

**CHARACTERISATION OF PP71
HOMOLOGUES ENCODED BY
MAMMALIAN
CYTOMEGALOVIRUSES**

by

Tanya N. Chaudry

A thesis presented for the degree of Doctor of Philosophy in the Faculty of
Biomedical and Life Sciences at the University of Glasgow

MRC Virology Unit

Institute of Virology
Church Street
Glasgow
G11 5JR

September 2008

Abstract

Human cytomegalovirus (HCMV) is a human pathogen that can cause severe disease in immunocompromised or immunosuppressed individuals and also in newborns infected *in utero*. Transcription of the viral genome occurs by a process in which three classes of HCMV genes, immediate early, early and late are expressed in a regulated temporal cascade. The HCMV protein pp71, encoded by gene UL82, is located in the tegument of the HCMV virion and is delivered to cells immediately upon infection. This protein has been identified as a transactivator of viral immediate early gene expression. It also stimulates expression from a number of heterologous promoters by a mechanism that is not promoter sequence specific. Protein pp71 has multiple properties; it can increase the infectivity of transfected viral DNA, modulate the cell cycle and interact with the retinoblastoma family of proteins. Within the cell nucleus, pp71 co-localises with the cellular proteins PML and hDaxx at sub-cellular structures named nuclear domain 10 (ND10). The interaction of pp71 with hDaxx is believed to promote the degradation of hDaxx, resulting in relief of repression at the HCMV major immediate early promoter. Protein pp71 has also been reported to have the unusual property of mediating long-term expression of reporter genes cloned into a herpes simplex virus type 1 (HSV-1) vector. This study describes a comparison of pp71 with the non-human UL82 homologues from simian CMV, baboon CMV, rhesus CMV and chimpanzee CMV, named S82, B82, RH82 and Ch82, respectively.

Plasmids expressing all of the UL82 homologues as enhanced yellow fluorescent protein (EYFP) or myc-tagged proteins were constructed and analysed for expression by transfection into HFFF2 cells. The EYFP-tagged UL82 homologues all directed β -gal expression in short-term assays, while only pp71 directed both short-term and long-term gene expression. Only myc-tagged pp71 was observed to direct gene expression in both the short-term and long-term assays.

The EYFP-tagged proteins and myc-tagged pp71 and Ch82 were cloned into a mutated HSV-1 vector to produce recombinant viruses. Functional assays in human glioblastoma (U373) cells confirmed that all of the EYFP-tagged and myc-tagged non-human UL82 homologues were able to direct short-term

expression but only EYFP- and myc-tagged pp71 directed long-term gene expression, confirming results obtained in transfection assays.

In agreement with previous reports, pp71 was shown to promote the resumption of gene expression from quiescent HSV-1 genomes. Comparison of the pp71 and Ch82 homologues indicated that pp71 is unique in its ability to do so. No reactivation was observed in cells infected with an HSV-1 recombinant that expressed EYFP-tagged Ch82.

In order to establish the region of pp71 responsible for mediating long-term gene expression six plasmids encoding EYFP-tagged hybrid proteins were constructed. The C-terminus, N-terminus and mid-regions of pp71 were substituted for the equivalent Ch82 regions using homologous restriction sites in both coding sequences. All EYFP-tagged hybrids mediated short-term gene expression, while only one protein, with the mid region of pp71 inserted between the C- and N-terminal regions of the Ch82 homologue, appeared to stimulate long-term gene expression. However, levels of expression were significantly lower than that achieved by pp71. A HSV-1 recombinant expressing the hybrid protein was used to confirm results from transfection assays, suggesting that the mid-region of pp71 may be involved in mediating its long-term properties. Given the significantly lower degree of gene expression directed by the hybrid protein in short-term assays it was concluded that alterations to pp71 may result in structural changes that prevent normal function of the protein.

Immunofluorescence studies revealed further differences between the non-human UL82 homologues and pp71. In confirmation of previously published findings, in the majority of HFFF2 cells infected with a HSV-1 recombinant expressing EYFP-tagged pp71, this protein localised to discrete punctate ND10 foci at all times tested. In cells infected with a HSV-1 recombinant expressing S82 a pattern distinct from that of pp71 was observed. S82 exhibited a punctate/diffuse pattern of fluorescence, which became increasingly diffuse at later times post-infection. The remaining non-human UL82 homologues, despite localising to the discrete punctate foci characteristic of pp71 at early times post-infection, all showed nuclear distribution patterns akin to that of S82 at later times, in cells infected with the HSV-1 recombinants expressing EYFP-tagged Ch82, B82 and Rh82. All non-human UL82 homologues, like pp71, co-localised with the endogenous cellular

proteins hDaxx and PML at the times tested. Interestingly, however, at later times post-infection, the S82 protein appeared to disperse hDaxx throughout the nucleus, a feature that was not observed with the remaining UL82 homologues. Examination of the hybrid protein observed to stimulate long-term gene expression revealed that, like pp71, it localised to discrete punctate foci, and co-localised with both PML and hDaxx at all times post-infection. In contrast to other published studies, it was not possible to demonstrate pp71-mediated hDaxx degradation, by either pp71 or the non-human UL82 homologues.

The work presented in this thesis confirms the previous observation that pp71 directs long-term gene expression, reactivates quiescent genomes and co-localises in the nucleus with hDaxx and PML. It also characterises the non-human UL82 homologues of pp71. This study shows that, while each non human UL82 homologue shares some characteristics with pp71, subtle functional differences exist between these proteins.

Table of Contents

Abstract	1
Table of Contents	4
List of Figures	8
Acknowledgements	12
Authors Declaration	12
Abbreviations used in this study	13
1. Introduction to herpesviruses	17
1.1. Herpesviridae classification	17
1.1.1. Alphaherpesvirinae.....	17
1.1.2. Betaherpesvirinae.....	17
1.1.3. Gammaherpesvirinae	18
1.2. HSV biology	18
1.2.1. HSV-1 virion and genome structure	18
1.3. HSV infection	20
1.4. Lytic infection	20
1.4.1. Viral attachment and penetration into the cell	20
1.4.2. Virion transport and genome insertion to the nucleus.....	20
1.4.3. HSV-1 viral IE proteins	21
1.4.3.1. ICP4	22
1.4.3.2. ICP22	22
1.4.3.3. ICP27	23
1.4.3.4. ICP47	23
1.4.3.5. ICP0	24
1.4.3.6. ICP0 and USP7.....	24
1.4.3.7. ICP0 and PML	25
1.4.3.8. ICP0 and ICP4.....	25
1.4.3.9. ICP0-null viruses	26
1.4.4. Viral transcription and translation.....	26
1.4.5. Capsid assembly, DNA replication, packaging and virion maturation	27
1.5. Latent infection	28
1.5.1. Reactivation from latency	30
1.5.2. Reactivation of quiescent genomes.....	31
1.6. HCMV Biology	32
1.6.1. The HCMV genome	32
1.6.2. HCMV capsid.....	35
1.7. HCMV pathogenesis	36
1.7.1. HCMV prevalence and disease	36
1.7.2. HCMV latency and reactivation	38
1.8. HCMV Lytic infection	41
1.8.1. Attachment and penetration	41
1.8.2. IE gene expression	42
1.8.2.1. IE1	43
1.8.2.2. IE2.....	44
1.8.2.3. Role of HCMV E and L genes	45
1.8.3. HCMV DNA replication and packaging	46
1.8.4. HCMV capsid transport	47
1.9. The HCMV MIEP	48
1.10. HCMV pp71 protein	49
1.10.1. The UL82 gene	49
1.10.2. Functional properties of pp71.....	50
1.10.3. Interaction of pp71 with cellular proteins	52
1.10.3.1. Rb Tumour suppressor proteins and pp71	52

1.10.3.2. hDaxx, PML and pp71	53
1.10.4. The interaction of pp71 with other tegument proteins	57
1.10.5. pp71 and the immune system.....	58
1.10.6. HSV-1 recombinant viruses impaired for IE gene expression	59
1.10.7. pp71 directs long-term gene expression	61
1.11. A comparison of pp71 with the HSV-1 proteins VP16 and ICP0.....	62
1.11.1. pp71 and VP16	62
1.11.2. pp71 and ICP0	63
1.12. Simian Cytomegalovirus Biology	65
1.12.1. SCMV genome.....	65
1.12.2. SCMV lytic infection	65
1.12.2.1. Attachment and penetration.....	65
1.12.2.2. IE gene expression.....	65
1.12.2.3. E and L gene expression	66
1.12.3. Capsid assembly and DNA packaging.....	66
1.12.4. Virion maturation and egress	67
1.13. Rhesus Cytomegalovirus biology.....	67
1.13.1. RhCMV genome	67
1.13.2. RhCMV lytic infection	68
1.13.2.1. Attachment and penetration.....	68
1.13.2.2. RhCMV IE gene expression.....	68
1.13.2.3. RhCMV E and L gene expression	69
1.13.2.4. Capsid assembly and DNA packaging	69
1.13.3. RhCMV prevalence and disease	69
1.14. BCMV biology	69
1.15. ChCMV biology	70
1.16. Project aims	72
2. Materials	73
2.1. Chemicals	73
2.1.1. Eukaryotic cells and tissue culture	73
2.1.2. Primary Antibodies	74
2.1.3. Secondary Antibodies	75
2.1.4. Plasmids	75
2.1.5. Viruses.....	76
2.1.6. Restriction endonucleases	76
2.1.7. Miscellaneous enzymes	76
2.1.8. Composition of commonly used solutions and buffers	77
2.1.8.1. Bacterial cell culture	77
2.1.8.2. DNA manipulation	77
2.1.8.2a. Small scale DNA preparation.....	77
2.1.8.2b. Large Scale DNA preparation	77
2.1.8.3. STET preparations	78
2.1.8.4. SDS polyacrylamide gel electrophoresis and western blotting	78
2.1.8.5. DNA electrophoresis.....	78
2.1.8.6. β -Galactosidase assays	78
2.1.8.7. SEAP assay	79
2.1.8.8. Immunofluorescence reagents	79
2.1.9. Commercial kits and other reagents	79
2.1.9.1. DNA Handling	79
2.1.9.2. Transfection reagents.....	79
2.1.9.3. Transformation reagents	79
2.2. Methods.....	80
2.2.1. DNA manipulation techniques	80

2.2.1.1. Restriction endonuclease digestion.....	80
2.2.1.2. Removal of phosphate groups from DNA 5' ends.....	80
2.2.1.3. Generation of blunt ended linear DNA fragments	80
2.2.1.4. Separation of DNA fragments by agarose gel electrophoresis	80
2.2.1.5. Isolation of DNA fragments from agarose gels	81
2.2.1.6. Phenol/Chloroform extractions.....	81
2.2.1.7. Ligation of compatible DNA fragments	81
2.2.1.8. Transformation of DNA into competent bacteria.....	82
2.2.1.9. Small scale DNA preparation	82
2.2.1.10. STET preparations	82
2.2.1.11. Large Scale DNA preparation.....	83
2.2.1.12. Nucleofection of adherent cells	83
2.2.1.13. Virus infection of mammalian cells	84
2.2.2. Protein manipulation techniques	84
2.2.2.1. Preparation of cell lysates.....	84
2.2.2.2. SDS polyacrylamide gel electrophoresis of proteins.....	84
2.2.2.3. Western blot analysis of denatured proteins.....	85
2.2.2.4. Histochemical staining for β -galactosidase in tissue culture monolayers	85
2.2.2.5. Carmalum staining	86
2.2.2.6. Digital imaging of β -gal positive cells	86
2.2.2.7. Secreted Alkaline Phosphatase (SEAP) assays	86
2.2.3. Virus propagation techniques	87
2.2.3.1. Preparation of recombinant HSV-stocks	87
2.2.3.2. Titration of recombinant HSV-1 stocks	87
2.2.4. Cell culture techniques	87
2.2.4.1. Serial passage of eukaryotic cells.....	87
2.2.4.2. Seeding of eukaryotic cells into tissue culture dishes	88
2.2.5. Microscopy techniques	88
2.2.5.1. Immunofluorescence	88
2.2.5.2. Confocal microscopy.....	89
3. Part I.....	90
3.1. Introduction	90
3.1.1. Sequence analysis of the UL82 homologues	90
3.1.2. EYFP-tagged UL82 homologues as transactivators of gene expression.....	91
3.1.3. Myc-tagged UL82 homologues as transactivators of gene expression.....	93
3. Part II.....	96
3.2. Introduction	96
3.2.1. Infection with the <i>in1312</i> recombinants expressing the EYFP-tagged UL82 homologues stimulates short-term gene expression	96
3.2.2. Analysis of long-term gene expression.....	98
3.2.3. Myc-tagged UL82 homologues expressed by <i>in1312</i> based recombinants are functional 24 hr post-infection.....	100
3.2.4. Only myc-pp71 directs long-term gene expression.....	101
3. Part III.....	103
3.3. Introduction	103
3.3.1. Reactivation Assay	103
3.4 Discussion	105
Figure 3.5. Expression of EYFP-tagged UL82 homologues 24 hr, 4 days, and 10 days post-transfection.	Error! Bookmark not defined.
4. Part I.....	108

4.1. Introduction	108
4.1.1. Construction of plasmids that express EYFP-tagged hybrids	108
4.1.2. EYFPpp71/EYFPCh82 hybrids as transactivators of gene expression.....	110
4. Part II.....	114
4.2. Introduction	114
4.2.1. Infection with the <i>in1312</i> recombinant <i>in0156</i> stimulates short-term gene expression	114
4.2.2. Analysis of long-term gene expression	115
4.3. Discussion	118
5. Part I.....	120
5.1. Introduction	120
5.1.1. Distribution patterns of EYFPUL82 homologues at 3 hr post-infection.....	121
5.1.2. Distribution patterns of the EYFPUL82 homologues 5 hr post-infection.....	121
5.1.3. Distribution patterns of the EYFPUL82 homologues at 7 hr post-infection	122
5. Part II.....	124
5.2. Introduction	124
5.2.1. The EYFPUL82 homologues co-localise with the cellular proteins hDaxx and PML at 3 hr 5 hr and 7hr post-infection.	124
5. Part III.....	126
5.3. Introduction	126
5.3.1 Hybrid TC6 co-localises with the cellular proteins hDaxx and PML at 3 hr post-infection.	126
5.3.2. Hybrid TC6 co-localises with the cellular proteins hDaxx and PML at 5 hr post-infection.	127
5.3.3. Hybrid TC6 co-localises with the cellular proteins hDaxx and PML at 7 hr post-infection.	127
5. Part IV	129
5.4. Introduction	129
5.4.1. Infection with the <i>in1312</i> recombinants expressing EYFP-tagged homologues does not result in the degradation of hDaxx.....	129
5.5. Discussion	131
6. Final Discussion	135
6.1. Introduction	135
6.1.1. UL82 homologues; short-term and long-term expression analyses	135
6.1.2. The UL82 homologues and long-term gene expression	136
6.1.3. Effects of the UL82 homologues on genome quiescence.....	137
6.1.4. Promoter analysis of the UL82 homologues	138
6.1.5. The LXCXD motif.....	139
6.2. The significance of the DIDs in the UL82 homologues	140
6.3. Conclusions.....	141
6.4. Future work.....	141
References	143
Appendices	163

List of Figures

Figure 1.1 Cartoon illustrating the structure of a herpes virion	19
Figure 1.2 Genome arrangement of HSV-1	19
Figure 1.3. Schematic view of the sequence of viral gene expression during HSV-1 infection	21
Figure 1.4 Regulation of HCMV gene expression during productive infection	43
Figure 1.5 Schematic representation of the HCMV genome	50
Figure 3.1. Conservation of UL82 amino acids in homologue primate CMV sequences	90
Figure 3.2. Phylogenetic analysis of UL82 homologues	90
Figure 3.3. Stimulation of β -gal expression by EYFP-tagged UL82 homologues at 24 hr post-infection	91
Figure 3.4. Stimulation of β -gal expression by EYFP-tagged UL82 homologues at 24 hr and 10 days post-infection.....	92
Figure 3.5. Expression of EYFP-tagged UL82 homologues 24 hr, 4 days, and 10 days post-transfection.	92
Figure 3.6. Stimulation of β -gal expression by the myc-UL82 homologues at 24 hr and 10 days post-infection	93
Figure 3.7.Expression of myc-tagged pp71 homologues 24 hr and 10 days post-transfection	94
Figure 3.8.Overview of the experimental plan employed in short-term analysis of the EYFP/myc-tagged UL82 homologues.	97
Figure 3.9. β -gal expression of the <i>in1312</i> recombinants expressing the EYFP-tagged UL82 homologues at 24 hr post-infection	97
Figure 3.10. Expression of the EYFP-tagged UL82 homologues at 24 hr post-infection.....	97
Figure 3.11. Activation of expression by infection with <i>in1312</i> recombinants expressing the EYFP-tagged UL82 homologues <i>in trans</i>	98
Figure 3.12.Overview of the experimental plan employed in long-term analysis of the EYFP/myc-tagged UL82 homologues.	99
Figure 3.13a β -gal expression directed by the <i>in1312</i> recombinants expressing the EYFP-tagged UL82 homologues at 10 days post-infection	99
Figure 3.13b. Response of the <i>in1312</i> recombinants expressing EYFP-tagged UL82 homologues to temperature downshift.....	99
Figure 3.13c. Response of the <i>in1312</i> recombinants expressing the EYFP-tagged UL82 homologues to super-infection with <i>tsK</i>	100
Figure 3.14. Expression of the EYFP-tagged UL82 homologues at 10 days post-infection	100
Figure 3.15. β -gal expression directed by the <i>in1312</i> recombinants expressing the myc-tagged UL82 homologues at 24 hr post-infection	101
Figure 3.16. Expression of the myc-tagged UL82 homologues at 24 hr post-infection.....	101
Figure 3.17. Activation of expression by infection with <i>in1312</i> recombinants expressing the myc-tagged UL82 homologue <i>in trans</i>	101
Figure: 3.18a β -gal expression directed by the <i>in1312</i> recombinants expressing the myc-tagged UL82 homologues at 10 days post-infection	102
Figure 3.18b. Response of the <i>in1312</i> recombinants expressing myc-tagged UL82 homologues to temperature downshift.....	102
Figure 3.18c. Response of the <i>in1312</i> recombinants expressing myc-tagged UL82 homologues to super-infection with <i>tsK</i>	102

Figure 3.19. Expression of the myc-tagged UL82 homologues 10 days post-infection.....	102
Figure 3.20. Reactivation of SEAP expression by <i>in1312</i> recombinants expressing EYFPpp71 and EYFPCh82 <i>in trans</i>	103
Figure 3.21 Activity of the <i>in1312</i> recombinants expressing EYFP-tagged pp71 or Ch82.....	104
Figure 3.22. Western analysis of the <i>in1312</i> recombinants expressing EYFP-tagged pp71 or Ch82 homologues at 24 hr and 10 days post-super-infection	104
Figure 4.1 Conservation of amino acid sequences between pp71 and Ch82 homologues	108
Figure 4.2. Schematic representation of the pEYFPpp71 and pEYFPCh82 plasmids	108
Figure 4.3. Schematic representation of the <i>Bgl</i> II and <i>Bss</i> HI restriction sites in homologous regions of the pp71 and Ch82 nucleotide sequences..	108
Figure 4.4 Schematic representation of the pEYFP/pEYFPCh82 hybrids....	110
Figure 4.5. Expression directed by the EYFPpp71/EYFPCh82 hybrids at 24 hr post-transfection	110
Figure 4.6. β -gal expression directed by EYFPpp71/EYFPCh82 hybrids at 24 hr and 10 days post-infection	111
Figure 4.7. Analysis of protein expression directed by the pEYFPpp71/pEYFPCh82 plasmids at 24 hr and 10-days post-transfection	112
Figure 4.8. β -gal expression directed by <i>in1312</i> recombinants expressing EYFP-tagged UL82 homologues or hybrid F at 24 hr post-infection	114
Figure 4.9. Expression of the EYFP-tagged UL82 homologues or TC6 at 24 hr post-infection.....	115
Figure 4.10. Activity of the <i>in1312</i> recombinants expressing either the UL82 homologues or TC6 <i>in trans</i>	115
Figure 4.11a. β -gal expression directed by the <i>in1312</i> recombinants expressing the EYFP-tagged UL82 homologues or TC6 at 10 days post-infection.....	116
Figure 4.11b. Response of the <i>in1312</i> recombinants expressing the UL82 homologues or TC6 to temperature downshift	116
Figure 4.11c. Response of the <i>in1312</i> recombinants expressing the UL82 homologues or TC6 to super-infection with <i>tsK</i>	116
Figure 4.12. Expression of the EYFP-tagged UL82 homologues or TC6 at 10 days post-infection.....	117
Figure 4.13 Showing the regions of disorder in the UL82 proteins.....	119
Figure 5.1 Patterns of fluorescence exhibited by the EYFPUL82 homologues	121
Figure. 5.2 Nuclear distribution of the EYFPUL82 homologues at 3 hr, 5 hr and 7 hr post-infection	121
Figure 5.3a. EYFPpp71 co-localises with hDaxx at 3 hr, 5 hr and 7 hr post-infection.....	124
Figure 5.3b. EYFPpp71 co-localises with PML at 3 hr, 5 hr and 7 hr post-infection.....	124
Figure 5.4a. EYFPCh82 co-localises with hDaxx at 3 hr, 5 hr and 7 hr post-infection.....	125
Figure 5.4b. EYFPCh82 co-localises with PML at 3 hr, 5 hr and 7 hr post-infection.....	125
Figure 5.5a. EYFPS82 and hDaxx at 3 hr, 5 hr and 7 hr post-infection	125
Figure 5.5b. EYFPS82 co-localises with PML at 3 hr, 5 hr and 7 hr post-infection.....	125

Figure 5.6a. EYFPB82 co-localises with hDaxx at 3 hr, 5 hr and 7 hr post-infection.....	125
Figure 5.6b. EYFPB82 co-localises with PML at 3 hr, 5 hr and 7 hr post-infection.....	125
Figure 5.7a. EYFPRh82 co-localises with hDaxx at 3 hr, 5 hr and 7 hr post-infection.....	125
Figure 5.7b. EYFPRh82 co-localises with PML at 3 hr, 5 hr and 7 hr post-infection.....	125
Figure 5.8a. EYFPTC6 co-localises with hDaxx at 3 hr, 5 hr and 7 hr post-infection.....	126
Figure 5.8b. EYFPTC6 co-localises with PML at 3 hr, 5 hr and 7 hr post-infection.....	126
Figure 5.9. Western blot analysis of lysates of cells infected with <i>in1312</i> recombinants expressing UL82 homologues at 7 hr post infection	129
Figure 5.10. β-gal expression directed by the <i>in1312</i> recombinants expressing the EYFP-tagged UL82 homologues at 7 hr post-infection	129
Figure 5.11. Western blot analysis of lysates of cells infected with <i>in1312</i> recombinants expressing UL82 homologues 24 hr post-infection	130
Figure 5.12. β-gal expression of the <i>in1312</i> recombinants expressing the EYFP-tagged UL82 homologues at 24 hr post-infection	130
Figure 6.1 Conservation of UL82 functional domains in homologous non-human CMV sequences.....	139

List of Tables

Table 2.1. Showing cells used and their sources.....	74
Table 2.2. Primary antibodies used, their targets and their source.....	74
Table 2.3. Secondary antibodies used and their source	75
Table 2.4. Plasmids used and their acknowledged sources	75
Table 2.5. Viruses used in this study	76
Table 3.1. Stimulation of β-gal expression by the EYFP-tagged UL82 homologues at 24 hr and 10 days post-infection.....	91
Table 4.1. Stimulation of β-gal expression directed by the pEYFPpp71/pEYFPCh82 hybrids at 24 hr and 10 days post-transfection	110
Table 5.1. Nuclear distribution patterns of the EYFPUL82 homologues at 3 hr, 5 hr and 7 hr post-infection	121
Table 5.2. Nuclear distribution patterns of the EYFPUL82 homologues at 3 hr 5 hr and 7 hr post-infection.....	121

Acknowledgements

I would like to thank Professor Duncan McGeoch for allowing me the opportunity to carry out my PhD within the MRC virology unit.

Thanks go to my project supervisor Dr. Chris Preston for his continuous help advice and support throughout my studies.

I would also like to express thanks to the occupants of Lab A408 for all their help and advice during my time in the laboratory. Particular thanks go to Steven McFarlane and Mary-Jane Nicholl for their invaluable advice and technical assistance. Special thanks go to Jane Sutherland for her endless support, encouragement and assistance with everything thesis related.

To all my friends: Amanda Bradley, Sarah Mole, Jon Hubb, Ross Watters, Louise Yule, David Dalrymple, James Towler, Ali Saville, Martin Higgs and Maureen O'Hara for providing coffee breaks, great nights out, humour, support and lots of random chat over the past few years.

To my brother Sam for always helping me find the humour in every situation!

My eternal gratitude goes to my parents, to whom this thesis is dedicated. A huge thank you for all your unconditional love, support and for always encouraging me in everything I have set out do.

Authors Declaration

The author was a recipient of a Medical Research Council Studentship. Except where specified, all of the results described in this thesis were obtained by the authors own efforts.

Tanya Chaudry

Abbreviations used in this study

AP	assembly protein
APS	ammonium persulphate
BCMV	baboon cytomegalovirus
BDGF	Bio-Gene Finder
bp	base pair
β -gal	β -galactosidase
BSA	bovine serum albumin
C	carboxy (-terminal end of protein)
CCMV	chimpanzee cytomegalovirus
CENP-C	centromere protein C
CIP	calf intestinal phosphatase
CLTs	cytomegalovirus latency-specific transcripts
CTCF	CCCTC-binding factor
DC	dendritic cells
dH ₂ O	distilled water
DID	Daxx interaction domain
DMEM	Dulbeccos modified Eagles medium
DMSO	dimethylsulphoxide
DNA	deoxyribonucleic acid
E	Early
EBV	Epstein-Barr virus
EC	endothelial cells
<i>E.coli</i>	<i>Escherichia coli</i>
ECL	enhanced chemiluminescence
EDTA	ethylenediaminetetra-acetic acid
EGFR	epidermal growth factor receptor
ER	endoplasmic reticulum
EYFP	enhanced yellow fluorescent protein
FCS	foetal calf serum
GAG	glycosaminoglycan
GMPs	granulocyte macrophage precursors
GST	glutathione S-transferase
HCF	host cellular factor
HCMV	human cytomegalovirus

HDAC	histone deacetylase
HFFF	human foetal foreskin fibroblasts
HHV-6	human herpesvirus type 6
HHV-7	human herpesvirus type 7
HIV	human immunodeficiency virus
HMBA	hexamethylbisacrylamide
HP1	histone deacetylase 1
hr	hours
HRP	horse radish peroxidase
HSV-1	herpes simplex virus type 1
HSV-2	herpes simplex virus type 2
HVEM	herpes virus entry mediator
ICP	infected cell protein
IE	immediate early
Ig	immunoglobulin
ITE	immediate transcript environment
KHSV	Kaposi's sarcoma-associated herpesvirus
L	Late
LAT	latency associated transcript
LTR	long-terminal repeat
LSM	laser scanning microscope
mcBP	minor capsid binding protein
MCMV	murine cytomegalovirus
MCP	major capsid protein
mcP	minor capsid protein
MCS	multiple cloning site
MHC	major histocompatibility complex
MIEP	major immediate early promoter
min	minutes
MOI	multiplicity of infection
mRNA	messenger RNA
MUP	4-methylumbelliferyl phosphate
N	amino (-terminal of protein)
NBCS	newborn calf serum
ND10	nuclear domain 10
NLS	nuclear localisation signal

NPC	nuclear pore complex
NP40	Nonidet p40
NT2D1	teratocarcinoma cells
ORF	open reading frame
<i>orilyt</i>	origin of lytic replication
PAGE	polyacrylamide gel electrophoresis
PBS	phosphate buffered saline
PBST	phosphate buffered saline+Tween 20
PCR	polymerise chain reaction
pfu	plaque forming unit
PML	promyelocytic leukaemia
Rb	retinoblastoma protein
RhCMV	rhesus cytomegalovirus
rpm	revolutions per minute
R _L	long inverted repeat region
R _S	short inverted repeat region
SCMV	simian cytomegalovirus
SCP	small capsid protein
SEAP	secreted alkaline phosphatase
ShRNA	short hairpin RNA
SiRNA	small inhibitory RNA
SIM	SUMO-interaction motif
SIV	simian immunodeficiency virus
SUMO-1	small ubiquitin-like modifier
TAP	transporter associated with antigen presentation
TBP	TATA-binding protein
TEMED	N'-N'-N'-N'-tetramethylethylenediamine
TF	transcription factor
THP1	myelomonocytic cells
TK	thymidine kinase
Tris	tris (hydroxymethyl) aminomethane
ts	temperature sensitive
TSA	trichostatin A
Tween 20	polyoxyethylene-sorbitanmonolaurate
U _L	unique long region
U _S	unique short region

USP7	ubiquitin specific protease
UV	ultra-violet
v/v	volume/volume
VZV	varicella-zoster virus
w/v	weight/volume
X-gal	5'bromo-4-chloro-3-indoyl- β -D-galactosidase
YFP	yellow fluorescent protein

Chapter 1

Introduction

1. Introduction to herpesviruses

1.1. Herpesviridae classification

Herpesviruses constitute a large group of viruses classified as the family Herpesviridae, containing over 120 members (Roizman, 2001). Herpesviruses differ widely in their pathogenic potential, but following primary infection can remain latent within the host. The Herpesviridae fall into three sub-families, *Alphaherpesvirinae*, *Betaherpesvirinae* and *Gammaherpesvirinae*. Classification of these sub-families is based on their biological characteristics such as the length of the viral replication cycle, host cell range, cytopathology and the disease resulting from productive infection (Roizman & Baines, 1991, Roizman, 2001).

1.1.1. Alphaherpesvirinae

Viruses in the sub-family *Alphaherpesvirinae* typically exhibit variable host range *in vitro*, a rapid reproductive cycle, and the capacity to establish latent infection within sensory ganglia. They are further divided into two genera; the *Simplexviruses* and *Varicelloviruses*. The *Simplexviruses* include herpes simplex virus type 1 (HSV-1), which typically infects mucosal tissue of the mouth resulting in cold sores, and herpes simplex virus type 2 (HSV-2), which infects genital mucosal epithelia causing genital lesions. The *Varicelloviruses* include varicella-zoster virus (VZV), which causes chickenpox during primary infection (Roizman, 2001).

1.1.2. Betaherpesvirinae

Viruses within the sub-family *Betaherpesvirinae* demonstrate a restricted host range and slow growth in cell culture models (Mocarski, 2001). Latency is established in lymphoreticular cells, and secretory glands (Sinclair & Sissons, 2006). This sub-family is further divided into three genera; the *Cytomegaloviruses*, *Roseloviruses* and *Muromegaloviruses*. Infection with human cytomegalovirus (HCMV) of the *Cytomegalovirus* genera poses a significant risk to immunocompromised individuals resulting in diseases such as retinitis and pneumonitis (Mocarski, 2001). HHV-6 and HHV-7 are both members of the *Roselovirus* genus of the *Betaherpesvirinae*. HHV-6 is associated with febrile disease in children and has been implicated in the aetiology of chronic fatigue syndrome and multiple sclerosis (Ablashi et al., 2000). HHV-7 has been

associated with post-transplant disease in immunosuppressed organ recipients. It has been reported that gastric mucosal cells are the site at which latent HHV-7 DNA is found (Gonelli et al., 2001). The murine cytomegalovirus (MCMV) of the *Muromegalovirus* genera is utilised as a model for both productive and persistent HCMV infection (Keil et al., 1984).

1.1.3. Gammaherpesvirinae

These viruses have variable host cell range, and duration of replication (Roizman, 2001). Members of this family replicate in lymphoblastoid cells some types of epithelioid and fibroblastic cells, and establish latency in either T or B lymphocytes (Roizman, 2001). Gammaherpesviruses are further divided into two genera; *Lymphocryptoviruses* (EBV) and *Rhadinoviruses* (HHV-8). HHV-8 is also known as Kaposi's sarcoma-associated herpesvirus (KSHV), and infection can result in Kaposi's sarcoma, primary effusion lymphoma or multicentric Castleman's disease in immunosuppressed patients (Roizman, 2001).

1.2. HSV biology

The herpes simplex viruses consist of two serotypes, HSV-1 and HSV-2, and were the first of the human herpesviruses to be discovered. Due to their ease of growth in culture both are amongst the most intensely investigated (Roizman, 2001). HSV-1 has a complex lytic life cycle (Roizman, 2001) and is able to establish life long latency in sensory neurons. This strategy secures the long-term survival of the virus as it is able to evade the host immune system during latent infection (Efstathiou & Preston, 2005).

1.2.1. HSV-1 virion and genome structure

As with other herpesviruses, the HSV-1 virion consists of four distinct components; the DNA core (contained within the capsid), capsid, tegument, and envelope (Adamson et al., 2006, Roizman, 2001). The HSV-1 capsid is icosohedral in shape with a diameter of 1,250 Å (Saad et al., 1999). Capsids are considered to exist in three forms, B-capsids, which contain scaffolding proteins, C-capsids, which contain viral DNA, and A-capsids that are empty capsids (Rixon, 1993). Capsids are composed of 162 capsomeres, which can be divided into three types:

150 hexons, 11 pentons and one portal. The hexons form the faces and edges of the capsid and the pentons form eleven of the twelve vertices. Triplexes of UL18 and UL38 hold the capsomeres together (Garner, 2003, Newcomb et al., 2005, Newcomb et al., 2006, Newcomb et al., 2003). A linear double stranded DNA genome of 152 kb is packaged into the capsids. It has been reported that the packaged DNA appears to exist in a liquid crystalline state, similar to that suggested for the double stranded DNA bacteriophages λ and T4 (Booy et al., 1991, Rixon, 1993). The capsid is surrounded by a tegument layer that contains at least 15 viral proteins including the HSV-1 immediate early (IE) proteins (McLauchlan & Rixon, 1992, Rixon et al., 1992). The outer surface of the virion is a tri-laminar viral lipid envelope with a diameter of 170-200 nm, containing embedded viral glycoproteins, which are seen as spikes under an electron microscope (Mettenleiter, 2002). A schematic representation of a herpes virion is presented in figure 1.1

The initial sequence of the HSV-1 genome, strain 17, was finally determined in 1988 by McGeoch et al. when the complete DNA sequence of the long unique region of HSV-1 was obtained (McGeoch et al., 1988). Prior to this the complete sequence of the unique short region (U_S) (McGeoch et al., 1985), and the complete sequence of the short inverted repeat region (R_S) (Davison & Wilkie, 1981, Murchie & McGeoch, 1982) were published. The complete sequence of the long inverted repeat (R_L) region was later published by Perry and McGeoch in 1988 (Perry & McGeoch, 1988), thus the complete sequence of HSV-1 was believed to contain 152260 residues in each strand with a base composition of 68% G+C (McGeoch et al., 1988). The sequence of HSV-1 was later updated and currently stands at 152261 base pairs (bp) (Dolan et al., 1998). The HSV-1 genome therefore consists of the U_L and U_S regions that are in turn flanked by inverted repeat sequences R_L and R_S . HSV-1 genes are distributed throughout the genome on both DNA strands; genes located within the inverted repeats are present in two copies (Weir, 2001). Three of the IE genes are located near the termini of the R_L and R_S regions of the genome. The IE genes encoding ICP0 and ICP4, are contained within the inverted repeats R_L and R_S , and therefore occur twice within the genome. The early (E) and late (L) genes are found throughout the unique regions (Roizman, 2001). Figure 1.2 shows the genome arrangement of HSV-1.

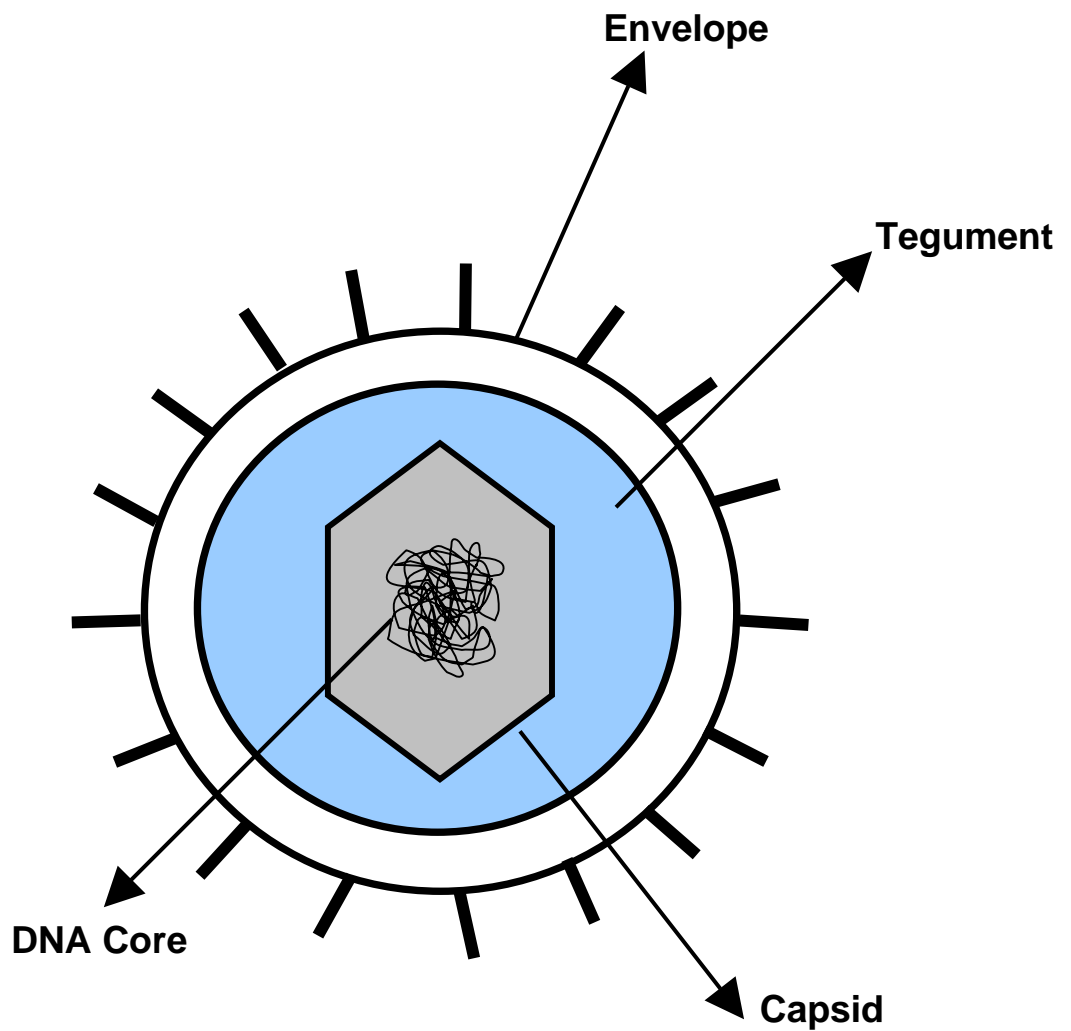


Figure 1.1 Cartoon illustrating the structure of a herpes virion

Schematic representation of the structure of an HSV-1 virion. It shows the double-stranded DNA core enclosed within the icosahedral capsid, surrounded by a proteinaceous tegument and enclosed within a lipoprotein membrane.

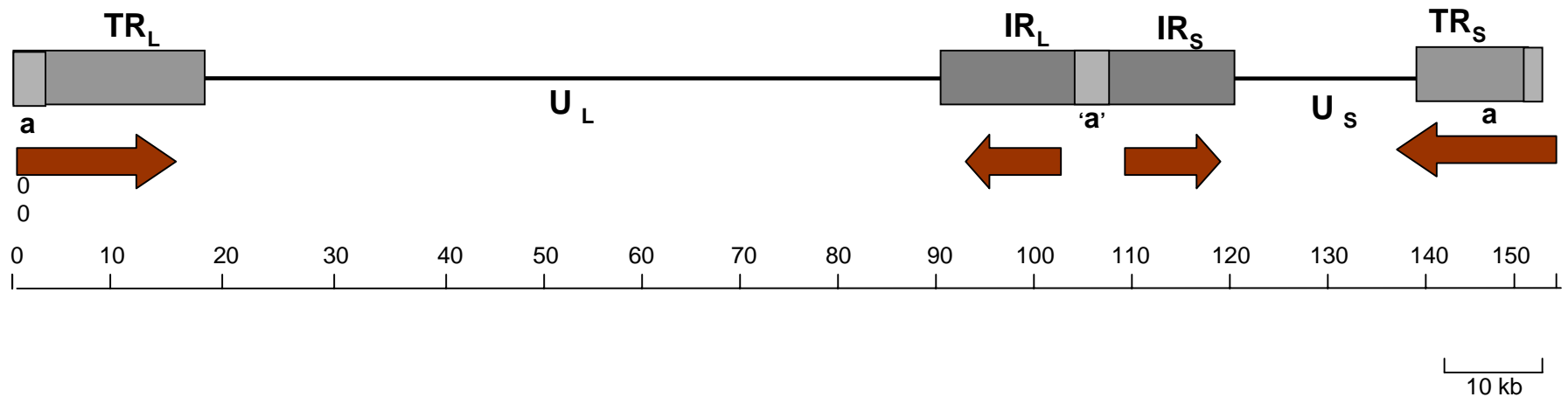


Figure 1.2 Genome arrangement of HSV-1

The genome has two unique regions, each of which is flanked by an inverted repeat. The repeat regions IR_L/TR_L and IR_S/TR_S, flanking U_L and U_S respectively. An additional repeat element the 'a' sequence, is found at both genomic termini and at the junction between the internal repeats (IR_L and IR_S). Both the U_L and U_S segments show a high frequency of inversion.

Adapted from Davison and McGeoch (1995).

1.3. HSV infection

The prevalence of both HSV-1 and HSV-2 infections varies markedly by country, region within country and population sub-group. The percentage of adults infected with HSV-1 is thought to be 60-90% in non-high risk groups, a rise from 40% at 15 years old (Smith & Robinson, 2002). Infection occurs when HSV is excreted from infected individuals to seronegative individuals via intimate personal contact. Infection occurs at mucosal surfaces or abraded skin (Whitley, 2001). The most common consequence of HSV-1 infection is cold sores, however severe infection with HSV-1 can result in stromal keratitis (infection of the cornea) and it is also the most common causative agent of viral encephalitis and, more rarely of meningoencephalitis (Whitley, 2001), while HSV-2 infection is the main cause of genital herpes (Roizman, 2001). Following infection HSV-1 can enter two modes of infection: lytic or latent (Efstathiou & Preston, 2005).

1.4. Lytic infection

1.4.1. Viral attachment and penetration into the cell

HSV-1 host cell entry is mediated by glycoproteins B (gB), gC, gD, gH, gJ, gK, gL, gM, and gN which are components of the viral envelope (Spear, 2004). Only gB, gD, gH, and gL are believed to be essential for cell fusion and entry (Spear, 2004). The virus initially binds to glycosaminoglycan (GAG) heparan sulphate on the host cell surface via gB and gC (Herold et al., 1994). Fusion of the viral envelope with the cell membrane is triggered by gD interaction with one of three cellular receptors: herpes virus entry mediator (HVEM), nectin-1 or nectin-2 (Spear, 2002).

1.4.2. Virion transport and genome insertion to the nucleus

Following internalisation the majority of tegument proteins dissociate from the capsids. However, tegument proteins that remain associated with the HSV-1 capsid are thought to assist in microtubule dependent transport, as is the case for pseudorabies virus (Granzow et al., 2005). The HSV-1 nucleocapsid is transported to the nuclear pore complex (NPC) via the microtubule network and the cellular motor dynein (Dohner et al., 2002).

Translocation of HSV-1 DNA into the nucleus occurs following capsid docking at the NPC, a process mediated by the one or more of the tegument proteins. The empty capsid remains in the cytoplasm (Ojala et al., 2000, Roizman, 2001). Shanin et al. (2006) suggested that the HSV-1 genome translocates through the nuclear pore in a condensed rod like structure. For this to occur the NPC is thought to dilate to allow entry (Shahin et al., 2006). Following entry of the genome into the nucleus it is thought to circularise (Roizman, 2001).

1.4.3. HSV-1 viral IE proteins

HSV-1 gene expression involves a sequential cascade of three sets of genes, IE, E and L, which are classified according to their time of expression during replication (Roizman, 2001). The IE genes are the first genes expressed, these are: ICP4, ICP27, ICP0, ICP22 and ICP47 (Efsthathiou & Preston, 2005). Expression of the IE genes is stimulated by binding of a tripartite complex, composed of the tegument protein VP16, and two cellular proteins Oct-1 and host cellular factor (HCF), to DNA elements containing the TAATGARAT sequence (where R is a purine) upstream of each of the IE gene promoters (Nicholl & Preston, 1996, Preston et al., 1988). Each component of the complex plays a specific role in the activation of IE gene expression (Weir, 2001). Transcriptional activation is a function of the acidic carboxy-terminus of VP16; studies have shown that this acidic domain can be tethered to DNA binding domains to activate transcription. Thus the target for VP16 activation is a component of the basal transcription machinery of the cell (Flint & Shenk, 1997). Oct-1 provides binding specificity, while HCF stabilises the tripartite complex and acts a nuclear import factor for VP16 (LaBoissiere & O'Hare, 2000).

Of the five IE gene products only four play a role in regulating viral gene expression (Weir, 2001). ICP0, ICP4, ICP22 and ICP27 are all involved in controlling gene expression, while ICP47 interferes with antigen presentation (York & Rock, 1996). A schematic over-view of HSV-1 viral gene expression is presented in figure 1.3. Below is a brief review of the HSV-1 IE proteins.

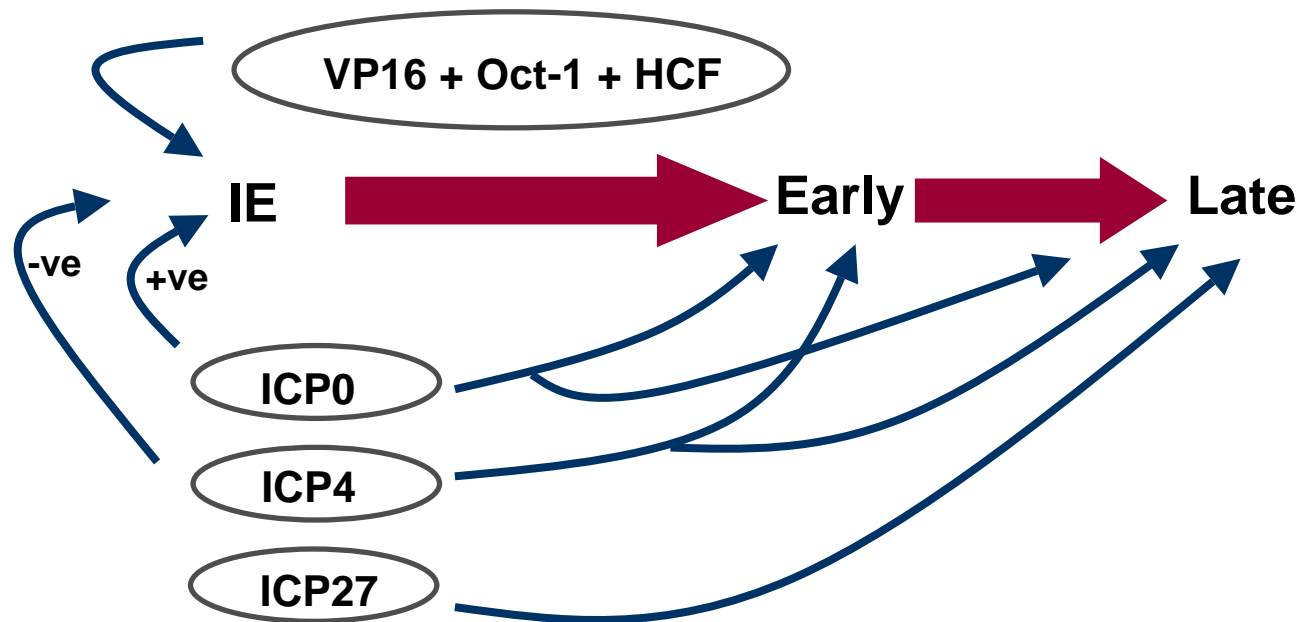


Figure 1.3. Schematic view of the sequence of viral gene expression during HSV-1 infection.

A scheme of viral gene expression in HSV-1 infection. VP16 activates IE gene expression upon forming a complex with Oct-1 and HCF. The subsequent production of ICP4 and ICP0 activates expression of Early and Late viral genes. Diagram adapted from Everett (2000).

1.4.3.1. ICP4

ICP4 has negative and positive effects upon transcription of viral genes and is composed of a number of discrete functional domains involved in transactivation, repression, dimerization, nuclear localisation and DNA binding (Gu et al., 1995). ICP4 acts as a transactivator of E and L gene expression (Weir, 2001) by promoting transcription by facilitating the formation of pre-initiation complexes through the recruitment of transcription factor (TF) IID (Grondin & DeLuca, 2000). It was also shown that ICP4 requires TFIIA to initiate transcription of the E genes (Zabierowski & DeLuca, 2004)

ICP4 is able to repress its own expression by negatively regulating the ICP4 promoter (Kuddus & DeLuca, 2007). Repression is thought to require direct binding of ICP4 to specific DNA binding sites near the transcription start site. Specific ICP4 interactions with general transcription factors including the TATA-binding protein (TBP) and TFIIB are involved in repression (Kuddus et al., 1995). Co-transfection experiments also showed that ICP4 acts to repress the latency associated promoter (LAP) by binding to the region spanning the LAP cap site sequences. Deletion of LAP cap site sequences effectively abolished ICP4 mediated repression (Batchelor et al., 1994).

More recent studies suggest ICP4 is important for circularisation of the HSV-1 genome, an event that may occur at a site where replication compartments later develop (Su et al., 2006).

1.4.3.2. ICP22

ICP22 is not required for virus replication in many cell systems. However, in certain rodent cell lines and primary human cells ICP22 is essential for efficient viral replication, expression of ICP0 and of a subset of viral L genes (Weir, 2001). It has been suggested that the primary role of ICP22 in lytic replication is to alter the expression, activity or post-translational modification of cellular proteins in order to provide a suitable environment for the expression of L genes (Orlando et al., 2006). Orlando et al. (2006) demonstrated that an ICP22-null virus (22/n199), produced virions that were of abnormal composition. Morphologically they contained reduced amounts of the L proteins, U_s11 and gC, but increased

amounts of ICP0 and ICP4, suggesting that ICP22 affects virion composition (Orlando et al., 2006).

1.4.3.3. ICP27

ICP27 is required for the switch between E and L viral gene expression, and for efficient DNA replication (Sacks et al., 1985). It has been shown to shuttle between the nucleus and the cytoplasm, suggesting a role for it in the nuclear export of viral transcripts and is also able to bind to intronless mRNAs (Sandri-Goldin, 1998). Koffa et al. (2001) proposed that ICP27 mediates viral mRNA transport by recruiting a TAP/NXF1 complex via an interaction with REF proteins (Koffa et al., 2001). This allows the otherwise inefficiently exported viral mRNAs to access the TAP-mediated export pathway. Studies have also shown that ICP27 associates with polyribosomes and its C-terminus is involved in the stimulation of translation (Larralde et al., 2006). ICP27 is able to interact with the C-terminus of RNA polymerase II (used by HSV-1 for viral gene transcription) to facilitate the recruitment of this cellular polymerase to sites of viral transcription (Dai-Ju et al., 2006).

1.4.3.4. ICP47

The HSV-1 IE protein ICP47 is able to block the major histocompatibility complex (MHC) class I antigen presentation pathway by binding to the transporter associated with antigen presentation (TAP), thus blocking the supply of peptide for the correct assembly and trafficking of MHC class I molecules (York et al., 1994). As a consequence antigenic presentation is turned off and infected cells are hidden from the immune system, suggesting a role for ICP47 in the persistence of HSV-1 infection (York & Rock, 1996). Recent studies *in vivo* showed that an ICP47-defective virus (Δ ICP47, F strain) was less able to invade organs of adult female mice than the wild-type virus employed in the study, indicating that ICP47 influences immune evasion (Burgos et al., 2006). This group also demonstrated that the neuroinvasiveness of the Δ ICP47 virus was recovered in TAP-deficient mice suggesting the TAP-ICP47 interaction is specific to neural tissues. Thus ICP47 appears to be essential for immune evasion, playing a role in infection while TAP production is regulated during viral challenge (Burgos et al., 2006).

1.4.3.5. ICP0

ICP0 is considered to be a promiscuous transactivator as it activates transcription from HSV-1 (Cai & Schaffer, 1992, Chen & Silverstein, 1992) and heterologous promoter elements independently of a single *cis*-acting element (Everett et al., 1991).

The functional domains of ICP0 have been established via mutational analysis. These include a RING finger domain located near the N-terminus (Everett, 1988). Many functions of ICP0 are dependent on its RING finger domain (Everett, 2000, Harris et al., 1989). ICP0 interacts with and can promote the degradation of various cellular proteins including the nuclear domain 10 (ND10) components (described in section 1.5.3.7), PML (Everett et al., 1998a), Sp100 (Parkinson & Everett, 2000), CENP-C (Everett et al., 1999a) and CENP-A (Lomonte et al., 2001). As ICP0 induces the accumulation of and co-localises with conjugated ubiquitin it is considered to be a part of the ubiquitin proteasome pathway and can act as a ubiquitin ligase (Boutell & Everett, 2003, Boutell et al., 2002). Boutell et al. (2002) demonstrated that full length ICP0 and its isolated RING finger domain possess E3 ubiquitin ligase activity *in vitro*. Furthermore, deletion of the RING finger domain resulted in an inactive protein

1.4.3.6. ICP0 and USP7

The 135 KDa protein, named ubiquitin-specific protease 7 (USP7) is a member of a family of proteins that cleave ubiquitylated cellular proteins. It interacts with ICP0 residues 594-633 (Everett et al., 1997, Meredith et al., 1995, Meredith et al., 1994). Studies have shown that ICP0 is able to induce its own ubiquitination *in vitro*, however, this is abolished when ICP0 binds to USP7 (Canning et al., 2004). More recent studies have shown reciprocal activity between ICP0 and USP7, suggesting that rather than ICP0 mediating degradation of USP7 at low multiplicity infections, USP7 stabilises ICP0 during the initial stages of HSV-1 infection (Boutell et al., 2005).

1.4.3.7. ICP0 and PML

ND10 domains are punctate nuclear structures (Ascoli & Maul, 1991), the major constituent of which is PML (Maul et al., 2000). In HSV-1 infection one of the early events is the association of the HSV-1 genome with ND10 domains (Everett & Murray, 2005). Various studies have linked ICP0 to the disruption of ND10 domains (Everett et al., 1998a, Everett & Maul, 1994, Maul & Everett, 1994) in a process that is dependent on its RING finger. Everett et al. (1998b) proposed during HSV-1 infection, ICP0 induces the loss of the high-molecular weight isoforms of PML, and the loss of these proteins is dependent on an active proteasome-dependent degradation pathway (Everett et al., 1998a). In 2003, using a transfection based approach and a family of deletion and point mutations, Boutell et al. demonstrated that sequences in the C-terminus and the lysine residue at position 160 of PML were necessary for ICP0-induced degradation of ND10 domains (Boutell et al., 2003). Initial infection with an ICP0-null virus showed the major ND10 components (PML, Sp100, and hDaxx) accumulating in replication compartments with ICP4 (Everett et al., 2004b). Everett and Murray (2005) showed that associated ND10-like complexes are formed in these replication compartments when ND10 proteins are deposited to create new aggregates in association with viral complexes, rather than by migration of pre-existing intact ND10 structures. Therefore ND10 constituent proteins migrate to the viral genome where ICP0 induced disruption and degradation takes place (Everett & Murray, 2005). More recently work using an siRNA approach was carried out where cells were depleted of PML and infected with HSV-1 ICP0-null virus. It was observed that depletion of PML increased the plaque forming and gene expression efficiencies of the ICP0-null HSV-1 mutants. This suggests that PML may contribute to a repressive mechanism that targets HSV-1 genomes and is countered by the activities of ICP0 (Everett et al., 2006).

1.4.3.8. ICP0 and ICP4

Both ICP0 and ICP4 have been shown to be present in the tegument of purified virions (Yao & Courtney, 1989), suggesting that upon entry of newly infected cells, these proteins function in synergy to activate viral gene expression (Yao & Schaffer, 1994). Using far-western blotting analysis and glutathione S-transferase (GST)-ICP0 affinity chromatography Yao and Schaffer (1994)

showed ICP0 to be capable of interacting directly and specifically with itself and ICP4. GST-ICP0 fusion protein affinity chromatography showed ICP4 to interact preferentially with the C-terminal amino acid residues 395-775 of ICP0. Further deletion analysis suggested amino acids 617-775 of ICP0 may represent the major domain for physical interaction of ICP4 and ICP0 (Yao & Schaffer, 1994).

1.4.3.9. ICP0-null viruses

In order to assess the biological activities of ICP0, an ICP0-null virus, *d/1403*, was constructed (Stow & Stow, 1986). HSV-1 viruses mutated for ICP0 are viable, but they exhibit a multiplicity and cell cycle-dependent defect in the onset of viral infection (Sacks & Schaffer, 1987, Yao & Schaffer, 1995). Cell type is also a complicating factor when working with ICP0-null viruses. This mutant virus has been shown to replicate to normal levels in the permissive osteosarcoma cell line U2OS (Yao & Schaffer, 1995). In Vero (African green monkey) and BHK (baby hamster kidney), replication efficiency is reduced, while replication efficiency in human fibroblast cell lines is extremely poor (Everett et al., 2004a, Hancock et al., 2006, Stow & Stow, 1986). Hancock et al. (2006) suggested gene expression is inhibited via a multi-step anti-viral gene silencing pathway and that VP16 and ICP0 act as inhibitors of separate steps in this pathway. This gene silencing pathway may be inactive in U2OS cells, accounting for the ability of these cells to complement defects in these viral functions.

Upon infecting non-permissive cell lines with ICP0-null viruses, at a low MOI, either quiescence or stalled infection is observed. Stalled infection displays one of three possible phenotypes; stalled with an incomplete set of expressed IE genes, stalled at the IE stage, or stalled with the expression of some E genes (Everett et al., 2004a). However, this inhibition of infection can be overcome at a high MOI, whereby infection proceeds normally even in the absence of ICP0 (Everett et al., 2004a, Stow & Stow, 1986).

1.4.4. Viral transcription and translation

The E genes are expressed after the IE genes. Transcription of this set of genes requires functional ICP4 (Watson & Clements, 1980) but not viral DNA synthesis (Roizman, 2001). The E genes include UL29, encoding ICP8 and UL23 encoding

thymidine kinase. UL29 is expressed shortly after the onset of the synthesis of the IE proteins, while UL23 is expressed with more significant delay following IE protein expression (Huszar & Bacchetti, 1981, Roizman, 2001).

The final class of genes to be expressed are the L genes, the expression of which begins with the initiation of DNA replication (Weir, 2001), which can be divided into two individual classes leaky-late and true-late genes (Roizman, 2001). The true-late genes (for example, UL38), require DNA replication for significant levels of protein expression, while leaky-late genes (for example, UL19) can be expressed in the absence of DNA replication (Roizman, 2001). The L genes encode for structural proteins of the virion including scaffolding proteins.

1.4.5. Capsid assembly, DNA replication, packaging and virion maturation

HSV DNA replication takes place in the nucleus of infected cells (Becker et al., 1968). The herpes simplex virus genome contains both *cis*- and *trans*-acting elements which are important in viral DNA replication (Wu et al., 1988). Three *cis*-acting replication origins are thought to exist, consisting of two distinct but related DNA sequences, *ori_L* of which there is one copy in the viral genome and *ori_S* of which there are two copies (Spaete & Frenkel, 1982, Stow, 1982, Stow & McMonagle, 1983, Weller et al., 1983). Studies have shown that plasmid DNAs containing either *ori_L* or *ori_S* are replicated when they are introduced into HSV-infected cells (Spaete & Frenkel, 1982, Stow, 1982, Stow & McMonagle, 1983, Weller et al., 1983), suggesting that *ori_L* and *ori_S* are sites at which viral DNA synthesis is initiated (Wu et al., 1988). Challberg (1986) showed that five cloned restriction fragments of HSV-1 DNA together can supply all of the *trans*-acting functions needed for the replication of plasmids containing *ori_L* or *ori_S* when co-transfected into Vero cells (Challberg, 1986). Using this approach in conjunction with data from large scale sequence analysis of the HSV-1 genome Wu et al. (1988) identified seven HSV genes which are necessary for transient replication of plasmids containing either *ori_L* or *ori_S*. As shown previously, two of these genes encode the viral DNA polymerase (UL30) and single-stranded DNA-binding protein (UL29). Wu et al. (1988) propose that the seven genes essential for plasmid replication comprise a set of genes whose products are directly involved in viral DNA synthesis.

It has been suggested that replication is a two-stage process. Initial theta replication is followed by rolling circle replication to generate, head to tail concatemers of double stranded viral DNA (Boehmer & Lehman, 1997). After replication viral DNA is incorporated into preformed capsids (Stow, 2001).

Capsids containing DNA leave the nucleus by a budding event at the inner nuclear membrane, a process involving UL34 and UL31. This results in the formation of enveloped virions in the perinuclear space. The primary envelope fuses with the outer part of the nuclear membrane releasing the nucleocapsids into the cytoplasm. The final stages of envelopment, including acquisition of tegument and envelope glycoproteins, occurs by budding into Golgi derived vesicles. Mature virions are released following fusion of the vesicle membrane with the membrane compartment of the cell (Mettenleiter, 2004).

Another model proposes multiple routes of egress for HSV-1, including budding of the capsids at the inner nuclear membrane into the perinuclear space where the tegument and a thick viral envelope are acquired. Virions travel via intraluminal transportation into the Golgi cisternae, where one or more of the virions are packaged into transport vacuoles. Alternatively, capsids may gain direct access to the cytoplasm via impaired nuclear pores. Cytoplasmic capsids may bud at the outer nuclear membrane, at membranes of the endoplasmic reticulum (ER), or at Golgi cisternae (Leuzinger et al., 2005).

1.5. Latent infection

A specific feature of all herpesviruses is their ability to establish life-long latency within their hosts (Efstathiou & Preston, 2005). Latency occurs due to a failure of the virus to initiate productive lytic infection as all the lytic genes are switched off (Preston, 2000). During HSV-1 infection, primary replication at oral mucosa results in the virus accessing sensory nerve terminals. The virions are then transported to neuronal cell bodies by retrograde axonal transport to trigeminal ganglia. The genome is maintained as a nucleosomal circular episome during latency (Efstathiou & Preston, 2005, Preston, 2000).

Latency is established when the viral genome is delivered to the nucleus but IE gene expression is not activated. IE gene activation fails if the three proteins (VP16, HCF, and Oct-1) involved in stimulating transcription do not interact

(Efstathiou & Preston, 2005). Kristie et al. (1999) attributed the failure of IE gene expression to occur because VP16 does not reach the neuronal nucleus in sufficient amounts to mediate IE gene expression. Other work suggests that HCF sequesters VP16 at the cytoplasm of sensory neurons thus restricting IE transcription (Kristie et al., 1999). It has also been proposed that a number of proteins related to Oct-1 fail to complex with VP16 thus acting as repressors of IE gene expression (Efstathiou & Preston, 2005).

During latency the expression of all IE genes is known to be switched off (Preston, 2000). However, this is not the only defining feature of latency as a set of viral transcripts known as the latency associated transcripts (LATs) accumulate (Margolis et al., 1992, Preston, 2000). Two major LAT products are produced from a 8.3 Kb polyadenylated transcript, a 2 Kb intron which is spliced and a 1.5 Kb product (Farrell et al., 1991, Margolis et al., 1992). These are located to the neuronal nucleus, and are transcribed anti-sense to and partially complementary to the ICP0 coding sequences (Preston, 2000). In 1988 Javier et al. demonstrated that a virus that was unable to express LAT could still establish latency in mice and was also able to be reactivated (Javier et al., 1988). This was confirmed by Steiner et al. (1989) who used a HSV-1 LAT deletion virus to infect mice. They showed that in explanted trigeminal ganglia, that LATs were not required for the maintenance of latency (Steiner et al., 1989). More recent studies have created a mouse transgenic for the LAT 5' exon and 2 Kb intron. When these mice were infected with HSV-1, no difference in lytic replication or in the establishment and maintenance of latency was observed when compared to non-transgenic mice. This suggests that LATs have no effect on these functions when supplied *in trans* (Gussow et al., 2006).

A number of studies have suggested that the LATs are effective at blocking virus induced apoptosis both *in vitro* and in the trigeminal ganglia of acutely infected rabbits (Inman et al., 2001, Perng et al., 2000). Ahmed et al. (2002) propose that the region of the LAT that includes the 2 Kb intron exhibits an antiapoptotic function. In cells transfected with a construct expressing the 2 Kb LAT as well as several LAT deletion constructs it was observed that the 5' region of the 2 Kb LAT intron and the exon 1 region of the LAT were vital for protection from apoptosis (Ahmed et al., 2002). It is possible that the proposed ability of the LATs to prevent HSV-1 induced apoptosis may be important in preventing the virus from causing

extensive neuronal damage and subsequent neuronal disorders (Perng et al., 2000).

HSV-1 latency is associated with chromatin modification and remodelling as the latent genomes are known to persist as circular episomes associated with histones (Deshmane & Fraser, 1989). Further work using cultured sensory neurones showed that the ICP0 promoter was activated by the histone deacetylase inhibitor trichostatin A (TSA), indicating that the latent genomes respond to changes in the acetylation state of histones (Arthur et al., 2001).

Studies have shown that during latency, the lytic regions of the virus exist in a hypoacetylated (transcriptionally non-permissive) state, while the LAT promoter and 5' exon/enhancer remain hyperacetylated (transcriptionally permissive) (Kubat et al., 2004). Amelio et al. (2006a) used latently infected dorsal root ganglia to assess relative levels of LAT and histone H3 acetylation of the LAT locus and ICP0 promoter at early time post-explant. The increase in levels of acetylation at the ICP0 promoter after deacetylation of the LAT enhancer suggested that chromatin remodelling at both the LAT locus and the ICP0 promoter may be directly linked during reactivation. Therefore the LAT could function to recruit a novel histone-modifying complex, which establishes and maintains active expression of the LAT during latency (Amelio et al., 2006a). Amelio et al. (2006b) identified a 1.5 kb region containing a CTCF (CCCTC-binding factor) motif in the LAT region. This motif was found to exhibit enhancer blocking and silencing activities by binding to motifs on the latent genome and insulating the LAT enhancer, thus suggesting that the CTCF motif may facilitate the formation of distinct chromatin boundaries during HSV-1 latency (Amelio et al., 2006b).

1.5.1. Reactivation from latency

Reactivation of a latent virus can be caused by a number of factors including immune suppression, emotional and physical stress and exposure to UV light (Wysocka & Herr, 2003). Given that during latency the viral genome is associated with non-acetylated histones, it would appear that the virus must act to overcome this repressive effect exerted by histones to overcome latency. Thus reactivation would employ a mechanism of IE gene activation that can be initiated in the absence of VP16 (Efstathiou & Preston, 2005).

In vivo reactivation studies have previously shown various stressful stimuli can lead to reactivation from latency (Wang et al., 2005). This induces changes in the physiological state of sensory neurons that contain the latent viral genome (Sawtell & Thompson, 2004). Latent HSV-1 in mouse ganglia was shown to be reactivated upon infection of dissociated ganglia with adenoviruses expressing VP16, ICP0 or ICP4 (Halford et al., 2001). These findings indicate that in the absence of ICP0, adenovirus directed expression of VP16 or ICP4 initiates reactivation in neurone based systems, possibly by exerting a general effect on the genome or by stimulating ICP0 production from the quiescent or latent genome. However Halford et al. (2001) showed that reactivation by ICP0-null mutants is considerably less efficient than that observed with wild type viruses upon explantation of ganglia suggesting reactivation can occur in the absence of ICP0.

Recent studies using wild type, revertant, ICP0-null or ICP0-mutant viruses have demonstrated that upon hyperthermic stress in mouse models, ICP0-defective viruses did not produce infectious virus, however, they did express 'lytic-phase viral proteins' at levels that were as easily detectable as in reactivating neurones infected with wild-type and revertant viruses. This suggested that ICP0 is not required for the initiation of reactivation, but instead is needed to activate productive infection once reactivation has been initiated (Thompson & Sawtell, 2006).

1.5.2. Reactivation of quiescent genomes

Work by Harris and Preston (1991), Preston and Nicholl (1997) and Samaniego et al. (1998) showed that after infection with mutants defective for IE proteins the virus establishes a quiescent state, during which promoters which would be active in the context of the cellular genome become repressed when placed in the context of the virus (Preston, 2000, Preston & Nicholl, 1997).

ICP0 was initially believed to be the HSV-1 protein involved in reactivation of quiescent viruses following studies carried out by Russell et al. (1987) whereby quiescent virus was observed to resume replication following super-infection of cultures with HSV-1, HSV-2 or HCMV (Russell et al., 1987). However it was observed that the mutant virus *d/1403* (deficient for ICP0) was unable to reactivate

HSV-2, thus suggesting a requirement for ICP0 in the reactivation of quiescent HSV (Preston, 2007). This was further confirmed when it was found that the mutant virus *d/1403* could be retained in a quiescent state in human fibroblasts, and super-infection of these cultures with wild-type HSV-1 resulted in reactivation (Stow & Stow, 1989). Therefore, it is possible that ICP0 can influence the balance between lytic and latent infection in cultured cells.

A further observation by Preston (2007) suggested quiescent HSV-1 genomes are reactivated by super-infection with the ICP0-null virus (*d/1403*) under appropriate conditions. Human fibroblasts were infected with *in1374* (HSV-1 recombinant mutated for VP16, ICP0 and ICP4) to establish quiescent infection. When super-infected with *d/1403* at various MOIs and stained with X-gal most plaques observed were β -gal positive at the lowest MOI. To eliminate effects of DNA replication, quiescent infected cells were super-infected with *in1330* (HSV-1 recombinant deleted for ICP0 and a temperature sensitive mutation in ICP4) or *d/1403* and maintained at 32°C or 38.5°C. β -gal expression was activated at 32°C, but only *d/1403* was active at 38.5°C therefore *d/1403* is dependent on functional ICP4 but not on DNA replication. It is possible that genomes retain different levels of silence and upon super-infection some are more susceptible to *trans* acting factors from *d/1403*, thus reactivation of some quiescent genomes is observed, and therefore highlights similarities between quiescence in fibroblasts and latency in neurons (Preston, 2007).

1.6. HCMV Biology

1.6.1. The HCMV genome

The HCMV genome is the largest within the herpesvirus family, consisting of a linear double stranded DNA molecule of 235646 bp with a G+C content of approximately 56%. It is organised into two segments, designated U_L and U_S , which are in turn flanked on one side by terminal repeated sequences (TR_L and TR_S) and on the other by internal repeats (IR_L and IR_S) yielding the overall gene configuration of $TR_L-U_L-IR_L-IR_S-U_S-TR_S$ (Chee et al., 1990, Mocarski, 2001).

The HCMV strain AD169 genome sequence, published in 1990, predicted 208 ORFs, 14 of which are duplicated within the TR_L/IR_L repeats (Chee et al., 1990).

However in 1997 Dargan et al. (1997) identified a novel 929 bp sequence in HCMV strain AD169 representing the upstream portion of the gene UL42 and an adjacent downstream portion of gene UL43. As the novel 929 bp sequence was observed to be present in most isolates of AD169, the revised sequence of AD169 was proposed to have a total genome length of 230283 bp (Dargan et al., 1997). AD169 is extensively used as a laboratory strain as, not only is the sequence available but it also replicates more efficiently than clinical isolates (Cha et al., 1996). However, it differs from clinical isolates in terms of genomic structure and biology (Prichard et al., 2001). For example AD169 lacks 19 ORFs that are present in clinical isolates and it fails to replicate in endothelial cells, which are permissive for replication of some clinical isolates (Murphy et al., 2003b). Comparisons of AD169 with data from other strains showed it to be a multiple mutant, containing frame shifts in three genes RL5A, RL13, and UL131A (Davison et al., 2003b).

Early work by Chee et al. (1990) established that the HCMV genome sequence (AD169) stood at 229354 bp. As laboratory strains have undergone deletions and re-arrangements during adaptation to growth in cell culture and since HCMV has not yet been sequenced directly from genetic material a full picture of the gene content of wild type HCMV is not available (Davison et al., 2003a). In order to improve interpretation, the HCMV sequence was compared with a close genetic relative, as most of the essential protein coding regions are conserved during evolution. The Chimpanzee CMV (ChCMV) genome was sequenced (the closest known relative of HCMV) and used to reassess the gene layout of HCMV. Of the 189 unique genes originally proposed in AD169 by Chee et al. (1990), 108 remained unchanged as a result of subsequent reinterpretations, 46 genes were discounted as being unlikely to encode proteins and five new AD169 genes (UL15A, UL21A, UL128, UL131A and US34A) were identified. Further comparison of the ChCMV genome with the HCMV Toledo strain confirmed that the AD169 sequence was correct. However, the additional region at the right end of U_L in Toledo (containing 19 genes absent from AD169) was found not to be co-linear with the corresponding part of the ChCMV genome (Davison et al., 2003a). Thus derivation of the ChCMV sequence showed both HCMV AD169 and ChCMV genomes to be co-linear, each possessing a few genes lacking in the other. The 40 core genes inherited from the common ancestor of the *Alpha*-, *Beta*- and *Gammaherpesvirinae* were found to be located in the central region, with most

non-core genes located nearer the genome termini. Genes nearer the genome termini generally exhibited higher levels of sequence divergence reminiscent of the two sub-species of HHV-6. Davison et al. (2003) concluded that ChCMV encodes 165 genes each present as single copies, while AD169 contains 145 genes, with four of these genes present in two copies in the R_L elements. Therefore, assuming that the wild type HCMV genome approximates to the AD169 genome plus a rearrangement of the additional genes at the right end of U_L in Toledo a complement of 164-167 genes was inferred (Davison et al., 2003a).

The coding potential of the HCMV AD169 genome was also re-evaluated by Murphy et al. in 2003 using a Bio-Gene Finder (BDGF) algorithm. The gene-finder algorithm was used to assess the potential of an ORF to encode a protein based on matches to a database of amino acid patterns derived from a large collection of proteins. The algorithm was used to score HCMV ORFs with the potential to encode polypeptides greater than 50 amino acids in length. The genomes of chimpanzee, rhesus and murine cytomegalovirus were also analysed using BDGF to search for orthologues of predicted HCMV ORFs as a further test for functionality. The analysis by Murphy et al. (2003) discounted 37 ORFs predicted by Chee et al. (1990), and further predicted 12 novel protein coding ORFs, predicting that the HCMV genome contains approximately 192 unique ORFs with the potential to encode a protein (Murphy et al., 2003a).

The genetic content of the HCMV genome was further investigated by sequencing the 235645 bp genome of a low passage strain Merlin. Comparative analyses with the genome of AD169 indicated that the strain Merlin accurately reflected the wild type complement of 165 genes (Dolan et al., 2004). This study by Dolan et al. (2004) however, discounted the 12 novel protein coding ORFs predicted by Murphy et al. (2003) as only modest levels of discrimination were thought to be achieved using the BDGF, even for recognised genes. Therefore, without additional data it was considered premature to include these ORFs in the gene layout.

The HCMV genome is densely packed with ORFs, but contains very few polyadenylation signals. Thus, many spliced and non-spliced HCMV genes share polyadenylation signals, leading to the generation of 3' co-terminal groups within specific regions of HCMV DNA, (Smuda et al., 1997). Further analysis revealed

ORFs such as UL146/UL147A (Lurain et al., 2006), UL122/UL123 and UL37 overlap (Adair et al., 2003, Awasthi et al., 2004).

1.6.2. HCMV capsid

Three types of HCMV capsids are produced: A capsids which are the products of abortive DNA packaging and lack the viral genome, B capsids which are precursors of fully mature particles, containing scaffolding proteins but again lack the DNA genome, and C capsids which are mature capsids containing the full length viral genome (Gibson et al., 1996).

The study of HCMV capsids has focused on the B capsid, which is the pre-formed capsid prior to DNA encapsidation, tegument formation and envelopment. It consists of proteins found in the capsid within the intact virus particle including an internal assembly protein (Chen et al., 1999). The HCMV capsid consists of four structural components: the major capsid protein (MCP), the minor capsid protein (mcP), the minor capsid binding protein (mCBP) and the small capsid proteins (SCP) (Borst et al., 2001). HCMV SCP is considered to be the homologue of HSV-1 VP26 and, similar to its HSV-1 counterpart, it is found located the tips of hexameric capsomers (Borst et al., 2001, Gibson et al., 1996).

HCMV B capsids are larger in diameter than HSV-1 capsids (130 nm and 125 nm respectively), allowing the HCMV B capsid to accommodate a DNA molecule that is 60% larger than the HSV-1 genome (Butcher et al., 1998). These differences in capsid size can be attributed to spacing and relative tilt of HCMV triplex proteins and the size of the scaffold core (Butcher et al., 1998). Electron-cryomicroscopy was used to image full and empty HSV-1 and HCMV capsids. Measurements obtained from images showed that the HCMV genome is packaged at a higher density, than the HSV-1 genome, with an inter-layer spacing of 23 Å compared to 26 Å of HSV-1 (Bhella et al., 2000).

1.7. HCMV pathogenesis

1.7.1. HCMV prevalence and disease

HCMV is thought to be acquired at an early age. In developed countries seroprevalence is thought to be around 30-70%. However, in developing countries, the prevalence exceeds 90% in certain socioeconomic groups and homosexual men (Gandhi & Khanna, 2004). The virus is transmitted via a number of routes that include sexual contact, saliva, placental transfer, breast-feeding, blood transfusion, solid organ transfer or haemopoietic stem cell transfer (Pass, 2001).

Infection with HCMV during pregnancy often results in severe consequences. Statistics show primary infection during gestation poses a 30-40% risk of clinical disease (Fisher et al., 2000). The risk to the infant is greatest if infection occurs during the first trimester of pregnancy (Gandhi & Khanna, 2004). The infant can be infected via viral transmission through the placenta, during delivery from cervical secretions, blood or from the mother by breast milk (Fisher et al., 2000).

Approximately 15% of women with primary HCMV infection during the early stages of pregnancy abort spontaneously (Griffiths & Baboonian, 1984). It is the placenta, not the foetus that shows evidence of infection, suggesting the placenta is infected before the embryo or the foetus (Mostoufi-zadeh et al., 1984). Recent studies by Fisher et al. (2000) used culture models of trophoblast populations from the maternal-foetal interface to observe HCMV infection of human placental cells *in vitro*. They observed the placenta to be an ineffective barrier to HCMV transmission, with cytotrophoblasts becoming infected in several locations. These locations suggest specific routes by which the virus reaches the foetus *in utero*. Currently no vaccine is available for HCMV infected infants, however, some studies have shown that administration of intravenous human immunoglobulin to a pregnant mother with a primary HCMV infection, could potentially protect the foetus (Malm & Engman, 2007).

Ten to seventeen percent of infants with asymptomatic infection develop hearing defects or neurodevelopmental sequelae. Furthermore 5-10% of congenitally infected neonates present with irreversible CNS involvement in the form of microcephaly, encephalitis, seizures, upper motor neuron disorders or

psychomotor retardation (Boppana et al., 1992). Infected newborn babies can also show other clinical features such as jaundice, petechiae and hepatitis, all of which tend to resolve without treatment. However long-term studies have indicated that 80% of affected infants display serious life long neurological abnormalities with severe life threatening organ dysfunction and death in 10-20% of patients (Gandhi & Khanna, 2004).

As HCMV can establish latent infections it is thought the foetus can in some cases become infected after reactivation of maternal infection. In this case, less severe clinical disease is observed in the offspring (Gandhi & Khanna, 2004).

Initial infection with HCMV results in a primary immune response, with subsequent establishment of long-term immunity preventing viral replication after reactivation from latency. However long-term immunosuppression can lead to uncontrolled replication of the virus in the host and can result in serious disease (Gandhi & Khanna, 2004). In cases of solid organ transfer such as kidney transplantation, HCMV is the single most frequent infectious complication observed (Sagedal et al., 2005), with the risk of infection being heightened because the patient is immunosuppressed. Those most at risk are serologically negative patients who receive organs from serologically positive donors. Limited organ availability means matching seronegative donors and recipients is not always possible (Gandhi & Khanna, 2004). HCMV associated disease in transplant/immunosuppressed patients manifests itself in the transplanted organ (i.e. hepatitis arises in liver transplant patients, pancreatitis arises in pancreas transplant patients). However, disease can spread rapidly leading to a host of other symptoms including pneumonitis, enteritis, retinitis and CNS involvement (Sagedal et al., 2005).

One method of preventing HCMV disease is pre-emptive anti-HCMV therapy. An antiviral agent is introduced at the first signs of HCMV antigenaemia (detection of HCMV pp65 antigen in leukocytes), positive HCMV PCR, or positive HCMV viraemia in the blood. When compared with prophylaxis this method means fewer patients are exposed to antiviral agents, resulting in less drug resistance (Sagedal et al., 2005).

1.7.2. HCMV latency and reactivation

As mentioned previously latency and reactivation are the defining characteristics of herpesviruses and HCMV is no exception. It is able to effectively establish lifelong persistence within the host following initial usually asymptomatic infection, by persisting in specific sites in the host. However the viral genome retains the ability to reactivate in response to specific stimuli (Sinclair & Sissons, 2006).

The presence of HCMV DNA in the peripheral blood leukocytes of healthy, HCMV seropositive individuals was only discovered by the technological advances of PCR (Stanier et al., 1992, Taylor-Wiedeman et al., 1991). It was established that peripheral blood monocytes are the major site of carriage of HCMV DNA in healthy individuals by using sorted peripheral blood monocytes (Larsson et al., 1998, Smith et al., 2004, Taylor-Wiedeman et al., 1991). Other studies have shown that HCMV DNA could be detected in CD34⁺ bone marrow progenitors (Mendelson et al., 1996). Although CD34⁺ cells give rise to B cells, T cells and polymorphonuclear leukocytes (PMNLs) as well as monocytes no evidence of HCMV has been detected in the PMNL, T-cell or B-cell fractions of peripheral blood, in normal healthy carriers (Taylor-Wiedeman et al., 1991). How the HCMV genome is maintained selectively in only particular sub-sets of cells arising from common CD34⁺ stem cells carrying viral DNA is as yet not understood (Sinclair & Sissons, 2006). Various studies have determined that in monocytic cells and their precursors, it appears that HCMV is carried in a true latent state, with little or no accompanying viral IE gene expression (Mendelson et al., 1996, Taylor-Wiedeman et al., 1994).

Various latent model systems have been set up to try to identify HCMV latent viral transcripts. Early work by Kondo et al. (1996) used infected granulocyte-macrophage precursors (GMPs) derived from foetal liver cells to identify HCMV transcripts expressed in the absence of virus production, termed cytomegalovirus latency-specific transcripts (CLTs). The CLTs were found to include novel spliced and unspliced RNA transcripts that mapped to both strands of the HCMV major IE region (Kondo et al., 1996). Some of these transcripts and antibodies to CLT ORFs were detected in healthy seropositive individuals, but many transcripts were also detected in infected cells in culture (Kondo et al., 1996), thus the true role of these transcripts remains to be established. Goodrum et al. (2002) identified multiple viral RNAs associated with the carriage of the virus in the absence of

production of infectious virions; many, if not all which were also detected in productive infection. However, it was not determined whether any of these transcripts were detected in mononuclear cells of normal, healthy carriers (Goodrum et al., 2002). Studies based on transcripts identified by Goodrum et al. (2002) identified viral RNA from monocytes of healthy seropositive carriers (Bego et al., 2005). These RNA transcripts were observed to be antisense to the UL81-82 region of the viral genome. As these RNA transcripts were partially antisense to the viral UL82 gene, encoding pp71 a transcriptional transactivator of the MIEP, it has been suggested this transcript (or its protein product) maybe involved in restricting IE gene expression in order to maintain latency (Bego et al., 2005).

It is generally considered that myeloid cells are an important site of true latency *in vivo*. However, the possibility remains that in healthy carriers other sites of latency may occur, this is mainly due to a number of cell types becoming rapidly infected upon clinical reactivation (Sinclair & Sissons, 2006). It was suggested that endothelial cells (ECs) may be a reservoir of latent virus as CD34⁺ bone marrow derived cells may give rise to ECs (Jarvis & Nelson, 2002, Quirici et al., 2001). This however, was disputed by Reeves et al. (2005), as latent HCMV genomes were not detected in ECs of healthy seropositive individuals, despite HCMV DNA being readily detected in monocytes at the same time. It is therefore possible that HCMV may persist in certain cells types, at a low level of productive infection (Sinclair & Sissons, 2006).

After establishing latency within its host, sporadic reactivation events can occur, that are generally controlled by cell-mediated immunosurveillance. However when reactivation occurs in immunocompromised or immunosuppressed individuals replication of the virus becomes uncontrolled leading to morbidity and mortality (Sinclair & Sissons, 2006). As with the other herpesviruses (EBV and HSV-1), reactivation from latency is dependent upon expression of viral IE genes which determine commitment of the virus to lytic infection (Sinclair & Sissons, 2006).

Myeloid cells appear to be classical sites of viral latency, in peripheral blood of healthy individuals carrying viral DNA no appreciable levels of infectious virus or lytic gene expression is observed (Mendelson et al., 1996, Taylor-Wiedeman et al., 1994). It is believed that the undifferentiated nature of these cells is important in maintaining latency of HCMV genomes (Reeves et al., 2005a). However, once

myeloid cells differentiate to macrophages and dendritic cells (DC) a fundamental change in their ability to support IE gene expression occurs (Taylor-Wiedeman et al., 1994). Differentiation of these myeloid cells, generated from healthy seropositive carriers, reactivated HCMV and suggested that latency and reactivation in these cells maybe controlled by chromatin remodelling of the MIEP to regulate lytic gene expression (Reeves et al., 2005a). Chromatin-mediated regulation of transcription is achieved by a number of post-translational modifications of histone N-terminal tails (Berger, 2002). Histone acetylation causes chromatin to adopt an open structure allowing access of DNA-binding factors to the DNA template resulting in an increase in gene expression. The recruitment of various silencing proteins e.g. heterochromatin protein 1 (HP1) or the deacetylation or methylation of histones causes a closed, transcriptionally silenced chromatin state preventing viral gene expression (Kouzarides, 2002).

Reeves et al. (2005b) showed that in CD34⁺ cells, the viral MIEP is associated with the HP-1 protein and not acetylated histones, consistent with CD34⁺ cells being non-permissive for HCMV IE gene expression. In contrast, differentiation of infected CD34⁺ cells to mature CD34⁺-derived DCs, ultimately resulted in reactivation of infectious virus. This was observed to be preceded by chromatin remodelling of the MIEP such that it was associated with acetylated histones. Thus repression of the HCMV lytic gene expression after infection of CD34⁺ cells correlates with the recruitment of repressive chromatin markers (HP1) to the MIEP promoter. The exact mechanism, however, remains unclear (Reeves et al., 2005b).

Murphy et al. (2002) showed using transformed human cell lines, teratocarcinoma cells (NT2D1) and the myelomonocytic (THP1) cells, that when undifferentiated (non-permissive for HCMV IE gene expression), repression of the MIEP in these cells was associated with a closed chromatin conformation. However, when differentiation of these cells was induced with retinoic acid or phorbol esters to allow them to become permissive for HCMV IE gene expression acetylated histones were associated with the MIEP, consistent with transcriptional activation at the MIEP. Recent studies have shown that cellular transcription factor, Ets-2 repressor factor, (ERF) physically interacts with HDAC1 to mediate the repression of the MIEP in undifferentiated non-permissive cells. This suggests that the changes in chromatin structure around the MIEP, observed by Murphy et al.

(2002) upon differentiation of cells from a non-permissive to permissive phenotype (Murphy et al., 2002) may be due to differential recruitment of chromatin remodellers such as HDAC1 by factors such as ERF (Wright et al., 2005).

1.8. HCMV Lytic infection

1.8.1. Attachment and penetration

The first event in HCMV infection is attachment to and penetration of the host cell membrane. During this process, glycoproteins on the viral envelope play an important role in adsorption and penetration of the virus into the cell (Cirone et al., 1994, Yurochko et al., 1997). The initial association of the virion with the cell membrane is followed by binding of viral glycoproteins to specific receptors (Navarro et al., 1993).

Three major glycoprotein complexes of the virus have been identified, the gCI, gCII, and gCIII. The gCI complex, which is composed of homodimeric molecules of gB, is a highly conserved herpesvirus glycoprotein, linked by disulphide bonds. This homodimeric complex can promote virion penetration into cells and promote transmission of infection from cell-to-cell (Bold et al., 1996, Compton et al., 1992, Navarro et al., 1993). The gCII complex is composed of glycoproteins gM and gN (Li et al., 1997), linked by non-covalent and disulphide bonds (Mach et al., 2000). The physical interaction between the two glycoproteins is presumed to be necessary for the correct post-translational modification and transport of the complex through the exocytic pathway (Mach et al., 2000). Deletion of the carboxy-terminal of gN resulted in a replication incompetent virus. However, when compared to wild-type virus it was found that complex formation of mutant gN with gM and transport of the complex to the viral assembly compartment seemed to be unaltered (Mach et al., 2007). Mach et al. (2007) suggest that gN may be involved in the secondary envelopment of the HCMV virion as disruption of the carboxy-terminus of gN resulted in a decrease in secondary envelopment of HCMV capsids.

The gCIII complex was initially thought to consist of two glycoproteins with average molecular masses of 145 and 86 kDa. These were thought to be differentially modified forms of gH (Bogner et al., 1992, Gretch et al., 1988). It was

later established that the gH homologue of HSV-1 required a second protein, gL, for intracellular transportation, and correct folding of gH. Thus, the gL homologue of HCMV was identified (Spaete et al., 1993). Spaete et al. (1993) showed gH and gL of HCMV complexed by forming disulphide bonds, suggesting the gCIII complex consisted of an oligomeric form of gH and gL. Later work identified a third member of this complex, gO (Huber & Compton, 1997, Huber & Compton, 1998, Li et al., 1997). The tripartite gH-gL-gO complex assembled in two steps with gH and gL associating by disulphide bonding to form the gH-gL complex, followed by subsequent association of gO. This forms a precursor pgCIII complex that is processed to the mature gCIII complex in a post-endoplasmic reticulum compartment (Huber & Compton, 1999). In addition a gO deletion mutant virus was impaired for viral growth and cell-to-cell spread, suggesting a role for gO in the fusion and entry process (Hobom et al., 2000).

Following interaction with gB and heparan sulphate binding, the gB homodimer is believed to interact with the epidermal growth factor receptor (EGFR) inducing an intracellular signalling cascade (Wang et al., 2003). Activation of EGFR initiates receptor homodimerization/hetero-oligomerization, leading to autophosphorylation at specific tyrosine residues, receptor internalization and the induction of associated intracellular signalling (Schlessinger, 2000, Ullrich & Schlessinger, 1990). Following release of the capsid into the cytoplasm some of the tegument components are lost. Transport of the capsid is thought to occur when viral tegument proteins interact with the host machinery involved in cellular transport systems (Sodeik, 2000). Studies have demonstrated a close association of the HCMV capsid with the microtubule network in fibroblasts infected with HCMV. (Towne strain). Disruption of the microtubule network with the microtubule depolymerising drugs nocodazole and colchicine resulted in capsids being unable to move to close proximity to the nucleus. This suggested that HCMV capsids associate with the microtubule network to facilitate their own movement to the nucleus prior to the onset of IE gene expression and that this association is required to start efficient gene expression (Ogawa-Goto et al., 2003).

1.8.2. IE gene expression

The expression of HCMV genes is temporally regulated. The first genes to be expressed are the IE genes. This is followed by expression of the E and L genes

(Chambers et al., 1999). At least 1 hr post-infection, four genomic regions, UL36-38, TRS1-IRS1, MIE and US3 begin producing IE transcripts (Mocarski, 2001). The majority of gene expression immediately after viral entry arises from a single locus, known as the major immediate early (MIE) locus, comprising the IE1/IE2 (alternatively spliced UL122 and UL123 genes). This generates proteins that are synthesised by alternative mRNA splicing, the two most important products of which are IE1/IE72 and IE2/IE86 (Mocarski, 2001). Both IE1 and IE2 share 85 amino-terminal amino acids that correspond to MIE exons 2 and 3 but have distinct carboxy-terminal parts encoded by exons 4 and 5 (IE1 and IE2 respectively) (Marchini et al., 2001). Regulation of HCMV gene expression by the IE proteins is presented in figure 1.4.

1.8.2.1. IE1

IE1 is able to augment transcription from a number of viral and cellular promoters, including the HCMV MIEP, various HCMV E promoters and the SV40 early promoter (Castillo & Kowalik, 2002, Mocarski, 2001). Studies using IE1-null viruses have shown that at high input multiplicities the viruses are able to replicate efficiently. However, at low MOI the absence of IE1 causes a block in HCMV E gene expression (Gawn & Greaves, 2002, Greaves & Mocarski, 1998). This defect of IE1 mutant viruses at low MOI is attributed to a failure/delay in the accumulation of E gene products. Examination of levels of IE2 protein in cells infected with these viruses showed it was comparable to levels in wild-type virus but the intranuclear localisation pattern was altered (Ahn & Hayward, 2000, Greaves & Mocarski, 1998).

The IE1 gene product behaves similarly to ICP0 by associating with and disrupting ND10 structures. IE1 accumulates at ND10 domains, disassembling their structure and allowing IE2 to gather juxtaposed to ND10 in a region where HCMV can initiate transcription (Ishov et al., 2002). Subsequently PML, Sp100, SUMO and IE1 are all displaced from ND10s into the cytoplasm (Ahn et al., 1998, Ahn & Hayward, 1997, Koriath et al., 1996, Mocarski, 2001). Ahn et al. (1998) proposed that a direct interaction of IE1 and the N-terminal RING finger domain of PML leads to the displacement of both PML and IE1 from ND10 domains into the nucleus.

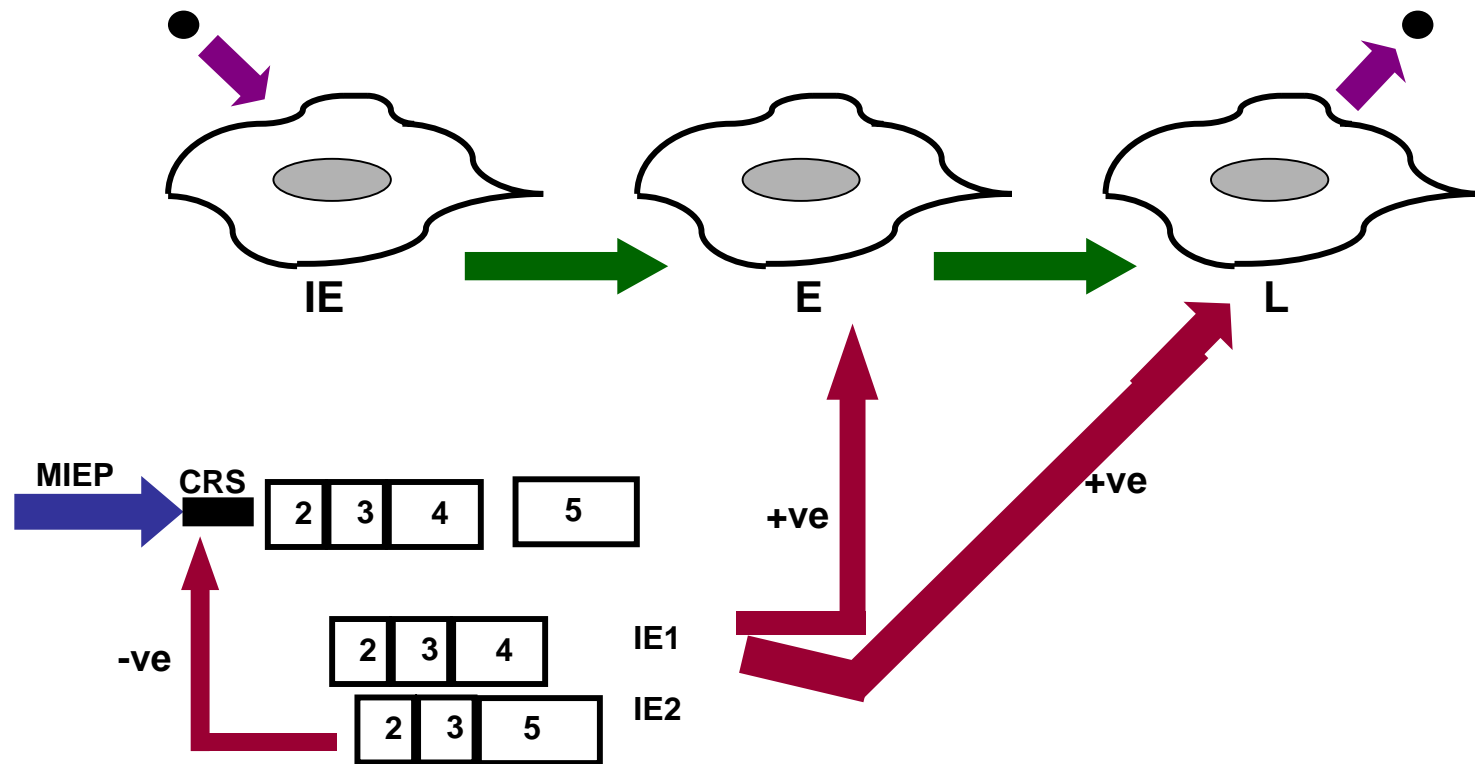


Figure 1.4 Regulation of HCMV gene expression during productive infection

Productive infection with HCMV results in a regulated cascade of viral gene expression designated IE, E and L. Expression of the major IE gene products, IE1 and IE2 is a result of differential splicing of the same primary transcript. IE1 is comprised of exons 2, 3, and 4 and IE2 of exons 2, 3, and 5. IE1 and IE2 act synergistically to activate viral E and L gene expression. IE2 can negatively auto-regulate its own promoter by binding to the *cis*-repression signal (CRS).
 Figure adapted from Sinclair and Sissons (2006).

IE1 is also post-translationally modified by covalent conjugation of SUMO-1 (Spengler et al., 2002). Mutant viruses deficient for SUMOylation of IE1 have shown that the SUMO modification of IE1 is necessary for efficient HCMV replication (Nevels et al., 2004a). Mutational analysis revealed the acidic C-terminal region of IE1 is dispensable, while the central hydrophobic region is required for binding to and deSUMOylation of PML. Mutant forms of IE1 that failed to bind to or deSUMOylate PML were also unable to target to or disrupt ND10s. This indicated that the disruption of ND10 domains by IE1 was linked to the deSUMOylation of PML (Lee et al., 2004)

An additional activity of IE1 is its ability to bind to cellular chromatin, which is dependent upon sequences within the acidic C-terminus (Wilkinson et al., 1998). Recently it has been proposed that IE1 can promote viral transcription by antagonising histone deacetylation (Nevels et al., 2004b). Nevels et al. (2004b) showed that IE1 and HDAC3 could be co-immunoprecipitated from extracts of transfected and virus infected cells, suggesting IE1 may interact with HDAC3 to inhibit its activity.

1.8.2.2. IE2

IE2 is able to control the switch between IE, E, and L gene expression during productive infection (Mocarski, 2001). The IE2 gene product regulates homologous/heterologous viral and cellular promoters in the absence of IE1, or more efficiently in the presence of IE1 (Kim et al., 1999, Mocarski, 2001). Like IE1, IE2 localises to or adjacent to ND10 domains however, it is unable to disrupt them. When acting in conjunction IE1 and IE2 cause efficient viral gene expression and DNA replication (Ahn & Hayward, 2000).

IE2 is a repressor of its own MIEP via direct DNA binding to the MIE *cis*-repression signal (CRS) near the 5' cap site in transient-co-transfection assays (Liu et al., 1991, Pizzorno & Hayward, 1990). Recent studies have shown that autorepression by IE2 at late times of infection correlates with changes in chromatin structure around the MIEP. IE2 can interact with HDAC1 and histone methyltransferases *in vitro* and *in vivo*, resulting in an increase in autorepression of the MIEP (Reeves et al., 2006).

IE2 (like IE1) is affected by SUMO-1; however, IE2 has both covalent conjugation and a direct protein-protein interaction with SUMO-1, SUMO-2, SUMO-3 and a SUMO-conjugating enzyme Ubc9 (Ahn et al., 2001). Two lysine residues were identified as the major alternative SUMO-1 attachment sites and it was established that the SUMOylation of IE2 is required for its transactivation function. The SUMO modification of IE2 is enhanced via an interaction with a protein inhibitor of STAT (PIAS1), which can act as an E3 ligase for IE2 (Lee et al., 2003).

Sommer et al. (1994) showed that IE2 interacts with a hypo-phosphorylated form of Rb (Sommer et al., 1994). They suggested this interaction takes place via two separate binding domains and IE2 can regulate gene expression through the formation of multimeric protein complexes (Hagemeier et al., 1994). Further studies showed that, not only does IE2 bind to Rb, but this complex also acts to relieve the IE2 repression of the MIEP (Choi et al., 1995).

1.8.2.3. Role of HCMV E and L genes

The classification of E and L genes is dependent on both their timing of expression and their sensitivity to inhibitors of viral DNA synthesis. Both E and L genes are thought to be activated by targeting the TATA box, initiator elements and upstream promoter elements located within 100-200 bp of transcription start sites by IE gene products (Mocarski, 2001). The timing of expression of these viral genes is modulated by transcriptional and post-transcriptional controls dictating the appearance of proteins and sensitivity of viral replication to the physiological control of the host cell. This influences events such as the activation of host cell protein degradation machinery and the accumulation of E and L gene products during infection (Mocarski, 2001). Most E and L genes have a polycistronic structure correlating with the few polyadenylation signals within the viral genome. Most of the 3' co-terminal families of transcripts are generated from a series of promoters each controlling a separate gene (Mocarski, 2001).

E genes have a promoter structure, consisting of an upstream region, spanning a 100-200 bp sequence containing a *cis*-acting regulatory element for transactivating viral and cellular promoters. Two E transcripts of 1.2 Kb and 2.7 Kb represent approximately 20%-40% of total viral transcription during early times of infection (Mocarski, 2001). E genes tend to code for non-structural proteins required for

DNA replication, packaging and maturation of virus particles (Chambers et al., 1999, Mocarski, 2001).

Investigations into L gene expression have been limited, thus little is known about these genes. Two types of transcripts known as the leaky late or true late genes are produced, the regulation of each being markedly different (Mocarski, 2001). The true late genes, for example, encoding pp28, have a very basic promoter structure in that they lack upstream *cis*-regulatory elements, thus true late gene expression is dependent on the replication of viral genomic DNA (Depto & Stenberg, 1992). The L genes are essentially expressed after the onset of viral DNA replication and their products are responsible for virion assembly and morphogenesis (Chambers et al., 1999).

1.8.3. HCMV DNA replication and packaging

HCMV contains a single lytic origin of replication, *ori*-Lyt, (Hamzeh et al., 1990) which is located near the centre of the U_L region upstream of the DNA binding protein ppUL57 ORF (Masse et al., 1992). The HCMV *ori*-Lyt is composed of a core that spans 1548 nucleotides, and contains two essential regions (I and II) (Anders et al., 1992, Masse et al., 1992). Both regions are a site of active transcription and are complex in nature, consisting of a pyrimidine-rich region, several transcription factor binding sites, and direct and inverted repeat sequences (Anders et al., 1992, Huang et al., 1996, Masse et al., 1992). In human fibroblasts *ori*-Lyt dependent DNA replication requires core replication machinery and the gene products of IE2, and UL36-38 (Reid et al., 2003, Sarisky & Hayward, 1996). However while Sarisky and Hayward (1996) perceived that UL84 was essential for *ori*-Lyt activity, Reid et al. (2003) found UL84 to be dispensable in their transient transfection assays. However, Reid et al. (2003) found UL84 inhibited both transactivation of E genes by IE2 and enhanced its activity as a negative autoregulator. This suggested that the balance between levels of IE2 and UL84 may have a significant effect on viral DNA replication (Reid et al., 2003). Recent studies however, have shown UL84 interacts with IE2 to activate the *ori*-Lyt promoter to initiate DNA replication, however, the precise mechanisms of this process remain unknown (Xu et al., 2004).

The majority of research regarding capsid assembly has been derived from studies of HSV-1 (see section 1.4.5). In the case of HCMV it is generally accepted that capsid assembly occurs in the nucleus of infected cells (Sanchez et al., 2000a). The virally encoded DNA polymerase produces large-head-to tail concatemers, which are cleaved into genomic-length pieces before being packaged into capsids. Genomes are packaged into capsids through a portal coded by UL104 that acts a dock for the terminase enzyme (Dittmer & Bogner, 2005, Nixon & McVoy, 2002). The driving force behind this process is the ATP-ase activity of the terminase enzyme, which pushes DNA into the capsid (Hwang & Bogner, 2002). Recently several putative functional domains in pUL89, such as the pUL89 zinc finger (pUL89-ZF), DNA cutting sites and portal binding sites, were identified as being involved in DNA cleavage and packaging (Champier et al., 2007).

1.8.4. HCMV capsid transport

The size of HCMV capsids prevents their transport into the cytoplasm through the NPC, therefore nuclear egress requires the penetration of nuclear membranes and the nuclear lamina. This occurs through an envelopment/de-envelopment process similar to that observed in HSV-1. Following release into the cytoplasm, the HCMV capsid acquires the majority of its tegument proteins (including UL25, UL32 and UL99 which are excluded from the nuclei during productive infection), which aggregate at the cytoplasmic surface of the membrane (Sanchez et al., 2000b). Of particular importance is UL32, which encodes the tegument protein pp150 that accumulates in a cytoplasmic inclusion adjacent to the nucleus at late times during infection. Use of a UL32 deletion mutant has shown that pp150 is critical for virion maturation in the cytoplasmic compartment and for virion egress at the final stages of envelopment (AuCoin et al., 2006). The capsids are enveloped at Golgi apparatus-derived cisternae by a wrapping process and released by fusion with the plasma membrane (Buser et al., 2007, Homman-Loudiyi et al., 2003). However given that several models of capsid assembly have been proposed for HSV-1 this might also be the case for HCMV.

1.9. The HCMV MIEP

The MIE regulatory region controls transcription of the IE1 and IE2 genes through both positive and negative *cis*-acting elements. The area upstream of the HCMV MIEP is divided into three regions: the modulator, the unique region and the enhancer. Deletion of the modulator region has no detectable effect on viral replication (Meier & Stinski, 1997). The unique region contains multiple protein binding sites however, deletion analysis of the unique region showed it has no effect on transcription from the MIEP (Lundquist et al., 1999).

The boundaries of the enhancer regions span –65 to –550 bp, with respect to the transcription start site at position +1 of the MIEP. It can be further divided into a distal and proximal enhancer and many of the *cis*-acting elements are found in the enhancer region (Isomura & Stinski, 2003).

The enhancer region is extremely complex and contains a strong transcriptional enhancer made up of an array of 17, 18, 19 and 21 bp repeat elements (Boshart et al., 1985, Ghazal et al., 1987). Activity of the MIE enhancer is dependent on an interaction of various cellular and viral proteins with the *cis*-acting elements in a number of transfection, *in vitro* or transgenic animal studies (Meier & Stinski, 1996, Meier & Stinski, 1997). The enhancer's activity can be stimulated by cellular transcription factors including Sp1, NF- κ B, ATF, ELK1, AP1 and serum response factor (SRF) (Ghazal et al., 1992, Ghazal et al., 1987, Ghazal et al., 1988). These transcription factors bind to the different repeat elements located throughout the enhancer, and many of them bind to multiple sites (Meier & Stinski, 1997). The cellular CREB/ATF proteins bind to the TTGACGTCAA sequence which forms the core of the 19 bp repeat element, five of which are located in the enhancer region. The Sp1 and NF- κ B transcription factors bind to 21 bp and 18 bp repeat elements respectively. Three copies of the 21 bp elements and four copies of the 18 bp elements have been found in the enhancer region (Cherrington & Mocarski, 1989, Liu & Stinski, 1992).

Studies have shown that the distal enhancer is necessary for efficient IE gene expression and viral replication at low MOIs (Meier & Pruessner, 2000). Various viral proteins including pp71 can also stimulate enhancer activity in the presence of one or more ATF sites within the region (Liu & Stinski, 1992) (The actions of pp71 are discussed in detail in a later section).

In contrast to the positive regulatory effects of the MIE enhancer region, its function can also be repressed by a transcription factor YY1. When YY1 binds to a 21 bp repeat element in the HCMV MIEP-regulatory region in un-differentiated non-permissive cells, it mediates a repressive effect on HCMV IE gene expression and may be a mechanism by which viral latency is maintained (Liu et al., 1994).

Although expression of the MIEP can be modulated by various cellular factors, its role in viral infection remains unclear. Murphy et al. (2002) demonstrated a role for HDAC in suppressing the MIEP. It has already been suggested that HDACs play a role in controlling HSV-1 latency, (Arthur et al., 2001) therefore the recruitment of chromatin silencing factors to the MIEP may be involved in repressing gene expression during HCMV latency. This HDAC-mediated repression of HCMV appears to occur within the MIEP in the region encompassing the modulator and 21 bp repeat elements of the enhancer region. Upon differentiation of cells, the histones surrounding the promoter are thought to become acetylated thus viral transcription and, in turn, productive HCMV infection occurs. In non-permissive cells the presence of high levels of HDACs causes inhibition of HCMV infection due to deacetylation of histones surrounding the MIEP, and recruitment of HP1 causes silencing of the promoter (Murphy et al., 2002).

1.10. HCMV pp71 protein

1.10.1. The UL82 gene

The two most abundant proteins in the HCMV tegument are pp65 (a lower matrix protein), encoded by the UL83 gene, and pp71 (an upper matrix protein), encoded by the UL82 gene. Transcript analysis of both genes show that a bicistronic 4 kb mRNA, encoding both pp71 and pp65 ORFs, is produced at both early and late times of infection (Nowak et al., 1984, Ruger et al., 1987). Work by Ruger et al. (1987) suggested that the 4 kb mRNA is formed through the splicing of a 39 nucleotide intron. It codes for pp65, the most abundant tegument protein, but contains all the information for pp71. The protein pp71 is itself encoded for by a rare, unspliced 1.9 kb mRNA. The two mRNAs are 3' co-terminal and employ a single polyadenylation signal (Ruger et al., 1987).

Studies show that two specific mRNAs (1.9 kb and 4 kb), coding for pp71 and pp65, can be detected at 5 hr post-infection (Hensel et al., 1996, Ruger et al., 1987). Both transcripts exhibit a biphasic pattern of expression during a single round of HCMV infection, peaking at 12 hr, and 72 hr post-infection. The biphasic pattern of pp71 expression suggests a bifunctional role for this protein in the nucleus: firstly during the IE and E phases as a transactivator of gene expression, and secondly in progeny maturation during the late phase of viral replication (Hensel et al., 1996). An overview of the HCMV genome and the two pp71 transcripts is presented in figure 1.5.

1.10.2. Functional properties of pp71

HCMV pp71 was first realised to be of importance when the HCMV virion was found to contain a structural component, homologous to HSV-1 VP16, able to transactivate transcription from the MIEP (Spaete & Mocarski, 1985, Stinski & Roehr, 1985). Co-transfection assays showed that pp71 was able to stimulate transcription from HCMV, SCMV and MCMV MIEPs and also SV40 promoters (Liu & Stinski, 1992). Promoter responsiveness to pp71 was associated with a number of 19 bp repeat elements containing ATF binding sequences in the MIEPs investigated. Mutations at the ATF site within these 19 bp repeat element abolished responsiveness of promoters to pp71 in co-transfection assays (Liu & Stinski, 1992).

In later work, infection with HSV-1 recombinant viruses expressing pp71 showed that pp71 could transactivate the HCMV MIEP in the absence of *de novo* protein synthesis. It was also demonstrated that recombinant HSV-1 viruses expressing pp71 showed that this tegument protein could transactivate a number of promoters in tissue culture cells including the already established HCMV MIEP, SCMV MIEP, the HSV-1 ICP4 and ICP0 promoters and the adenovirus VAI promoter (Homer et al., 1999, Marshall et al., 2002). Some of these data disagree with that put forward by Liu and Stinski (1992), in that pp71 transactivated promoters that did not contain consensus ATF motifs including the HSV-1 ICP4 and adenovirus VAI promoters (Homer et al., 1999).

The protein pp71 can enhance the infectivity of viral DNA and accelerate the infectious cycle (Baldick et al., 1997). Alone, viral HCMV DNA has low intrinsic

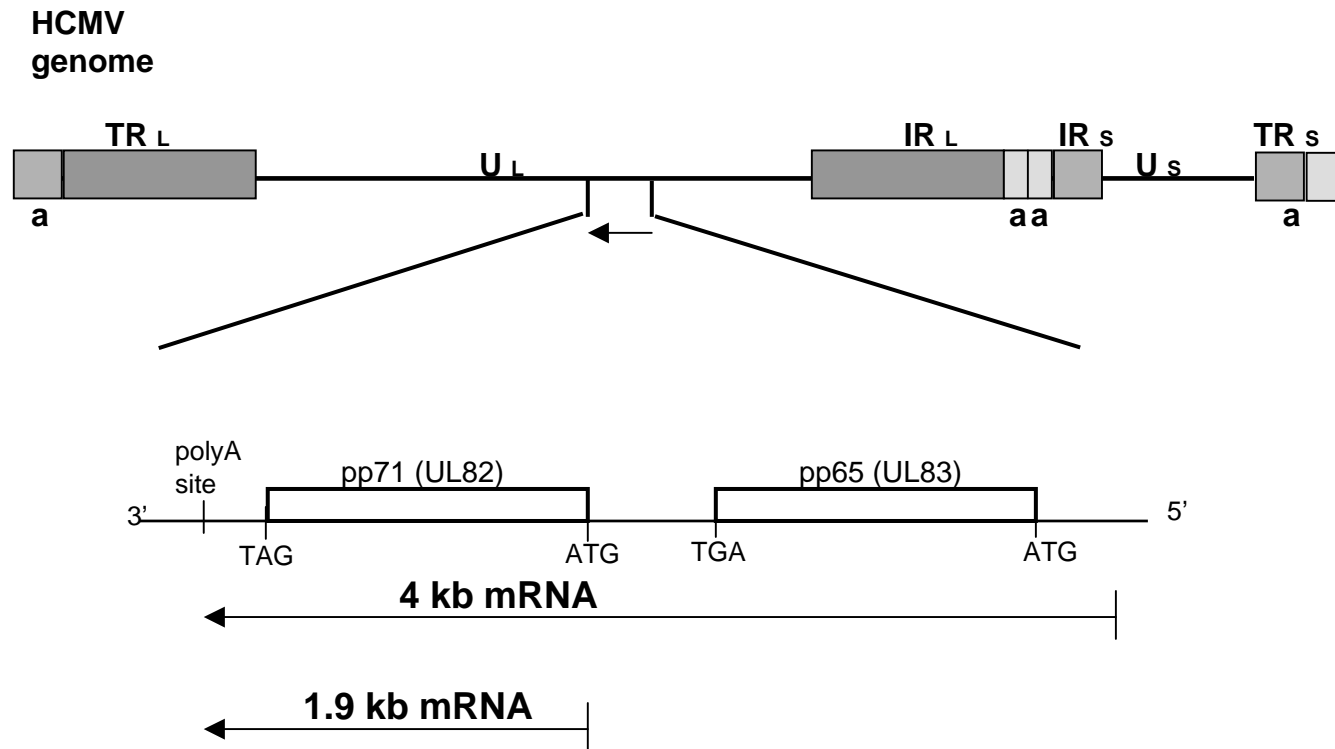


Figure 1.5 Schematic representation of the HCMV genome

A scheme of the HCMV genome showing the location of the UL82 and UL83 genes encoding the upper matrix (pp71) and lower matrix (pp65) proteins. Translation initiation, and translation termination signals are indicated. The 3' end of the transcription unit is designated by polyA. The direction of transcription is indicated by an arrow. Both the 4 kb and 1.9 kb transcripts are shown.

Diagram adapted from Liu and Stinski (1992).

infectivity, however when co-transfected with a plasmid expressing pp71, a 30 to 80-fold increase in infectivity was observed due to increased expression levels of the IE1 and IE2 proteins. When plasmids expressing the IE proteins IE1 and IE2 were co-transfected into cells with HCMV viral DNA the increase in production of infectious virions was not as great as observed after transfection of plasmids expressing pp71. Also co-expression of plasmids expressing IE1, IE2 and pp71 only modestly increased DNA infectivity beyond that seen with pp71 alone (Baldick et al., 1997). This group concluded that pp71 and the IE proteins have different roles during early times after infection, and that it is possible that pp71 transactivates other IE genes which have important functions early in infection.

Further work by Bresnahan and Shenk. (2000) was in agreement with that of Baldick et al. (1997) in that pp71 acts to increase the infectivity of viral DNA and activates the MIEP to allow expression of IE1 and IE2 proteins. They also demonstrated that pp71 facilitates mRNA accumulation from other IE genes including UL37exon1, UL38, UL106-109 and UL115-UL119 by constructing a HCMV mutant which lacks a substantial portion of the pp71 coding region. This mutant, named *ADsubUL82*, is derived from the AD169 strain of HCMV and has nucleotides 117648-119185 deleted.

ADsubUL82 displays a multiplicity dependent growth phenotype whereby at a low MOI its replication is restricted. At higher MOIs, replication is restored to nearly that of wild-type virus. A decrease in viral DNA accumulation in cells infected with *ADsubUL82* was observed compared with DNA levels in wild-type infected cells, suggesting that pp71 functions before or during viral DNA synthesis. DNA array analysis was used to investigate mRNA accumulation in cells infected with *ADsubUL82*. A deficiency was observed at early times of infection (8 hr), thus confirming that the defect associated with *ADsubUL82* occurs early in the replication cycle (Bresnahan & Shenk, 2000). Gene array and northern blot analyses were also used to confirm previous work showing that virion-associated pp71 facilitates the activation of IE genes. Expression of a number of IE genes (IE1, IE2 UL37 and UL38) were significantly decreased in cells infected with *ADsubUL82* compared to wild-type HCMV (Bresnahan & Shenk, 2000).

1.10.3. Interaction of pp71 with cellular proteins

1.10.3.1. Rb Tumour suppressor proteins and pp71

Various studies have shown that HCMV is able to alter cell cycle regulation, possibly as means to suit its own needs by causing arrest at the G₁/S phase of the cell cycle (Dittmer & Mocarski, 1997, Kalejta & Shenk, 2003b). Infection of quiescent cells with HCMV forces re-entry into the cell cycle, a process that is modulated by pp71 (Kalejta et al., 2003a). Kalejta et al. (2003a) illustrated that pp71 stimulated cell cycle progression through the G₁ phase into S phase by binding to and degrading hypophosphorylated forms of the Retinoblastoma (Rb) family of tumour suppressor proteins p107, p130 and p105 (Kalejta et al., 2003a). The oncoproteins of the DNA tumour viruses adenovirus E1A, SV40 T antigen and papillomavirus E7 show a degree of similarity with pp71, as they are also able to interact with Rb family members to stimulate cell cycle progression. These proteins share a similar motif (LXCXE, or LXCXD in the case of pp71) that mediates binding in the pocket domains of the Rb family members. As in the case of E1A a single point mutation in the conserved C residue of the LXCXD motif of pp71 resulted in its inability to degrade Rb proteins. Other than this motif, however, the general mechanisms and effects of cell cycle stimulation differ significantly between pp71 and the DNA tumour virus oncoproteins despite the sequence and functional homologies (Kalejta et al., 2003a).

The ubiquitin-proteasome pathway is the main intracellular machinery involved in eliminating unfolded proteins and destroying regulatory proteins involved in cellular processes (Glickman & Ciechanover, 2002). Substrates are usually targeted to the 26S proteasome by polyubiquitination on internal lysine residues. The polyubiquitin chains mediate the binding of targeted proteins to the proteasome and assist in their unfolding but are removed from the substrate before proteasomal degradation takes place (Glickman & Ciechanover, 2002). Therefore the actual substrate for proteasomal degradation is a partially denatured, non-ubiquitinated protein, indicating that if a protein is delivered to the proteasome in a denatured or partially unfolded state, ubiquitination may not be essential for its degradation (Kalejta & Shenk, 2003c). Work by Kalejta and Shenk (2003c) provided a mechanism whereby pp71 degrades the Rb proteins. It was shown that, in the absence of pp71, the degradation of Rb p130 occurred via a

ubiquitin-dependent pathway, whilst in its presence, p130 was degraded independently of ubiquitin. Also, in the presence of a proteasome inhibitor, pp71 mediated degradation of p130 was prevented. These experiments established that the pp71-mediated degradation of the hypophosphorylated Rb family proteins is via a proteasome-dependent, ubiquitin-independent pathway that then stimulates quiescent cells to re-enter the cell cycle and progress to the S phase (Kalejta & Shenk, 2003c).

Having established that pp71 can stimulate progression of the cell cycle by inducing the proteasome-dependent, ubiquitin-independent degradation of the Rb family of proteins (Kalejta et al., 2003a, Kalejta & Shenk, 2003c), this group went on to show that pp71 accelerates progression through the G₁ phase of the cell cycle via a mechanism that is independent of its ability to target Rb proteins (Kalejta & Shenk, 2003b). Studies by Kalejta (2003b) demonstrated that the major component of G₁ acceleration caused by pp71 is not due to Rb degradation. A pp71 mutant that failed to degrade Rb family members retained the ability to accelerate movement through the G₁ phase. This suggested that the acceleration could be due to the ability of pp71 to degrade another unidentified cell cycle regulatory protein, its ability to regulate transcription or due to a currently unknown function of pp71 (Kalejta & Shenk, 2003b).

1.10.3.2. hDaxx, PML and pp71

ND10s are spherical structures of approximately 0.3-1.0 µm in diameter. They are present in virtually all cell types and each cell nucleus usually contains between 5 and 20 of these punctate sub-structures. They consist of a central core surrounded by an electron dense capsule and are defined by the presence of PML (Dyck et al., 1994). ND10 domains are thought to behave as nuclear depots for the homeostatic maintenance and release of proteins and are altered in size and number in response to the cell cycle e.g. during mitosis (Everett et al., 1999b) and S-phase (Dellaire et al., 2006).

The human PML locus is 35 Kbp in length and consists of nine exons. PML gene transcripts undergo alternative splicing to produce multiple mRNAs that encode for 13 different PML isoforms (Fagioli et al., 1992, Ruggiero et al., 2000). PML is known to be the major protein of ND10 domains and is essential for recruiting

other cellular proteins associated with ND10 such as hDaxx, Sp100 and SUMO-1 (Everett et al., 2006). Other proteins associated with ND10s are p53 (Fogal et al., 2000), BRCA1, (French et al., 2006), USP7 (Everett et al., 1997) and ATRX (Ishov et al., 2004). ND10s have been associated with a number of processes including transcriptional regulation, genome stability response to viral infection, apoptosis and are also considered as nuclear depots (Bernardi & Pandolfi, 2003, Negorev & Maul, 2001).

It is known that PML is covalently modified by SUMO-1, and it is this SUMOylation that is vital for targeting polypeptides to specific cellular compartments, and is required by PML for the formation of ND10 domains (Ishov et al., 1999). A recent model for ND10 formation proposed the RING finger of PML to be essential for both self-SUMOylation and ND10 formation. Furthermore, its SUMO binding motif independently can interact with nearby SUMOylated PML molecules and allow the formation of a PML network. Together with other SUMOylated proteins e.g. hDaxx, these networks may eventually form higher order structures, i.e. ND10 domains (Shen et al., 2006). In the case of hDaxx, a SUMO-interacting motif (SIM) has been identified which is thought to be crucial for recruiting hDaxx to ND10 domains. It is thought that the SIM acts *in trans* to repress several SUMO-modified transcription factors (Lin et al., 2006).

The hDaxx protein was first identified as a protein able to bind to the death domain of FAS in the cytoplasm and to mediate signal transduction pathways, which lead to apoptosis (Chang et al., 1999, Yang et al., 1997). hDaxx is also known to interact with at least eighteen other cellular proteins leading to functional consequences ranging from activation of transcription to apoptosis (Salomoni & Khelifi, 2006).

The cellular protein hDaxx is presumed to be involved in the repression of transcription due to its interaction with HDAC molecules. This interaction causes chromatin to be condensed into a state that is unfavourable for transcription (Li et al., 2000b). More recently, immunoprecipitation and co-fractionation studies have shown that both HDAC and hDaxx are associated with histones and interact with Dek, a chromatin associated protein (Hollenbach et al., 2002). Moreover, Woodhall et al. (2006) have suggested that hDaxx, localising at ND10 domains, is

able to repress transcription of incoming HCMV genomes through the recruitment of HDACs for chromatin remodelling at the viral MIEP (Woodhall et al., 2006).

Using confocal microscopy the HCMV tegument protein pp71 has been demonstrated to localise directly at the nucleus in a punctate pattern in transient transfection assays. This led to the tentative idea that pp71 co-localises at specific locations within the nucleus involved in transcription (Hensel et al., 1996). Work by Hofmann et al. (2002) determined that the central glutamine rich region of hDaxx spanning amino acids 409-501 was a strong binding region for pp71. As it was not possible to narrow down a putative hDaxx binding site within pp71 by deletion analysis internal domains were identified using sequence analysis. Two putative hDaxx interaction domains (DIDs) were mapped to amino acids 206-213 (DID I) and 324-331 (DID II) of pp71, which exhibited sequence similarity to the DID within centromere protein C (CENP-C). Transfection experiments using a vector expressing pp71 fused to a green fluorescent protein (GFP), showed pp71 co-localising with the ND10 proteins PML and Sp100 in nuclear speckles, correlating with that observed by Hensel et al. (1996). Upon deletion of these binding domains the pp71-hDaxx interaction was blocked, preventing pp71 localisation to ND10s and resulting in the inability of pp71 to transactivate the MIEP in transient transfection assays. This suggested that pp71 was recruited to ND10 domains via binding to hDaxx, a process essential for the efficient onset of IE gene expression (Hofmann et al., 2002). This observation was confirmed by Ishov et al. (2002) who showed that, during HCMV infection, pp71 accumulates at ND10s prior to the production of IE proteins. It is the interaction of pp71 and hDaxx, mediated by the interaction of the C-terminus of hDaxx with SUMO modified PML, which trafficks pp71 to ND10s (Ishov et al., 2002). This was confirmed by the observation that pp71 failed to accumulate at ND10s in hDaxx deficient cells and PML deficient cells. In the PML deficient cells pp71 was distributed throughout the nucleus in a diffuse pattern.

In 2005, Cantrell and Bresnahan showed that the pp71-hDaxx interaction regulated efficient HCMV replication. Viral mutants deleted for pp71 or DIDs within pp71 were seriously attenuated for replication at low MOI, but this was overcome at higher MOI. Both mutant viruses showed a significant decrease in the abundance of IE1 and IE2 and also a delay in their expression compared to wild-type virus, suggesting that the pp71-hDaxx interaction is an essential

requirement for efficient gene expression and viral replication. It was also noted that the pp71-hDaxx interaction was involved in enhancing the infectivity of viral DNA, as co-transfection of plasmids expressing pp71-hDaxx binding mutants and viral DNA failed to enhance plaque production (Cantrell & Bresnahan, 2005).

More recent studies have proposed that that the pp71-hDaxx interaction may act to relieve repression of the genome and stimulate IE gene expression (Cantrell & Bresnahan, 2006, Preston & Nicholl, 2006, Saffert & Kalejta, 2006). Work by Saffert and Kalejta. (2006) initially proposed that the mechanism by which pp71 activates the MIEP is by inducing the degradation of hDaxx to permit viral gene expression. Their work showed that pp71 alone is necessary for hDaxx degradation in HCMV-infected cells and that HCMV IE gene expression can be rescued in the presence of hDaxx by inhibiting HDACs. A model was proposed in which the viral MIEP is silenced by hDaxx through the recruitment of HDAC, a process that is reversed when pp71 degrades hDaxx. Work by Preston and Nicholl. (2006) also showed a role for hDaxx in HCMV IE gene expression. In hDaxx depleted cells there was no effect upon wild-type HCMV IE gene expression or MIEP activity in the presence of pp71, suggesting that the pp71-hDaxx interaction does not have a positive effect on IE transcription. However, in the absence of pp71, an increase in the activity of the MIEP was observed in hDaxx depleted cells following infection with AD_{sub}UL82 indicating an involvement of hDaxx in the repression of the MIEP activity. This work was in agreement with that of Cantrell and Bresnahan (2006). Using HCMV permissive cell lines (U373) that were depleted for hDaxx expression (using shRNA) it was shown that wild-type virus replication was increased. Furthermore, the pp71 deletion mutant-associated defects in viral replication and IE gene expression were abolished in these knock down cells. In cell lines over-expressing hDaxx, wild-type virus replication and IE gene expression were inhibited in a multiplicity-dependent manner. These findings suggest that hDaxx acts as a repressor during HCMV infection and that pp71 is responsible for relieving this repression (Cantrell & Bresnahan, 2006).

It has been suggested that the mechanism by which pp71 facilitates the degradation of hDaxx is via a proteasome-dependent, ubiquitin-independent pathway (Hwang & Kalejta, 2007). Using a mouse ts20 cell line (containing a temperature sensitive E1 ubiquitin activating enzyme) transduced with a

recombinant adenovirus expressing pp71, Hwang and Kalejta (2007) showed that at both the permissive temperature (35°C) and non-permissive temperature (39°C) the steady state level of endogenous hDaxx protein was decreased. This indicated that the pp71-mediated degradation of hDaxx occurs through a ubiquitin-independent mechanism. Mouse ts20 cells were infected with either wild-type HCMV or AD_{sub}UL82 to establish if this mechanism was true for HCMV tegument-delivered protein. It was observed that wild-type HCMV induced the degradation of endogenous hDaxx, while the AD_{sub}UL82 virus did not (Hwang & Kalejta, 2007). The proteasomal aspect of this degradation process was established when HCMV-infected ts20 cells treated with the proteasome inhibitor lactacystin, showed stabilisation of hDaxx (Hwang & Kalejta, 2007). Therefore pp71 is presumed to promote the degradation of hDaxx in a proteasome-dependent, ubiquitin-independent manner, in a way similar to pp71 degradation of the Rb family (see section 1.10.3.1).

It is possible that hDaxx acts as a control of HCMV latency by exerting a repressive effect upon the MIEP to induce a repressed chromatin structure, and prevent expression of the IE genes, unless neutralised by pp71. This repressed chromatin state (whereby there is an association of HP1 and a lack of acetylated histones at the MIEP) is similar to that observed at the MIEP in naturally latently infected and incompletely differentiated CD34⁺ cells (Saffert & Kalejta, 2007). Saffert and Kalejta (2007) proposed that hDaxx is essential in establishing quiescent HCMV infections, as loss of hDaxx causes initiation of the lytic cycle. They showed that in undifferentiated cells, viral IE gene expression needs to be silenced to establish latency and prevent abortive infection. Thus this silencing of the genome serves to establish lifelong latent infection (Saffert & Kalejta, 2007). However, this has recently been disputed by Groves et al. (2007) who showed that down-regulation of hDaxx using siRNA in undifferentiated NT2D1 cells did not cause changes in the chromatin structure around the viral MIEP. Productive infection and IE gene expression were only observed in differentiated cells (Groves & Sinclair, 2007).

1.10.4. The interaction of pp71 with other tegument proteins

The UL35 open reading frame has been identified as an early-late gene, which is transcribed into two co-terminal transcripts, directing the synthesis of two

phosphorylated protein products ppUL35 and ppUL35A (Liu & Biegelke, 2002). PpUL35A localises to the nucleus, and it has been reported that it inhibits activation of the MIEP by pp71 (Liu & Biegelke, 2002). The interaction between pp71 and both forms of ppUL35 was identified by yeast two-hybrid screening, with a specific interaction of pp71 and ppUL35 confirmed by co-immunoprecipitation of both proteins from transfected and infected cells (Schierling et al., 2004). Co-localisation of these tegument proteins in human fibroblast cells was demonstrated by immunofluorescence. Alone, ppUL35 appeared as diffuse nuclear staining, however in the presence of pp71, discrete punctate foci were observed. The proteins co-localised with ND10 domains, leading to the suggestion that pp71 recruits both hDaxx and ppUL35 for efficient initiation of the viral replication cycle. Transient luciferase experiments showed strong co-operative activation of the HCMV MIEP by pp71 and ppUL35, whereas each protein alone showed a weak stimulation only (Schierling et al., 2004).

1.10.5. pp71 and the immune system

As discussed in section 1.8 HCMV infects a large proportion of individuals across the world. As HCMV infection can cause serious disease, development of a vaccine is vital. In order to develop a HCMV subunit vaccine, proteins which induce protective immune responses in humans were identified by studying the T cell proliferative response to five HCMV proteins: IE1, IE2, pp71, gpUL18 and gB (He et al., 1995). In the majority of individuals tested, gB was one of the most commonly recognised proteins of the five tested, followed by IE2. Both IE1 and gpUL18 were less frequently recognised. In the case of pp71, 10 out of 23 seropositive patients responded, indicating that pp71 may play a role in the immune response to HCMV in some individuals. Therefore in order to develop a feasible vaccine a combination of proteins would have to be used as different seropositive individuals responded to different proteins (He et al., 1995).

The tegument protein pp71 was found to be able to stimulate the activation of the US11 promoter (Chau et al., 1999). The HCMV US11 gene is already known to be non-essential for replication in tissue culture and plays an essential role in HCMV pathogenesis (Chau et al., 1999). The product of US11, a glycoprotein found in the ER, causes the destruction of the MHC class I proteins, resulting in down regulation of their cell surface expression (Wiertz et al., 1996). Studies by

Chau et al. (1999) revealed two sequence elements (a CREB and an ATF site) within the promoter of US11 which are important for activation by IE proteins, the ATF site being especially critical for US11 promoter activation. The tegument protein pp71 is already known to bind to ATF sites within the MIEP of HCMV (Liu & Stinski, 1992), but as discussed previously pp71 is also able to transactivate promoters that do not contain this motif (Homer et al., 1999). It was observed by Chau et al. (1999) that in combination with viral IE proteins, pp71 could up-regulate the US11 promoter in transient assays and this up-regulation required both CREB and ATF sites to be intact. US11 promoter mutants inactivated for both of these sites were used to show that mutating CREB alone reduced mRNA levels to 25% of that observed with the wild-type promoter. Inactivation of ATF alone reduced US11 mRNA levels to 6% of that of the wild-type promoter. When both CREB and ATF elements were mutated, US11 gene expression was almost undetectable; indicating that both sites co-operate to regulate the US11 promoter in HCMV infected cells (Chau et al., 1999).

More recently a novel function for pp71 has been suggested in relation to the MHC class I antigen presentation pathway. Work by Trgovcich et al. (2006) showed pp71 to be capable of interfering with cell surface expression of MHC class I complexes. Ectopic expression of pp71 in human glioblastoma cells caused a dose-dependent decrease in the accumulation of cell surface MHC class I complexes. It was established that pp71 delayed transport of MHC class I complexes from the ER to *cis* Golgi apparatus, but did not interfere with accumulation of either MHC class I heavy chain transcript or protein. In cells silenced for pp71 and infected with a recombinant adenovirus mutated for the unique short region MHC class I evasion genes, an increase in the accumulation of cell surface MHC class I complexes was observed. It was proposed that pp71 can, at late times of infection, interfere with the transport and cell surface expression of MHC class I complexes (Trgovcich et al., 2006).

1.10.6. HSV-1 recombinant viruses impaired for IE gene expression

The study of pp71 at the MRC Virology Unit has previously relied on the use of HSV-1 recombinant viruses rather than plasmids to express the protein and as reporters to measure its activity (Preston & Nicholl, 2005). The basic HSV-1 mutant used in these studies was termed *in1312* and this virus is impaired for

transcriptional activity of VP16 and the IE proteins ICP0 and ICP4. A 12 bp insertion mutation in the HSV-1 UL48 gene rendered VP16 incapable of transactivating IE gene expression (Ace et al., 1988). The mutated VP16 was incorporated into HSV-1 to produce a mutant *in1814*, and all subsequent recombinant HSV-1 vectors were derived from this virus (Ace et al., 1989). Harris and Preston. (1991) found that the virus *in1814* exhibited a multiplicity dependent phenotype. At high MOIs lytic replication levels were equivalent to those of wild type HSV-1, however, at low MOI *in1814* replicated poorly. This defect could be complemented by the addition of VP16 prior to infection or ICP0 post-infection, demonstrating that the *in1814* replication block was due to low levels of IE proteins. It was also observed that in cells infected with *in1814*, the viral genomes was retained in a non-linear form and that these quiescent genomes were unresponsive to VP16 but remained responsive to ICP0. It was concluded that the *in1814* genome established quiescent infections *in vitro* that resembled latent wild type HSV-1 genomes *in vivo* in some respects (Harris & Preston, 1991).

The virus *in1814* was modified by homologous recombination to replace the ICP0 promoter with the LTR of Moloney murine leukaemia virus to yield *in1820* (Jamieson et al., 1995, Preston & Nicholl, 1997). The LTR is inactive under IE conditions therefore *in1820* lacks functional VP16 and ICP0. Upon infection it can establish quiescent infection, which is reactivated by the addition of ICP0. *In1820* was then further modified to produce the virus *in1820K* through homologous recombination of viral DNA with a plasmid containing a temperature sensitive mutation in ICP4. This mutant (*in1820K*) failed to produce virus at temperatures greater than 31°C (Preston et al., 1997). It was also determined that transgenes, such as the *E.coli lacZ* gene and the neomycin phosphotransferase gene could be inserted into the *in1820K* genome under the control of a variety of promoters including the HCMV MIEP, and that short-term expression of the transgene was observed (Preston et al., 1997, Preston & Nicholl, 1997). Expression of the transgenes, driven by the HCMV MIEP in particular, was repressed considerably at 24 hr post-infection, indicating that repression of gene expression observed in *in1814* derivatives is not confined specifically to the HSV-1 IE genes (Preston & Nicholl, 1997).

In 1998 Preston et al. inserted a mutation into the ICP0 coding sequence by deleting the RING finger, substituting this mutation for the previous ICP0 promoter

mutation in *in1820*. This resulted in the virus *in1312* (Preston et al., 1998), the parental genome used to create the various recombinant viruses used in the study of pp71. Derivatives of this virus may have the *E.coli lacZ* gene inserted into either the TK locus or the UL43 locus of this genome or they may be employed as expression vectors.

Recombinant viruses such as *in1312* are particularly useful as they can be retained in a quiescent state following infection of cultured cells. Due to the mutations rendering the critical HSV-1 transcription factors inactive, the absence of IE gene expression ensures that the infected cells survive infection, but do not support lytic infection (Preston & Nicholl, 2005). The input viral genomes are responsive to transcription factors immediately after infection, however, a few hours post-infection they become repressed i.e. quiescent. In this quiescent state the viral genomes are transcriptionally inactive and retained in a non-linear configuration (Preston & Nicholl, 2005). This quiescent state established by the HSV-1 recombinant viruses is believed to resemble the latent state attained by wild type HSV-1 in some respects (Preston, 2000). The quiescent genome is believed to be stably repressed, but gene expression can be provoked by the addition of ICP0 (Hobbs et al., 2001, Preston et al., 1997, Samaniego et al., 1998) as ICP0 can disrupt the chromatin structure into which the quiescent genome is packaged.

1.10.7. pp71 directs long-term gene expression

The HSV-1 recombinant virus *in1312* was used to construct the recombinant virus *in1324* which was *in1312* with the coding sequence of pp71 inserted into the TK locus of the *in1312* genome. Homer et al. (1999) showed that infecting human fibroblasts with *in1324* stimulated short-term gene expression from the HCMV MIEP promoter. A novel property of pp71 was observed whereby it was able to stimulate gene expression from the HCMV MIEP, cloned into the *in1324* genome, over extended periods in cell culture (Preston & Nicholl, 2005). Using the HSV-1 recombinant *in1360* (derived from inserting HCMV IE-*lacZ* into the UL43 locus of *in1324*) to infect human foetal foreskin fibroblast cells (HFFF2), a biphasic pattern of β -gal expression was observed. At early times of infection, β -gal positive cells were observed which were indicative of short-term gene expression. β -gal positive cells indicative of longer term gene expression were not observed until 5-7 days

post-infection, possibly because the HCMV MIEP was not fully activated at early times of gene expression. In cells that did not respond to short-term gene expression the virus, *in1360*, initially became quiescent but was slowly turned on by pp71. Low level expression of pp71 unblocked the remainder of the genome, increasing expression of pp71 itself along with HSV-1 IE proteins (Preston & Nicholl, 2005). These observations suggest that there may be two populations of cells present; one immediately subject to active virus infection and the second where the virus becomes quiescent. This second population of cells does not support short-term gene expression but as the MIEP is slowly turned on by low levels of pp71, the remainder of the genome is unblocked and the IE proteins, and pp71, are expressed.

1.11. A comparison of pp71 with the HSV-1 proteins VP16 and ICP0

Much work has been carried out in order to determine if pp71 has any functional analogy with the proteins found in the tegument of HSV-1. To date pp71 has been compared in function to the protein VP16 and the IE protein ICP0.

1.11.1. pp71 and VP16

The HSV-1 tegument protein VP16 activates IE transcription by forming a complex with the cellular proteins Oct-1 and HCF at the TAATGARAT sequence. The HCMV tegument protein pp71 activates expression from the MIEP in transfection assays by targeting ATF or AP-1 recognition sites in the 19 bp repeated units of the promoter (Liu & Stinski, 1992). It is the most likely candidate for a functional counterpart of VP16.

Using a HSV-1 recombinant *in1324* that expresses pp71 Homer et al. (1999) showed that pp71 is the virion component of HCMV that effects activation of a variety of promoters. Removal of the pp71 ORF from *in1324* abolished this activity, demonstrating that pp71 is able to act alone. Unlike VP16, pp71 dependent promoter activation is not sequence specific (Homer et al., 1999). Furthermore despite their similar roles, the broader specificity exhibited by pp71 may imply that HCMV differs from HSV-1 in its requirements for a virion transactivator. During HSV-1 infection VP16 is essential for the early increase in IE gene expression that allows the IE proteins to maintain transcription of the viral

genome. It also ensures that sufficient levels of ICP0 accumulate to prevent the HSV-1 genome from becoming quiescent. Homer et al. (1999) suggest that pp71 is important for the efficient expression of IE loci other than those controlled by the MIEP, themselves lacking potent promoters. In addition, it may function to maintain the accessibility of the genome to other transcription factors.

1.11.2. pp71 and ICP0

The HCMV tegument protein pp71 exhibits broad promoter specificity and can activate a variety of promoters, including the HCMV MIEP, SCMV MIEP, the HSV-1 ICP0 and HSV-1 ICP4 promoters (Homer et al., 1999, Marshall et al., 2002). ICP0 is also considered to be a promiscuous transactivator, in as much as it activates transcription from HSV-1 and heterologous promoter elements independently of a single *cis*-acting element (Everett et al., 1991). Marshall et al. (2002) showed that the expression of pp71 partially complements the replication of an HSV-1 ICP0 null mutant indicating that there exists a degree of functional interchangeability between these proteins.

Both ICP0- and pp71-null viruses have been produced in order to better examine the biological activities of the proteins. It has been demonstrated that at low MOIs, in human fibroblasts, infection with HSV-1 ICP0-null viruses can result in quiescence of the genome (Stow & Stow, 1989). Absence of ICP0 also leads to stalled infection with an incomplete set of expressed IE genes, stalling at the IE stage of infection or stalling with the expression of some E proteins but no DNA replication (Everett et al., 2004a). Human fibroblasts infected with a MOI of 10 of both ICP0-null and wild-type viruses show little difference in levels of productive infection. However, human fibroblasts infected with the same viruses at a lower MOI of 1 shows little progress into productive infection in cells infected with the ICP0-null virus (Everett et al., 2004a).

The HCMV mutant virus deficient for pp71, AD_{sub}UL82, also displays a multiplicity dependent phenotype in human fibroblasts. The growth of this mutant, like that of the ICP0-null virus, is restricted at low MOIs. However this defect, like that of the ICP0-null virus, is overcome at higher MOIs whereby AD_{sub}UL82 replicates to wild-type levels. Again the absence of pp71 means that infection is stalled, as AD_{sub}UL82 is unable to effectively activate IE genes (Bresnahan & Shenk, 2000),

As discussed in section 1.5.1, ICP0 is known to facilitate viral replication and reactivation from latency. When HSV-1 gene expression is repressed in human fibroblasts in the absence of viral IE gene expression, ICP0 is required to reactivate gene expression from quiescence (Harris et al., 1989, Zhu et al., 1990). It has been reported that ICP0 may counteract repression by stimulating the degradation of various cellular proteins via a ubiquitin-proteasome pathway (Everett et al., 1998a, Everett et al., 1997). HCMV pp71 has also been reported to reactivate viral expression from quiescent genomes (Preston & Nicholl, 2005), however the kinetics of reactivation were considerably slower than that of ICP0. Moreover, pp71 was observed to be less effective than ICP0 in reactivating quiescent genomes (Preston & Nicholl, 2005).

ICP0 and pp71 both localise to ND10 domains following infection. However, how they get there and what they do at these sites differs. The initiation of gene expression due to localisation of ICP0 and degradation of PML at ND10 domains is well documented (Boutell et al., 2003, Everett & Maul, 1994, Everett et al., 1998b, Everett et al., 2006). Everett and Murray (2005) showed, using live cell microscopy that it is not ICP0 that localises to ND10 components, but it is ND10 domains that are recruited to viral genomes at the periphery of nuclei. Here ICP0 targets the disruption of ND10 domains and the degradation of PML.

Marshall et al. (2002) and Hensel et al. (1996) showed that pp71 localises to ND10 domains but, unlike ICP0, does not induce their disruption. Also, IE gene expression is not initiated by the degradation of PML. Instead, pp71 participates in the degradation of hDaxx in order to relieve IE gene repression (Cantrell & Bresnahan, 2006, Preston & Nicholl, 2006, Saffert & Kalejta, 2006).

ICP0 and pp71 differ in sequence and structure. Analysis of the HCMV pp71 sequence using 'Scanprosite' showed that no homologous sequence motifs such as the ICP0 consensus RING finger motif were present in HCMV pp71; however, both proteins contain a bipartite nuclear localisation signal (NLS). The crystal structure of pp71 has not been solved and searches of structural databases using the amino acid sequence have shown that there are no structural homologues to pp71, apart from the functional cytomegalovirus homologues of pp71 described previously, which show up to 60% amino acid sequence homology (Jane Sutherland personal communication).

1.12. Simian Cytomegalovirus Biology

1.12.1. SCMV genome

The simian cytomegalovirus (SCMV) is also known as CMV strain Colburn. It is composed of a linear, double stranded DNA molecule of 220 kbp (Gibson, 1981). Like the other herpesviruses, it is replicated and packaged into an icosohedral capsid in the nucleus of infected cells, and is surrounded by an envelope.

Various sequence elements and proteins encoded by SCMV have been described. These include IE94 (Jeang et al., 1982), an upstream regulatory region which directs the expression of IE94 (Jeang et al., 1987), an assembly protein and the *oriLyt* (Anders & Punturieri, 1991, Jeang et al., 1987, Robson & Gibson, 1989). A nuclear DNA binding protein, structural proteins of the mature virus particle, three intracellular capsid forms (Gibson, 1981) and a basic phosphoprotein (BPP) (Baxter & Gibson, 2001) have also been identified

1.12.2. SCMV lytic infection

1.12.2.1. Attachment and penetration

The little which is known about the lytic cycle of SCMV has been derived by extrapolation from the study of HCMV. Glycoproteins gB and gH are conserved in all herpesviruses and are known to be involved in viral attachment and penetration of the virion into the host cell (Bold et al., 1996). It is assumed that these glycoproteins play the same role in SCMV attachment and penetration. Following entry into the cell the genome is probably transported to the nucleus by a microtubule network system, in a similar manner to HCMV (Ogawa-Goto et al., 2003).

1.12.2.2. IE gene expression

The HCMV tegument protein pp71 transactivates the MIEP to stimulate production of IE proteins, which in turn transactivate the E and L genes to stimulate lytic replication. Sequence comparison of HCMV and SCMV revealed a structural

protein named S82, which is functionally homologous to HCMV pp71 as it stimulates IE gene expression (Nicholson, 2004). S82 also co-localises with hDaxx and PML at ND10 domains, possibly exerting its effect on the SCMV MIEP in a similar manner to HCMV pp71.

As mentioned previously, the IE1 gene of SCMV, IE94, and its associated upstream promoter-regulatory region have been characterised (Jeang et al., 1987). Studies have shown that this promoter-regulatory region consists of two distinct domains. Two NF1 binding sites have been identified within this region, the functional significance of which is not yet known (Jeang et al., 1987).

1.12.2.3. E and L gene expression

Little information is available regarding expression of the SCMV E and L genes. It is assumed that E and L gene expression occurs in a similar manner to that of HCMV.

1.12.3. Capsid assembly and DNA packaging

In herpesvirus virion assembly, various kinds of capsids have been identified, these include A capsids, C capsids, and B capsids. Using cryoelectron microscopy and image reconstruction, B-capsids recovered from SCMV-infected cells have been investigated (Trus et al., 1999). It was observed that these capsids contain an inner shell composed mainly of the assembly protein (Ap) in its mature, proteolytically processed form. An interaction between capsid and tegument was observed, as the B capsid revealed two sites of tegument attachment (Trus et al., 1999).

Capsid assembly of all herpesviruses is a closely conserved process whereby a procapsid is assembled requiring the involvement of several proteins. In HCMV these are the MCP, mc-BP, and pAP homologues all of which have been identified in SCMV (Gibson, 1981). The pAP protein is modulated by proteolytic cleavage, which is essential for capsid maturation and production of infectious virus. It is also modulated by phosphorylation. Plafker et al. (Plafker et al., 1999) established that the SCMV pAP could be phosphorylated on two adjacent serine residues on a casein kinase II (CKII) consensus sequence. Later studies identified two more

sites, Thr231 and Ser235, the phosphorylation of which resulted in conformational changes in the pAP. Inhibition of phosphorylation at these sites was found to alter the interaction of pAP with itself and with the MCP. This indicates that phosphorylation of this protein has a functional significance in the capsid assembly of herpesviruses (Casaday et al., 2004).

1.12.4. Virion maturation and egress

As with HCMV, tegumentation of SCMV capsids occurs in the cytoplasm of infected cells (Trus et al., 1999). It is likely that the egress of these SCMV virions proceeds via a similar pathway to that of HCMV.

1.13. Rhesus Cytomegalovirus biology

1.13.1. RhCMV genome

The complete genome sequence of rhesus cytomegalovirus (RhCMV) has been determined using the shotgun approach (Hansen et al., 2003). Sequence analysis showed a significant degree of homology with the HCMV genome.

As with other herpesviruses the RhCMV has a long, double-stranded unique sequence within its genome. It was found to be 221,459 bp in length, 7895 bp shorter than the HCMV genome, with a G+C content of 49% evenly distributed throughout the genome. No large internal or terminal repeats were found in the RhCMV genome. Of the 230 ORFs, 138 ORFs dispersed throughout the genome were found to encode proteins homologous to HCMV proteins. RhCMV was also found to encode almost all classified HCMV gene families, including RL11, UL25, UL82, US1, US2/6, US12 and US22 (Hansen et al., 2003).

RhCMV encodes enzymes homologous to those of HCMV that are required for nucleotide metabolism, replication and repair. This includes uracil-DNA glycosylase, ribonucleotide reductase, and dUTPase all of which have very high homologies to their HCMV counterparts (Hansen et al., 2003).

HCMV UL82 family members consist of the upper and lower matrix proteins pp71 and pp65. RhCMV homologues to these proteins are Rh110 (pp71) and

Rh111/Rh112 (pp65). The RhCMV pp71 protein has 39% identity with HCMV pp71, while the two pp65 copies of RhCMV have 32% (Rh111) and 35% (Rh112) identity with the HCMV protein (Hansen et al., 2003). In HCMV, pp65 illicit protective immune responses in humans and represents an important vaccination target (Yue et al., 2006). The RhCMV homologue (Rh112) was characterised by Yue et al. (2006) and analysed for its ability to induce host immune responses. Rh112 is expressed at L times of infection and localises to the nucleus following expression. It elicits both humoral and cellular immune responses.

1.13.2. RhCMV lytic infection

1.13.2.1. Attachment and penetration

The gB of RhCMV was identified and characterised by Kravitz et al. (1997) and Kropff and Mach (Kropff & Mach, 1997). This RhCMV gene had extensive homology to gB of HCMV (75% similarity and 60% identity), with many structural, modifying and processing signals being maintained (Kravitz et al., 1997). The RhCMV gB protein was also found to be proteolytically processed similarly to HCMV gB. Therefore, gB is an important component of the viral envelope and is involved in virus attachment, penetration and viral spread. RhCMV cross-reacted and cross-neutralised with various HCMV gB-specific monoclonal antibodies, which revealed homologous immunogenic epitopes between the two molecules (Kravitz et al., 1997). RhCMV infection in rhesus macaques could provide a model in which to study HCMV pathogenesis and immune surveillance of cytomegaloviruses.

Sequencing of the RhCMV genome identified 21 further glycoproteins, as well as gB, encoding homologues to gH, gL, gM, gN and gO of HCMV (Hansen et al., 2003).

1.13.2.2. RhCMV IE gene expression

The IE region of RhCMV was cloned and sequenced by Barry et al. (1996) and was found to span 9.2 kb. Within this region, ORFs corresponding to the IE1 and IE2 genes were identified (Barry et al., 1996). The predicted IE1 protein was

found to share 29% identity with HCMV IE1, while the predicted IE2 protein shared 48% identity with HCMV IE2.

1.13.2.3. RhCMV E and L gene expression

Little information is available regarding expression of the RhCMV E and L genes. It is assumed that E and L gene expression occurs in a similar manner to HCMV.

1.13.2.4. Capsid assembly and DNA packaging

Capsid assembly proteins are conserved amongst the betaherpesviruses. RhCMV encodes homologues to the MCP, a mc-BP of HCMV. Also present in RhCMV is a UL80 homologue thought to be involved in assembly and packaging (Hansen et al., 2003).

1.13.3. RhCMV prevalence and disease

RhCMV was first identified as an incidental infection of rhesus macaques and is now known to be ubiquitous in captive rhesus macaques (Kalter & Heberling, 1990). The majority of RhCMV infections, like HCMV infections, are subclinical. Healthy individuals shed virus in their urine, saliva, semen, cervical secretions and breast milk.

As with humans, rhesus macaques are susceptible to infection with simian immunodeficiency virus (SIV). Various studies using SIV-infected rhesus macaques have shown that disseminated cytomegalovirus disease is fairly similar to that observed in HIV-infected humans (Baskin, 1987). Symptoms include orchitis, encephalitis and respiratory tract disease.

1.14. BCMV biology

Baboons are known to harbour viruses which are closely related to EBV, HHV6 and VZV (Blewett et al., 2001). An alphaherpesvirus called herpesvirus papio 2 (HPV2), bearing significant similarity to human HSV was discovered in a colony of captive baboons (Jenson et al., 2000). Recently CMV-like viruses were isolated

from three sub-species of baboon, all of which were found to be closely related to both HCMV and RhCMV (Blewett et al., 2001).

The baboon CMV-like viruses had similar characteristics to other CMVs, including slow growth in fibroblast cell cultures, and production of virions with similar size and morphology to HCMV (Blewett et al., 2001). Phylogenetic analysis and predicted protein sequences of the gB gene confirmed baboon cytomegalovirus (BCMV) to be a member of the cytomegalovirus group, closely related to both HCMV and RhCMV. More detailed analysis via ELISA and western blotting showed that BCMV shared greater homology with RhCMV than HCMV (Blewett et al., 2001). gB genes have been isolated from various strains of BCMV, which were isolated from three sub-species of cynocephalus baboons (olive, yellow and chacma) (Ross et al., 2005). However, similarities between the gB coding sequences were too similar to differentiate by PCR assay. This similarity may be due to a range overlap between two central African baboon subspecies allowing transfer of BCMV strains between populations (Ross et al., 2005).

Baboons are perceived to be a possible species for xenogeneic organ donors as they are relatively easy to breed in captivity and their organ size is appropriate for humans (Blewett et al., 2000). However baboon to human transplants have been restricted due to possible cross-species transfer of baboon viruses to xenotransplant patients. BCMV was isolated from the peripheral blood of the recipient of a baboon liver transplant four weeks post-transplantation (Michaels et al., 2001). Furthermore, it has been observed that BCMV was reactivated (detected as an increase in BCMV DNA copy numbers by PCR) in baboon recipients. The pattern of reactivation observed was similar to that of HCMV in human transplant patients (Mueller & Fishman, 2004).

1.15. ChCMV biology

Chimpanzee cytomegalovirus (ChCMV) is the closest known relative to HCMV. It is thought that the two viruses evolved with their hosts, with a divergence date of approximately 5-6 million years ago. Sequencing of ChCMV revealed a 241,087 bp genome, with U_L, U_S, R_L, and R_S components, and a G+C content of 67.7%. The greatest degree of sequence similarity was observed in the central part of the U_L region with similarity decreasing towards the genome termini. ChCMV was found to lack counterparts of HCMV UL1 (a member of the RL11 glycoprotein

family), UL111A (which encodes an interleukin-10 homologue in HCMV), and UL3. ChCMV was also found to contain a number of genes absent in HCMV AD169 and Toledo strains, including: UL146A (encodes a α -chemokine in HCMV), UL155, UL156, and UL157 (Davison et al., 2003a).

The Toledo strain of HCMV produces the functional viral chemokine vCXCL-1 (UL46), which has been implicated in HCMV virulence. A similar gene, vCXCL-1_{chcmv}, was identified in ChCMV. It was found that vCXCL-1_{chcmv} had similar activation potentials, chemotactic and signalling properties to its HCMV counterpart and could provide a model for assessing the role of vCXCL-1 in CMV pathogenesis (Miller-Kittrell et al., 2007).

1.16. Project aims

Previous work comparing HCMV and SCMV pp71 proteins, by cloning and sequencing, had shown that these two homologues can locate to ND10 domains and play an active role in transactivating gene expression. However, only HCMV pp71 was able to direct long-term gene expression (Nicholson, 2004). Homologues of pp71 obtained from other CMV viruses including RhCMV, BCMV and ChCMV had been sequenced but not yet studied. Close examination of the predicted amino acid sequences showed a significant degree of homology between the UL82 proteins, especially in the middle region where a large degree of similarity is seen. Therefore the pp71 homologues were expected to behave in a similar manner to HCMV pp71.

This study aimed to:

1. Investigate the activation of gene expression by comparing the non-human homologues to HCMV pp71 using transfection assays and HSV-1 vectors. To determine how the pp71 homologues behave in short-term and long-term gene expression assays.
2. Map the region of HCMV pp71 involved in long-term gene expression.
3. Further characterise the non-human homologues by comparing the intracellular localisation of these proteins with that of HCMV pp71.

Chapter 2

Materials and Methods

2. Materials

2.1. Chemicals

All chemicals were of analytical grade, and unless otherwise stated, purchased from VWR Ltd, Sigma Aldrich Company Ltd. UK, or Invitrogen.

2.1.1. Eukaryotic cells and tissue culture

Culture media

D5+5

Dulbecco's modified Eagle's medium containing 1 mM sodium pyruvate and 2 mM L-glutamine, supplemented with 5% newborn calf serum (NBCS), 5% foetal calf serum (FCS), 100 U/ml penicillin, 100 µg/ml streptomycin and 1% non-essential amino acids (NEAA).

DF2

Dulbecco's modified Eagle's medium containing 1 mM sodium pyruvate and 2 mM L-glutamine, supplemented with 2% FCS, 100 U/ml penicillin, 100 µg/ml streptomycin and 1% NEAA.

ETC10

BHK-21 medium supplemented with 10% NBCS, 100 U/ml penicillin, 100 µg/ml streptomycin, 7% tryptose phosphate broth and 2 mM L-glutamine.

RPMI

RPMI 1640 medium containing 25 mM HEPES buffer, supplemented with 10% FCS, 1% NEAA, 100 U/ml penicillin, 100 µg/ml streptomycin and 2 mM L-glutamine.

Tissue culture solutions

PBSA: 170 mM NaCl, 3.4 mM KCl, 1.8 mM KH₂PO₄, pH 7.5.

Trypsin: 0.25% trypsin in Tris saline pH 7.7 (140 mM NaCl, 0.7 mM Na₂HPO₄, 5.6 mM D-glucose, 24.8 mM Tris).

Versene: 0.6 mM EDTA with 0.002% phenol red in PBSA.

Tryptose Phosphate Broth: 29.5 g/L tryptose phosphate (Becton Dickinson).

Eukaryotic cells

Name	Description	Source	Growth Medium
HFFF2	Human foetal foreskin fibroblasts	Provided by C.M. Preston	D5+5
U2OS	Human osteosarcoma cells	Provided by C.M. Preston	D5+5
BHK	Baby hamster kidney fibroblasts	Provided by J.Mitchell	ETC10
U373	Human glioblastoma	Provided by C.M. Preston	D5+5

Table 2.1. Showing cells used and their sources

2.1.2. Primary Antibodies

Antibody	Target	IF/WB*	Source
Anti-hDaxx (mouse monoclonal)	Endogenous hDaxx	IF	Courtesy of G.Maul
Anti-PML A-20 (goat polyclonal)	Endogenous PML	IF	Santa Cruz
Anti-GFP (rabbit polyclonal)	EYFP-tag	WB	AbCam
Anti-myc (mouse monoclonal)	myc-tag	WB	Santa Cruz
Anti-Actin (mouse monoclonal)	Actin	WB	Sigma Aldrich UK
Anti-hDaxx (rabbit polyclonal)	Endogenous hDaxx	WB	Sigma Aldrich UK

Table 2.2. Primary antibodies used, their targets and their source

*Abbreviations: IF=immunofluorescence, WB=western blotting

2.1.3. Secondary Antibodies

Antibody	IF/WB*	Source
Anti-mouse IgG-Cy5 conjugate	IF	Amersham Biosciences UK Ltd
Alexa 647-chicken anti-goat	IF	Invitrogen
Anti-rabbit IgG-HRP conjugated	WB	Sigma Aldrich UK
Anti-mouse IgG-HRP conjugated	WB	Sigma Aldrich UK

Table 2.3. Secondary antibodies used and their source

*Abbreviations: IF=immunofluorescence, WB=western blotting

2.1.4. Plasmids

Plasmid	Description	Source
pEYFP-C1	EYFP expression vector containing a multiple cloning site (MCS) allowing inserts to be fused to the EYFP terminus driven by the HCMV MIEP	CM.Preston
pEYFPpp71	EYFP fused to the N-terminus of the HCMV pp71 ORF driven by the HCMV MIEP	C.M.Preston
pEYFPS82	EYFP fused to the N terminus of the SCMV S82 ORF driven by the HCMV MIEP	C.M.Preston
pEYFPB82	EYFP fused to the N terminus of the BCMV B82 ORF driven by the HCMV MIEP	C.M.Preston
pEYFPCh82	EYFP fused to the N terminus of the ChCMV Ch82 ORF driven by the HCMV MIEP	M.J.Nicholl
pEYFPRh82	EYFP fused to the N terminus of the RhCMV Rh82 ORF driven by the HCMV MIEP	T. Chaudry
pmycpp71	c-myc tag fused to N-terminus of HCMV pp71 driven by the HCMV MIEP	C.M.Preston
pmycS82	c-myc tag fused to N-terminus of SCMV S82 driven by the HCMV MIEP	M.J.Nicholl
pmycB82	c-myc tag fused to N-terminus of BCMV B82 driven by the HCMV MIEP	M.J.Nicholl
pmycRh82	c-myc tag fused to N-terminus of RhCMV Rh82 driven by the HCMV MIEP	M.J.Nicholl
pmycCh82	c-myc tag fused to N-terminus of ChCMV Ch82 driven by the HCMV MIEP	C.M.Preston
pCP1082	HCMV MIEP controlling <i>E.coli lacZ</i> gene in HSV-1 thymidine kinase locus	C.M.Preston

Table 2.4. Plasmids used and their acknowledged sources

2.1.5. Viruses

Virus	Promoter	Transgene locus
<i>in1382</i>	HCMV MIEP (-750 to +7)	<i>E.coli lacZ</i> (TK locus)
<i>in1374</i>	HCMV MIEP (-750 to +7)	<i>E.coli lacZ</i> (UL43) locus
<i>in1310</i>	HCMV MIEP (-750 to +7)	HCMV EYFPpp71 (TK locus), <i>E.coli lacZ</i> (UL43 locus)
<i>in0150</i>	HCMV MIEP (-750 to +7)	SCMV EYFPS82 (TK locus), <i>E.coli lacZ</i> (UL43 locus)
<i>in0146</i>	HCMV MIEP (-750 to +7)	ChCMV EYFPCh82 (TK locus), <i>E.coli lacZ</i> (UL43 locus)
<i>in0144</i>	HCMV MIEP (-750 to +7)	RhCMV EYFPRh82 (TK locus), <i>E.coli lacZ</i> (UL43 locus)
<i>in0145</i>	HCMV MIEP (-750 to +7)	BCMV EYFPB82 (TK locus), <i>E.coli lacZ</i> (UL43 locus)
<i>in0149</i>	HCMV MIEP (-750 to +7)	ChCMV mycCh82 (TK locus), <i>E.coli lacZ</i> (UL43 locus)
<i>in0151</i>	HCMV MIEP (-750 to +7)	HCMV mycpp71 (TK locus), <i>E.coli lacZ</i> (UL43 locus)
<i>in0156</i>	HCMV MIEP (-750 to +7)	EYFPTC6 (TK locus), <i>E.coli lacZ</i> (UL43 locus)
<i>in1318</i>	HCMV MIEP (-750 to +7)	Secreted alkaline phosphatase (SEAP) (TK locus)

Table 2.5. Viruses used in this study

All mutant HSV-1 recombinant viruses were derived from the HSV-1 virus *in1312* (see introduction section 1.10.6). All HSV-1 recombinant viruses used in this study are impaired for the transcriptional stimulating activity of VP16 and additionally, the IE proteins ICP0 and ICP4 are rendered non-functional by deletion and temperature sensitive mutations respectively.

2.1.6. Restriction endonucleases

All restriction endonucleases were purchased from New England Biolabs Ltd (UK) or Roche Diagnostics Ltd (UK) and were supplied with the appropriate reaction buffers.

2.1.7. Miscellaneous enzymes

T4 DNA ligase and calf intestinal phosphatase (CIP) were obtained from New England Biolabs. Klenow DNA Polymerase was purchased from Roche Diagnostics Ltd. All enzymes were supplied with the appropriate reaction buffers.

2.1.8. Composition of commonly used solutions and buffers

2.1.8.1. Bacterial cell culture

L-Broth: 10 mg/ml tryptone peptone (Becton Dickinson), 5 mg/ml yeast extract (Becton Dickinson), 10 mg/ml NaCl pH 7.5.

L-Broth agar: L-broth plus 15 mg/ml agar (Becton Dickinson).

2.1.8.2. DNA manipulation

2.1.8.2a. Small scale DNA preparation

Resuspension buffer p1: 50 mM Tris.HCl, 10 mM EDTA, 100 µg/ml RNase A pH 8.0.

Lysis buffer p2: 200 mM NaOH, 1% SDS.

Neutralisation buffer N3: 3.0 M potassium acetate pH 5.5.

Wash buffer 1 PB: Qiagen proprietary information.

Wash buffer 2 PE: Qiagen proprietary information.

Elution buffer EB: 10 mM Tris.HCl, pH 8.5.

2.1.8.2b. Large Scale DNA preparation

Resuspension buffer: 50 mM Tris.HCl, pH 8.0, 10 mM EDTA, 100 µg/ml RNase A.

Cell lysis buffer: 200 mM NaOH, 1% SDS.

Neutralisation buffer: 3.0 M potassium acetate pH 5.5.

Filter wash buffer: 1 M potassium acetate pH 5.0.

Equilibration buffer: 750 mM NaCl, 50 mM MOPS, pH 7.0, 15% isopropanol, 0.15% Triton X-100.

Column wash buffer: 1.0 M NaCl, 50mM MOPS, pH 7.0, 15% v/v isopropanol.

Elution buffer I: 1.25 M NaCl, 50 mM MOPS, pH 7.0, 15% v/v isopropanol.

Elution buffer II: 1.6 M NaCl, 50 mM MOPS, pH 7.0, 15% v/v isopropanol.

TE buffer: 10 mM Tris.HCl pH 8.0, 1 mM EDTA.

2.1.8.3. STET preparations

STET: 8% sucrose, 5% Triton-X 100, 500 mM EDTA, 500 mM Tris.HCl pH 8.0

2.1.8.4. SDS polyacrylamide gel electrophoresis and western blotting

Running gel buffer: 52 mM Tris.HCl, 53 mM glycine, 1% SDS, pH 6.8.

Transfer Buffer: 25 mM Tris.HCl, 192 mM glycine, 20% methanol, pH 8.3

SDS gel loading buffer: 50 mM Tris.HCl, pH 6.8, 100 mM DTT, 2% SDS, 10% glycerol, 0.1% bromophenol blue.

PBSA+TWEEN: PBSA+1% TWEEN 20 (Calbiochem).

2.1.8.5. DNA electrophoresis

TBE (10X): 1.25 M Tris, 27mM EDTA, 0.4 M boric acid.

Ficoll loading buffer: 10% Ficoll, 5XTBE, 0.1% bromophenol blue.

2.1.8.6. β -Galactosidase assays

β -Gal reaction mix (histochemical): 5 mM $K_4Fe(CN)_6$, 5 mM $K_3Fe(CN)_6$, 2 mM $MgCl_2$, 0.01% NP40, 1 mg/ml 5-Bromo-4-Chloro-3-Indolyl- β -D-galactoside (X-gal) (Melford) in PBSA.

Carmalum Stain: 5 g Carmine red, 5 ml glacial acetic acid 120 ml dH_2O , 5 g aluminium potassium sulphate, 80 ml dH_2O , 1 crystal thymol.

2.1.8.7. SEAP assay

SEAP 2x buffer: 2 M diethanolamine, 1 M MgCl₂, 1 M homoarginine, 12 mM pNitrophenyl phosphate.

2.1.8.8. Immunofluorescence reagents

Fix buffer: 5% Formaldehyde, 2% sucrose in PBSA

Permeabilisation buffer: 0.5% NP40, 2% sucrose, in PBSA

2.1.9. Commercial kits and other reagents**2.1.9.1. DNA Handling**

QIAEXII Extraction kit	Qiagen
Endofree plasmid Maxi kit	Qiagen
1KB DNA ladder	NEB
Klenow Buffer 10 X	66 mM Tris.HCl, 0.5 M NaCl, 66 mM MgCl ₂ , pH 7.5.
Rainbow Marker	GE Healthcare
AF1 mounting fluid	Citiflour
Aquamount fluid	VWR Ltd

2.1.9.2. Transfection reagents

NucleofectorTM Solution Amaxa Biosystems

2.1.9.3. Transformation reagents

E.Coli DH5 α chemically competent cells Invitrogen Life Technologies

2.2. Methods

2.2.1. DNA manipulation techniques

2.2.1.1. Restriction endonuclease digestion

DNA was digested in a final volume of 10-20 μ l, in buffer reaction conditions according to manufacturer's guidelines. The number of units of enzyme added per reaction was dependent on the quantity of DNA present. Typically 10 units of enzyme were used per 5 μ g of DNA. Restriction enzyme digests were incubated, unless otherwise stated, at 37°C for 1-3 hr.

2.2.1.2. Removal of phosphate groups from DNA 5' ends

1 unit of CIP was added to restriction endonuclease digests to remove phosphate groups from 5' ends of DNA fragments to prevent vector re-ligation.

2.2.1.3. Generation of blunt ended linear DNA fragments

DNA fragments generated by digestion with the appropriate restriction enzyme were blunt ended using fill in reactions containing 2 units Klenow DNA polymerase, 100 μ g/ μ l BSA, 5 mM DTT, 100 μ M dATP, 100 μ M dTTP, 100 μ M dGTP, 100 μ M dCTP, 1xKlenow buffer. Reactions (20 μ l) were incubated at 37°C for 1 hr.

2.2.1.4. Separation of DNA fragments by agarose gel electrophoresis

DNA fragments were separated and identified using 50-100 ml gels containing 1%-1.2% agarose. The DNA samples were analysed by gel electrophoresis with 50-100 ml 1xTBE and 1 μ g/ml ethidium bromide at 50 V. DNA was visualised by UV transillumination and photographed using a camera with Polaroid 667 film.

2.2.1.5. Isolation of DNA fragments from agarose gels

Long wave UV transillumination was used to visualise DNA fragments to be isolated and purified. Appropriate DNA fragments were excised using a sterile scalpel. DNA was extracted using a QIAquick gel extraction kit (QIAGEN). Purified fragments were checked on 1% agarose gels.

2.2.1.6. Phenol/Chloroform extractions

DNA eluted using the QIAquick method was phenol/chloroform extracted to give more concentrated preparations. The final volume of DNA solutions was brought up to 50 μ l by the addition of dH₂O. An equal volume of phenol/chloroform (1:1) was added and the mixture vortexed prior to centrifugation at 13000 rpm (MSE microfuge) for 2 min. The resulting upper aqueous phase was transferred to a fresh microfuge tube and an equal volume of chloroform was added. The mixture was vortexed briefly and centrifuged again at 13000 rpm (MSE microfuge) for 2 min. For ethanol precipitations 2.5 volumes of 100% ethanol, 0.3 M sodium acetate and 5 mM EDTA was added to the aqueous phase and incubated at -20°C for 2 hr. For isopropanol precipitations an equal volume of isopropanol was added to the aqueous phase with 0.3 M sodium acetate and 5 mM EDTA. The mixture was left to precipitate at room temperature for 1 hr and spun down at 13000 rpm (MSE microfuge) for 5 min. The resulting pellet was washed with 0.5 ml 100% ethanol, and air dried and resuspended in an appropriate volume of dH₂O.

2.2.1.7. Ligation of compatible DNA fragments

Vector and insert were digested with the appropriate restriction endonuclease and purified by phenol/chloroform extraction, as described above. DNA was analysed by gel electrophoresis and purified using a gel extraction kit (QIAGEN). The purified DNA fragments were ligated using a variety of vector-insert ratios depending on the size of vector and insert. Final reaction volumes of 10 μ l containing 1xT4 DNA ligase buffer and 10 units T4 ligase were used per ligation mixture. Reactions were ligated for 4-12 hr at 16°C. Ligated DNA was stored at -20°C.

2.2.1.8. Transformation of DNA into competent bacteria

Approximately 1-5 μ l ligation mix with 25-50 μ l of *E-coli* DH5 α bacterial cells was incubated on ice for 20 min. The transformation mix was heat shocked at 37°C for 30 sec and followed by a further 2 min incubation on ice. 500 μ l of pre-warmed L-broth was added to the transformed cells and the mixture placed in an orbital shaker (200 rpm) at 37°C for 1 hr. 150 μ l of the transformed cells was plated onto L-broth agar plates containing 50 μ g/ml of the appropriate antibiotic to allow selection of the transformants. The plates were incubated overnight at 37°C to allow the growth of single colonies.

2.2.1.9. Small scale DNA preparation

Starter cultures were generated by inoculating 1 ml L-broth containing the appropriate antibiotic with a single bacterial colony. This was placed in an orbital shaker at 200 rpm overnight at 37°C. Plasmid DNA was extracted from pellets using a QIAGEN Mini-prep kit according to manufacturer's guidelines, as follows: Starter cultures were centrifuged at 3000 rpm in a bench top centrifuge for 30 min at 4°C with the resulting supernatant being discarded. The bacterial pellet was resuspended in 4 ml buffer P1 and the cells lysed by the addition of 4 ml buffer P2, and incubated at room temperature for 5 min. 4 ml buffer P3 was added to the mixture and the tube inverted 4-6 times and incubated on ice for 15 min. The supernatant was applied to a QIAGEN tip, previously equilibrated with 4 ml buffer QBT, and allowed to enter the resin. The column was washed with buffer QC. DNA was eluted using 5 ml buffer QF and precipitated by adding 3.5 ml room temperature isopropanol to the eluted DNA and centrifuged at 11000 rpm (Sorvall SS-34) for 30 min at 4°C. The DNA pellet was washed with 2 ml 70% room temperature ethanol and centrifuged at 11000 rpm (Sorvall SS-34) for 10 min at 4°C. The supernatant was decanted and the DNA pellet air dried and resuspended in 300 μ l of 10 mM Tris.HCl pH 8.5.

2.2.1.10. STET preparations

Bacterial colonies were picked from selective plates and inoculated in 2 ml L-broth containing the appropriate selective antibodies and incubated overnight at 37°C in an orbital shaker (200 rpm). The following day 1.5 ml of the culture was

transferred into a 1.5 ml eppendorf tube and centrifuged for 2 min at 6000 rpm (MSE microfuge). The medium was removed and the bacteria were resuspended in 100 μ l STET plus 5 μ l 10 mg/ml lysozyme, and the mixture was vortexed. The eppendorf tubes were transferred to a boiling water bath for 1 min and then centrifuged for 10 min at 13000 rpm (MSE microfuge). The resulting supernatant was transferred to a new eppendorf tube containing 400 μ l 0.3 M sodium acetate pH 7 and 0.5 ml isopropanol and vortexed. The mix was centrifuged at 13000 rpm (MSE microfuge) for 5 min and the resulting supernatant discarded and the pellet air dried and resuspended in 33 μ l of dH₂O.

2.2.1.11. Large Scale DNA preparation

100 μ l of starter culture containing the required DNA plasmid was used to inoculate 200 ml of L-broth, containing 50 μ g/ml of the appropriate antibiotic, and shaken overnight at 200 rpm in an orbital shaker at 37°C. Cultures were centrifuged at 3000 rpm for 30 min at 4°C (Sorvall RT60000B) and the resulting supernatant discarded. Plasmid DNA was extracted according to manufacturers guidelines using a Qiagen Maxi-prep kit as follows. The bacterial pellets were resuspended in 10 ml buffer P1 and lysed with 10 ml buffer P2. Lysis was stopped by the addition of buffer P3. The lysate was filtered through a QIA filter cartridge. 2.5 ml buffer ER was added to filtered lysate mix and incubated on ice for 30 min. The filtered lysate was transferred to an equilibrated QIAGEN-tip 500 to allow DNA to bind to the resin and the column was washed twice with 30 ml buffer QC. DNA was eluted using buffer QN and precipitated by adding 10.5 ml room temperature isopropanol to the DNA and centrifuged at 11000 rpm in a Sorvall SS-34 rotor for 30 min at 4°C. The DNA pellet was washed with 5 ml endotoxin free 70% ethanol and centrifuged at 11000 rpm (Sorvall SS-34 rotor) for 10 min at 4°C. The supernatant was discarded and the DNA pellet air dried and re-dissolved in 350 μ l buffer TE and transferred to a fresh microfuge tube.

2.2.1.12. Nucleofection of adherent cells

Transfection of adherent cells was carried out using a Nucleofector™ (Amaxa). HFFF2 cell monolayers maintained in 175 cm² tissue culture flasks were trypsinised and resuspended in RPMI growth medium. Cell density was determined (2×10^5 - 2×10^7 cells/ml) and cells were centrifuged at 1000 rpm using a

RTH-250 rotor for 10 min at 20°C. The supernatant was discarded and the cell pellet resuspended in room temperature Nucleofector™ Solution R to a final concentration of 2×10^5 - 2×10^7 cells/100 μ l. Each 100 μ l of cell suspension was mixed with 5 μ g of the required DNA, transferred to a cuvette and placed in the Nucleofector™ at the appropriate program and transfected. 500 μ l pre-warmed RPMI medium was added to the transfected cells prior to samples being seeded into 24 well plates and incubated at 37°C overnight.

2.2.1.13. Virus infection of mammalian cells

24 well plates seeded with 1.5×10^5 cells, 13 mm coverslips seeded with 8×10^4 cells or 35 mm plates seeded with 1×10^6 cells (unless otherwise stated) in 1 ml (24 well plate) or 2 ml (35 mm plates and 13 mm coverslips) D5+5 medium were incubated overnight at 37°C. The growth medium was removed, the following day and cells were infected with the appropriate virus in a volume of either 100 μ l (24 well plate) or 200 μ l (35 mm plates and 13 mm coverslips) and incubated at 37°C with plates being rocked gently every 10 min for 1 hr. Following incubation either 1 ml (24 well plate) or 2 ml (35 mm plates and 13 mm coverslips) of fresh medium was added to the cell monolayers and the incubation continued at 38.5°C. For longer incubation periods cell culture medium was changed every 2 days.

2.2.2. Protein manipulation techniques

2.2.2.1. Preparation of cell lysates

Culture medium was removed from cell monolayers grown in 24 well tissue culture plates and the monolayers were washed with 1 ml PBSA. 40 μ l 1xSDS gel loading buffer was added to each cell monolayer. The resulting lysates were scraped into 1.5 ml microfuge tubes and stored at -20°C.

2.2.2.2. SDS polyacrylamide gel electrophoresis of proteins

Cell lysates were boiled for 10 min at 100°C to ensure complete denaturation of the proteins to be resolved by electrophoresis. SDS-PAGE was carried out using Bio-Rad mini Protean II apparatus. Resolving gels containing 4.17 ml distilled

water, 2.5 ml resolving gel buffer, 3.33 ml 30% acrylamide, 80 μ l 10% ammonium per sulphate, 8 μ l TEMED were overlaid with ethanol. Following polymerisation the ethanol was rinsed off before overlaying with the stacking gel containing 1 ml distilled water, 0.6 ml stacking gel buffer, 0.4 ml acrylamide, 20 μ l 10% ammonium per sulphate and 3 μ l TEMED. Samples were analysed by gel electrophoresis at 150 V in running gel buffer till the dye front reached the bottom of the gel. Prior to blotting the gel was removed from electrophoresis apparatus.

2.2.2.3. Western blot analysis of denatured proteins

SDS-PAGE gels were transferred to nitrocellulose membranes by the assembly of a blotting sandwich, the components of which were pre-soaked in transfer buffer and assembled as follows: The gel was placed on a 9.5 cm x 8.0 cm piece of Whatman No.1 filter paper and overlaid with nitrocellulose membrane cut to 8.5 cm x 7.0 cm and a second piece of Whatman No.1 filter paper, cut as before, placed on top and air bubbles expelled. The assembled sandwich was placed in a Bio-Rad mini-transblot apparatus and the proteins electroblotted at 250 mA for 2-4 hr at 4°C. The membrane was blocked in 25 ml PBSA+TWEEN and 5% dried milk for 1 hr at room temperature. The membrane was washed 3 times in 100 ml PBSA+TWEEN for 5 min and incubated with primary antibody at the appropriate dilution in 20 ml PBSA+TWEEN and 5% dried milk for 4-12 hours at 4°C. The membrane was washed 3 times in 100 ml PBSA+TWEEN for 5 min. The blot was incubated for 1 hr at room temperature in secondary antibodies which were diluted to appropriate concentrations in 20 ml PBSA+TWEEN and 2% dried milk. The membrane was washed 3 times in 100 ml PBSA+TWEEN for 5 min and proteins were detected using ECL reagents (Amersham). A 2 ml mixture of ECL western blotting reagents was applied to the drained membrane for 1 min after which the membrane was placed between 2 sheets of Melinex hazy 23-micron film and exposed to Kodak X-omat S film.

2.2.2.4. Histochemical staining for β -galactosidase in tissue culture monolayers

Cell culture medium was removed from cell monolayers, grown in 24 well plates. Each cell monolayer was fixed with 1 ml 1% glutaraldehyde in a fume cupboard. The fix solution was removed after 45 min incubation at room temperature and the

cell monolayers washed with 2 ml PBSA. 1 ml of β -gal reaction mixture was added to the cell monolayers and the plates incubated at 37°C for 2-4 hr until blue cells became visible under a low power light microscope. The cell monolayers were washed with 2 ml dH₂O and positive blue cells counted.

2.2.2.5. Carmalum staining

Cell monolayers to be retained for digital imaging were washed with dH₂O to remove the β -gal reaction mixture. Prior to monolayers drying out, 1 ml of Carmalum stain was added and monolayers were incubated at 4°C for 4-5 days. Following staining the dye was removed and the plates were washed with dH₂O, dried and stored until required.

2.2.2.6. Digital imaging of β -gal positive cells

Digital images of β -gal positive cells were obtained by mounting a clean coverslip of the appropriate size over the stained monolayers using aquamount fluid. Images were taken using a Nikon TS100 microscope and a SPOT INSIGHT camera and software.

2.2.2.7. Secreted Alkaline Phosphatase (SEAP) assays

Analysis of SEAP was carried out by infecting cell monolayers with a HSV-1 recombinant virus expressing SEAP at 38.5°C. 150 μ l of growth medium was harvested and samples were incubated at 65°C to destroy endogenous alkaline phosphatase and allowed to cool to room temperature. 25 μ l of sample was transferred to a fresh 1.5 ml microfuge tube and the remaining samples stored at -20°C. To each sample 25 μ l of assay buffer, containing 25 μ l 2xSEAP buffer and 1 μ l 4-methylumbelliferyl phosphate (MUP) was added. Reactions were vortexed and incubated in the dark for 1 hr at room temperature. The reaction was stopped by placing samples on ice and fluorescence measured when 25 μ l of each reaction was added to 2 ml dH₂O in a cuvette in a HSI DNA fluorometer.

2.2.3. Virus propagation techniques

2.2.3.1. Preparation of recombinant HSV-stocks

Recombinant HSV-1 stocks were propagated in BHK-21 cells grown at 37°C in tissue culture roller bottles to approximately 90% confluency. The cells were inoculated with 0.2 ml of seed stock in 100 ml ETC10 medium containing 3 mM HMBA. The cells were incubated at 31°C until CPE was observed. The cell suspension was transferred to a Sorvall goose necked bottle and centrifuged at 5,000 rpm in a Sorvall SLA-1500 GSA rotor for 10 min at 4°C. The supernatant was transferred to a fresh goose necked bottle and centrifuged at 12,000 rpm for 2 hr in a Sorvall SL-1500 GSA rotor. The resulting cell pellets were resuspended in 4.5 ml ETC10 medium and sonicated in a bath sonicator to disaggregate the virus. The suspension was dispensed into 1.5 ml microfuge tubes and stored at -70°C.

2.2.3.2. Titration of recombinant HSV-1 stocks

Recombinant HSV-1 stocks were titrated on U2OS cell monolayers grown in 35 mm dishes to 90-100% confluency. Cell monolayers were infected with 200 µl serial dilutions of the viruses, with titrations being produced in duplicate. After a 1 hr incubation at 37°C the cells were overlaid with fresh D5+5 medium containing 3 mM hexamethylbisacetamide (HMBA) and 2% human serum. The cells were incubated at 31°C till plaques were observed. Upon observation of plaques medium was removed and the monolayers fixed with 1 ml 1% glutaraldehyde for 45 min. The fix solution was removed and the cells washed with 2 ml PBSA. 1 ml β-gal reaction mixture was added to the monolayers and incubation continued at 37°C for 2-3 hours until blue plaques could be observed. The β-gal reaction mix was washed off prior to counting plaques.

2.2.4. Cell culture techniques

2.2.4.1. Serial passage of eukaryotic cells

Eukaryotic cells were maintained in 175 cm² tissue culture flasks (NUNC) in 50 ml of the appropriate growth medium. For serial passage the growth medium was removed and cell monolayers washed with 10 ml versene, which was

subsequently poured off. 10 ml versene containing 2 ml trypsin was washed over the cells and all but 5 ml removed. Gentle agitation was applied to the flask for 5 min, allowing the cell monolayer to detach. 10 ml of appropriate fresh growth medium was added to the cell suspension and seeded into tissue culture flasks containing 40 ml fresh growth medium. HFFF2 cells were typically split at a ratio of 1:4, while both U373 cells and U2OS cells were split at a ratio of 1:3.

2.2.4.2. Seeding of eukaryotic cells into tissue culture dishes

Eukaryotic cell monolayers maintained in 175 cm² tissue culture flasks were trypsinised and re-suspended in appropriate growth medium as described above. Cells were seeded, into 24 well plates or 35 mm plates.

2.2.5. Microscopy techniques

2.2.5.1. Immunofluorescence

Cells were grown on sterile 13 mm diameter coverslips in 24 well tissue culture plates to approximately 75% confluency. After incubation with virus or DNA plasmid, culture medium was removed and monolayers washed twice with PBSA. Monolayers were fixed with 0.5 ml fixing solution, at room temperature, for 10 min. After fixation cells were washed 3 times with PBSA+1% FCS and permeabilised with 0.5 ml permeabilisation buffer for 5 min at room temperature. Following removal of permeabilisation buffer cells were washed 3 times with PBSA+1% FCS. 20 µl of the appropriate primary antibody dilutions, in PBSA+1% FCS, were applied to each coverslip and incubated at room temperature for 1 hr. Coverslips were washed 3 times with PBSA+1% FCS and 20 µl of the appropriate secondary antibody, diluted in PBSA+1% FCS was applied to the coverslips. After incubation in the dark for 30 min at room temperature, coverslips were washed 3 times with PBSA+1% FCS, once with dH₂O and air-dried. The coverslips were mounted onto glass microscope slides using 5 µl Citifluor, the edges sealed with clear nail varnish and stored at 4°C.

2.2.5.2. Confocal microscopy

Immunolabelled cells and those expressing EYFP conjugates were examined using a Zeiss LSM 510 confocal microscope attached to a computer with the appropriate LSM software. Images were exported and saved.

Chapter 3

Short-term and long-term expression analyses of the UL82 homologues

3. Part I

3 1. Introduction

The HCMV tegument protein pp71 is important for transactivating IE gene expression and initiating lytic replication. This protein has also been shown to stimulate transcription from IE promoters in HSV-1 genomes. Studies showed that pp71 stimulates expression of genes under the control of the HCMV MIEP in short-term assays (Homer et al., 1999, Liu & Stinski, 1992, Marshall et al., 2000). Preston and Nicholl (2005) showed, using various reporter based assays, that pp71 could direct long-term gene expression (see Introduction section 1.10.7 for details).

In the study described here a HSV-1 mutant, *in1382*, which contains the *lacZ* gene inserted in the TK locus under the control of the MIEP was employed. This virus was impaired for transcriptional activity due to mutations at VP16, ICP0, a temperature sensitive mutation at ICP4 therefore was unable to enter lytic replication, due to the absence of IE proteins. In the presence of pp71 quiescence was overcome, as pp71 allowed continued expression from the HCMV IE promoter cloned into the genome. In the study presented here a comparison of pp71 with UL82 homologues from Simian CMV (S82), Baboon CMV (B82), Rhesus CMV (Rh82), and Chimpanzee CMV (Ch82) was carried out to establish if pp71 was unique in its ability to stimulate long-term gene expression.

3.1 1. Sequence analysis of the UL82 homologues

Amino acid sequences of pp71 (Chee et al., 1990, Dargan et al., 1997, Davison et al., 2003a), and its homologues S82 (Nicholson, 2004), B82 (Accession number AF324835), Rh82 (Hansen et al., 2003) and Ch82 (Davison et al., 2003a) were analysed using Vector NTI (Vector NTI suite 9.0) in order to determine their degrees of homology. The analysis of the primate CMV UL82 amino acid sequences in figure 3.1 shows a large number of conserved regions between all five homologues, indicating a significant degree of homology. A more detailed sequence analysis of the homologues, carried out by Nicholson (2004), led to the construction of a phylogenetic tree showing the relative evolutionary distances of the proteins from one another (Nicholson, 2004) (figure 3.2). The tree shows that

		1		50
B82	(1)	----	MDRP-QEER EPRPSTSRPLSLSATFERLSQV MRVISTQNT-TLEA	
Ch82	(1)	MSRSPS-	PGEGPSAAGPGGAPGDNGSTFGRMHCQVLRRLVTNHDS-SLEP	
pp71	(1)	MSQASSS	PGEGPSSEAAAISEAEAASGSFGRLHCQVLRRLITNVEGG-SLEA	
Rh82	(1)	----	MDRPP EEEEE EPRPSTSRALAPAATFERLTQQLRLVCTQHS-PLDV	
S82	(1)	----	MDRPP EEEEE EPRPSTSRAPAAPATFDRLTCHVLRMITTQST-TMET	
Consensus	(1)		MDRP EEE EPRPSTSR A AATFERLTCQVLRRLITTQ S SLE	
		51		100
B82	(45)		DAVKVNWHTHVQVANPAVICAFQESTCTRDALQLTDISIKGRSSSTLRD	
Ch82	(49)		DRLKILDLRTSVEVSRVSVLCLFQENKSKQHDVLDLTLNKGHC AVGERD	
pp71	(51)		GRLRLDLRTNIEVSRPSVLCFQENKSPHDTVLDLTLNKGRCVVGEQD	
Rh82	(46)		DAVQTMNWHTSVEVANRAVICAFQEMKSSRDALQLTDLNLKGHCSTFRD	
S82	(46)		NAVKVIDWHANIQVANPAVICTFQEVKSPRDLQLTDLNLKGRCSSSTLRD	
Consensus	(51)		DAVKVLDWHT VEVANPAVIC FQE KS RD LQLTDLNLKGRCSSST RD	
		101		150
B82	(95)		QLRTDVGNYANKRLKSGT--HTKSM LVFALPLLRVPVTGIHLFRG--KAK	
Ch82	(99)		QLKADLINYSQRRMSPGS--STPI SVLAFGLPLERVVSGIHLFQAHPRGD	
pp71	(101)		RLLVDLNNEGPRRLTPGSENNTVSVLAFALPLDRVPVSGLHLFQSQRGG	
Rh82	(96)		SLRTDACNYANRRLSPGS--QTSAM LVFALPIVRVPVTGIHLFRG--RGN	
S82	(96)		SLRTDVCNFSDTRLRSGS--NTMSV LVFALPLVRVPVTGIHLFRG--RAQ	
Consensus	(101)		LRTDL NYANRRLSPGS NTISV LVFALPLVRVPVTGIHLFRG RG	
		151		200
B82	(141)		NENRPLKANARATIRRQYMWKVLNLDKI IWNRRRDPNIEGGQFFTTDF	
Ch82	(148)		EENRL-RTEARVDIRR TAYHWGVRTTVSPR-WRRKVDRSLEAEQIFTTDF	
pp71	(151)		EENRP-RMEARAIIRR TAHHWAVRLTVPN-WRRRTDSSLEAGQIFV SQF	
Rh82	(142)		SQNRPPRANARTTIRRAQYTWTVKVNVAITWTRKR DQYVEGGYTFATDF	
S82	(142)		SENRP PRANARVTIRRAQYMWTVKVNLAGINWSRRRDSHTEGGQFFTSDF	
Consensus	(151)		ENRP RANAR TIRR QY W VKLNVS I W RRRD LEGGQ FTTDF	
		201		250
B82	(191)		IFSTELIPLTVVDAMDQLACSDGYTHVQKAETVGENLVRVFLINLSHHP	
Ch82	(196)		IFRAGAIPLRLVDAVELLS CDRNTYIHK AETDARGQWVNVHLQHETLHP	
pp71	(199)		AFRAGAIPLTLVDALEQLACSDPNTYIHK TETDERGQWIMLFLHHDSPHP	
Rh82	(192)		TFLTGLIPLTVDAIDQLACSN GDTYVQKVETIGEENLILVSLIHFSLHP	
S82	(192)		TFATDLMPLTVVDAMDQLACSDADTYIQKAETVGEQNLI RVIYIHL SGHP	
Consensus	(201)		F TGLIPLTLVDAAMDQLACSDG TYIQKAETVG NLI VFLIH S HP	
		251		300

B82 (241) PQELFLQLSVYSHRAEVMCRHNPEPFFQRHSDNGFLVKNTKGV TIP-AHH
 Ch82 (246) PPSVFLHFSLYTHGAEVVLRHNPHYHLTRHGDNGFTLHAPRGFTLSRLHR
 pp71 (249) PTSVFLHFSLYTHRAEVARHNPHYHLRRLPDNGFQLLIPKSFTLTRIHP
 Rh82 (242) PTEVFLQLSVYAHRAEVMWRHNPEPFFERHSENGFLVKCPLHVTIP-AHQ
 S82 (242) PAEMFLQMSVYSHRAEVI CRHNPAEPFFERHAENGFLVRNPHTVNIIP-AHH
 Consensus (251) P EVFLQLSVYSHRAEVM RHNPEPFF RHSDNGFLVK PK VTIP AH
 301 350
 B82 (290) THVAHFNNAFETQNTCSFLFFPVDIPGLSIECGPLQNRMKITIKMQNLTK
 Ch82 (296) EYIVQVQNAFETNNTHDVIFFPADIPGVSMEAGPLPDRVIRITIRLTWTGE
 pp71 (299) EYIVQIQNAFETNQTHDTIFFPENIPGVSIEAGPLPDRVIRITLRVTLTGD
 Rh82 (291) TYVVQFNNALETQDTCYAVFFPLELPGISMDAGPLPNRMKITINVQNLTA
 S82 (291) THVAHFNNAIETQGTCHLFFPIDIPGLSIEAGPLTSRMKITLKIQNLTK
 Consensus (301) TYVVQFNNAFETQNTC IFFPIDIPGLSIEAGPLP RMKITIKVQNLTK
 351 400
 B82 (340) TEISVSFMQTI GLIHFPRGTLTYTMPNKTLSACSQIRLRAGLCPRESIA
 Ch82 (346) NSVRIEHMQILGTIHLFKRGVNLNLLPGKTEKIKRPQIQLRAGLFPRAVM
 pp71 (349) QAVHLEHRQPLGRIFHFRRGFWTLTPGKPKIKRPQVQLRAGLFPASNVM
 Rh82 (341) NAITLAHMQMLGFIHFRRGVGLPNKTETPRCSQIRLRAGLFPDSDIL
 S82 (341) TAITVNYMQMLGFIHFRRGSLATMPNRTQTPRCSQIRLRAGLFPDSDVIM
 Consensus (351) NAITL HMQMLG IHFFRRGSL LLPNKTET KCSQIRLRAGLFPDSDIM
 401 450
 B82 (390) RG- ISQFAEQ-----HS SSSE---DEDELPGTTPPIVTEAIFNPFQ
 Ch82 (396) RGEVSEFRPQSPGELPLEGEEEEEE---EEERSSTPTPPALSESVFAAFE
 pp71 (399) RGAVSEFLPQSPGLPPTEEEEEEEDDEDDLSSTPTPPPLSEAMFAGFE
 Rh82 (391) RG- ISEFAQQP-----NNSSSSE---DEEEGPPITPPIITEAIFDPFQ
 S82 (391) RGVISQFVEQ-----NS SSSEE---EEDEPVPLTPPILTEAIFAPFQ
 Consensus (401) RG ISEF Q SSSEE DEEDE TPPILTEAIFAPFQ
 451 500
 B82 (428) SENESTSDEDDER-----KRGGRPATPHIS-DQLSPTSMLLTLP
 Ch82 (443) -ESSEEEESDTEEG-----LSRALALTGRRRPRRGAGEGEDLMLVIP
 pp71 (449) -EASGDESDTQAG-----LSPALILTGQRR---RSGNNGALTLVIP
 Rh82 (431) SEDSSDEDEPQTTMDRLRREAHKAKREGTAAVPVTHRERLPKTAMLLVVP
 S82 (431) SENDSTSDDEEPEPTTSARLRAEARARREAGQPVP-ERPPPITVQLLSLP
 Consensus (451) SE SDEDED E SRA TG P E TALLLVIP
 501 550
 B82 (467) CWNMYMHLENLMPITASVEDNAVKN TSYLKSEMDGDICTAADIDVAYQTL

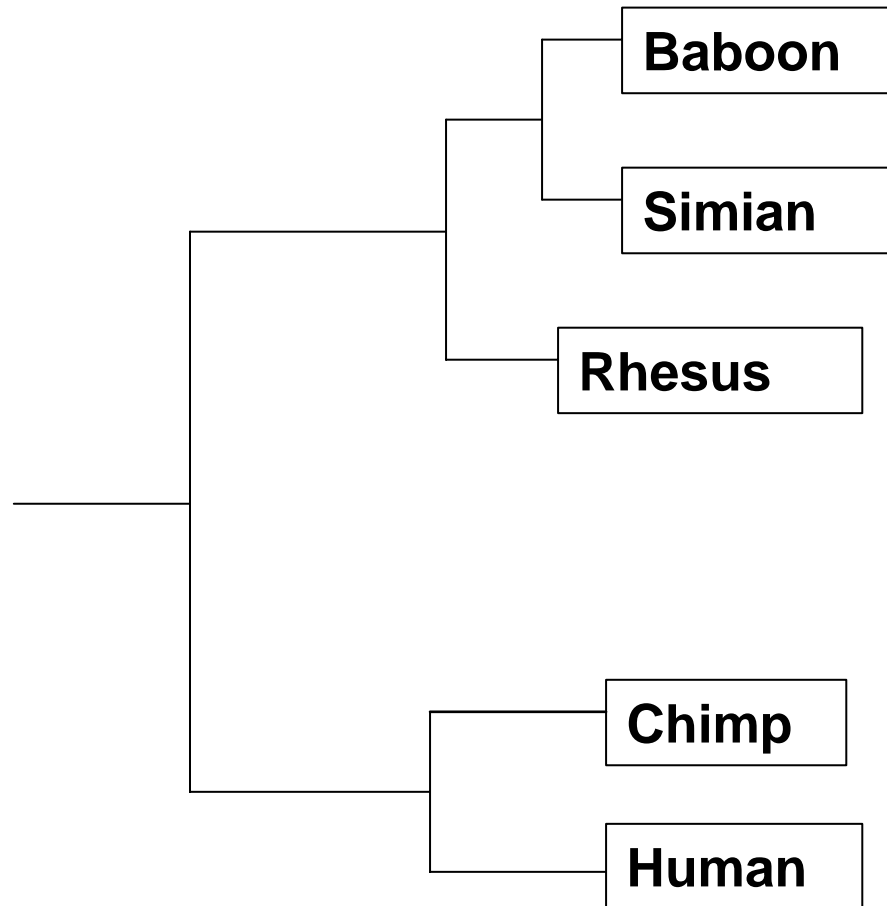


Figure 3.2. Phylogenetic analysis of UL82 homologues

Phylogenetic tree showing evolutionary relatedness between primate UL82 homologues and HCMV pp71. HCMV pp71 and Ch82 proteins appear to be evolutionarily distinct from S82, which shows greater homology to B82 and Rh82. The tree was constructed by the alignment of sequences using ClustalW using a multipurpose multiple peptide program, which employs the Blosum62 matrix (Nicholson, 2004).

the pp71 and Ch82 proteins form a distinct group due to a greater degree of homology between their sequences (Davison et al., 2003a), while the S82 protein exhibits a greater degree of sequence homology with the B82 protein in a group separate from the Rh82 protein (Nicholson, 2004).

Studies with an HSV-1 recombinant expressing YFP-tagged S82 under the control of the HCMV MIEP showed S82 to be a transactivator of short-term gene expression. However the S82 protein was unable to direct long-term gene expression (Nicholson, 2004). The study described here investigated whether the Ch82, B82 and Rh82 homologues behaved like pp71 or S82 in terms of long-term gene expression.

3.1.2. EYFP-tagged UL82 homologues as transactivators of gene expression

The role of pp71 as a transactivator of short-term gene expression is well known (Homer et al., 1999, Liu & Stinski, 1992, Marshall et al., 2002). Work by Nicholson. (2004) showed that the S82 protein also stimulated short-term gene expression from the HCMV MIEP (Nicholson, 2004). To determine if the non-human UL82 homologues (B82, Rh82, and Ch82) also transactivated short-term gene expression, plasmids pEYFPpp71, pEYFPS82, pEYFPB82, pEYFPRh82, pEYFPCh82 and pEYFP-C1 all under the control of the HCMV MIEP were transfected into HFFF2 cells using the Nucleofector™ system (Amaxa). The transfected cells were cultivated in 24 well plates overnight at 37°C. To investigate the activities of the homologues, transfected cells were infected with 3×10^5 pfu, 1×10^5 pfu or 3×10^4 pfu of the HSV-1 recombinant virus *in1382* and maintained at 38.5°C. This HSV-1 mutant is inactive for VP16 and the IE proteins ICP0 and ICP4, but contains *lacZ* under control of the HCMV MIEP (Preston et al., 1998). This virus is unable to progress past the IE stage of infection so can be used to assess the activity of the UL82 homologues by observing expression of the reporter gene. At 24 hr post-infection cell monolayers were stained with X-gal and the numbers of β -gal positive cells counted. Figure 3.3 shows the average numbers of β -gal positive cells at 24 hr post-infection from three individual experiments, the raw data for which are presented in table 3.1. Cultures transfected with each of the plasmids expressing a UL82 homologue gave more β -gal positive cells than those transfected with the control vector, pEYFP-C1, when subsequently infected with 3×10^5 pfu, or 1×10^5 pfu of *in1382*. At the highest

		Experiment 1		Experiment 2		Experiment 3	
Plasmid	Titre (pfu)	24 hours	10 days	24 hours	10 days	24 hours	10 days
	3x10 ⁵	18	0	59	0	45	0
pEYFP-C1	1x10 ⁵	11	0	14	0	0	0
	3x10 ⁴	4	0	0	0	0	0
	3x10 ⁵	74	300	262	379	66	121
pEYFPpp71	1x10 ⁵	3	62	24	78	2	35
	3x10 ⁴	0	0	1	9	1	14
	3x10 ⁵	102	9	205	0	33	0
pEYFPS82	1x10 ⁵	12	6	41	0	0	0
	3x10 ⁴	0	0	1	0	0	0
	3x10 ⁵	79	8	115	0	52	0
pEYFPB82	1x10 ⁵	9	1	33	0	0	0
	3x10 ⁴	2	0	2	0	0	0
	3x10 ⁵	46	19	134	0	46	0
pEYFPRh82	1x10 ⁴	8	2	11	0	1	0
	3x10 ⁴	3	0	1	0	0	0
	3x10 ⁵	81	4	159	0	54	0
pEYFPCh82	1x10 ⁵	4	0	21	0	1	0
	3x10 ⁴	2	0	1	0	0	0

Table 3.1. Stimulation of β -gal expression by the EYFP-tagged UL82 homologues at 24 hr and 10 days post-infection

HFFF2 monolayers were transfected with plasmids expressing EYFP-tagged UL82 homologues, and infected with *in1382* at 24 hr post-transfection. After a further 24 hr or 10 days, monolayers were stained with X-gal and β -gal positive cells were counted.

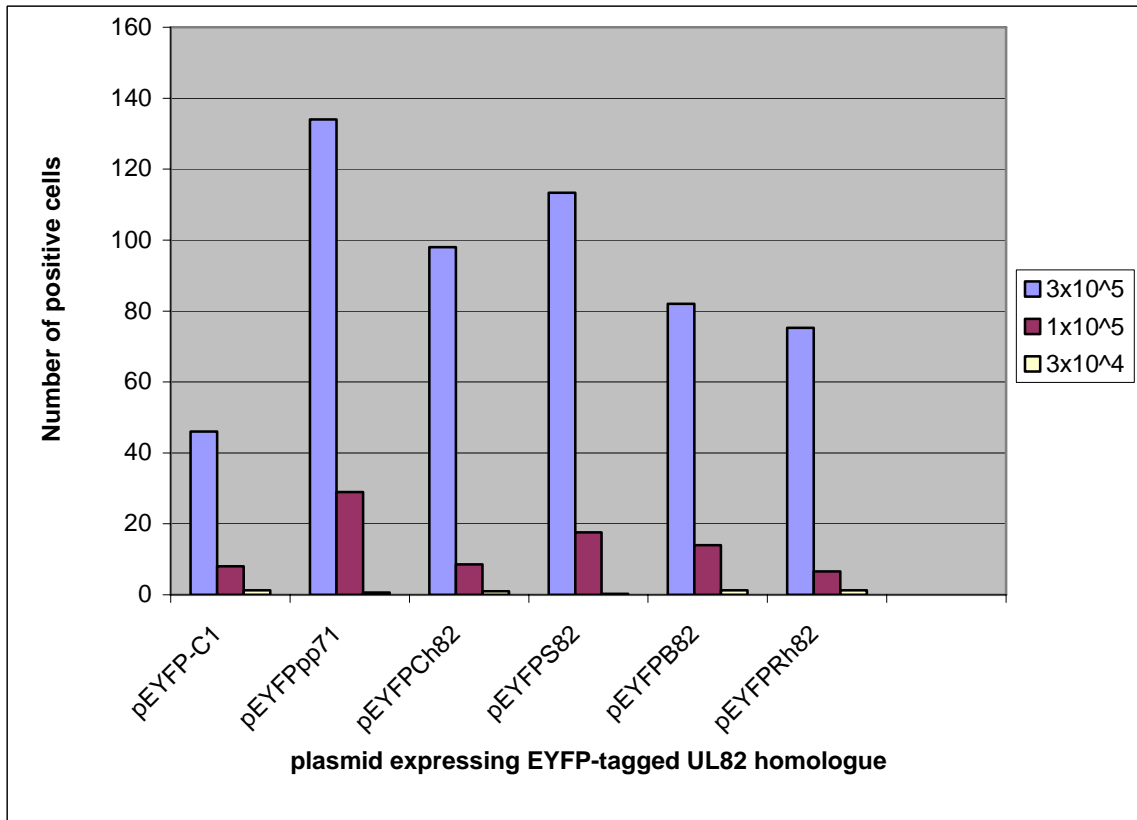


Figure 3.3. Stimulation of β -gal expression by EYFP-tagged UL82 homologues at 24 hr post-infection

HFFF2 monolayers were transfected with plasmids expressing the EYFP-tagged UL82 homologues, and infected with various amounts of *in1382* at 24 hr post-transfection. After a further 24 hr monolayers were stained with X-gal and β -gal positive cells were counted.

value of 3×10^5 pfu, in cultures transfected with the non-human UL82 homologues numbers of β -gal positive cells were greater than the control pEYFPC1. However, cultures transfected with plasmids expressing the non-human homologues all produced fewer β -gal positive cells than those transfected with pEYFPpp71. A similar pattern was observed from the numbers of β -gal positive cells in cultures infected with 1×10^5 pfu of virus.

At 10 days post-infection cell monolayers were stained with X-gal and β -gal expression was analysed. Figure 3.4 shows the average numbers of β -gal positive cells at 10 days post-infection. At the highest value of 3×10^5 pfu, the number of positive cells in cultures transfected with pEYFPpp71 increased in comparison to that at 24 hr. Cultures transfected with plasmids expressing the non-human homologues all showed a decrease in numbers of β -gal positive cells at 10 days post-infection compared to that observed at 24 hr.

Due to the large degree of variability in numbers of β -gal positive cells between individual transfection experiments, (table 3.1), it was not possible to carry out statistical analysis. Further experiments are needed to determine if the numbers are due to the alternative behaviour of these proteins or a result of experimental variability. However, the transfection experiments did indicate that that all the EYFP-tagged UL82 homologues were functional in the short-term while only pEYFPpp71 appeared to stimulate long-term gene expression. This was further confirmed using western analysis.

Lysates of HFFF2 cells transfected with plasmids pEYFP-C1, pEYFPpp71, pEYFPCh82, pEYFPS82, pEYFPB82, or pEYFPRh82 were analysed by gel electrophoresis, transferred onto nitrocellulose membranes and probed with an anti-GFP antibody to detect EYFP-tagged proteins. Figure 3.5 shows levels of UL82 proteins present at 24 hr post-infection. Plasmids pEYFPpp71, pEYFPCh82, pEYFPS82 and pEYFPB82 all expressed similar levels of protein at 24 hr post-transfection. However lysates transfected with pEYFPRh82 expressed lower levels of protein in comparison to those transfected with the other homologues. At 4 days post-transfection extracts from cells transfected with the plasmids expressing the non-human UL82 homologues continued to express similar levels of protein in comparison to lysates transfected with pEYFPpp71. At 10 days post-transfection, protein expression of the non-human UL82 homologues

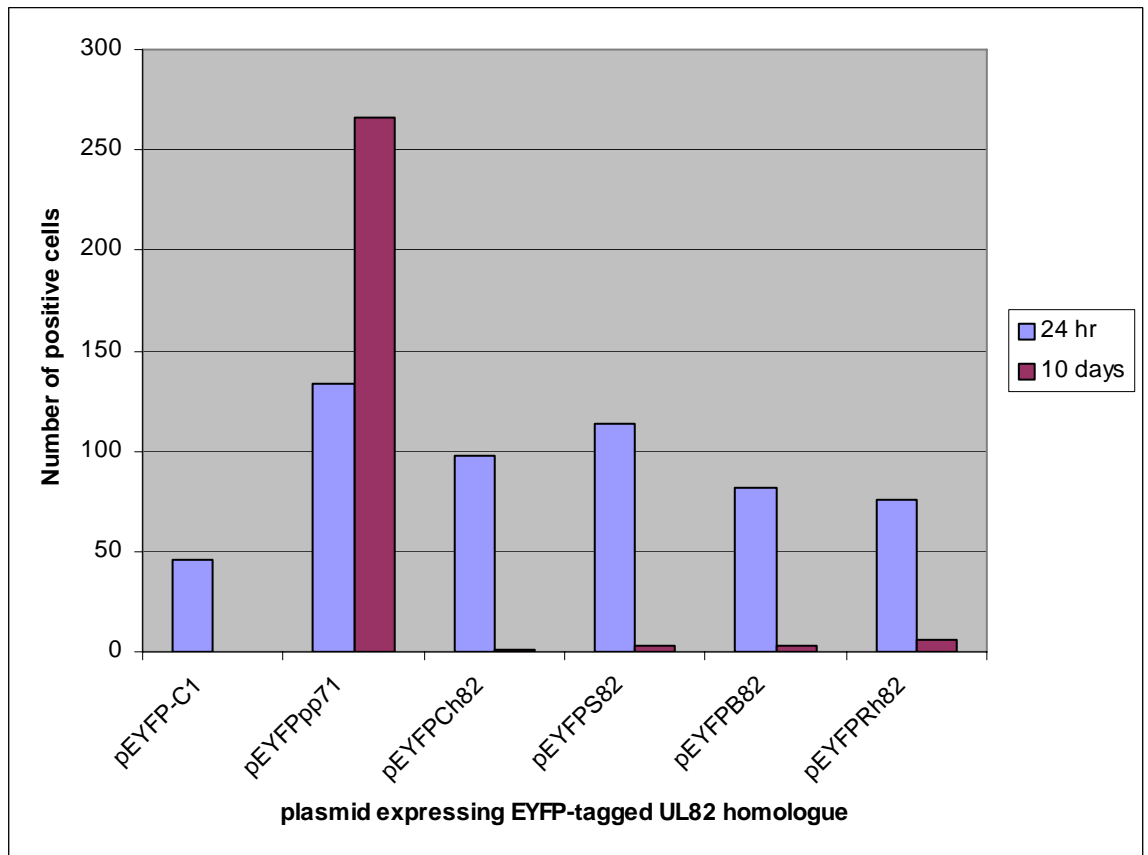


Figure 3.4. Stimulation of β -gal expression by EYFP-tagged UL82 homologues at 24 hr and 10 days post-infection

HFFF2 monolayers were transfected with plasmids expressing EYFP-tagged UL82 homologues, and infected with 3×10^5 pfu *in1382* at 24 hr post-transfection. After a further 24 hr or 10 days, monolayers were stained with X-gal and β -gal positive cells counted.

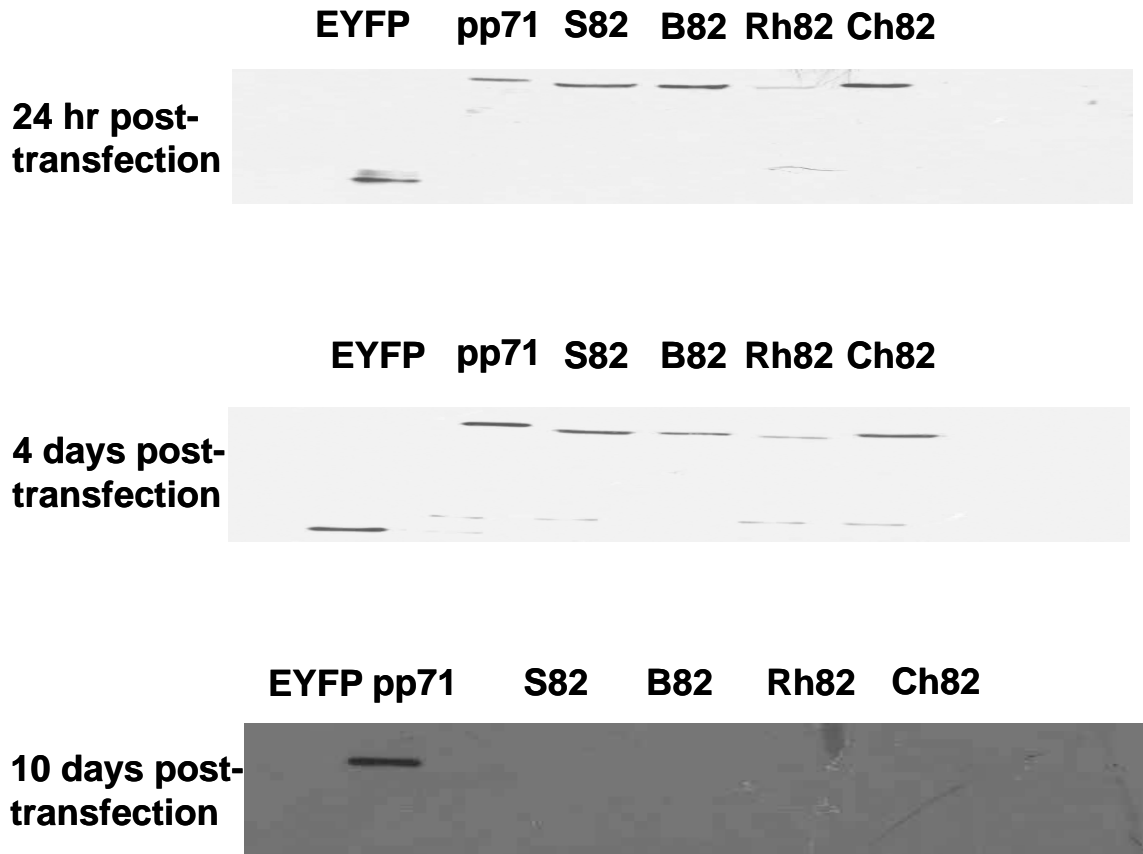


Figure 3.5. Expression of EYFP-tagged UL82 homologues 24 hr, 4 days, and 10 days post-transfection.

HFFF2 monolayers were transfected with plasmids expressing the EYFP-tagged UL82 homologues. Cell lysates were harvested at either 24 hr, 4 days or 10 days post-transfection and electrophoresed via SDS PAGE. EYFP-tagged UL82 homologues were detected using an anti-GFP primary antibody, and an anti-rabbit HRP-conjugated secondary antibody.

was not detectable. In cultures transfected with pEYFPpp71 an increase in levels of pp71 expression was observed indicating that only pEYFPpp71 was able to maintain self transcription.

Therefore transfection assays showed all five non-human UL82 homologues to be functional and able to stimulate gene expression from the HCMV MIEP in short-term assays but only pp71 to be able to simulate long-term gene expression.

3.1.3. Myc-tagged UL82 homologues as transactivators of gene expression

In order to confirm that the EYFP tag did not affect the properties of the UL82 homologues, each homologue was fused to a myc tag at its N-terminus. The myc-tagged plasmids expressing pp71 and the non-human UL82 homologues were used to analyse if myc-tagged pp71, like EYFP-tagged pp71, was unique in stimulating LT gene expression.

Plasmids pEYFP-C1 (control), pmyc-pp71, pmyc-S82, pmyc-B82, pmyc-Rh82 or pmyc-Ch82 were transfected into HFFF2 cells using the Nucleofector™ system, and monolayers were incubated at 37°C. At 24 hr post-transfection cell monolayers were infected with 3×10^5 pfu, 1×10^5 pfu, or 3×10^4 pfu of *in1382* and incubated at 38.5°C. Following incubation at either 24 hr or 10 days cell monolayers were stained with X-gal and β -gal positive cells were counted. Figure 3.6 shows the average numbers of positive cells. The data presented here show that only pmyc-pp71 was able to stimulate short-term gene expression from the HCMV MIEP. The plasmids pmyc-Ch82, pmyc-S82, pmyc-B82 and pmyc-Rh82 did not direct β -gal expression above the levels of the control (pEYFP-C1).

At 10 days post-infection in cultures transfected with pmyc-pp71 and infected with 3×10^5 pfu of *in1382*, the numbers of β -gal positive cells, increased at 10 days compared to numbers of β -gal positive cells seen at 24 hr post-infection, thus pmyc-pp71 was able to direct long-term gene expression. At 10 days post-transfection in cultures transfected with the myc-tagged non-human UL82 homologues no β -gal expression was detected. However as numbers of positive cells in cultures transfected with the myc-tagged non-human UL82 homologues did not exceed that of the control it is not possible to say that the non-human homologues are unable to direct long-term gene expression, as they did not

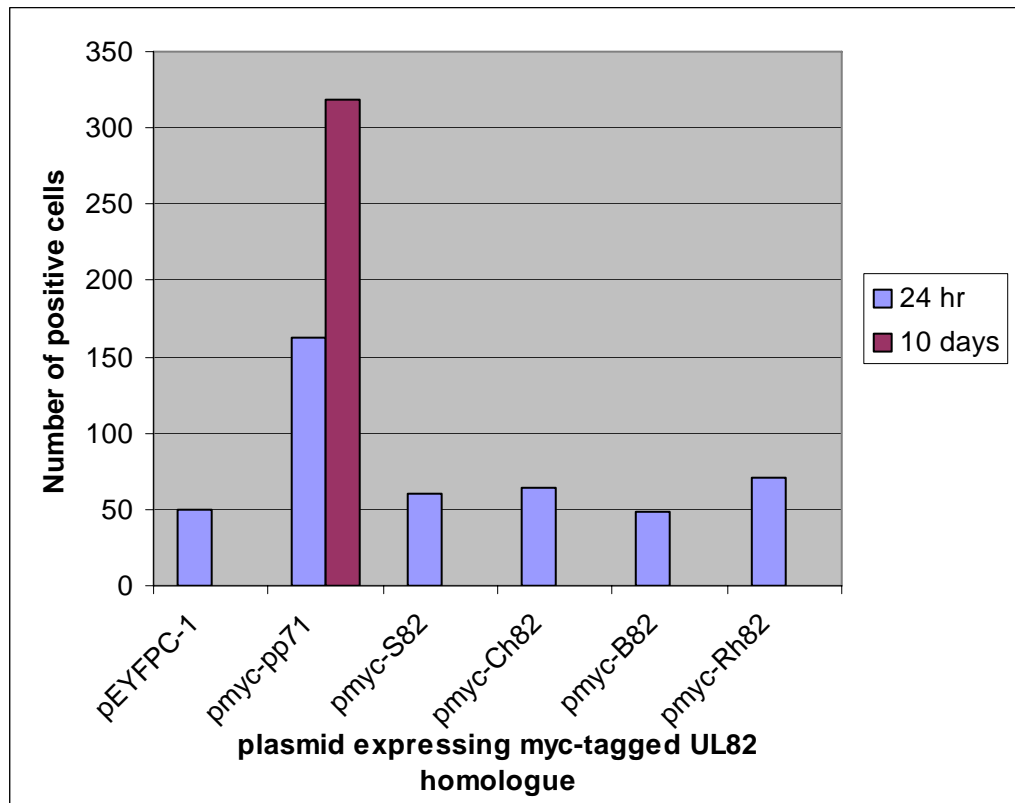


Figure 3.6. Stimulation of β -gal expression by the myc-UL82 homologues at 24 hr and 10 days post-infection

HFFF2 monolayers were transfected with plasmids expressing myc-tagged UL82 homologues, and infected with 3×10^5 pfu of *in1382* at 24 hr post-transfection. After a further 24 hr or 10 days, monolayers were stained with X-gal and β -gal positive cells were counted.

stimulate short-term gene expression. Protein expression of the myc-tagged UL82 homologues was analysed at 24 hr and 10 days post-transfection to confirm the data obtained from β -gal analysis.

Cell lysates transfected with pEYFP-C1 (control), pmyc-pp71, pmyc-Ch82, pmyc-S82, pmyc-B82 or pmyc-Rh82 were harvested at either 24 hr or 10 days post-transfection, electrophoresed by SDS PAGE and transferred onto nitrocellulose membranes. The myc-tagged proteins were detected using an anti-myc antibody (9E10). Figure 3.7 shows levels of protein present in lysates of cells transfected with plasmids expressing all five myc-tagged UL82 homologues. In lysates of cells transfected with pmyc-pp71 a greater amount of protein was expressed compared to that in lysates of cells transfected with the plasmids pmyc-Ch82, pmyc-S82, pmyc-B82 and pmyc-Rh82 indicating that all the myc-tagged homologues were able to show protein expression in the short-term. The differences in levels of protein expression between the myc-tagged UL82 homologues observed in figure 3.7 maybe be due to different expression efficiencies of pp71 compared to the non-human homologues. All myc-tagged plasmids were under the control of the HCMV MIEP, thus it is possible that pp71 is able to drive expression better from its own promoter than the non-human homologues when fused to the myc-tag. However, this is only one explanation as these differences may be due to transfection discrepancies.

At 10 days post-transfection protein was only detected in lysates transfected with pmyc-pp71, indicating that pp71 was the only protein able to maintain transcription, and thus that pmyc-pp71 is unique in directing long-term gene expression.

Initial data from transfection experiments showed that while the EYFP-tagged UL82 homologues were all functional in the short-term, only EYFP-tagged pp71 stimulated long-term gene expression. Upon fusing the UL82 homologues to a myc-tag the data obtained was controversial. β -gal assays showed only myc-tagged pp71 was functional in both short-term and long-term assays. Numbers of β -gal positive cells observed in cultures transfected with the myc-tagged UL82 non-human homologues were lower than numbers of β -gal positive cells observed in cultures transfected with the control plasmid. However

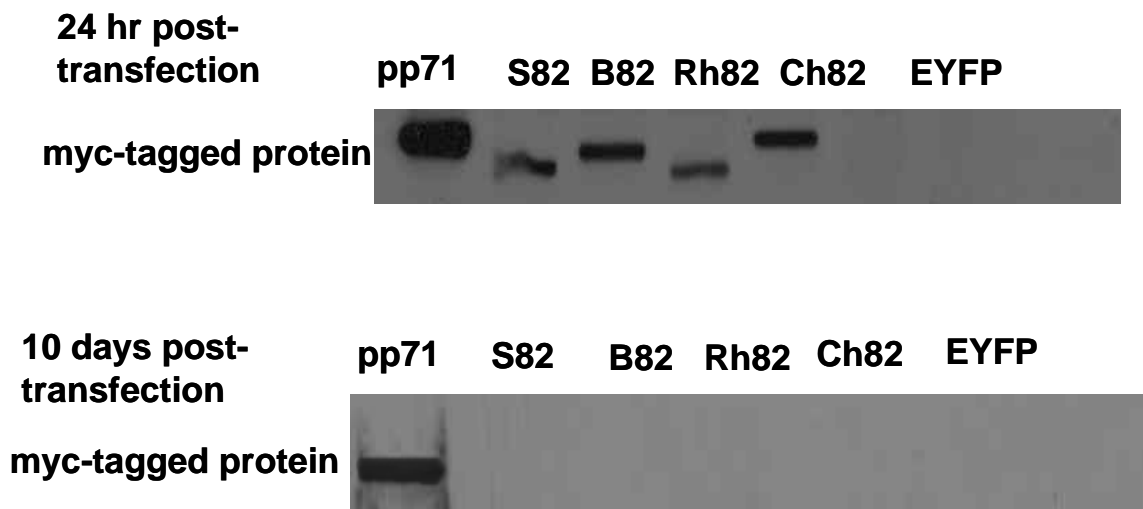


Figure 3.7. Expression of myc-tagged pp71 homologues 24 hr and 10 days post-transfection.

HFFF2 monolayers were transfected with plasmids expressing the myc-tagged homologues. Cell lysates were harvested either 24 hr or 10 days post-transfection and subjected to SDS PAGE. The myc-tagged UL82 proteins were detected using an anti-myc (9E10) primary antibody, and an anti-mouse HRP conjugated secondary antibody.

all myc-tagged UL82 homologues showed protein expression in the short-term, albeit at lower levels than lysates transfected with myc-tagged pp71.

In order to confirm results obtained from transfection assays, and to establish if the myc-tagged UL82 non-human homologues do behave differently from the EYFP-tagged non-human homologues the UL82 homologues were recombined into the HSV-1 genome.

3. Part II

3.2. Introduction

HCMV pp71 has been shown to have a number of effects on gene expression including the ability to maintain reporter gene expression from *in1312*-derived recombinants for extended periods in cell culture (Preston & Nicholl, 2005).

Plasmid transfection assays have demonstrated that EYFP-pp71, along with its homologues EYFPS82, EYFPB82, EYFPRh82, and EYFPCh82, can stimulate gene expression controlled by the HCMV MIEP in short-term assays. However only EYFPpp71 was able to mediate gene expression in long-term assays. To eliminate the disadvantages of the NucleofectorTM system, and to confirm the results obtained from the transfection assays, all plasmids of interest were recombined into a HSV-1 virus named *in1312*.

In1312 is a HSV-1 multiple mutant, which is defective for the functions of the three major HSV-1 transcription activators (VP16, ICPO and a temperature sensitive mutation in ICP4) at 38.5°C. The mutant is unable to progress past the IE stage of infection, and in HFFF2 and U373 cells the *in1312* genome becomes repressed within 24 hr, resulting in 'quiescent' infection. Insertions (under the control of the HCMV MIEP) at the non-essential thymidine kinase (TK) or UL43 loci of *in1312* (see materials and methods section 2.1.5 for further details) yields mutants that express reporter genes in tissue culture cells. The *in1312*-based virus *in1374*, which has *lacZ* inserted in the UL43 locus was used as a vector to express pp71 and its non-human homologues after insertion at the TK locus. Using a HSV-1 recombinant virus system expressing the proteins of interest allowed pp71 and its non-human UL82 homologues to be examined in an environment similar to that of HCMV wild-type, unlike the transfection based system where only a single protein in a plasmid vector could be examined.

3.2.1. Infection with the *in1312* recombinants expressing the EYFP-tagged UL82 homologues stimulates short-term gene expression

Expression vectors were constructed by inserting each EYFP-tagged UL82 homologue into the plasmid pCP1802. This plasmid contains a cassette comprising the HCMV MIEP, a multiple cloning site and an SV40 terminator in the

TK locus. The TK locus allows construction of HSV-1 vectors by recombination of the cassette into HSV-1 DNA. The *in1312* UL82 recombinant viruses were constructed by recombining the pCP1802 derived plasmids containing the coding regions of each of the EYFP homologues, into the TK locus of a HSV-1 mutant, *in1374* (*in1374* is derived from the mutant *in1312*, with the *lacZ* coding region controlled by the HCMV MIEP inserted in the UL43 locus). See Appendix 1 for further details).

To establish that the EYFP-tagged UL82 homologues expressed by the *in1312* recombinants were functional and able to stimulate short-term gene expression, 1.5×10^5 U373 cells were infected with 5×10^5 pfu (MOI 3.3) of *in1310* (which expresses EYFPpp71), *in0150* (EYFPS82), *in0146* (EYFPCh82), *in0144* (EYFPRh82), *in0145* (EYFPB82), *in1374* (negative control), or mock-infected. An overview of the experimental plan is presented in figure 3.8.

Infected cells were incubated at 38.5°C, at 24 hr post-infection, cell monolayers were fixed and stained with X-gal reaction mix and expression of β -gal assessed by observation. The results in figure 3.9 show cells infected with the *in1312* recombinant viruses expressing the EYFP-tagged UL82 homologues. All five of the recombinant viruses showed β -gal expression at levels above those of the negative control, *in1374*, implying that each homologue acts on the HCMV MIEP to drive short-term gene expression to a similar extent. This confirms the results from the plasmid transfection assays, which showed that all the UL82 homologues were able to drive short-term gene expression.

The protein levels of the UL82 homologues expressed by *in1312* recombinants in lysates of U373 cells were investigated by SDS PAGE and western blot analysis, using a polyclonal anti-GFP antibody. As shown in figure 3.10, no protein was recognised by the anti-GFP antibody in lysates of cells infected with *in1374* however, the results show that levels of protein produced by each of the *in1312* recombinant viruses expressing the non-human UL82 homologues were somewhat lower than that produced by *in1310*. Nonetheless, the results confirm, as found in the transfection assays, that all five UL82 homologues are able to stimulate short-term gene expression.

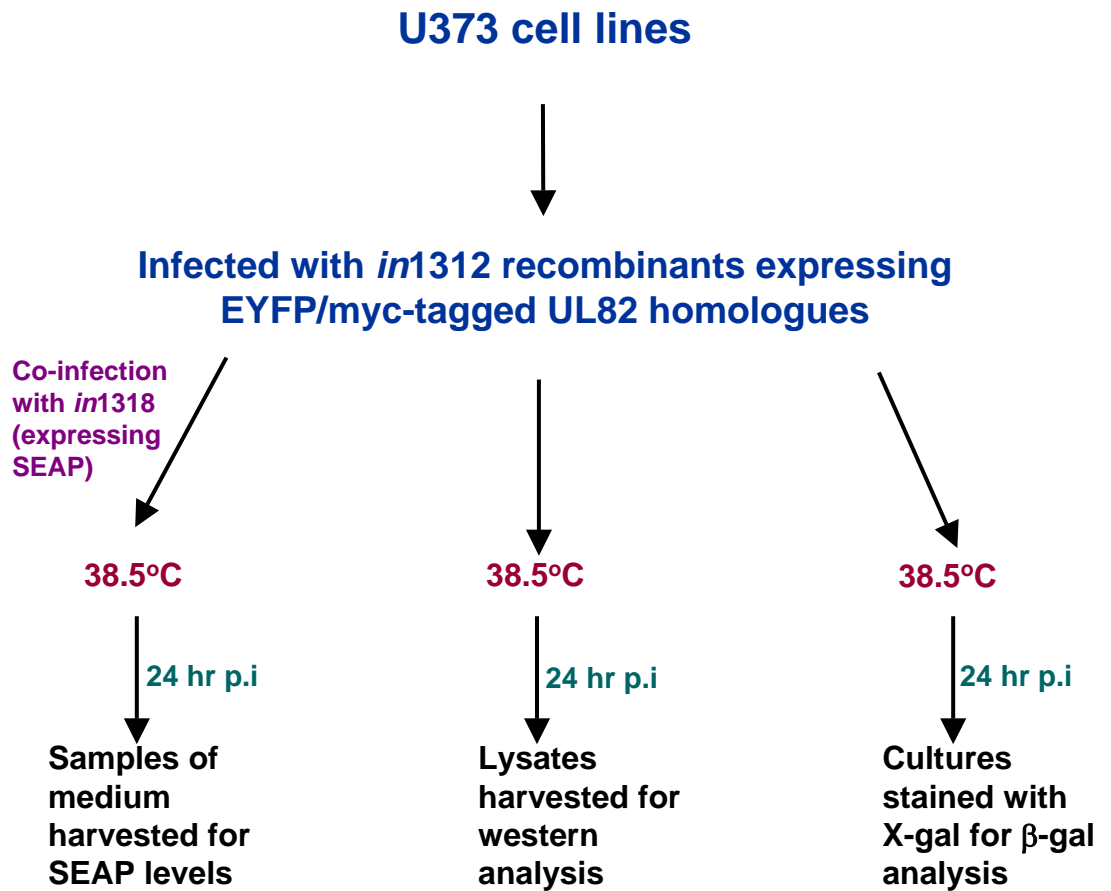


Figure 3.8.

Overview of the experimental plan employed in short term analysis of the EYFP/myc-tagged UL82 homologues.

p.i (post-infection)

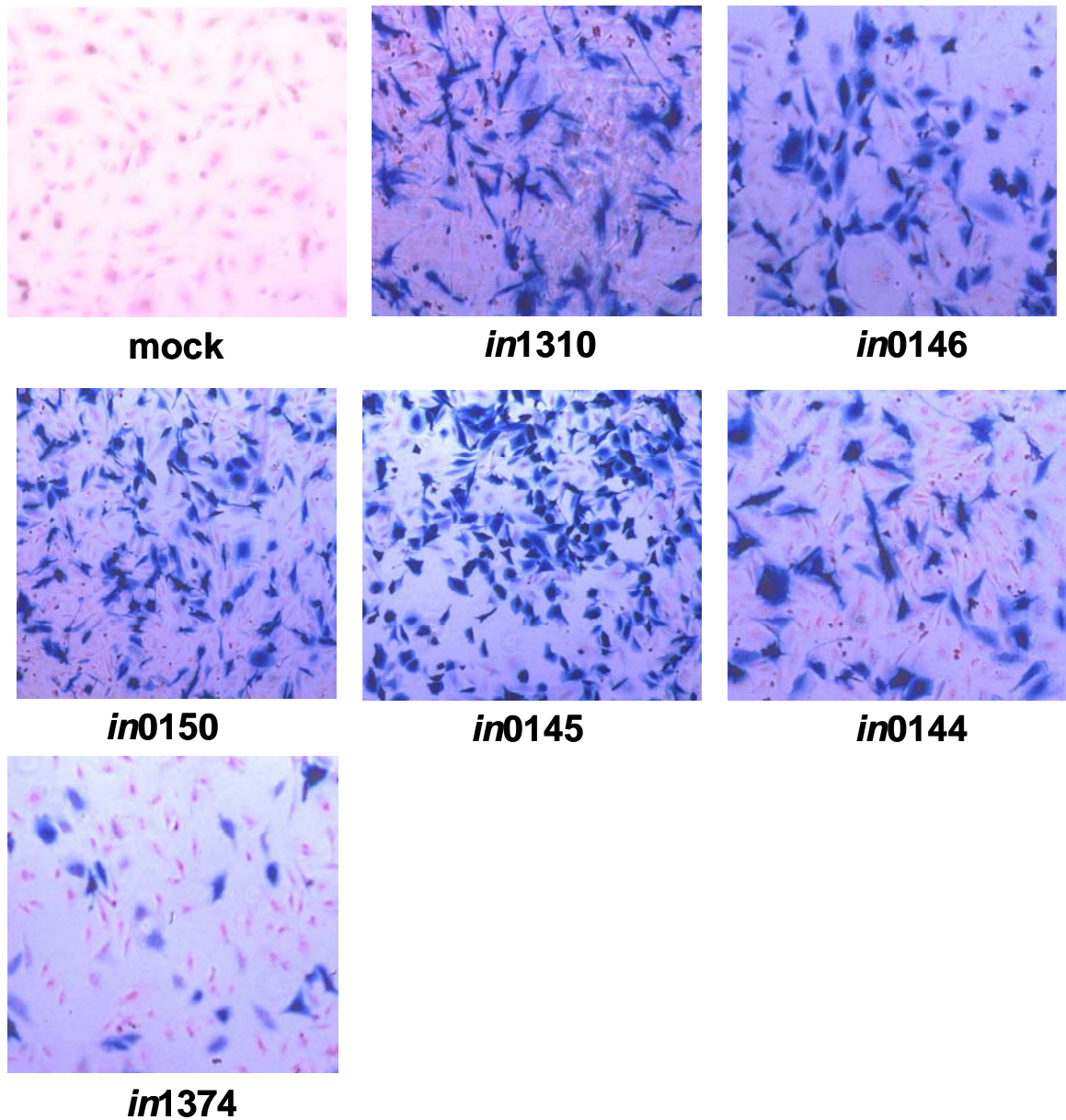


Figure 3.9. β -gal expression of the *in1312* recombinants expressing the EYFP-tagged UL82 homologues at 24 hr post-infection

U373 cell monolayers were mock-infected or infected with 5×10^5 pfu (MOI 3.3) of the *in1312* recombinants expressing the UL82 homologues and incubated at 38.5°C . At 24 hr post-infection cell monolayers were stained with X-gal.

The *in1310* virus expresses EYFPpp71, *in0146* expresses EYFPCh82, *in0150* expresses EYFPS82, *in0145* expresses EYFPB82, *in0144* expresses EYFPRh82, and *in1374* was used as a negative control.

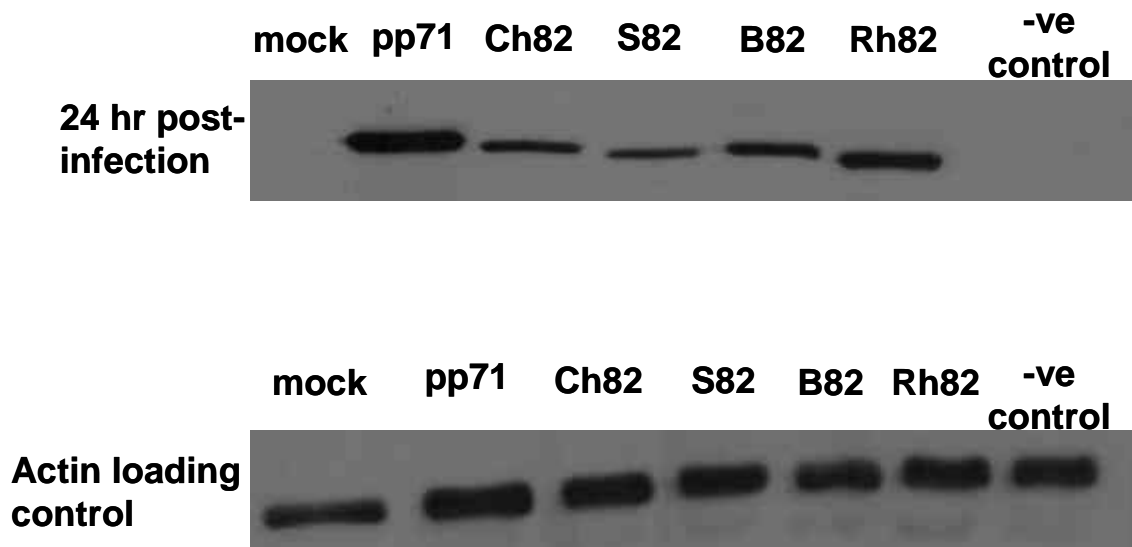


Figure 3.10. Expression of the EYFP-tagged UL82 homologues at 24 hr post-infection

U373 cell monolayers were cultivated in 24 well plates. Cells were either mock-infected or infected with 5×10^5 pfu (MOI 3.3) of the *in1312* recombinants expressing the UL82 homologues and incubated 38.5°C . *In1374* was used as a negative control. At 24 hr post-infection cell lysates were harvested and were subjected to SDS PAGE. EYFP-tagged UL82 proteins were detected using an anti-GFP primary antibody and an anti-rabbit HRP conjugated secondary antibody. Blots were stripped and reprobbed with an anti-actin primary antibody and an anti-mouse HRP-conjugated secondary antibody, to act as a loading control.

As levels of β -gal expression were in infection experiments were analysed by observation an experiment was developed to quantify levels of the promoter activity during the short-term assays. A dual infection system was used, the results of which could be measured quantitatively. In this experiment U373 cells cultured in 24 well plates were infected with *in1312* recombinants expressing the UL82 homologues and co-infected with *in1318*. The HSV-1 recombinant virus *in1318*, which encodes secreted alkaline phosphatase (SEAP) under the control of the HCMV MIEP, was used because this protein is secreted into the culture medium and synthesis of this protein can therefore be measured by simply assaying the growth medium for SEAP at various time points without having to create cell lysates or stain cultures for the presence of β -gal.

Figure 3.11 shows the average number of arbitrary units of fluorescence from two experiments. The results from figure 3.11 show that cells mock-infected or infected with *in1374* virus alone produced relatively low amounts of SEAP. Cells infected with the *in1312* recombinants expressing the EYFP-tagged UL82 homologues showed SEAP synthesis was stimulated. However levels of SEAP synthesis stimulated by *in1310* were lower than those observed for viruses expressing the non-human UL82 homologues. The lower levels of SEAP synthesis stimulated by *in1310* in this study is surprising as in previous transfection and infection experiments pp71 appeared to stimulate levels of expression greater than or equivalent to the EYFP-tagged UL82 non-human homologues. It is possible that the lower levels of SEAP synthesis in this experiment could be attributed to experimental artifacts such as cell viability. Further experiments would have to be carried out to obtain a larger range of data to establish if this is the case or if in this method of analysis pp71 is less efficient in the short-term.

3.2.2. Analysis of long-term gene expression

Studies by Preston and Nicholl (2005) showed that, as HFFF2 cells could be maintained at 38.5°C in medium containing 2% serum for two weeks with no serious deterioration in cell viability, viral gene expression of pp71 could be investigated at later times post-infection. Preliminary experiments suggested that β -gal could be detected for many days in cell monolayers co-infected with *in1324*, (HCMV pp71 inserted into the TK locus, with mutations to VP16, ICP0 and a

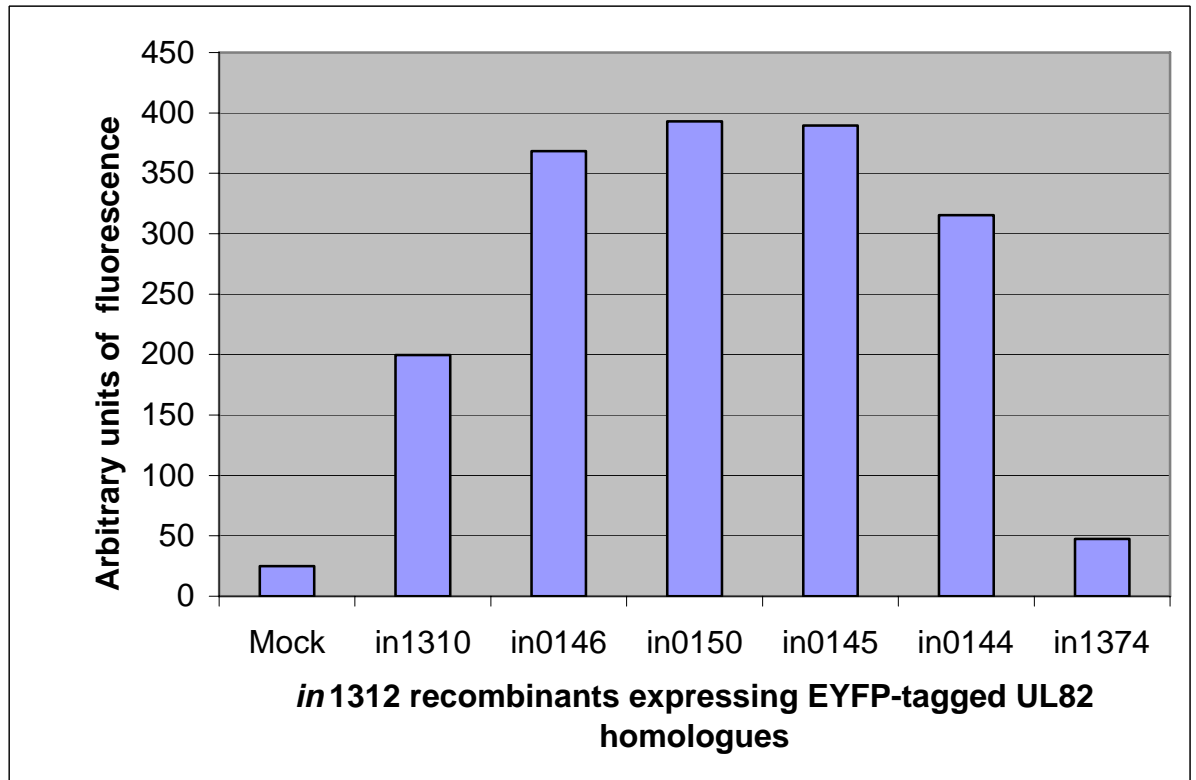


Figure 3.11. Activation of expression by infection with *in1312* recombinants expressing the EYFP-tagged UL82 homologues *in trans*

U373 cell monolayers were infected with 5×10^5 pfu (MOI 3.3) of the *in1312* recombinants expressing the UL82 homologues and incubated at 38.5°C for 2 hr. Cell monolayers were infected with 5×10^5 pfu *in1318* and incubation was continued at 38.5°C . At 24 hr post-infection samples of medium were analysed for SEAP activity.

temperature sensitive mutation to ICP4) and the reporter virus *in1382* (containing the *lacZ* coding sequences in the TK locus controlled by the HCMV MIEP promoter). Continued β -gal expression was not observed with *in1382* alone, suggesting that pp71 expressed by *in1324* exerted an effect at late times post infection (Preston & Nicholl, 2005).

Previous transfection based assays in the study presented here showed that EYFP-tagged pp71 was the only homologue able to direct long-term gene expression. To confirm that pp71 was unique in its ability to do so, and also to confirm results from the transfection assays and work by Preston and Nicholl. (2005), *in1312* recombinants expressing the EYFP-tagged UL82 homologues were used to investigate the effects of the UL82 homologues at late times post-infection.

Three sets of HFFF2 monolayers consisting of 1×10^6 cells on 35 mm plates were each infected with 3×10^6 pfu (MOI 3) of *in1310* (expressing EYFPpp71), *in0150* (EYFPS82), *in0146* (EYFPCh82), *in0144* (EYFPB82), *in0145* (EYFPRh82), *in1374* (negative control) or mock-infected. Following infection, D5+5 medium was replaced with DF2 medium and incubation continued at 38.5°C for 10 days, with medium changes every 2 days. At 9 days post-infection one set of infected HFFF2 cells was super-infected with 3×10^6 pfu of *tsK*, a HSV-1 mutant that produces ICP0, and the cells were incubated for a further 24 hr at 38.5°C. A second set of infected cells was overlaid with DF2 medium containing 2% human serum at 9 days post-infection and downshifted to the permissive temperature of 31°C for a further 5 days. The third set of infected HFFF2 cells remained untreated at 38.5°C for 10 days. An overview of the experimental plan is presented in figure 3.12.

At day 10 post-infection cell monolayers super-infected with *tsK* and those left untreated were stained with X-gal. β -gal expression at 10 days post-infection showed that only the recombinant virus expressing pp71 was able to maintain gene expression. β -gal expression was not observed in those monolayers infected with viruses that express the non-human UL82 homologues (Figure 3.13a). This was further confirmed by the results from the downshift experiment (figure 3.13b) where infected monolayers were stained with X-gal 14 days post-infection. Downshift of the cells to a permissive temperature of 31°C allowed

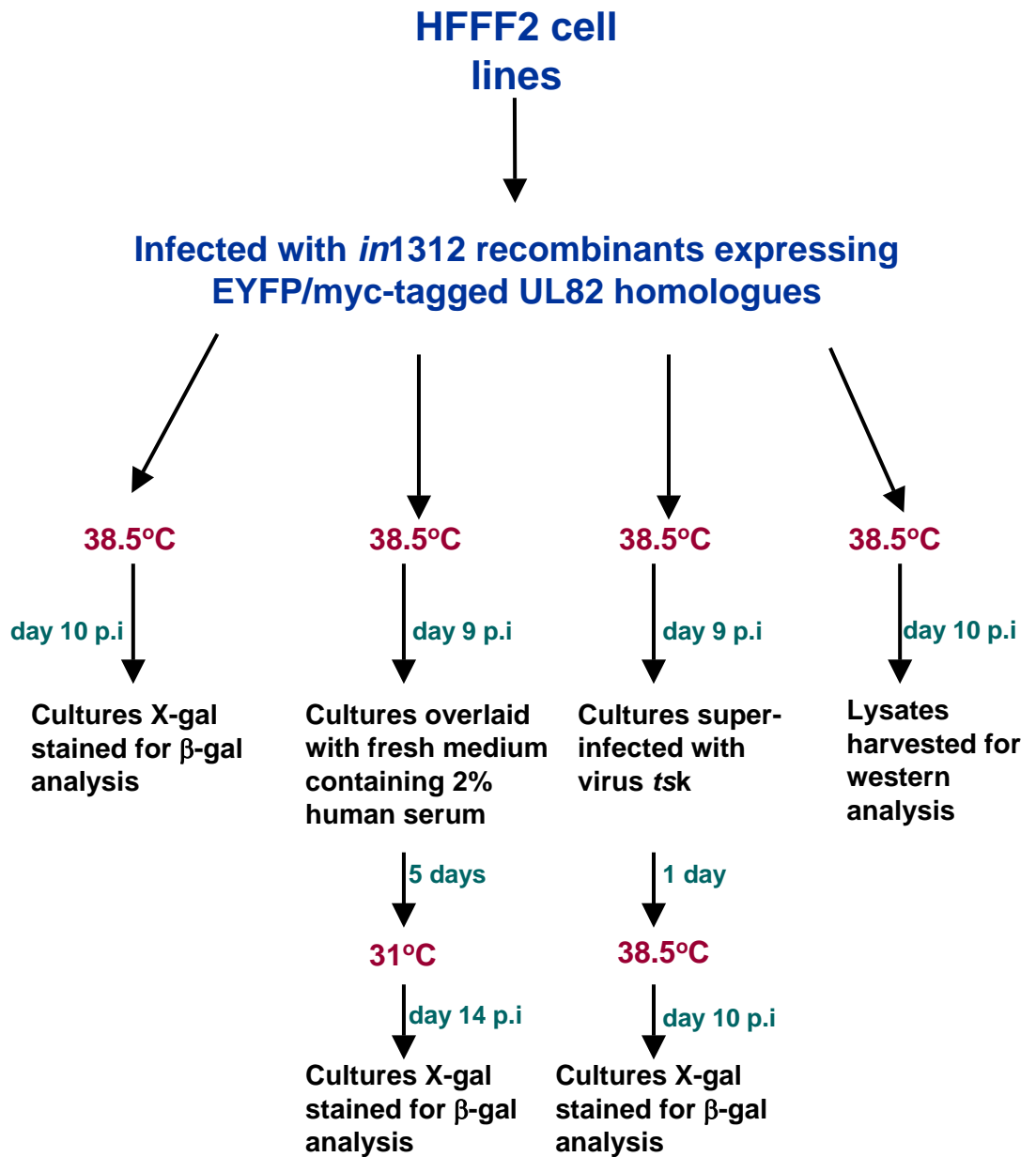


Figure 3.12.

Overview of the experimental plan employed in long term analysis of the EYFP/myc-tagged UL82 homologues.

p.i (post-infection)

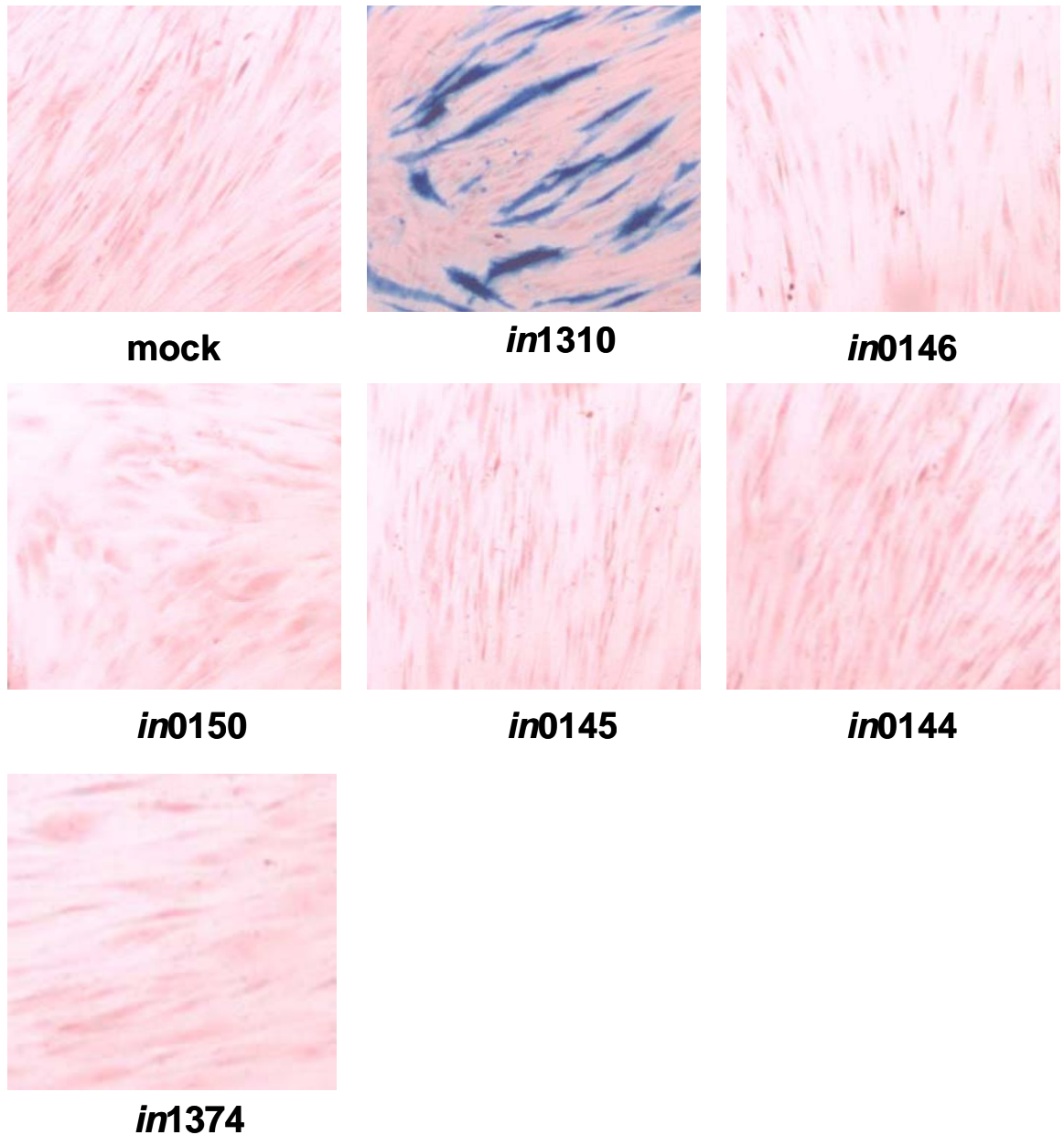


Figure 3.13a β -gal expression directed by the *in1312* recombinants expressing the EYFP-tagged UL82 homologues at 10 days post-infection. HFFF2 cell monolayers were infected with 3×10^6 pfu (MOI 3) of the *in1312* recombinants expressing the UL82 homologues, and incubated at 38.5°C . *In1374* was used as a negative control. At 10 days post-infection cell monolayers were stained with X-gal.

The *in1310* virus expresses EYFPpp71, *in0146* expresses EYFPCh82, *in0150* expresses EYFPS82, *in0145* expresses EYFPB82, *in0144* expresses EYFPRh82, and *in1374* was used as a negative control.

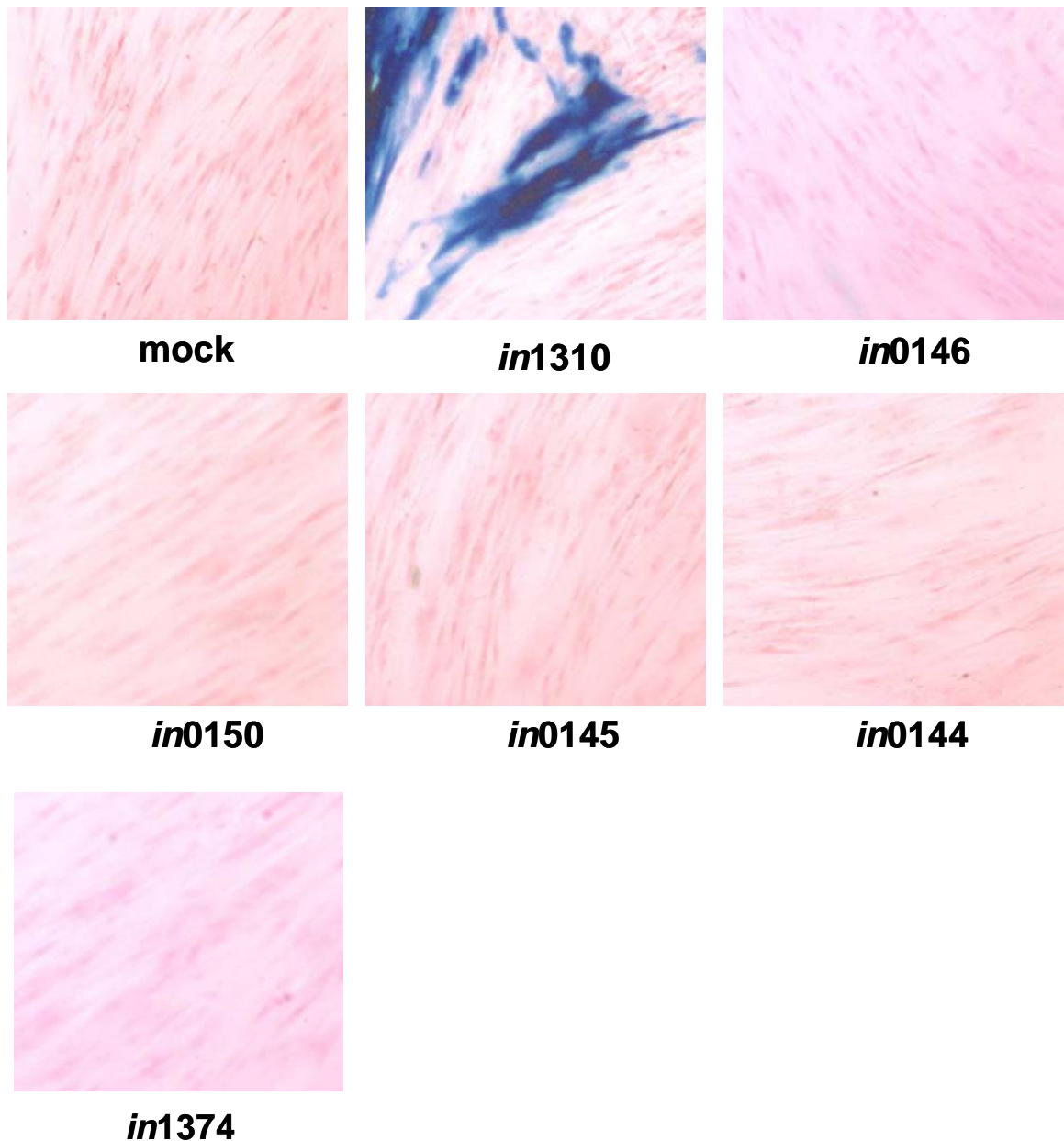


Figure 3.13b. Response of the *in1312* recombinants expressing EYFP-tagged UL82 homologues to temperature downshift

HFFF2 monolayers were infected with 3×10^6 pfu (MOI 3) of the *in1312* recombinants expressing the UL82 homologues and incubated at 38.5°C . At 9 days post-infection cell monolayers were overlayed with medium containing 2% human serum, and downshifted to 31°C . At 14 days post-infection cell monolayers were stained with X-gal.

The *in1310* virus expresses EYFPpp71, *in0146* expresses EYFPCh82, *in0150* expresses EYFPS82, *in0145* expresses EYFPB82, *in0144* expresses EYFPRh82, and *in1374* was used as a negative control.

expression of ICP4 and consequently replication of the viruses if they remained potentially replication competent. Plaques were observed only in those monolayers infected with *in1310*. Figure 3.13c shows monolayers super-infected with *tsK* and stained with X-gal at 10 days post-infection. As VP16 and ICP0 are both functional in the super-infecting virus, *tsK*, the superinfection allows ICP0 to reactivate the quiescent genomes by driving expression from the *lacZ* gene. β -gal expression at 10 days post-infection showed that all genomes were present at functionally comparable levels. Therefore at 10 days post-infection there remained a significant number of cells retaining the genomes of the viruses expressing the non-human UL82 homologues despite the HCMV MIEP *lacZ* cassette remaining inactive.

At 9 days post-infection samples of cells were subcultured into 24 well plates and incubated overnight at 38.5°C. Lysates were harvested, analysed by gel electrophoresis and transferred onto nitrocellulose membrane before western blotting, using an anti-GFP antibody. Figure 3.14 shows that at 10 days post-infection EYFPpp71 was the only homologue detectable. Stripping and re-probing blots for actin demonstrated that protein loading was equivalent.

3.2.3. Myc-tagged UL82 homologues expressed by *in1312* based recombinants are functional 24 hr post-infection

Data from transfection experiments using myc-tagged UL82 homologues gave inconclusive results as only myc-tagged pp71 appeared to be able to direct β -gal expression in both short-term and long-term assays (section 3.1.3). However, all five homologues were able to stimulate protein expression in the short-term while only myc-tagged pp71 stimulated protein expression in long-term assays. To eliminate transfection discrepancies and in order to determine if myc-tagged pp71 and its non-human homologue myc-tagged Ch82 behave as the EYFP-tagged homologues HSV-1 recombinants expressing myc-tagged pp71 or myc-tagged Ch82 were constructed. The HSV-1 recombinants expressing myc-tagged pp71 and myc-tagged Ch82 were constructed by homologous recombination of each into *in1312*, as described for the production of viruses expressing EYFP-tagged proteins (section 3.2.1).

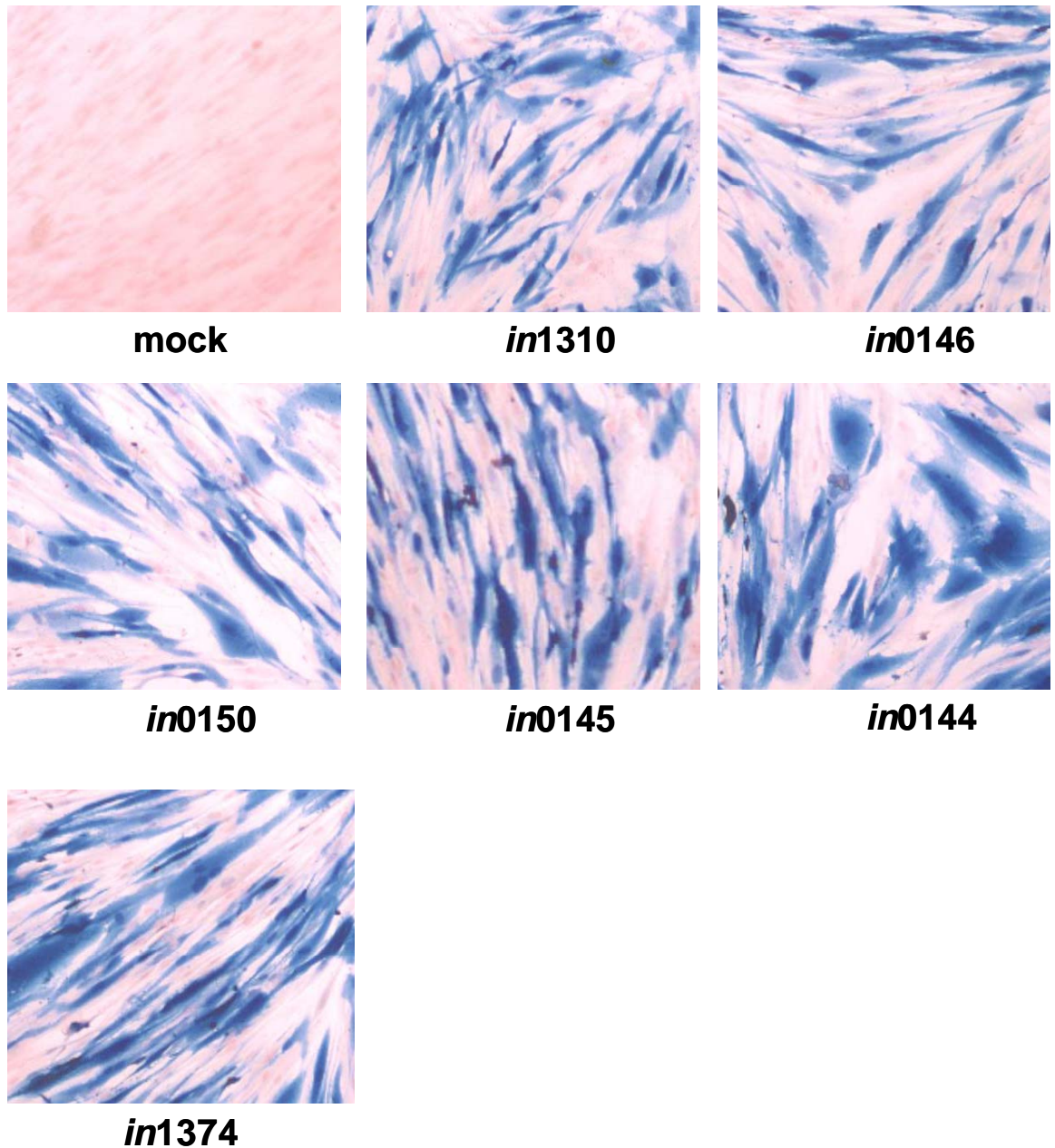


Figure 3.13c. Response of the *in1312* recombinants expressing the EYFP-tagged UL82 homologues to super-infection with *tsK*.

HFFF2 monolayers were infected with 3×10^6 pfu (MOI 3) of the *in1312* recombinants expressing the UL82 homologues and incubated at 38.5°C . *In1374* was used as a negative control. At 9 days post-infection cell monolayers were super-infected with 3×10^6 pfu of *tsK* and incubated at 38.5°C for a further 24 hr. At 10 days post-infection cell monolayers were stained with X-gal.

The *in1310* virus expresses EYFPpp71, *in0146* expresses EYFPCh82, *in0150* expresses EYFPS82, *in0145* expresses EYFPB82, *in0144* expresses EYFPRh82, and *in1374* was used as a negative control.

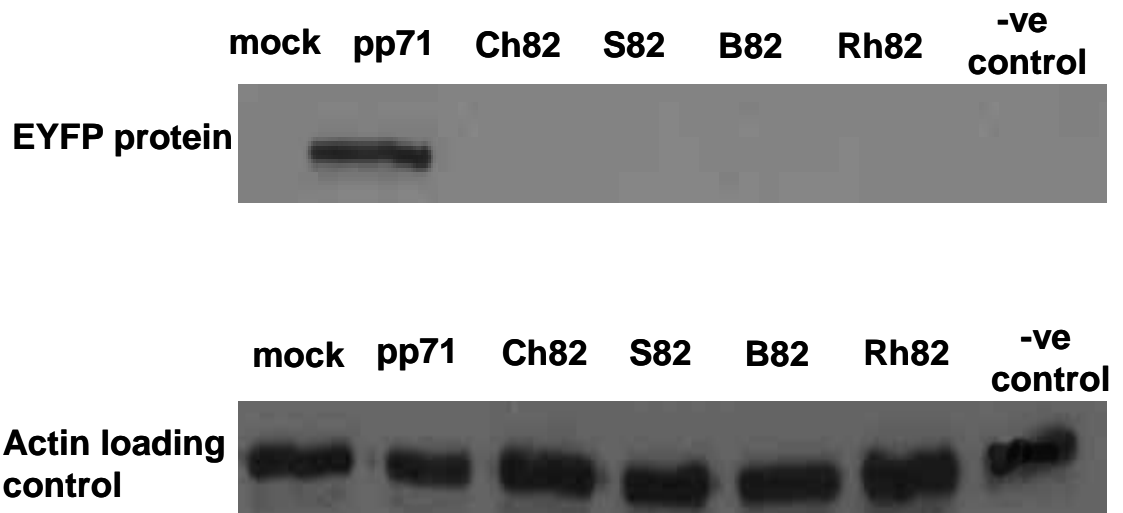


Figure 3.14. Expression of the EYFP-tagged UL82 homologues at 10 days post-infection

HFFF2 cell monolayers cultivated in 35 mm plates were either mock-infected or infected with 3×10^6 pfu (MOI 3) of the *in1312* recombinants expressing the UL82 homologues and incubated at 38.5°C. At 10 days post-infection cell lysates were harvested, and subjected to SDS PAGE. EYFP-tagged protein was detected using an anti-GFP primary antibody and an anti-rabbit HRP conjugated secondary antibody. Blots were stripped and reprobbed with an anti-actin primary antibody and an anti-mouse HRP-conjugated secondary antibody to act as a control for loading.

To assess whether the myc-pp71 and myc-Ch82 proteins expressed by the *in1312* recombinants were functional each virus was tested in short-term assays (an overview of the experimental plan is presented in figure 3.8). U373 cells seeded at 1.5×10^5 cells per 13 mm well were infected with 5×10^5 (MOI 3.3) of *in0151* (expressing myc-pp71), *in0149* (myc-Ch82), *in1374* (negative control), or were mock-infected and incubated at 38.5°C. At 24 hr post-infection cell monolayers were fixed and stained with X-gal reaction mix and β -gal expression was assessed by observation. Figure 3.15 shows that both *in0151* and *in0149* produced levels of β -gal above those seen in cultures infected with the parent virus *in1374*. This implies that the myc-tagged homologues expressed by the *in1312* recombinants were functional in the short-term.

The protein levels in U373 cells infected with the *in1312* recombinants expressing myc-pp71 or myc-Ch82 homologues were investigated by SDS PAGE and western blot analysis, using an anti-myc antibody (9E10). Figure 3.16 shows that extracts of cells infected with *in0151* and *in0149* contained equivalent amounts of myc-tagged protein. Therefore when fused to the myc tag both pp71 and Ch82 stimulated gene expression.

To quantify the levels of expression directed by the homologues, confluent U373 cell monolayers were infected with 5×10^5 pfu of each *in1312* recombinant virus expressing the UL82 homologues and were co-infected with *in1318*. At 24 hr post-infection samples of growth medium were harvested and assayed for the amount of SEAP present. Figure 3.17 shows that samples harvested from monolayers mock-infected or infected with *in1374* contained relatively low quantities of SEAP. In cell monolayers infected with *in0151* and *in0149* similar levels of SEAP were observed at levels greater than those infected with the negative control.

3.2.4. Only myc-pp71 directs long-term gene expression

In order to establish whether the myc-pp71 or myc-Ch82 proteins were able to direct long-term gene expression, three individual sets of HFFF2 cell monolayers were seeded in 35 mm plates each containing 1×10^6 cells. Cells were mock-infected, or infected with 3×10^6 pfu of *in0151* (myc-pp71), *in0149* (myc-Ch82), *in1374* (negative control). Following infection, D5+5 medium was

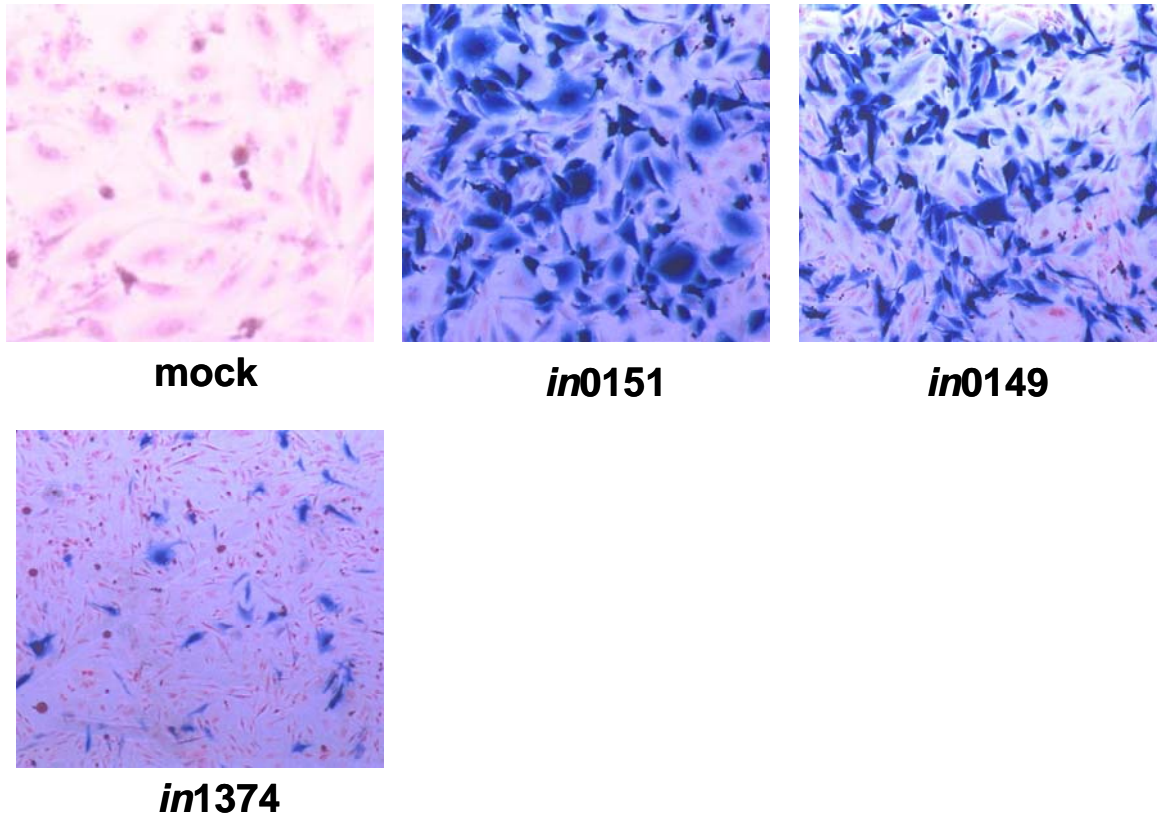


Figure 3.15. β-gal expression directed by the *in1312* recombinants expressing the myc-tagged UL82 homologues at 24 hr post-infection

U373 cell monolayers were mock-infected or infected with 5×10^5 pfu (MOI 3.3) of the *in1312* recombinants expressing the UL82 homologues and incubated at 38.5°C. At 24 hr post-infection cell monolayers were stained with X-gal.

In0151 (expressing myc-pp71), *in0149* (expressing myc-Ch82) *in1374* (negative control).

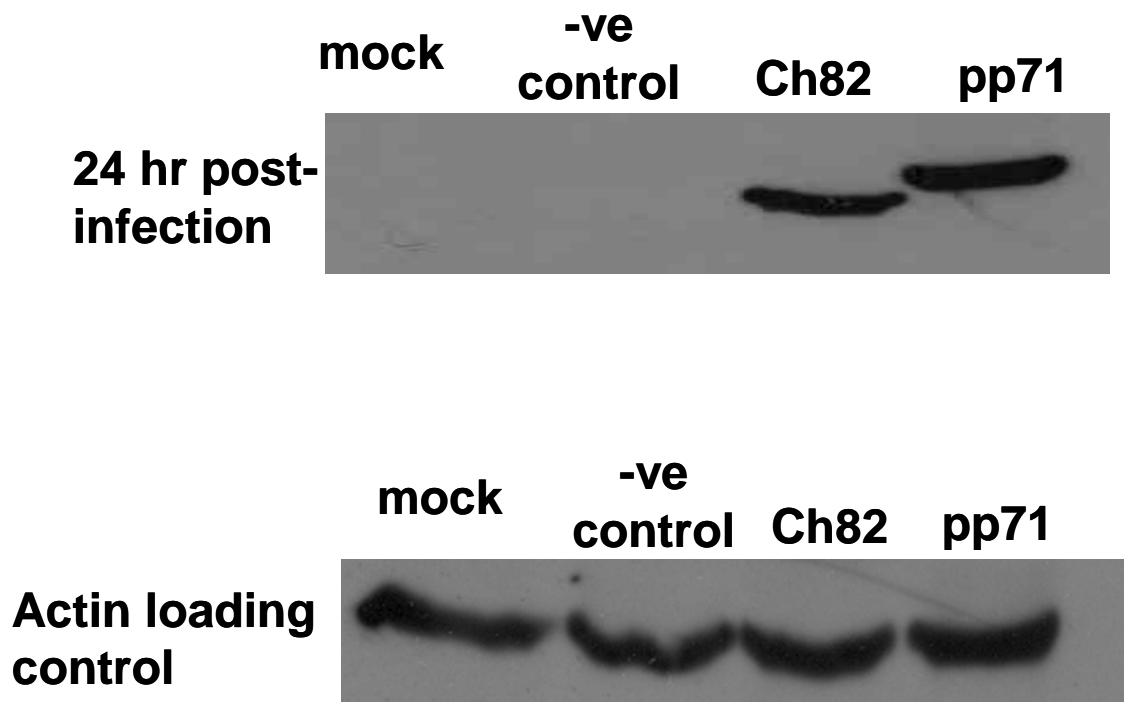


Figure 3.16. Expression of the myc-tagged UL82 homologues at 24 hr post-infection.

U373 cell monolayers were mock-infected or infected with 5×10^5 pfu (MOI 3.3) of the *in1312* recombinants expressing the myc-tagged UL82 homologues and incubated at 38.5°C. At 24 hr post-infection cell lysates were harvested and analysed by SDS PAGE. The myc-tagged proteins were detected using an anti-myc (9E10) primary antibody and an anti-mouse HRP-conjugated secondary antibody. Blots were stripped and reprobbed with an anti-actin antibody and an anti-mouse HRP-conjugated secondary antibody, to act as a loading control.

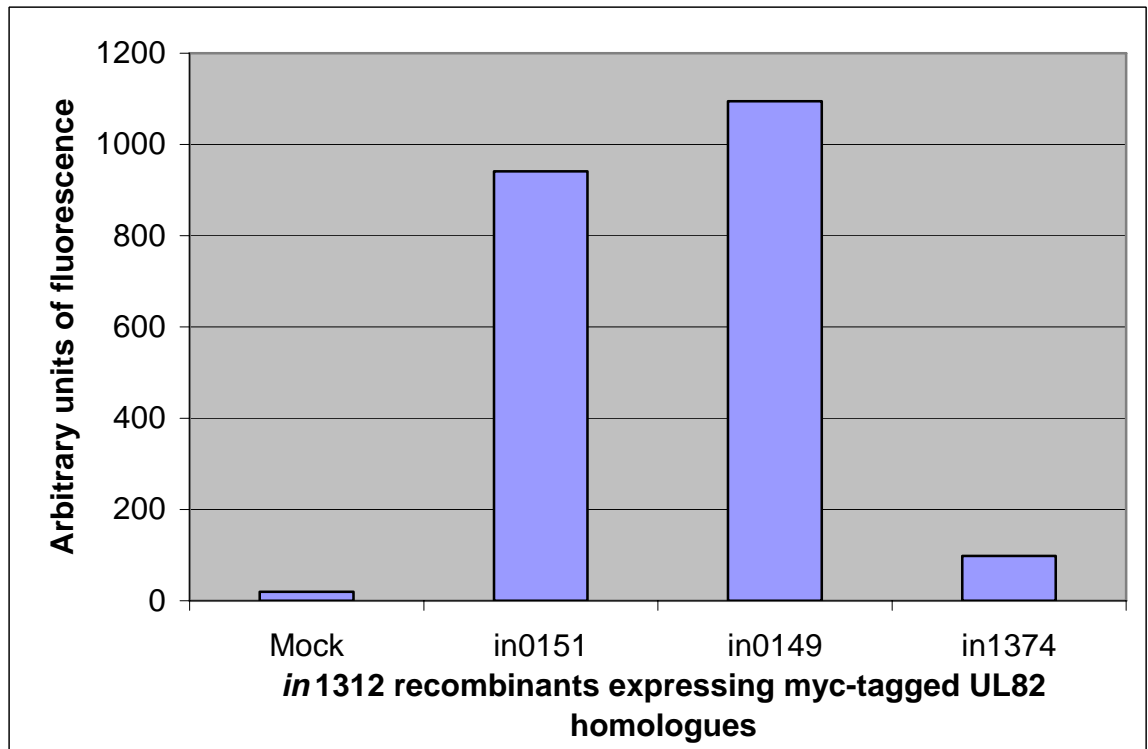


Figure 3.17. Activation of expression by infection with *in1312* recombinants expressing the myc-tagged UL82 homologue *in trans*

U373 cell monolayers were infected with 5×10^5 pfu (MOI 3.3) of the *in1312* recombinants expressing myc-tagged pp71 or Ch82 and incubated at 38.5°C for 2 hr. The cell monolayers were super-infected with 5×10^5 pfu of *in1318* and incubation was continued at 38.5°C . At 24 hr post-infection samples of medium were analysed for alkaline phosphatase activity.

replaced with DF2 medium and infected monolayers were incubated at 38.5°C for 10 days with medium changes every two days. At 9 days post-infection one set of infected HFFF2 cells was super-infected with 3×10^6 pfu of *tsK*, and incubated for a further 24 hr at 38.5°C. A second set of infected cells was overlaid with DF2 medium containing 2% human serum at 9 days post-infection and downshifted to the permissive temperature of 31°C for a further 5 days. The third set of infected cells remained untreated at 38.5°C for 10 days (an overview of the experimental plan is presented in figure 3.12).

At day 10 post-infection cell monolayers super-infected with *tsK*, and those which were left untreated, were stained with X-gal. Analysis of β -gal expression at 10 days post-infection showed that only *in0151* was able to maintain gene expression. β -gal expression was not observed in those monolayers infected with *in0149* (Figure 3.18a). This was further confirmed by staining infected cells which were downshifted to the permissive temperature of 31°C (figure 3.18b), in which infected monolayers were stained with X-gal 14 days post-infection. Plaques were observed only in those monolayers infected with *in0151*. Figure 3.18c shows monolayers super-infected with *tsK* and stained with X-gal at 10 days post-infection. As VP16 and ICP0 are both functional in *tsK*, the super-infection allows ICP0 to reactivate the quiescent genomes by driving expression from the *lacZ* gene. β -gal expression at 10 days post-infection showed that all genomes were present at functionally comparable levels.

In order to monitor protein expression of myc-tagged proteins at later times of infection, cell lysates infected with *in0151*, *in0149*, *in1374* or mock-infected were harvested and subjected to SDS PAGE. Protein was transferred to a nitrocellulose membrane prior to being probed with an anti-myc antibody (9E10). Figure 3.19 shows that *in0151* was the only recombinant virus to produce protein. No protein was detected in lysates of cells infected with *in0149*. Equivalent levels of a protein assumed to be endogenous c-myc were also observed.

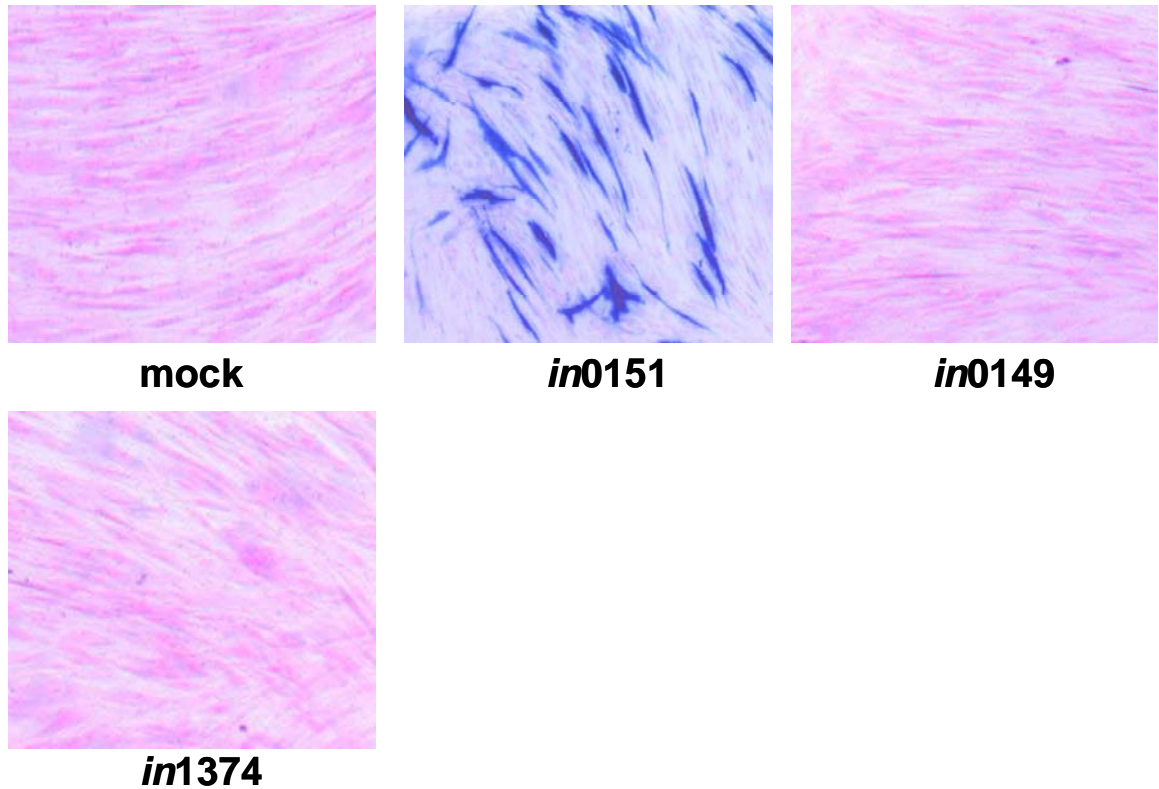


Figure: 3.18a β -gal expression directed by the *in1312* recombinants expressing the myc-tagged UL82 homologues at 10 days post-infection.

HFFF2 cell monolayers were infected with 3×10^6 pfu (MOI 3) of the *in1312* recombinants expressing the myc-tagged UL82 homologues and incubated at 38.5°C . *In1374* was used as a negative control. At 10 days post-infection cell monolayers were stained with X-gal.

In1310 (expressing EYFPpp71), *in0149* (expressing EYFPCh82) *in1374* (negative control).

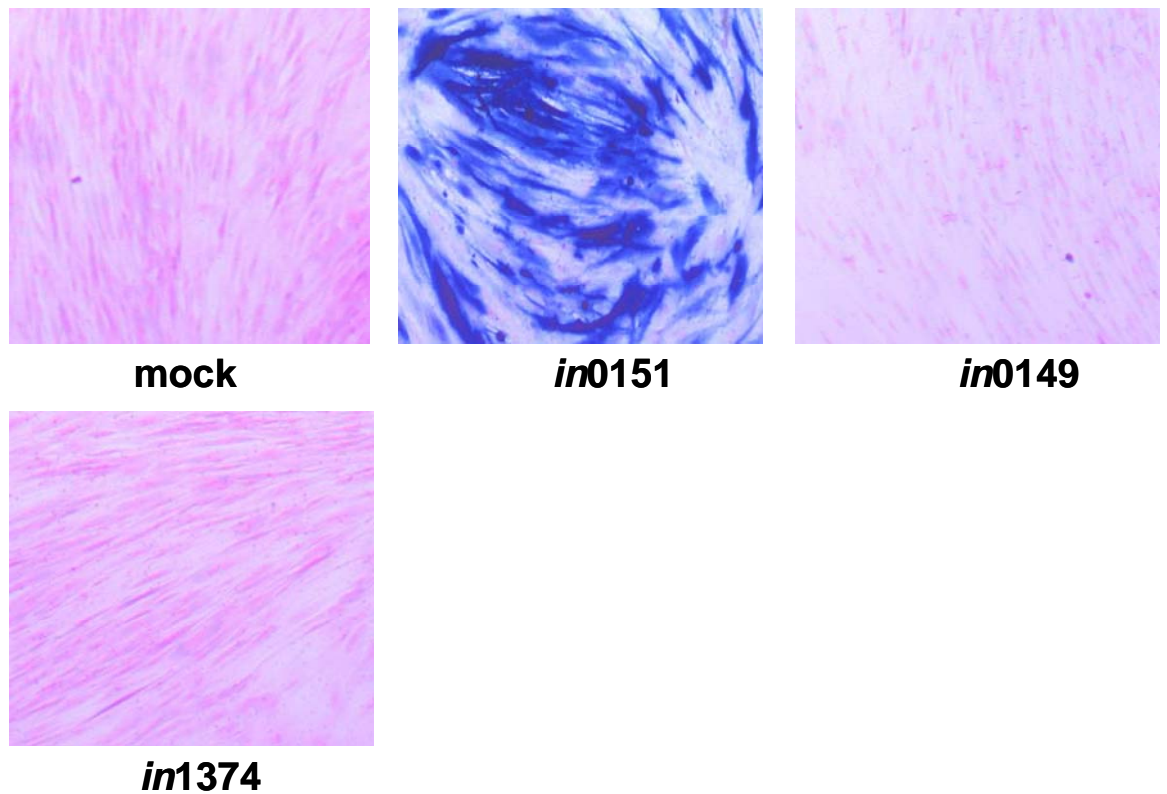


Figure 3.18b. Response of the *in1312* recombinants expressing myc-tagged UL82 homologues to temperature downshift.

HFFF2 monolayers were infected with 3×10^6 pfu (MOI 3) of the *in1312* recombinants expressing the myc-tagged UL82 homologues and incubated at 38.5°C. At 9 days post-infection cell monolayers were overlayed with medium containing 2% human serum and downshifted to 31°C. At 14 days post-infection cell monolayers were stained with X-gal.

In1310 (expressing EYFPpp71), *in0149* (expressing EYFPCh82) *in1374* (negative control).

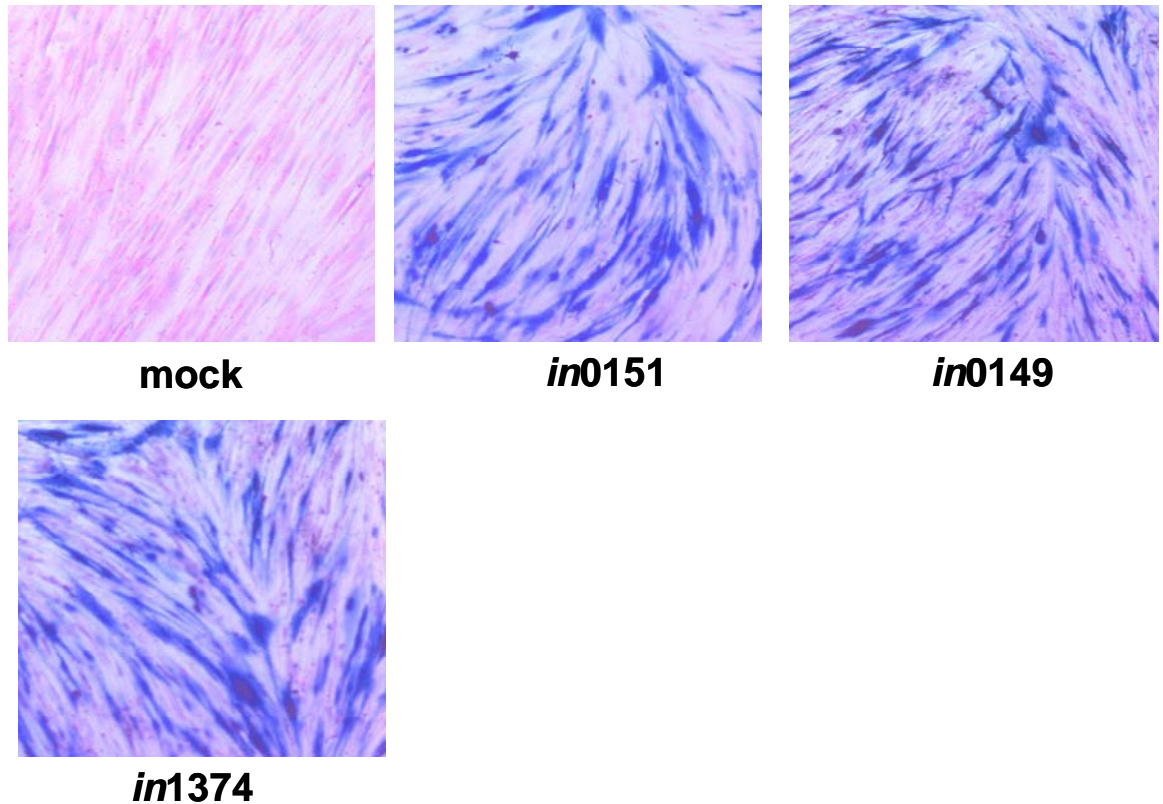


Figure 3.18c. Response of the *in1312* recombinants expressing myc-tagged UL82 homologues to super-infection with *tsK*.

HFFF2 monolayers were infected with 3×10^6 pfu (MOI 3) of the *in1312* recombinants expressing the myc-tagged UL82 homologues and incubated at 38.5°C . *In1374* was used as a negative control. At 9 days post-infection cell monolayers were super-infected with 3×10^6 pfu *tsK* and incubated at 38.5°C for a further 24 hr. At 10 days post-infection cell monolayers were stained with X-gal.

In1310 (expressing EYFPpp71), *in0149* (expressing EYFPCh82) *in1374* (negative control).

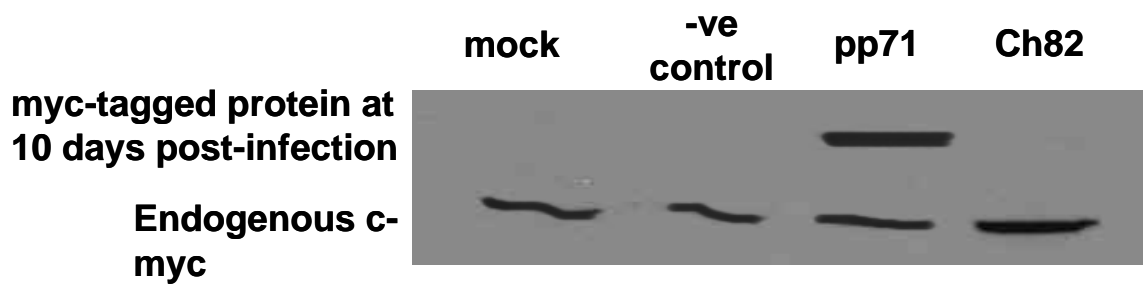


Figure 3.19. Expression of the myc-tagged UL82 homologues 10 days post-infection

HFFF2 cell monolayers cultivated in 35 mm plates were either mock-infected or infected with 3×10^6 pfu (MOI 3) of the *in1312* recombinants expressing the myc-tagged UL82 homologues and incubated at 38.5°C . At 10 days post-infection cell lysates were harvested and analysed by SDS PAGE. Lysates of cells infected with *in1312* recombinants expressing myc-tagged UL82 proteins were detected using an anti-myc (9E10) primary antibody and an anti-mouse secondary antibody.

3. Part III

3.3. Introduction

The tegument protein pp71 has been shown to have the unique property of stimulating gene expression for a prolonged period of time. The protein pp71 has also been shown to act *in trans* on quiescent genomes to reactivate gene expression (Preston & Nicholl, 2005) in a manner similar to that of ICP0. The *in1312* recombinant viruses expressing EYFP-tagged Ch82 or pp71 were used to determine whether Ch82 exhibited the same property as pp71 in terms of being able to reactivate a quiescent virus.

3.3.1. Reactivation Assay

In order to quantitatively assay the activity of both pp71 and Ch82 homologues, HFFF2 cells seeded at 1×10^6 cells in 35mm plates were infected with 3×10^6 pfu (MOI 3) of *in1318* at 38.5°C. At 10 days post-infection cells were subcultured into 24 well plates and super-infected with *in1310* (expressing EYFPpp71) or *in0146* (EYFPCh82) and incubated at 38.5°C. The levels of SEAP in the growth medium were measured each day over a further 10 days. Figure 3.20 shows that there was no detectable SEAP in the growth medium of mock-infected cells. Cells infected with *in0146* produced relatively low levels of SEAP which peaked at three days post-infection and then declined to levels similar to those observed in mock-infected cells. Cell monolayers super-infected with *in1310* showed levels of SEAP in the growth medium gradually increasing from days one and two post-infection to peaking at day six post-infection. This represented a 6 fold increase in levels of SEAP stimulated by EYFPpp71 compared to EYFPCh82 at three days post-infection. The level of SEAP found in the growth medium of cells infected with *in1310* dipped slightly at day seven and remained constant until day 10 when the experiment was terminated. Levels of SEAP remained constant from days 7-10 due to SEAP continuing to be synthesised. These results indicate that pp71 is able to act *in trans* to reactivate expression from a quiescent virus whereas Ch82 does not possess this property.

As each of the super-infecting viruses contained the *lacZ* gene, cell monolayers were stained with X-gal at 24 hr post-super-infection to show that the recombinant

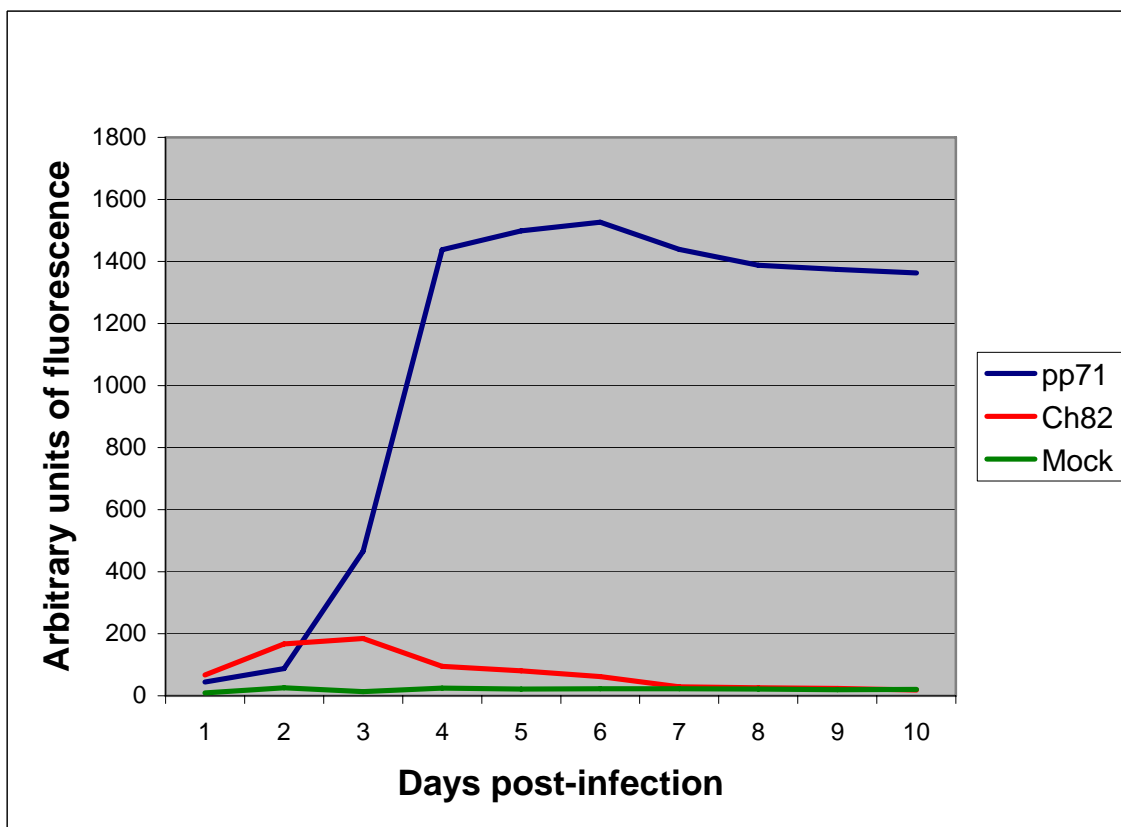


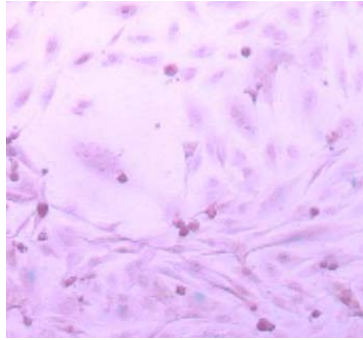
Figure 3.20. Reactivation of SEAP expression by *in1312* recombinants expressing EYFPpp71 and EYFPCh82 *in trans*

HFFF2 monolayers were infected with 3×10^6 pfu of *in1318*, and incubated at 38.5°C. At 10 days post-infection cell monolayers were trypsinised, replated and super-infected with *in1312* recombinants expressing either pp71 or Ch82 and incubated at 38.5°C. Samples of medium harvested at days 1-10 were analysed for alkaline phosphatase activity.

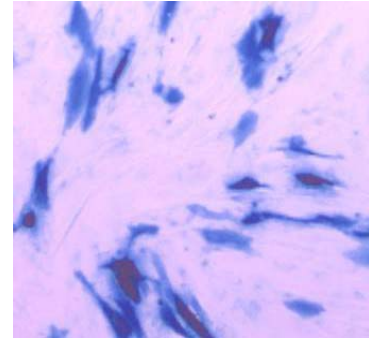
viruses used, (*in1310* and *in0146*), expressed proteins that were functional in the short-term. Figure 3.21 shows that in mock-infected cell monolayers no β -gal positive cells were detected. In monolayers infected with the *in1312* recombinant viruses expressing pp71 or Ch82 homologues showed, as expected, significant numbers of β -gal positive cells indicating that both homologues are functional at 24 hr post-super-infection. However by 10 days post-super-infection β -gal positive cells were detected in cell monolayers infected with *in1310* but not in those infected with *in0146* (data not shown).

HFFF2 lysates of cells super-infected with *in1310* and *in0146* were analysed by SDS PAGE and EYFP-tagged proteins were detected using an anti-GFP antibody. Figure 3.20 shows that at 24 hr post-super-infection, equivalent levels of pp71 and Ch82 protein were expressed. However at 10 days post-super-infection, no protein product was not detected in lysates of cells that were mock-infected or infected with the Ch82 homologue. Figure 3.22 shows only the EYFPpp71 band was observed indicating only pp71 is capable of directing its own transcription.

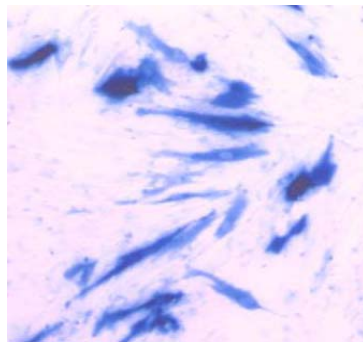
Thus pp71 is not only able to stimulate long-term gene expression from its own promoter but is also able to reactivate quiescent genomes whereas Ch82 does not possess this property.



Mock



in1310



in0146

Figure 3.21 Activity of the *in1312* recombinants expressing EYFP-tagged pp71 or Ch82.

HFFF2 monolayers were infected with 3×10^6 pfu of *in1318* and incubated at 38.5°C. At 10 days post-infection cell monolayers were trypsinised, replated and super-infected with the *in1312* recombinants expressing either pp71 or Ch82 and incubated at 38.5°C. Cell monolayers were stained with X-gal 24 hr post-super-infection.

The *in1310* virus expresses EYFPpp71, *in0146* expresses EYFPCh82, and *in1374* was used as a negative control.

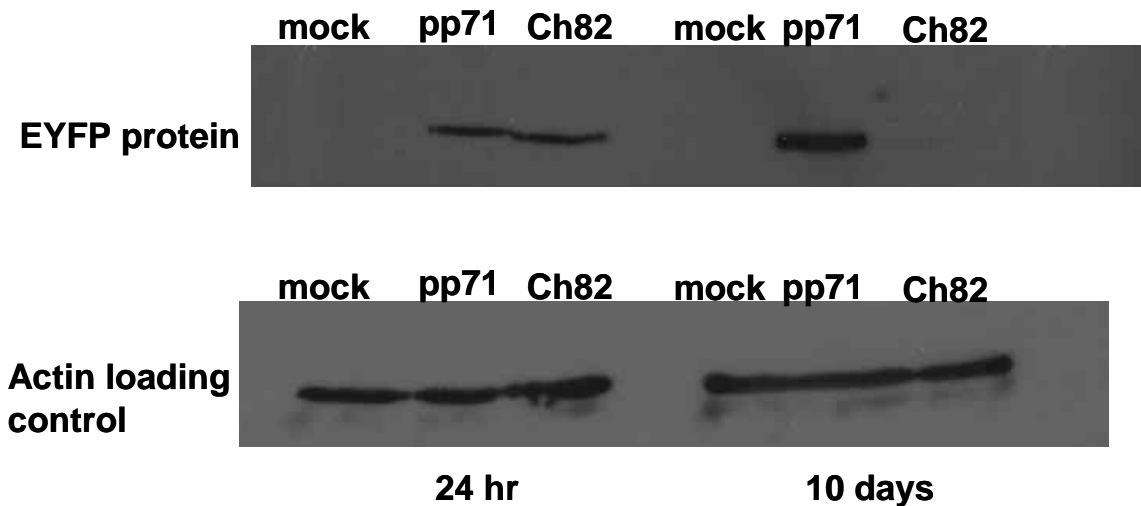


Figure 3.22. Western analysis of the *in1312* recombinants expressing EYFP-tagged pp71 or Ch82 homologues at 24 hr and 10 days post-super-infection HFFF2 monolayers were infected with 3×10^6 pfu of *in1318* and incubated at 38.5°C . At 10 days post-infection the cell monolayers were trypsinised, replated and super-infected with the *in1312* recombinants expressing either pp71 or Ch82 and incubated at 38.5°C . At 24 hr or 10 days post super-infection cell lysates were harvested and samples analysed via SDS PAGE. The EYFP-tagged *in1312* recombinants were detected using an anti-GFP primary antibody and an anti-rabbit HRP conjugated secondary antibody. Blots were stripped and reprobed with an anti-actin primary antibody and an anti-mouse HRP-conjugated secondary antibody to control for loading.

3.4 Discussion

The first part of this study compares the transactivation efficiency of HCMV pp71 with the non-human UL82 homologues. To do this, a system was employed, where plasmids expressing EYFP- or myc-tagged homologues were transfected into HFFF2 cells.

Transfection assays were carried out using the Nucleofector™ system (Amaxa), which employs electroporation to introduce the DNA into HFFF2 cell monolayers. This method of transfection is more efficient in this cell type than other transfection systems e.g. Lipofectamine (Invitrogen). Cells transfected with EYFP-tagged plasmids were observed to fluoresce green allowing transfection levels to be ascertained visually using a UV microscope at 24 hr post-transfection. Satisfactory levels of transfection were classed as 60-70% of transfected cells fluorescing at 24 hr post-transfection. Transfected cells were infected with replication impaired HSV-1 recombinant reporter viruses expressing β -gal driven by the HCMV MIEP.

Data obtained from plasmid transfection assays showed that at the highest values of *in1382* used (3×10^5 pfu and 1×10^5 pfu), all of the plasmids expressing EYFP-tagged non-human homologues stimulated gene expression from the HCMV MIEP at levels above the control (pEYFP-C1). None however stimulated gene expression to the same degree as pp71. Data from long-term experiments showed that only pEYFPpp71 was able to direct gene expression over a period of 10 days post-infection. Activity of the non-human UL82 homologues appeared to be switched off after short times of infection, as confirmed by both western blotting and β -gal analysis. The raw data for EYFP-tagged plasmid transfections showed variations in the numbers of β -gal positive cells in individual experiments, although trends in the overall data remained unaltered. The variations in numbers could be attributed to transfection discrepancies. This was again seen in transfection experiments where myc-tagged UL82 homologues were transfected into HFFF2 cells. The myc-tagged non-human homologues failed to show numbers of β -gal positive cells above levels of the control (pEYFP-C1), only pmyc-pp71 was able to direct β -gal expression in short-term experiments. However protein corresponding to all the myc-tagged homologues was detected by western analysis in the short-term. Since the myc-tagged non-human UL82 homologues did not direct β -gal

expression in short-term experiments, it was uncertain whether they were able to direct long-term gene expression. The low levels of β -gal positive cells detected in this assay may be attributed to a low efficiency of transfection as the Nucleofection system does not allow control of how much DNA enters each cell. Consequently the low levels of expression observed in some assays could be a result of under loading cells with the plasmid of interest.

To eliminate the disadvantages of the Nucleofector™ system, and to confirm the results obtained from the transfection assays, all plasmids of interest were recombined into HSV-1 viruses (impaired for VP16, ICP0 and ICP4 activity to attain quiescence) and used to infect either U373 or HFFF2 cells. Using a recombinant virus system expressing the protein of interest allowed the protein to be examined in an environment akin to that of HCMV wild type, unlike the transfection based system where only the single protein in a plasmid vector could be examined. All short-term infection assays showed that the *in1312* recombinant viruses expressing the EYFP-tagged non-human UL82 homologues were able to stimulate reporter gene expression at levels above that of the negative control. A similar result was obtained from assays using U373 cells infected with myc-tagged pp71 and Ch82, suggesting that myc-tagged Ch82 like, myc-tagged pp71 was functional in short-term assays eliminating discrepancies in the data observed in the transfection assays (section 3.1.1). Therefore, changing the EYFP-tag to a myc-tag did not affect functionality of the homologues in short-term β -gal assays. The differences in levels of protein expression observed from myc-tagged transfection assays was also eliminated in infection experiments, where similar levels of protein were expressed by myc-tagged pp71 and myc-tagged Ch82. The different levels of protein expression observed in transfection experiments (section 3.1.1) were unlikely to be due to different expression efficiencies as suggested previously, and more likely caused by experimental artefacts.

Long-term infection experiments carried out in HFFF2 cells, using the *in1312* recombinant viruses expressing the EYFP-tagged UL82 homologues or myc-tagged homologues, showed only pp71 continued to drive gene expression, as full viral replication was only observed in down shift experiments where the medium of infected cells was replaced with fresh medium containing 2% human serum and downshifted to the permissive temperature of 31°C.

Data from both transfection and infection experiments presented here showed that pp71 is not only able to stimulate long-term gene expression, confirming work by Preston and Nicholl (2005), but is unique in its ability to do so. Long-term gene expression by the non-human UL82 homologues was not detected. The most surprising result observed from this study was that the Ch82 homologue was able to stimulate only short-term gene expression. Given that it shares a significant degree of homology with pp71, it was initially hypothesised that it would be likely to behave in a similar manner, however this was not observed to be the case. It was found to stimulate short-term gene expression only, therefore behaving like the S82 homologue that had previously been shown to stimulate short-term gene expression and not long-term (Nicholson, 2004).

Results from SEAP assays showed that upon super-infecting quiescent genomes with *in1310* and *in0146*, only pp71 was able provoke resumption of gene expression. Cells that were super-infected with *in0146* (expressing EYFPC82) produced low levels of SEAP, peaking at three day post-super-infection then declining to levels similar to those observed in mock-infected cells. In cell monolayers super-infected with *in1310*, an increase in levels of SEAP were observed, peaking at 6 days post-super-infection to become steady for the remainder of the experiment. This data confirmed work by Preston and Nicholl (2005) that pp71 is able to act *in trans* to reactivate quiescent genomes, however, the data presented in this study shows that pp71 appears to be unique amongst the UL82 homologues in its ability to do so. It also provides further evidence that this protein has similar functions to HSV-1 ICP0 (see final discussion for further details).

Chapter 4

Investigation into the region of pp71 responsible for long-term gene expression

4. Part I

4.1. Introduction

The transfection and infection experiments described in chapter 3 showed that pp71 is unique among the UL82 homologues in its ability to stimulate long-term gene expression. Surprisingly, despite its amino acid homology with pp71, the Ch82 homologue was unable to direct gene expression at later times after transfection or infection. Given the significant degree of homology between the pp71 and Ch82 proteins, it was possible to construct six hybrid proteins in order to map the region of pp71 that mediates this unusual property of long-term gene expression.

4.1.1. Construction of plasmids that express EYFP-tagged hybrids

Analysis of the pp71 and Ch82 amino acid sequences (figure 4.1) shows residues conserved between the homologues. A 65% homology between the sequences was calculated. The only functional difference observed was the inability of the Ch82 homologue to stimulate long-term gene expression. A closer examination of the amino acid sequences showed conserved regions to be spread throughout the protein, with the greatest degree of homology occurring in the middle. Analysis of the DNA sequences of both pp71 and Ch82 (figure 4.2) showed a conserved *Bgl*II site and *Bss*HII site in both sequences (figure 4.3). Using these conserved sites plasmids expressing six individual hybrids were constructed by exchanging the C-terminal, N-terminal and the middle regions between the homologues. Figure 4.3 shows the nucleotide sequence and amino acid sequences around the *Bss*HII and *Bgl*II sites in pEYFPpp71 and pEYFPCh82. These homologous sites were utilised to construct plasmids expressing the hybrids without altering the immediate coding sequences of pEYFPpp71 and pEYFPCh82. Figure 4.4 shows maps of the plasmids that express the hybrids. These plasmids were used to determine the features of pp71 that mediate long-term gene expression.

Plasmid pEYFPTC1 was constructed by exchanging the C-terminal end of pp71 with that of the Ch82 protein. Plasmids pEYFPpp71 and pEYFPCh82 were digested with the restriction endonucleases *Spe*I and *Bss*HII. Reaction mixtures were analysed by gel electrophoresis and the 550 bp fragment containing the C-terminus of pp71 was ligated to the large fragment of pEYFPCh82 and

		1		50
Ch82	(1)	MSRSPS-PGEGPSAAGGPGGAPGDNGSTFGRMHCQVLRRLVTNHDS-SLEP		
pp71	(1)	MSQASSPGEGPSSAAAISEAEASGSFGRLLHCQVLRRLITNVEGGSLA		
Consensus	(1)	MS A S P G E G P S A A A	S F G R L H C Q V L R L I T N D	S L E
		51		100
Ch82	(49)	DRLKILDLRTSVEVSRTSVLCCLFQENKSQHDTVDLTDLNVKGHC AVGERD		
pp71	(51)	GRRLRLDLRTNIEVSRPSVLCCLFQENKSPHDTVDLTDLNKGRCV VGEQD		
Consensus	(51)	RLKILDLRT IEVSR SVLC FQENKS HDTVDLTDLNKG C VGE D		
		101		150
Ch82	(99)	QLKADLINYSQRRMSPGS-STPTISVLAFGLPLERVPVSGIHLFQAHPRGD		
pp71	(101)	RLLVDLNNGP RRLTPGS ENNTVSVLAFALPLDRVPVSGIHLFQSQRGG		
Consensus	(101)	L DL NF RRLSPGS ISVLAFALPLDRVPVSGIHLFQA RG		
		151		200
Ch82	(148)	EENRLRTEARVDIRRTAYHWGVRTTVSPRWRKVDRSLEAEQIFTFEFIF		
pp71	(151)	EENRPRMEARAIIRRTAHHWAVRLTVTPNWRRTDSLEAGQIFVSQFAF		
Consensus	(151)	EENR R EAR IRRTAHHWAVR TVSP WRRK D SLEA QIF S F F		
		201		250
Ch82	(198)	RAGAIPLRLVDAVEQLLSCSDRNTYIHKAE TDARGQWVNVHLQHETLHPPP		
pp71	(201)	RAGAIPLTLVDALQLACSDPNTYIHKTE TD ERGQWIMLFLHHDSPHPP T		
Consensus	(201)	RAGAIPL LVDAL LACSD NTYIHK ETD RGQWI L L HDS HPP		
		251		300
Ch82	(248)	SVFLHFSLYTHGAEVVL RHNYPHILTRHG DNGFTLHAPRGFTLSRLHREY		
pp71	(251)	SVFLHFSLYTHRAEVVARHNYPHILRLP DNGFQLLIPKSF T LTRIHP EY		
Consensus	(251)	SVFLHFSLYTH AEVV RHNYPHIL R DNGF L PK FTLSRIH EY		
		301		350
Ch82	(298)	IVQVQNAFETNNTHDVIFFPADIPGVSMEAGPLPDRVRITIRLTW TGENS		
pp71	(301)	IVQIQNAFETNQTHDTIFFPENIPGVSIEAGPLPDRVRITLRVTLTG DQA		
Consensus	(301)	IVQIQNAFETNNTHD IFFP IPGVSIEAGPLPDRVRITIRLT TGDNA		
		351		400
Ch82	(348)	VRIEHMQILGTIHLFKRGLVNL L PGKTEKIKRPQIQLRAGLFPRRAVMRG		
pp71	(351)	VHLEHRQPLGR IHFERRGFWTLTPGKPKIKRPQVQLRAGLFPRSNVMRG		
Consensus	(351)	V IEH Q LG IH FKRGL L PGK DKIKRPQIQLRAGLFPR VMRG		
		401		450
Ch82	(398)	E VSEFR PQSPGELPLEGEEEEEE---EEER SSTPTPALSESVFAAF EES		
pp71	(401)	A VSEFL PQSPGLPTEEEEEEEEDD EDDL SSTPTPTP LSEAMFAGFEEA		
Consensus	(401)	VSEF PQSPG P E EEEEE EDD SSTPTP LSEAMFAAFEEA		

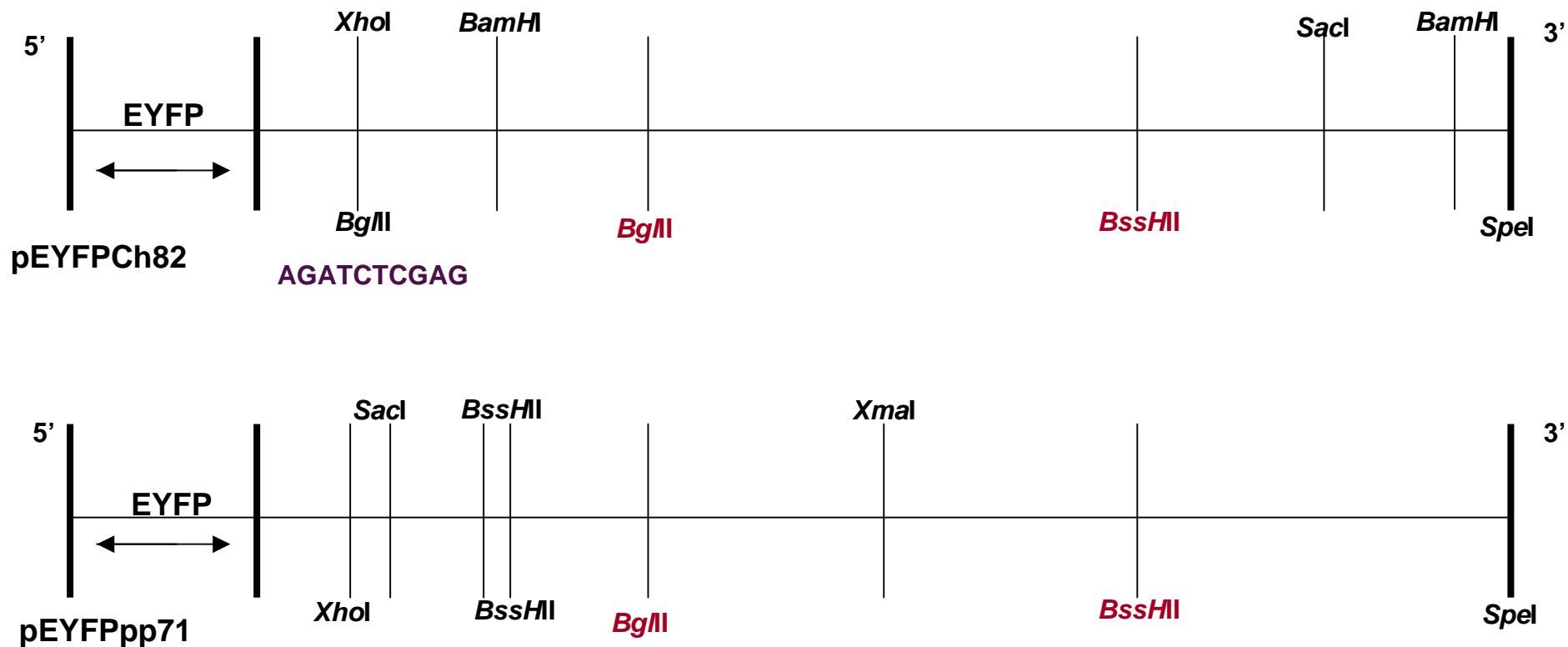
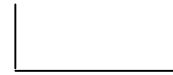


Figure 4.2. Schematic representation of the pEYFPpp71 and pEYFPCh82 plasmids

Maps showing the restriction sites used in constructing the EYFPpp71/EYFPCh82 plasmids. Conserved *BssHII* and *BglII* sites are marked in red. The 5' *XhoI* and *BglII* sites in EYFPCh82 plasmid overlapped (sequence marked in purple), this was taken into account when constructing the plasmids expressing the EYFPpp71/EYFPCh82 hybrids. Diagrams not to scale.

a

Amino acid sequence → **A E Q I F** Ch82
Nucleotide sequence → **gcc gag cag atc ttc**



BglII

Amino acid sequence → **A G Q I F** pp71
Nucleotide sequence → **gca ggg cag atc ttt**



BglII

b

Amino acid sequence → **Q L R A G** Ch82
Nucleotide sequence → **cag ctg cgc gcc ggc**



BssHII

Amino acid sequence → **Q L R A G** pp71
Nucleotide sequence → **cag ctg cgc gcc ggt**



BssHII

Figure 4.3 Schematic representation of the *BglII* and *BssHII* restriction sites in homologous regions of the pp71 and Ch82 nucleotide sequences.

The homologous restriction sites marked were used in constructing the pEYFPpp71/pEYFPCh82 plasmids.

transformed into competent *E.coli*. 24 hr later colonies were picked and amplified to make small scale DNA preparations. The plasmid DNA was screened by digestion with the restriction endonuclease *SacI* and *BssHII* to cut out the C-terminus fragment.

Plasmids pEYFPTC2 and pEYFPTC3 were created by exchanging the N-terminal ends of pEYFPpp71 and pEYFPCh82. In the case of pEYFPCh82 the *XhoI* and *BglII* sites overlapped (see figure 4.2). In order to release the N-terminal region the plasmid was digested first with *XhoI*, to linearise the plasmid. A second digest with *BglII* was carried out to isolate the region of interest. The plasmid pEYFPpp71 was digested with *XhoI* and *BglII* to separate the N-terminal region from the rest of the plasmid. As there was no overlapping *XhoI/BglII* site there was no need to linearise the plasmid initially. The fragment representing the N-terminus of pEYFPCh82 was ligated to the large pEYFPpp71 fragment while the isolated fragment containing the N-terminal of pp71 was ligated to the large pEYFPCh82 fragment. Small scale DNA preparations were screened for the correct insertions by digestion with restriction endonucleases *SacI* and *BamHI*.

To create plasmid pEYFPTC4, the C-terminal of Ch82 was transferred to pp71 via three way cloning. Plasmid pEYFPCh82 was digested with the restriction endonucleases *SpeI* and *BssHII* to release the 550 bp C-terminus region, while pEYFPpp71 was digested with *XmaI* and *SpeI* to release the large pEYFPpp71 fragment or with *XmaI* and *BssHII* to release a 190 bp fragment. The fragments were isolated, purified and the Ch82 550 bp C-terminus ligated to the isolated pEYFPpp71 190 bp and large fragments. Small scale DNA preparations were made and plasmid DNA was screened using the restriction endonucleases *SpeI* and *BssHII*.

The two remaining plasmids pEYFPTC5 and pEYFPTC6 were created by exchanging the middle coding regions of each homologue, again using three way cloning. Plasmid pEYFPTC5 was constructed by digesting pEYFPpp71 DNA with *XhoI* and *BglII* to release a 600 bp fragment, or with *XhoI* and *BssHII* to release the large fragment. pEYFPCh82 plasmid DNA was digested with the restriction endonucleases *BssHII* and *BglII* to release a 585 bp fragment containing the middle coding region of Ch82. Fragments were isolated, purified and the 585 bp pEYFPCh82 fragment was ligated to both isolated pEYFPpp71 fragments. Small

scale DNA preparations were screened using *Xma*I and *Xho*I restriction endonucleases.

Plasmid pEYFPTC6 was constructed by digesting pEYFPpp71 with *Bss*HI and *Bgl*II releasing 583 bp and 450 bp fragments. The pEYFPCh82 plasmid was digested with *Xho*I and *Bgl*II to release a 600 bp fragment or digested with *Xho*I and *Bss*HI to isolate the large pEYFPCh82 fragment. The large Ch82 fragment and the 600 bp fragment were ligated to the pp71 583 bp fragment. Plasmid DNA was prepared and screened for by digestion with restriction endonucleases *Xma*I and *Bss*HI to check for correct insertions.

A schematic representation of the six resulting plasmids is presented in figure 4.4. The hybrid proteins specified by pEYFPTC1 to 6 are named TC1 to TC6 respectively.

4.1.2. EYFPpp71/EYFPCh82 hybrids as transactivators of gene expression

The role of pp71 as a transactivator of short-term gene expression has been described previously (see chapter 3 for further details). To investigate functionality of the EYFPpp71/EYFPCh82 hybrid proteins constructed, plasmids pEYFPTC1, pEYFPTC2, pEYFPTC3, pEYFPTC4, pEYFPTC5, pEYFPTC6 were transfected into HFFF2 monolayers using a NucleofectorTM. Plasmids pEYFP-C1, pEYFPpp71 and pEYFPCh82 were used as controls as EYFPpp71 has previously been shown to stimulate long-term gene expression while EYFPCh82 did not. The transfected cells were incubated overnight at 37°C. Fluorescence levels of cells transfected with the EYFP-tagged plasmids were ascertained visually using a UV microscope at 24 hr post-infection. Satisfactory levels of fluorescence were classed as 60-70% of cells fluorescing.

To investigate the activities of the hybrids, the transfected cells were infected with 3×10^5 pfu, 1×10^5 pfu or 3×10^4 pfu of *in1382* (a HSV-1 recombinant impaired for transcriptional activity, expressing β -gal driven by the HCMV MIEP) and incubated at 38.5°C for a further 24 hr. Following infection the cell monolayers were stained with X-gal reaction mix and the β -gal positive cells were counted. Figure 4.5 shows the average numbers of β -gal positive cells counted from two individual experiments, the raw data for which are presented in table 4.1. The results

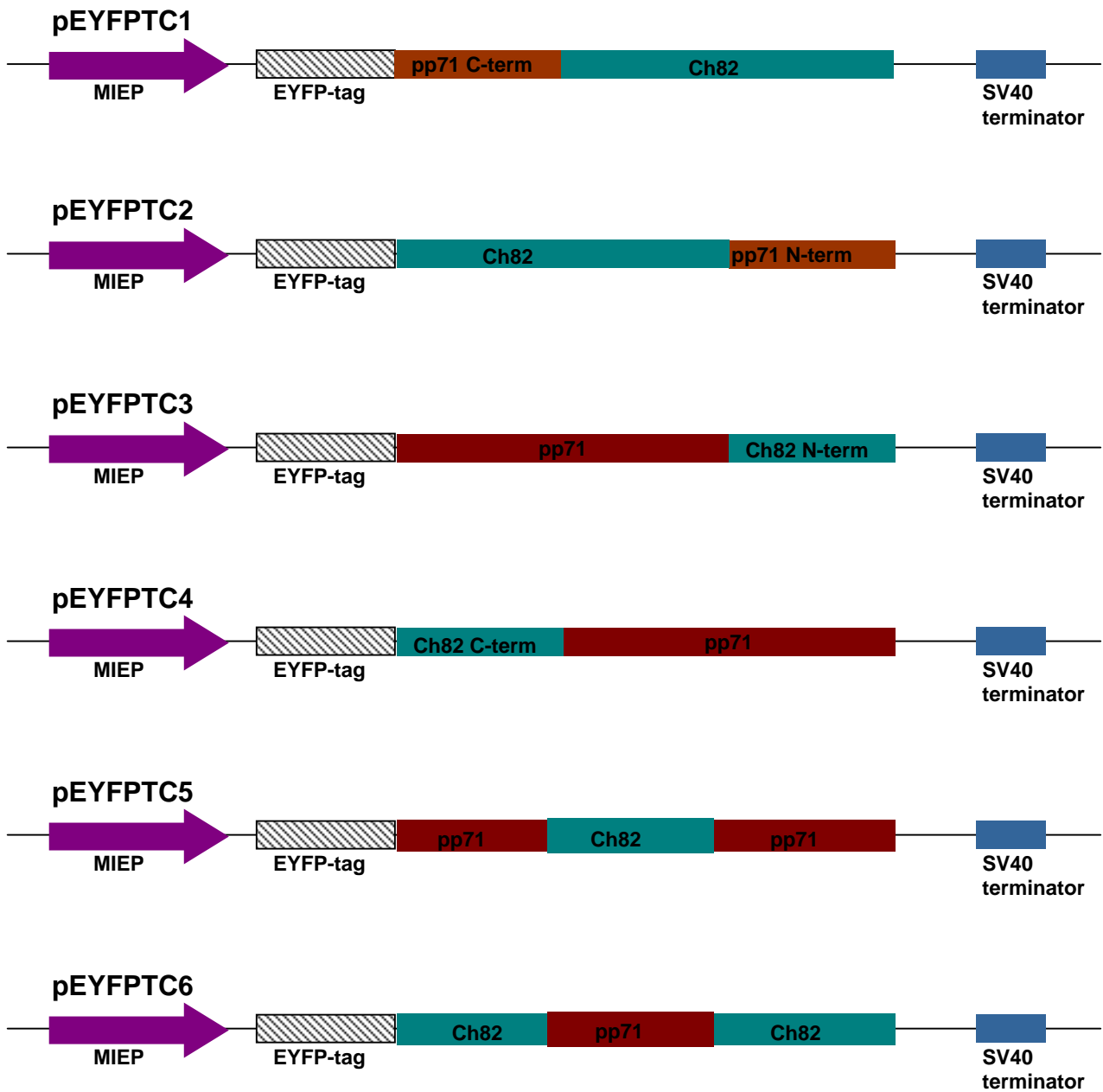


Figure 4.4 Schematic representation of the pEYFPpp71/pEYFPCh82 hybrids

Plasmid maps of the EYFPpp71/EYFPCh82 hybrids. Six hybrids were constructed by exchanging the C-terminal. N-terminal and middle regions off pp71 with those of Ch82. Plasmid maps show the MIEP, EYFP-tag and the SV40 terminator.

		Experiment 1		Experiment 2		Experiment 3		Experiment 4	
Plasmid	Titre	24 hours	10 days						
	3x10 ⁵	24	0	17	2	19	9	17	0
pEYFP-C1	1x10 ⁵	6	0	13	0	6	0	22	0
	3x10 ⁴	0	0	0	0	0	0	0	0
	3x10 ⁵	39	93	243	976	118	183	76	608
pEYFPpp71	1x10 ⁵	3	4	102	336	101	101	24	380
	3x10 ⁴	0	0	0	18	0	0	0	14
	3x10 ⁵	54	0	146	12				
pEYFPCh82	1x10 ⁵	2	0	102	0				
	3x10 ⁴	0	0	3	0				
	3x10 ⁵	37	0	171	8				
pEYFPTC1	1x10 ⁵	15	0	49	2				
	3x10 ⁴	0	0	0	0				
	3x10 ⁵	27	0	161	5				
pEYFPTC2	1x10 ⁵	7	0	51	2				
	3x10 ⁴	0	0	0	0				
	3x10 ⁵	58	0	153	11				
pEYFPTC3	1x10 ⁵	6	0	51	0				
	3x10 ⁴	0	0	0	0				
	3x10 ⁵	164	41	174	57				
pEYFPTC4	1x10 ⁵	41	6	51	0				
	3x10 ⁴	0	0	0	0				
	3x10 ⁵	47	0	151	0				
pEYFPTC5	1x10 ⁵	0	0	0	0				
	3x10 ⁴	0	0	0	0				
	3x10 ⁵	82	108	27	0	102	102	44	69
pEYFPTC6	1x10 ⁵	4	0	2	0	41	20	2	5
	3x10 ⁴	0	0	0	0	0	0	0	0

Table 4.1. Stimulation of β -gal expression directed by the pEYFPpp71/pEYFPCh82 hybrids at 24 hr and 10 days post-transfection. HFFF2 monolayers were transfected with plasmids expressing the required EYFP-tagged UL82 homologues or EYFPpp71/EYFPCh82 hybrids and infected with virus *in1382* at 24 hr post-transfection. After a further 24 hr or 10 days, monolayers were stained with X-gal and β -gal positive cells were counted.

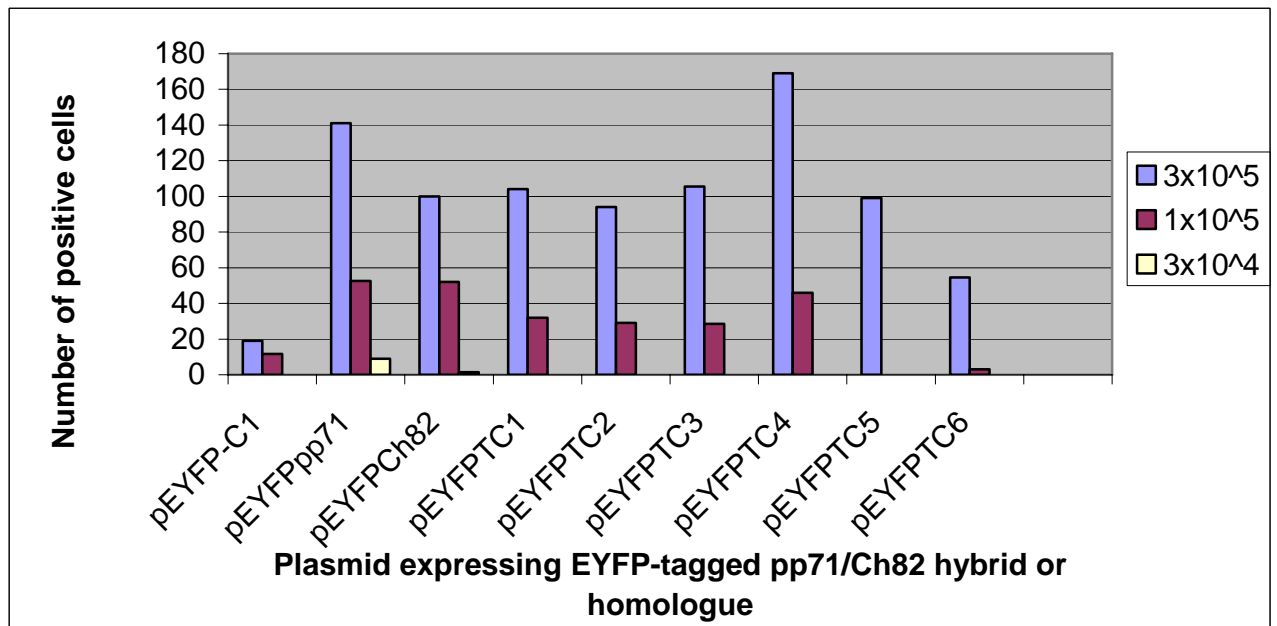


Figure 4.5. Expression directed by the EYFPpp71/EYFPCh82 hybrids at 24 hr post-transfection

HFFF2 monolayers were transfected with plasmids expressing EYFP-tagged UL82 homologues or EYFPpp71/EYFPCh82 hybrids, and infected with various amounts of *in1382* at 24 hr post-transfection. After a further 24 hr, monolayers were stained with X-gal and β -gal positive cells were counted.

presented in figure 4.5 show that cultures transfected with each of the plasmids expressing a EYFPpp71/EYFPCh82 hybrid gave more β -gal positive cells than those transfected with the control vector pEYFP-C1, when subsequently infected with 3×10^5 pfu or 1×10^5 pfu of *in1382*. Cells transfected with plasmids pEYFPTC1, pEYFPTC2, or pEYFPTC3 all showed similar numbers of β -gal positive cells, when infected with 3×10^5 pfu or at 1×10^5 pfu of virus, to each other and to cultures transfected with pEYFPCh82 but fewer β -gal positive cells than cultures transfected with pEYFPpp71. However pEYFPTC5 only directed β -gal expression in cells infected with 3×10^5 pfu of *in1382*, no β -gal positive cells were observed when transfected cells were infected with 1×10^5 pfu or 3×10^4 pfu of *in1382*. Levels of expression directed by this plasmid at 3×10^5 pfu were similar to those directed by pEYFPCh82. Cultures transfected with pEYFPTC4 showed a greater number of β -gal positive cells than those transfected with plasmids pEYFPCh82 or pEYFPpp71 when infected with 3×10^5 pfu of *in1382*. Figure 4.5 shows that the lowest levels of β -gal expression were directed by the plasmid pEYFPTC6. When infecting cells with 3×10^5 pfu or 1×10^5 pfu of *in1382* fewer β -gal positive cells were observed than after transfection with pEYFPpp71, pEYFPCh82 or the other pEYFPpp71/pEYFPCh82 plasmids. However all of the plasmids expressing the EYFPpp71/EYFPCh82 hybrids were able to direct levels of β -gal expression above the control (pEYFP-C1), indicating that the hybrid proteins expressed by the plasmids were functional and able to stimulate short-term gene expression in a similar manner to that of pp71.

At 10 days post-infection cell monolayers were stained with X-gal reaction mix and β -gal positive cells were counted. Figure 4.6 shows the average numbers of β -gal positive cells at 10 days post-infection in transfected cultures infected with 3×10^5 pfu of *in1382*. An increase in the number of β -gal positive cells was observed in cultures transfected with pEYFPpp71, compared to that observed at 24 hr post-infection. Cultures transfected with pEYFPCh82 showed, as expected, a decrease in the numbers of β -gal cells observed at 10 days post-infection. A similar result was observed in cultures transfected with plasmids pEYFPTC1, pEYFPTC2, pEYFPTC3, pEYFPTC4 or pEYFPTC5, all of which directed low levels, or no, β -gal expression at 10 days post-infection. Cultures transfected with plasmid pEYFPTC6, however, showed levels of β -gal expression at 10 days that were

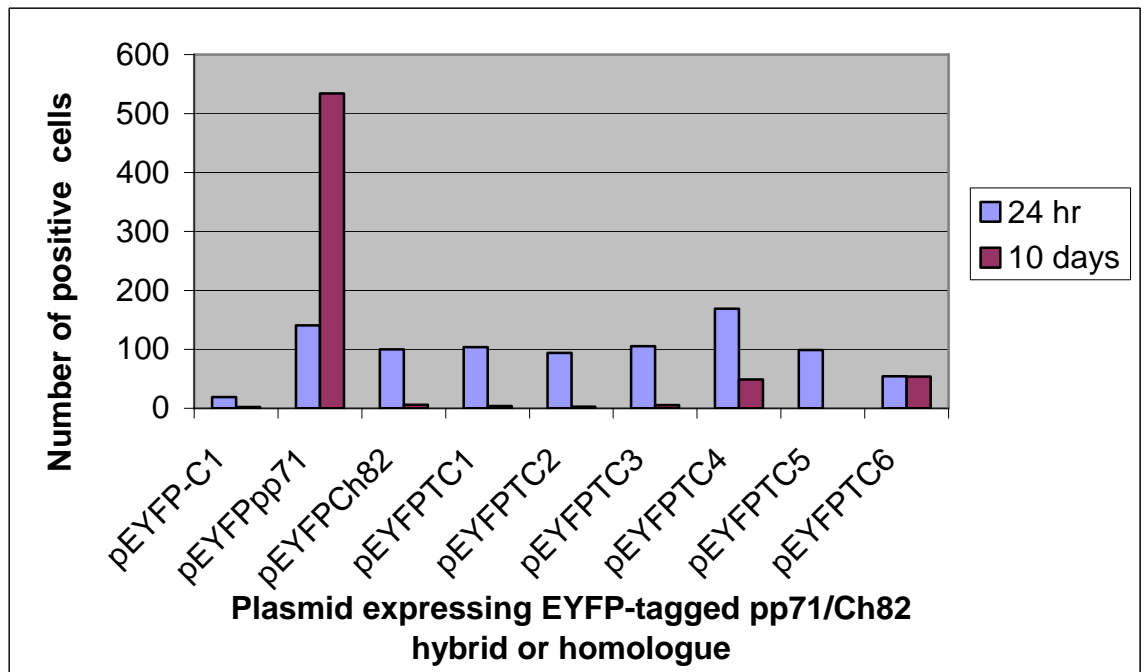


Figure 4.6. β -gal expression directed by EYFPpp71/EYFPCh82 hybrids at 24 hr and 10 days post-infection.

HFFF2 monolayers were transfected with plasmids expressing EYFP-tagged UL82 homologues or hybrids, and infected with 3×10^5 pfu of *in1382* at 24 hr post-transfection. After a further 24 hr or 10 days, monolayers were stained with X-gal and β -gal positive cells were counted.

similar to those observed at 24 hr post-infection. Numbers of β -gal positive cells were however, lower than those observed in cultures transfected with pEYFPpp71.

This result was reflected in the individual experiments as presented in table 4.1. Experiment one showed an increase in the number of β -gal positive cells at day 10 compared to 24 hr, while experiment two showed no β -gal positive cells at 10 days post-infection in cultures transfected with pEYFPTC6. Further investigation into the functionality of plasmid pEYFPTC6 showed that in two out of four experiments, the number of β -gal positive cells counted either stayed constant or increased at 10 days post-infection (table 4.1). Due to the large degree of variability in numbers of β -gal positive cells between individual transfection experiments, it was not possible to carry out statistical analysis on the numbers. Therefore all that could be confirmed from these experiments was that all of the hybrids were functional in short-term assays. However, in the context of long-term gene expression, plasmids pEYFPTC1, pEYFPTC2, pEYFPTC3, pEYFPTC4, and pEYFPTC5 all resembled the pEYFPCh82 homologue as they were unable to direct long-term gene expression. The only exception was pEYFPTC6, which contained the middle coding sequence of pp71. At 10 days post-infection conflicting results were observed which made it impossible to determine whether pEYFPTC6 was able to drive long-term gene expression, however it was clear that some activity was present.

Lysates of HFFF2 cells transfected with the plasmids pEYFP-C1, pEYFPpp71, pEYFPCh82, pEYFPTC1, pEYFPTC2, pEYFPTC3, pEYFPTC4, pEYFPTC5, or pEYFPTC6 were analysed by gel electrophoresis and transferred onto nitrocellulose membranes. The EYFP tagged proteins were detected using an anti-GFP antibody. Figure 4.7 shows levels of protein present in lysates of transfected cells at 24 hr post-transfection. Blot i shows that plasmids pEYFPTC1 and pEYFPTC3 directed similar levels of protein expression compared to that in lysates of cells transfected with pEYFPpp71, while plasmid pEYFPTC2 expressed levels of protein similar to that observed in lysates of cells transfected with pEYFPCh82. Blot ii shows that in lysates of cells transfected with both pEYFPpp71 and pEYFPCh82 low levels of protein were expressed, at equivalent levels to that observed in lysates of cells transfected with pEYFPTC5. In lysates of cells transfected with pEYFPTC6 very low levels of protein were detected.

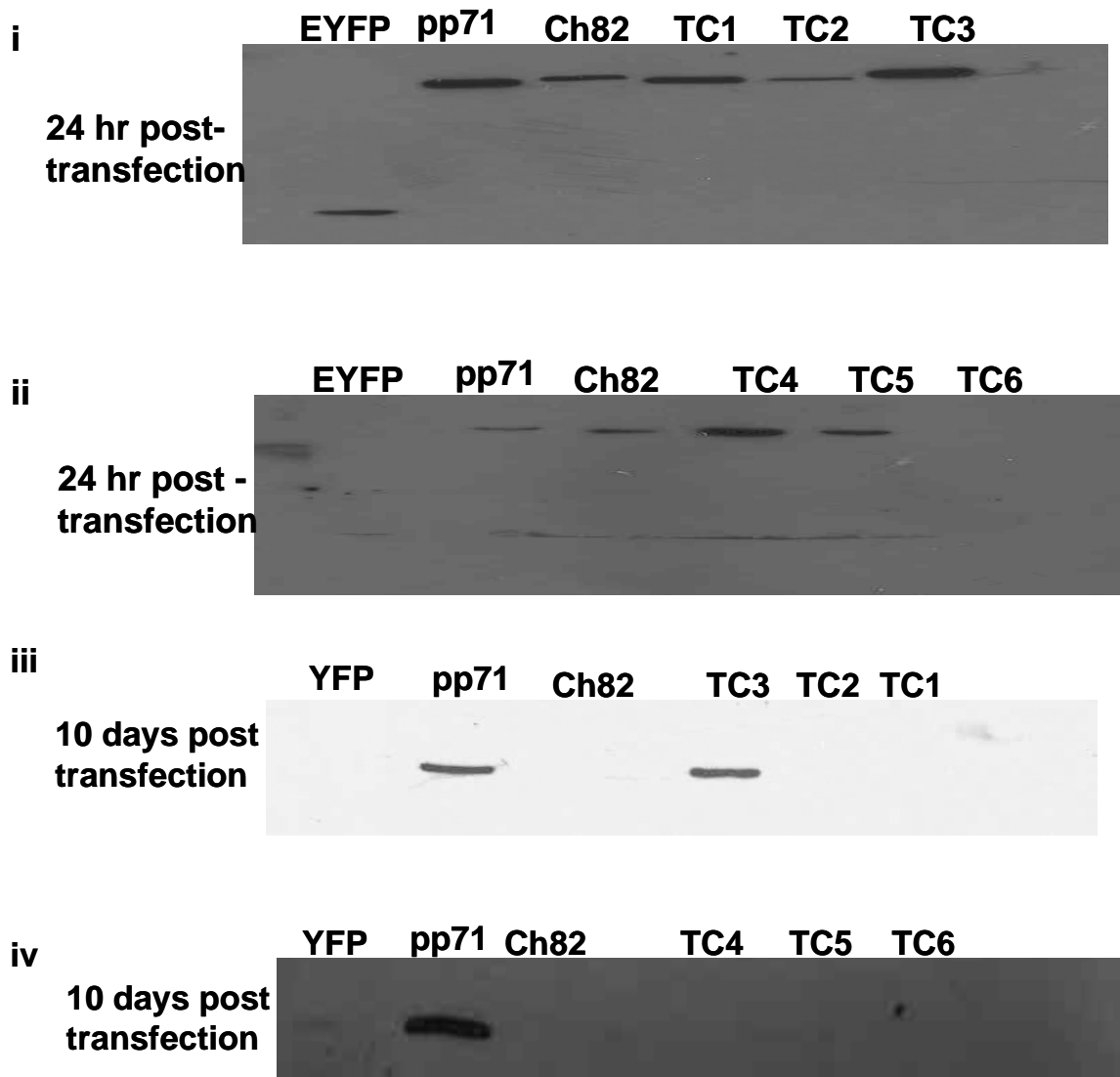


Figure 4.7. Analysis of protein expression directed by the pEYFPpp71/pEYFPCh82 plasmids at 24 hr and 10-days post-transfection.

HFFF2 monolayers were transfected with plasmids expressing pEYFPpp71, pEYFPCh82 or the pEYFPpp71/pEYFPCh82 hybrids. Cell lysates were harvested at either 24 hr or 10 days post-transfection and EYFP-tagged proteins were subjected to SDS PAGE. The EYFP-tagged proteins were detected using an anti-GFP primary antibody and an anti-rabbit HRP conjugated secondary antibody.

However plasmid pEYFPTC4 expressed protein at levels greater than for pEYFPpp71.

Blots iii and iv show protein expression of pEYFPpp71 and pEYFPCh82 and EYFPpp71/EYFPCh82 hybrids at 10 days post-transfection. Both blots showed increased levels of protein expression in lysates of cells transfected with pEYFPpp71, while no protein was detected in lysates of cells transfected with pEYFPCh82, indicating that protein expression was switched off. No protein was detected in lysates of cells transfected with pEYFPTC1, pEYFPTC2, pEYFPTC4, pEYFPTC5 and pEYFPTC6, however in lysates of cells transfected with pEYFPTC3 protein expression was similar to that after transfection of pEYFPpp71. The western blot in figure 4.7 shows contrasting results to those in figure 4.5 in that pEYFPTC3 was able to continue producing protein after 10 days post-infection but did not direct β -gal expression at 10 days. Surprisingly, given the results of the β -gal assays, no protein was detected in cells transfected with pEYFPTC6 at 10 days post-infection.

Data from transfection assays showed that it was possible to construct hybrid proteins using particular regions of the pp71 and Ch82 proteins which were functional in short-term assays. However in long-term assays, while it was again confirmed that pp71 could stimulate long-term gene expression, conflicting results were obtained from the plasmid pEYFPTC6. It appeared that this hybrid was unable to stimulate protein synthesis at late times post-infection, while the numbers of β -gal positive cells gave conflicting results as to whether this hybrid was able to direct long-term gene expression or not. To establish the true behaviour of this protein, TC6 was recombined into a HSV-1 recombinant virus (*in1312*).

4. Part II

4.2. Introduction

Plasmid transfection assays using EYFP-tagged pp71/Ch82 hybrids showed all of the hybrids to be functional because they stimulated short-term gene expression. However in terms of long-term gene expression, plasmid pEYFPTC6 (mid region of pp71 cloned into the Ch82 homologue) produced conflicting results. Expression assays showed that pEYFPTC6 might direct long-term gene expression, while western analysis showed protein expression to be at a considerably lower level than that of pp71 at 24 hr post-transfection with no detectable protein expressed by pEYFPTC6 at 10 days post-transfection. In order to determine if this hybrid was able to direct long-term gene expression and to eliminate the problem of variability in numbers incurred from transfection assays, the HSV-1 *in1312* recombinant, *in0156*, was constructed. This recombinant virus was analogous to *in1310* but contained the DNA sequence encoding EYFPTC6 in place of the EYFPpp71 coding region and β -gal inserted into the non-essential UL43 locus under the control of the MIEP. The HSV-1 recombinant virus, *in0156*, again contained mutations at of VP16, ICP0 and a temperature sensitive mutation in ICP4 ensuring the virus became quiescent shortly after infection. The DNA sequences encoding EYFPTC6 was recombined into the HSV-1 recombinant using a method similar to that described in section 3.2.1.

4.2.1. Infection with the *in1312* recombinant *in0156* stimulates short-term gene expression

The *in1312* recombinant virus expressing EYFPTC6, *in0156*, was first analysed for short-term gene expression. 1.5×10^5 U373 cells were seeded in a 24 well plate and infected, with 5×10^5 pfu (MOI 3.3) of *in1310* (expressing EYFPpp71), *in0146* (EYFPCh82), *in0156* (EYFPTC6), *in1374* (negative control) or mock-infected and incubated at 38.5°C. At 24 hr post-infection cell monolayers were stained with X-gal reaction mix and β -gal positive cells were observed. Figure 4.8 shows that, in U373 monolayers infected with *in1310* or *in0146*, equivalent numbers of β -gal expressing cells were detected at levels above those of *in1374*. U373 cells infected with *in0156* showed numbers of β -gal expressing cells that were similar to, or slightly higher than, those in *in1310* or *in0146* infected cultures.

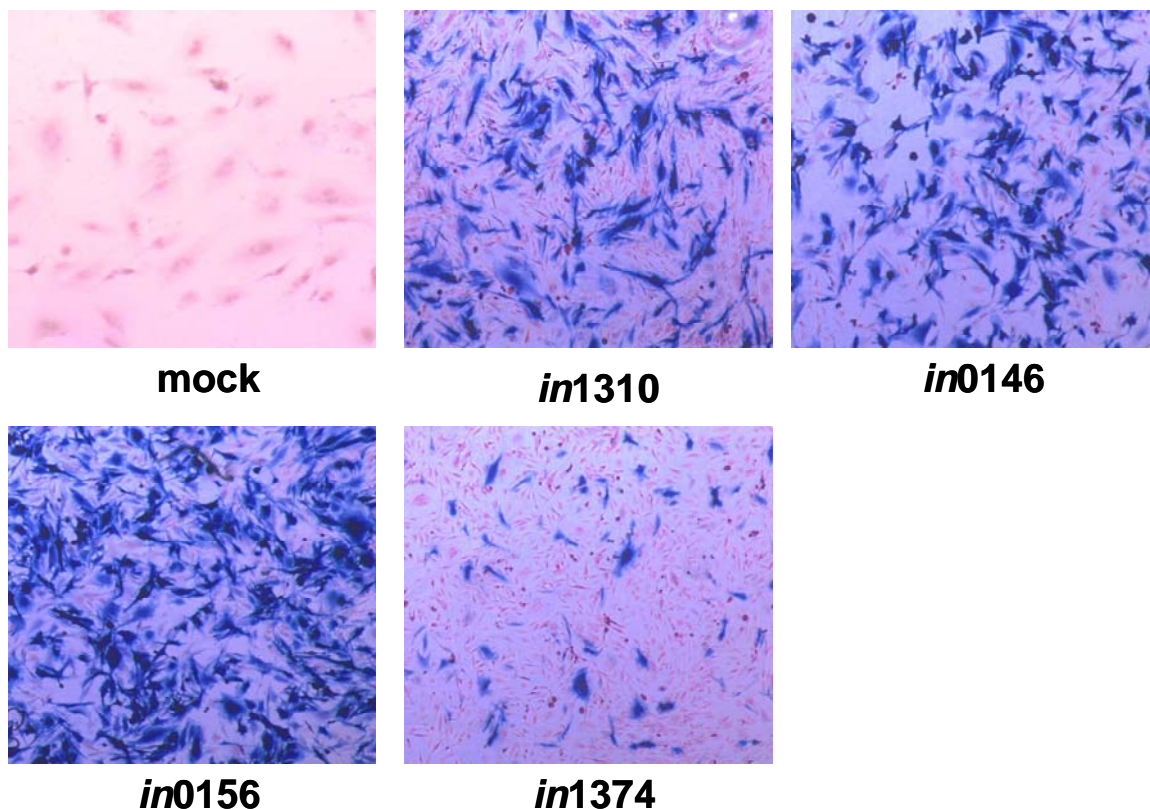


Figure 4.8. β -gal expression directed by *in1312* recombinants expressing EYFP-tagged UL82 homologues or hybrid EYFPTC6 at 24 hr post-infection U373 cell monolayers were mock-infected or infected with 5×10^5 pfu (MOI 3.3) of the *in1312* recombinants expressing either the UL82 homologues or EYFPTC6 and incubated at 38.5°C . *In1374*, a virus lacking the ORF of the UL82 homologues was used as a control. At 24 hr post-infection cell monolayers were stained with X-gal.

The *in1310* virus expresses EYFPpp71, *in0146* expresses EYFPCh82, *in0156* expresses EYFPTC6 and *in1374* was used as a negative control.

U373 cells were mock-infected or infected with 5×10^5 pfu of *in1310*, *in0146*, *in0156* or *in1374* and lysates were analysed SDS PAGE and transferred onto a nitrocellulose membrane. Protein expression was detected using an anti-GFP antibody. Figure 4.9 shows that lysates from cells infected with *in1310* and *in0146* produced equivalent amounts of protein at 24 hr post-infection while lysates from cells infected with *in0156*, contained lower levels of protein compared to those in lysates from cells infected with *in1310* or *in0146*. As expected no EYFP-tagged protein was observed in lysates from mock-infected or cells infected with *in1374*. Mock-infected and infected cell lysates were analysed by SDS PAGE again and blots were probed with an anti-actin antibody and an anti-mouse secondary antibody, to control for loading.

In order to quantify expression levels, U373 cells infected with 5×10^5 pfu of *in1310*, *in0146*, *in0156* *in1374* or mock-infected were super-infected with *in1318* (expressing SEAP under the control of the MIEP) and incubated at 38.5°C for 24 hr. Following infection, samples of the growth medium were harvested and endogenous alkaline phosphatase was eliminated by heating samples to 65°C prior to assaying for the amount of SEAP. Figure 4.10 shows the average number of arbitrary units of fluorescence from two experiments. The results show that samples of growth medium harvested from mock or *in1374* infected monolayers exhibited low levels of alkaline phosphatase activity. Cell monolayers infected with *in1310* and *in0156* showed similar levels of alkaline phosphatase activity. However, medium harvested from cells infected with *in0146* appeared to release levels of alkaline phosphatase activity to higher levels than cells infected with *in1310* and *in0156*.

4.2.2. Analysis of long-term gene expression

Data from transfection assays (presented in section 4.1.2) showed that of all the six EYFPpp71/EYFPCh82 hybrids constructed for this study only one showed any indication of stimulating long-term gene expression. However, variability in the numbers of β -gal positive cells was observed between individual experiments. To overcome this and to establish if the hybrid EYFPTC6 had any role in long-term gene expression, the HSV-1 recombinant virus *in0156* was used to investigate the ability of this hybrid protein to direct β -gal expression at late times post infection.

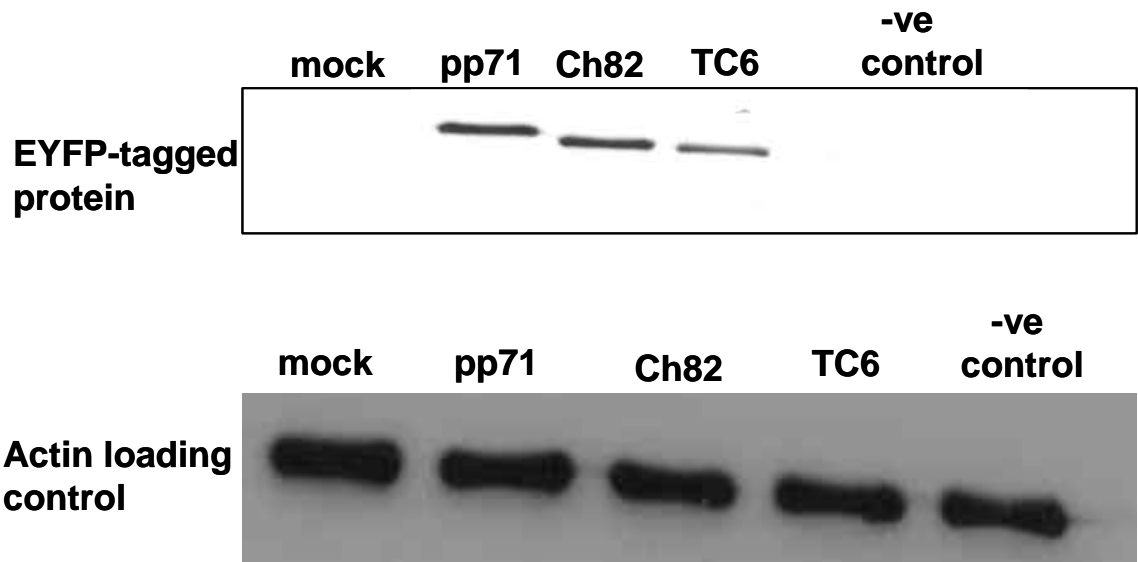


Figure 4.9. Expression of the EYFP-tagged UL82 homologues or TC6 at 24 hr post-infection.

U373 cell monolayers were mock-infected or infected with 5×10^5 pfu (MOI 3.3) of the *in1312* recombinants expressing either the UL82 homologues or TC6 and incubated at 38.5°C . At 24 hr post infection cell lysates were harvested, and subjected to SDS PAGE. Proteins were transferred to a nitrocellulose membrane and were probed with an anti-GFP primary antibody and an anti-rabbit HRP conjugated secondary antibody. Lysates were subjected to SDS PAGE again and probed with an anti-actin antibody and an anti-mouse HRP-conjugated secondary antibody, to act as a loading control.

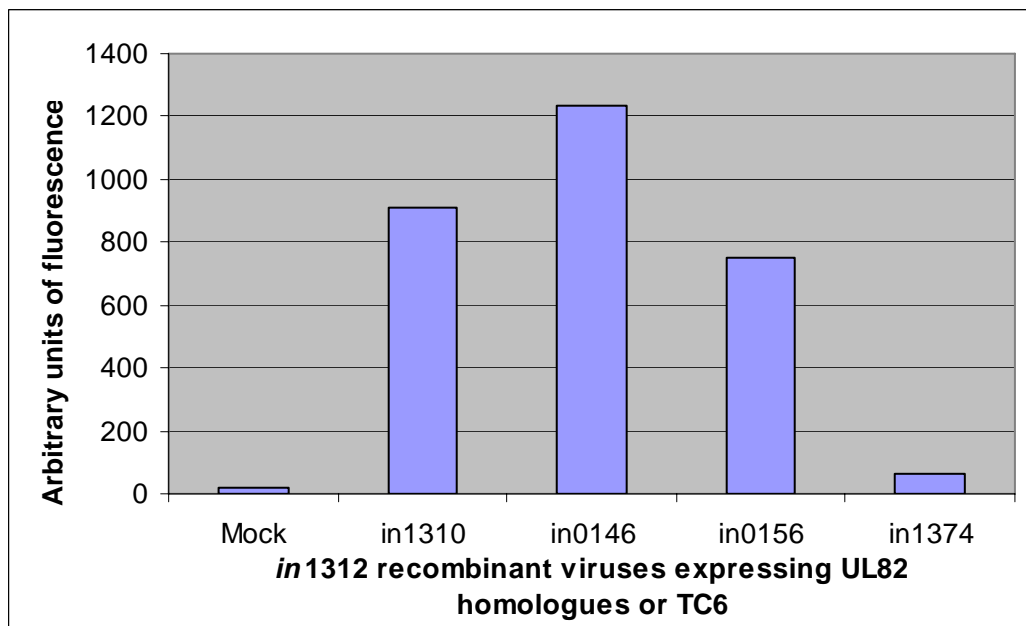


Figure 4.10. Activity of the *in1312* recombinants expressing either the UL82 homologues or EYFPTC6 *in trans*

U373 monolayers were infected with 5×10^5 pfu (MOI 3.3) of the *in1312* recombinants expressing either the UL82 homologues or EYFPTC6 and incubated at 38.5°C for 2 hr. The cell monolayers were super-infected with 5×10^5 pfu of *in1318* and incubation was continued at 38.5°C . At 24 hr post-infection samples of medium were analysed for alkaline phosphatase activity.

Three sets of HFFF2 cells were seeded at 1×10^6 cells per 35 mm dish. Confluent cell monolayers were either mock-infected or infected with 3×10^6 pfu (MOI 3) of *in1310* (expressing EYFPpp71), *in0146* (EYFPCh82), *in0156* (EYFPTC6) or *in1374* and incubated in DF2 medium at 38.5°C for 10 days with medium changes every two days. At 9 days post-infection one set of HFFF2 cells was super-infected with 3×10^6 pfu of *tsK* and incubation was continued for a further 24 hr at 38.5°C . The growth medium on one set of cells was replaced with fresh medium supplemented with 2% human serum and the cultures were downshifted to 31°C for a further 5 days. One set of cells remained untreated at 38.5°C . At 10 days post-infection cell monolayers super-infected with *tsK*, and those left untreated, were fixed and stained with X-gal. Cells that were downshifted to the permissive temperature of 31°C were stained at 14 days post-infection.

Figure 4.11a shows that untreated cell monolayers that were mock-infected or infected with *in1374* exhibited no β -gal expression. Monolayers infected with *in0146* showed no β -gal expression while those infected with *in1310* expressed, as expected, significant levels of β -gal. Monolayers infected with *in0156* still showed some β -gal expression, as some positive cells were observed at 10 days post-infection. The levels of expression observed however were significantly lower than those seen in monolayers infected with *in1310*. These results were confirmed by the downshift assay where figure 4.11b shows no β -gal expression in cell monolayers infected with *in1374*, *in0146* or mock-infected. In HFFF2 monolayers infected with *in1310*, large plaques could be observed indicating that the virus was able to replicate at its permissive temperature. Cell monolayers infected with *in0156* also showed a number of plaques, indicating that, by moving the cultures to 31°C the virus retained some replicative properties. However the numbers of plaques observed in this case were significantly fewer and the plaques were smaller in size than those seen in cells infected with *in1310*. Figure 4.11c shows cell monolayers super-infected with *tsK* at day 9 post-infection. Functional ICP0 expressed by the *tsK* virus allowed quiescent genomes to reactivate. β -gal expression at 10 days post-infection showed that viral genomes were present in all of the cell monolayers at functionally comparable levels.

At 9 days post-infection a proportion of untreated cells was subcultured into 24 well plates and incubated at 38.5°C for a further 24 hr. At 10 days post-infection lysates were harvested, analysed by gel electrophoresis and subjected to SDS

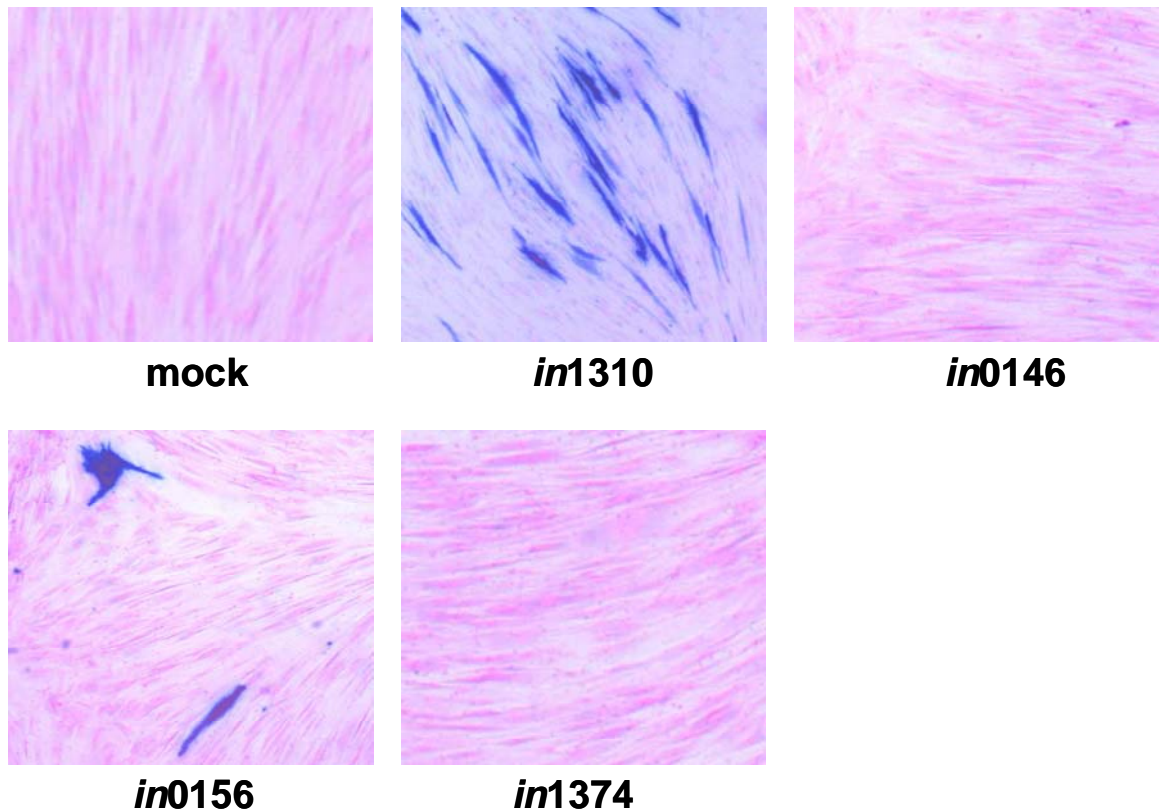


Figure 4.11a. β -gal expression directed by the *in1312* recombinants expressing the EYFP-tagged UL82 homologues or TC6 at 10 days post-infection.

HFFF2 cell monolayers were infected with 3×10^6 pfu (MOI 3) of the *in1312* recombinants expressing either the UL82 homologues or TC6 and incubated at 38.5°C . *In1374*, a virus lacking the ORF of the UL82 homologues was used as a control. At 10 days post-infection cell monolayers were stained with X-gal.

The *in1310* virus expresses EYFPpp71, *in0146* expresses EYFPCh82, *in0156* expresses EYFPTC6 and *in1374* was used as a negative control.

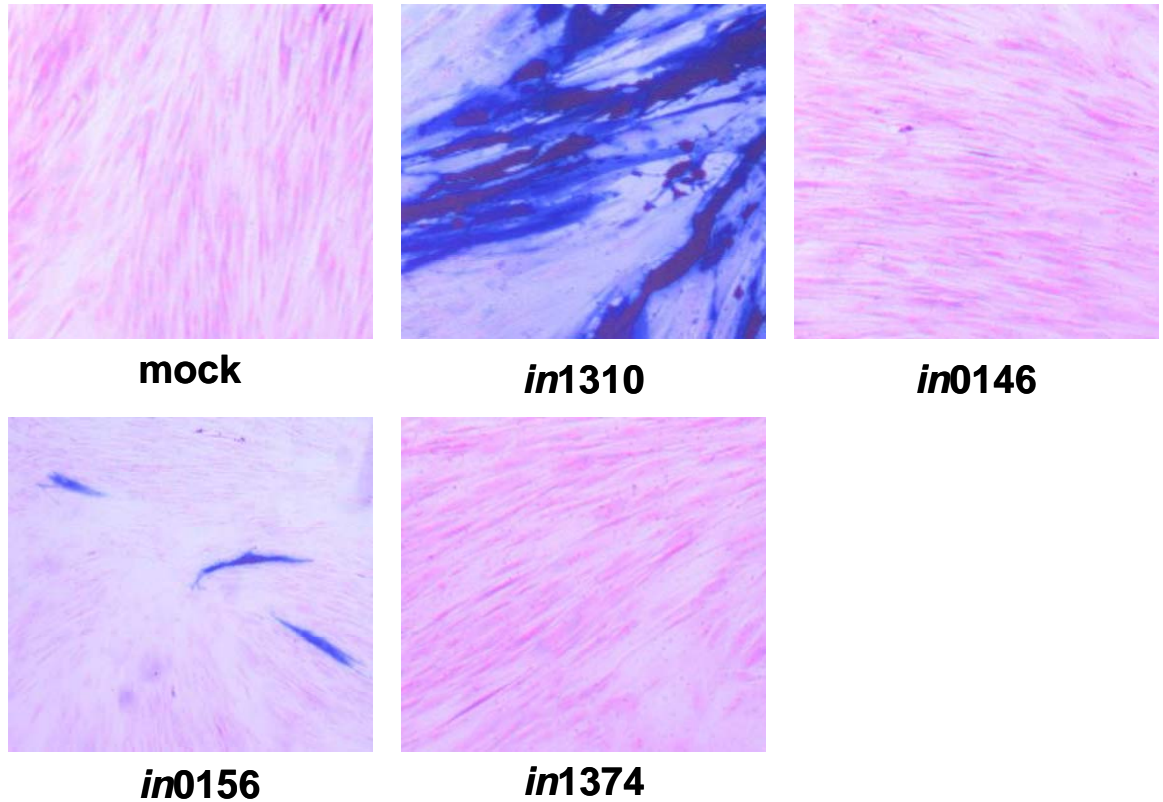


Figure 4.11b. Response of the *in1312* recombinants expressing the UL82 homologues or TC6 to temperature downshift.

HFFF2 monolayers were infected with 3×10^6 pfu (MOI 3) of the *in1312* recombinants expressing either the UL82 homologues or TC6 and incubated at 38.5°C . *In1374*, a virus lacking the ORF of the UL82 homologues was used as a control. At 9 days post-infection cell monolayers were overlayed with medium containing 2% human serum and downshifted to 31°C . At 14 days post-infection cell monolayers were stained with X-gal.

The *in1310* virus expresses EYFPpp71, *in0146* expresses EYFPCh82, *in0156* expresses EYFPTC6 and *in1374* was used as a negative control.

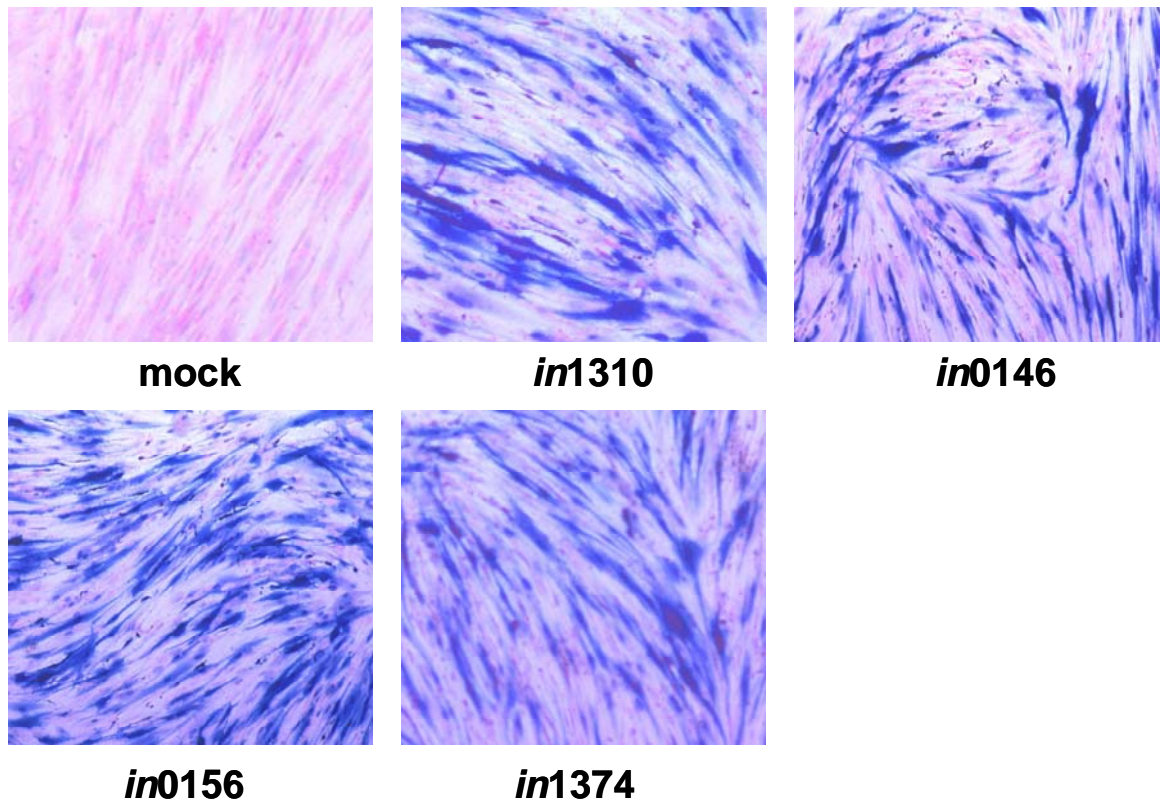


Figure 4.11c. Response of the *in1312* recombinants expressing the UL82 homologues or TC6 to super-infection with *tsK*.

HFFF2 monolayers were infected with 3×10^6 pfu (MOI 3) of the *in1312* recombinants expressing either the UL82 homologues or TC6 and incubated at 38.5°C. *in1374*, a virus lacking the ORF of the UL82 homologues was used as a control. At 9 days post-infection cell monolayers were super-infected with *tsK* and incubated at 38.5°C for a further 24 hr. At 10 days post-infection cell monolayers were stained with X-gal.

The *in1310* virus expresses EYFPpp71, *in0146* expresses EYFPCh82, *in0156* expresses EYFPTC6 and *in1374* was used as a negative control.

PAGE. Protein expression was detected using an anti-GFP antibody. Figure 4.12 shows at 10 days post-infection, as shown previously in figure 4.7, pp71 protein could be detected whereas in lysates of cells infected with *in0146*, no protein was detected. Furthermore no protein was detected in lysates of cells infected with *in0156* suggesting reduced production of the protein at late times of infection.

Data from the infection assays presented here show again that pp71 is able to stimulate long-term gene expression. Interestingly however, cells infected with *in0156* still exhibited some β -gal activity at 10 days post-infection. Levels of β -gal expression observed appeared to be lower than observed in cells infected with *in1310*. Therefore EYFPTC6 seems to retain some of the properties involved in long-term gene expression of pp71.

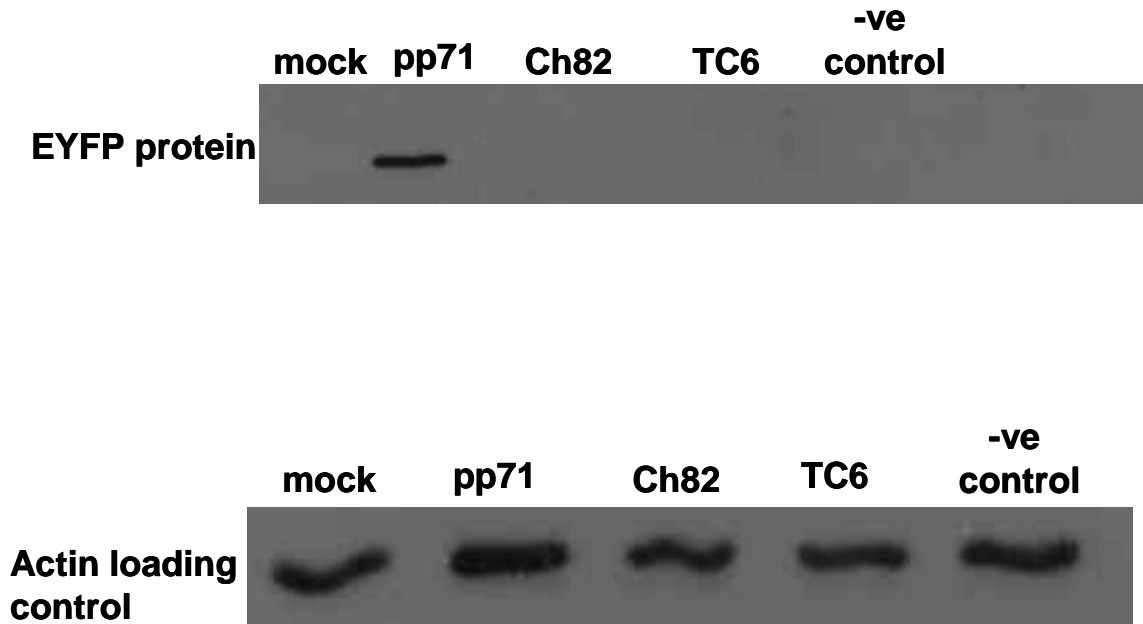


Figure 4.12. Expression of the EYFP-tagged UL82 homologues or TC6 at 10 days post-infection.

HFFF2 cell monolayers were either mock-infected or infected with 3×10^6 pfu (MOI 3) of the *in1312* recombinants expressing the UL82 homologues or TC6 and incubated at 38.5°C . At 10 days post-infection cell lysates were harvested, subjected to SDS PAGE and proteins transferred onto a nitrocellulose membrane. EYFP-tagged proteins expressed by the *in1312* recombinants were detected using an anti-GFP primary antibody and an anti-rabbit HRP conjugated secondary antibody. Blots were stripped and reprobed with an anti-actin primary antibody and an anti-mouse HRP-conjugated secondary antibody to act as a control for loading. Proteins were detected using ECL prior to exposure to autoradiographic film.

4.3. Discussion

Having established that pp71 is unique in its ability to stimulate long-term gene expression, the second part of this study aimed to investigate the region of pp71 involved in this. Due to the significant degree of homology between the pp71 and Ch82 homologues, hybrid proteins were constructed in order to closely examine the effects on gene expression of their C-termini, N-termini and mid-regions.

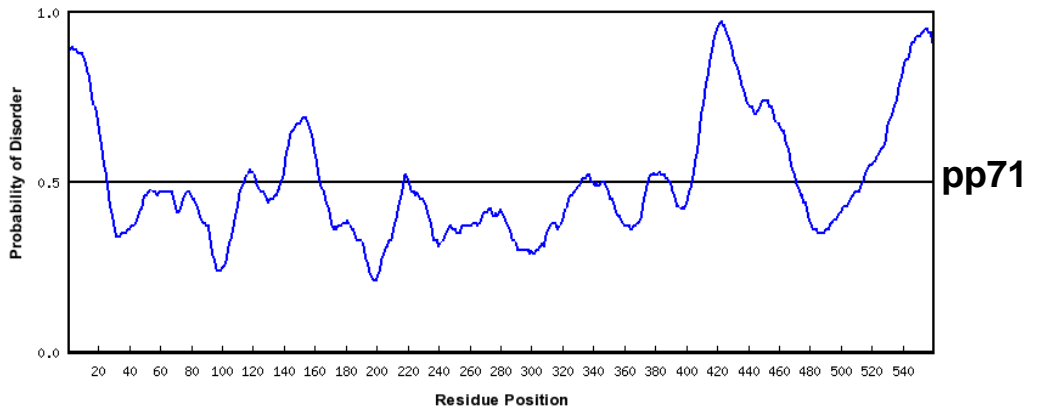
Initial experiments using plasmid based transfection assays showed all six hybrids were functional in short-term assays, as numbers of β -gal positive cells were observed at levels above the control. These results were also reflected in the western analysis whereby all six hybrids stimulated protein expression. In the long-term expression studies pEYFPpp71 continued to direct β -gal expression at 10 days post-infection. No activity was observed in cells transfected with pEYFPCh82 or the majority of pEYFPpp71/pEYFPCh82 hybrids, the only exception being cells transfected with pEYFPTC6. There was no difference in the average numbers of β -gal positive cells at 10 days post-transfection compared to 24 hr post-transfection although there were variabilites in numbers within individual experiments. With regards to western analysis no protein was detectable at 10 days post-transfection. From this it was concluded that some activity may have been retained, however the degree of activity was lower than that observed with pEYFPpp71.

Variability in numbers of β -gal positive cells was also observed with the remaining hybrids and was attributed to transfection discrepancies. However, the variability in numbers between experiments meant that statistical analysis could not be performed.

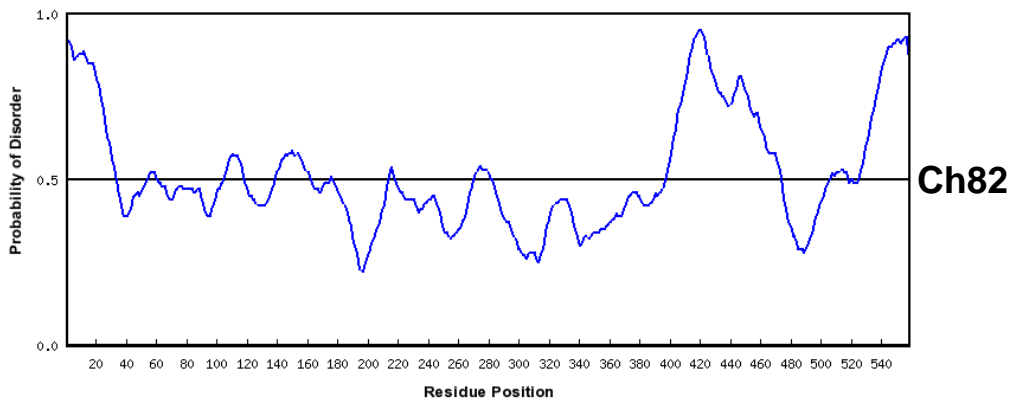
To eliminate the problem of variable numbers of β -gal positive cells observed in the transfection assays, a HSV-1 recombinant virus (*in0156*) was constructed containing the DNA cassette encoding EYFPTC6. All three assays employed in the short-term studies showed that *in0156* was able to stimulate levels of reporter gene expression above the negative control, confirming results from the transfection assays that this hybrid, like the pp71 protein, was functional in the short-term.

Results from long-term assays in HFFF2 cells showed that at 10 days post-infection, cell monolayers infected with *in0156*, contained β -gal positive plaques when the infected cells were downshifted to the permissive temperature of 31°C. However, numbers of β -gal positive plaques observed were fewer and smaller in size than those observed in cell monolayers infected with *in1310* (no β -gal expression was observed in cells infected with *in0146*). This suggests that the hybrid TC6 protein retains a degree of functionality that can be attributed to the middle region of pp71. Results from this part of the study showed that it is possible to exchange regions of the DNA coding sequences of the pp71 and Ch82 homologues, while retaining functionality.

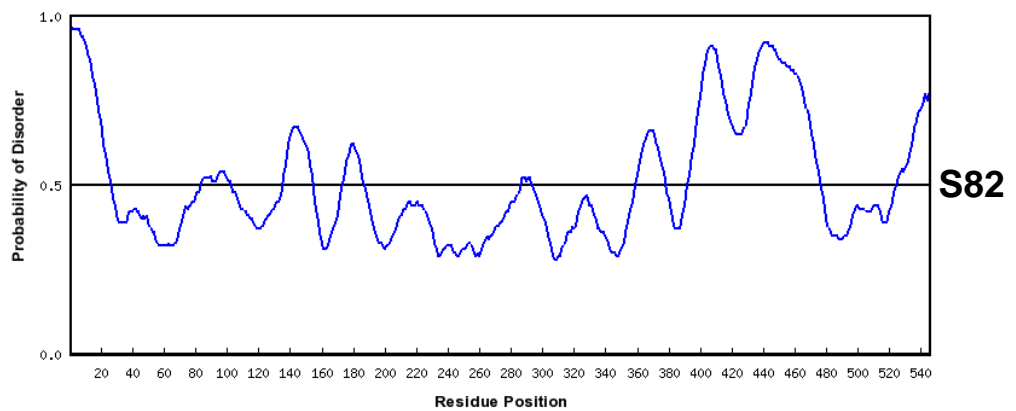
In infection assays EYFPTC6 appeared to direct a lower degree of gene expression compared to pp71 at 10 days post-infection. This could be attributed to the region of pp71 that was inserted into the Ch82 homologue. The middle region of pp71 appears to be the most highly ordered region of the protein (figure 4.13), with less order observed at the C- and N-termini. Incidentally, the other non-human UL82 homologues show a very similar pattern to pp71 in the RONN structural analysis program (figure 4.13). Some of the most important features of pp71 are found in the central third of this protein including the DIDs (Hofmann et al., 2002) and the LASCD (Kalejta & Shenk, 2003c) motif. It is possible that some part of this region of pp71 may contribute to the continued expression seen in cultures infected with *in0156* at 10 days post-infection. The EYFPpp71/EYFPCh82 hybrid proteins were constructed so as not to destroy the immediate coding sequence of the proteins, however, it is possible that while the coding sequences were not altered, the folding of the protein was affected. Small changes to the more ordered mid-section of pp71 could alter its structure and may affect its ability to direct long-term gene expression. Hofmann et al. (2002) suggested that internal deletion of the putative DIDs may cause an alteration in the 3D protein structure of pp71, causing a loss of interaction between pp71 and hDaxx. Davison and Stow (2005) also suggested that alterations to this region of the protein could result in gross structural changes to the protein. Therefore it is possible that the minor alterations to pp71 protein in the construction of the EYFPpp71/EYFPCh82 hybrid proteins may have affected the ability of this protein to drive long-term gene expression. To gain a better understanding of how the folding and structure of pp71 affects its ability to drive long term gene expression, the structures of both pp71 and Ch82 would have to be solved.



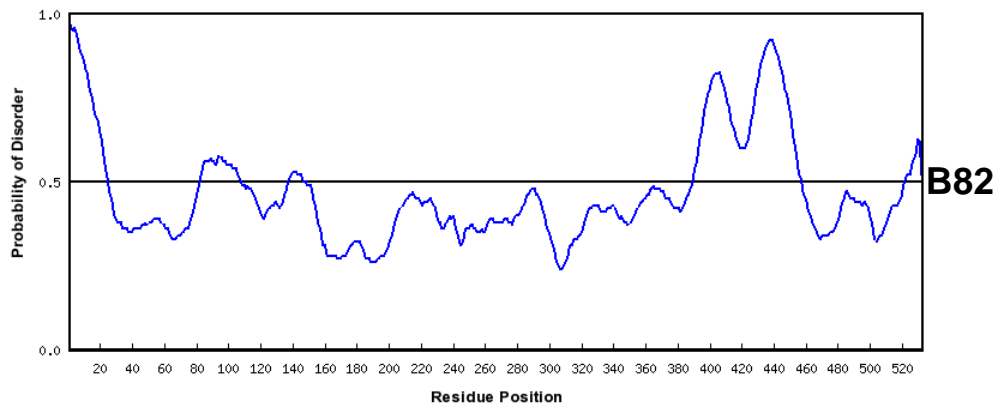
Regions of disorder: 1-25, 115-121, 139-163, 218-220, 333-338, 376-388, 404-470, 515-559



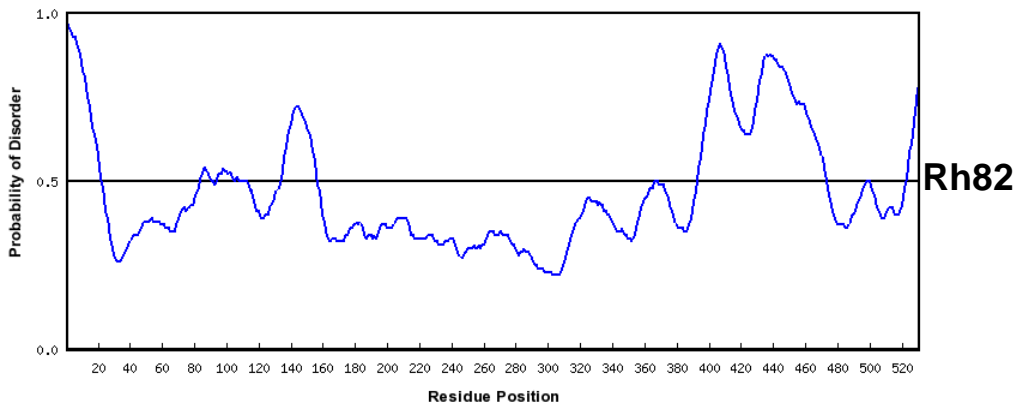
Regions of disorder: 1-33, 55-60, 105-118, 139-162, 176-176, 214-217, 271-281, 398-473, 507-518, 526-558



Regions of disorder: 1-26, 84-102, 136-154, 174-186, 287-292, 360-378, 393-476, 525-545



Regions of disorder: 1-24, 83-107, 138-146, 390-457, 522-532



Region of disorder: 1-22, 84-90, 95-104, 106-107, 134-156, 394-473, 523-530

Figure 4.13 Showing the regions of disorder in the UL82 proteins.

The graphs show that the greatest degree of order within these proteins is conserved within their middle regions, while the most significant disorder is observed at the C- and N- termini. All analysis was carried out using RONN software.

Yang et al. 2005

Chapter 5

Intracellular distribution and co-localisation of the UL82 homologues

5. Part I

5.1. Introduction

A large number of proteins, including PML, hDaxx, SUMO, and Sp100 are associated with ND10 structures. The protein hDaxx has been reported to be involved in various cellular processes including embryo development, apoptosis and transcription regulation (Salomoni & Khelifi, 2006). It has also been shown to co-localise with pp71 in the nucleus of transfected cells (Hofmann et al., 2002), and studies have shown that pp71 co-localises with PML at ND10 domains via an interaction with hDaxx (Hofmann et al., 2002, Ishov et al., 2002).

In the study described here the four non-human UL82 homologues (Ch82, S82, B82, and Rh82) were further characterised by comparing them to their human counterpart pp71, by examining the nuclear distribution patterns of the homologues and their abilities to co-localise with either hDaxx or PML.

Initial experiments to examine the nuclear distribution patterns of the UL82 homologues were carried out at 7 hr and 24 hr post-infection. Data obtained at these times of infection showed that the non-human homologues (Ch82, B82 and Rh82) behaved more like the S82 homologue than pp71. In the majority of cells infected with *in1310*, at 7 hr post-infection EYFP-tagged pp71 localised to discrete punctate foci whereas at 24 hr a number of infected cells showed pp71 accumulating as large aggregates in the nucleus (data not shown). At 7 hr post-infection in cells infected with *in0150*, EYFP-tagged S82 predominantly exhibited a diffuse pattern of fluorescence, while in some infected cells S82 was observed in punctate foci superimposed on a diffuse background. In HFFF2 cells infected with the *in1312* recombinants expressing EYFP-tagged Ch82, B82 or Rh82, in the majority of cells all three non-human homologues exhibited a punctate/diffuse pattern of fluorescence. Few infected cells showed these homologues localising to discrete punctate foci at 7 hr post-infection. Again at 24 hr post-infection in some infected cells the non-human homologue proteins accumulated in large masses (data not shown). Therefore in order to establish whether the non-human homologues localised to discrete punctate foci, like pp71, before forming the patterns of fluorescence observed at 7 hr and 24 hr post-infection, experiments were carried at the earlier time points of 3 hr and 5 hr as well as 7 hr post-infection.

5.1.1. Distribution patterns of EYFPUL82 homologues at 3 hr post-infection

To obtain comparisons between the nuclear distribution patterns of pp71 and the non-human homologues, 8×10^4 HFFF2 cells, cultivated on 13 mm coverslips in D5+5 medium, were infected with 5×10^5 pfu of *in1310* (expressing EYFPpp71), *in0146* (EYFPCh82), *in0150* (EYFPS82), *in0145* (EYFPB82), or *in0144* (EYFPRh82). At 3 hr post-infection cells were fixed and mounted onto microscope slides. Nuclear distribution patterns of each of the homologues were identified and tabulated (table 5.1). Figure 5.1 shows the various patterns of fluorescence observed. Figure 5.1a shows a typical pattern of discrete punctate foci, usually associated with pp71. Infected cells displaying foci that became larger were termed punctate/diffuse (figure 5.1b). The diffuse pattern of fluorescence was characterised by signal throughout the nucleus as presented in figure 5.1c.

Table 5.2 shows that in 95% of the cells infected with *in0146* the Ch82 homologue localised to discrete punctate foci, while in the remaining 5% Ch82 exhibited a punctate/diffuse pattern of fluorescence. Cells infected with *in0145* and *in0144* showed a slightly different distribution to that in cells infected with *in1310* and *in0146*. Upon infection with *in0145* and *in0144*, the B82 and Rh82 proteins localised primarily to discrete punctate foci (figure 5.2). However table 5.2 shows that despite the dominant nuclear pattern of discrete punctate foci, a greater percentage of cells showed these proteins in a punctate/diffuse pattern of fluorescence. Cells infected with *in0150* showed a different distribution pattern. The majority of infected cells (84%) examined contained S82 in a diffuse pattern of fluorescence, while in some cells punctate/diffuse patterns of fluorescence were observed.

At 3 hr post-infection the UL82 homologues exhibited varied distribution patterns ranging from the well-documented discrete punctate foci to increasingly diffuse patterns of fluorescence.

5.1.2. Distribution patterns of the EYFPUL82 homologues 5 hr post-infection

HFFF2 cell monolayers (8×10^4 cells) infected with 5×10^5 pfu of the *in1312* recombinant viruses expressing EYFP-tagged UL82 homologues were fixed at 5 hr post-infection. Nuclear distribution patterns exhibited by each homologue were

	Patterns of Distribution	3 hr post-infection	5 hr post-infection	7 hr post-infection
<i>in1310</i> (pp71)	Number of punctate foci	95	939	730
	Number of punctate/diffuse patterns of fluorescence	5	42	167
<i>in0146</i> (Ch82)	Number of punctate foci	124	45	24
	Number of punctate/diffuse patterns of fluorescence	7	39	95
<i>in0150</i> (S82)	Number of punctate foci	0	0	0
	Number of punctate/diffuse patterns of fluorescence	27	13	37
	Number of diffuse patterns of fluorescence	149	84	78
<i>in0145</i> (B82)	Number of punctate foci	31	42	3
	Number of punctate/diffuse patterns of fluorescence	58	35	54
<i>in0144</i> (Rh82)	Number of punctate foci	163	44	8
	Number of punctate/diffuse patterns of fluorescence	46	17	67

Table 5.1. Nuclear distribution patterns of the EYFPUL82 homologues at 3 hr, 5 hr and 7 hr post-infection.

HFFF2 cells were infected with 5×10^5 pfu of the *in1312* recombinant viruses expressing the EYFP-tagged UL82 homologues. Cell monolayers were fixed at 3 hr, 5 hr and 7 hr post-infection and the various patterns of fluorescence were examined and categorised as presented in figure 5.1. Cells expressing the different patterns of fluorescence were counted, in a range of fields, and the results tabulated.

	Patterns of Distribution	3 hr post-infection	5 hr post-infection	7 hr post-infection
<i>in1310</i> (pp71)	Percentage of punctate foci	95	95	81
	Percentage of punctate/diffuse patterns of fluorescence	5	5	19
<i>in0146</i> (Ch82)	Percentage of punctate foci	95	54	20
	Number of punctate/diffuse patterns of fluorescence	5	46	80
<i>in0150</i> (S82)	Percentage of punctate foci	0	0	0
	Percentage of punctate/diffuse patterns of fluorescence	16	13	12
	Percentage of diffuse patterns of fluorescence	84	87	88
<i>in0145</i> (B82)	Percentage of punctate foci	65	55	5
	Percentage of punctate/diffuse patterns of fluorescence	35	45	95
<i>in0144</i> (Rh82)	Percentage of punctate foci	78	72	11
	Percentage of punctate/diffuse patterns of fluorescence	22	28	89

Table 5.2. Nuclear distribution patterns of the EYFPUL82 homologues at 3 hr, 5 hr and 7 hr post-infection.

HFFF2 cells were infected with 5×10^5 pfu of the *in1312* recombinant viruses expressing the EYFP-tagged UL82 homologues. Cell monolayers were fixed at 3 hr, 5 hr and 7 hr post-infection and patterns of fluorescence were examined using a confocal microscope.

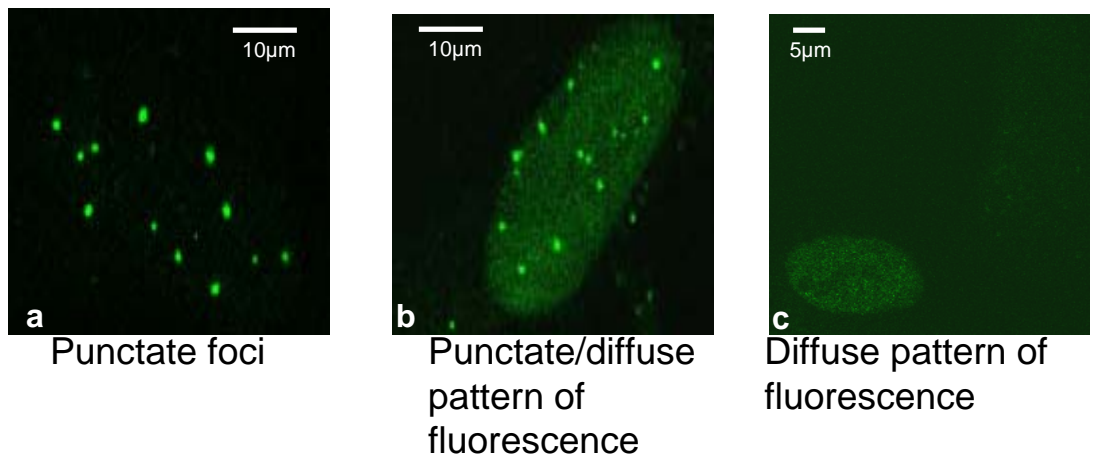


Figure 5.1 Patterns of fluorescence exhibited by the EYFPUL82 homologues

HFFF2 monolayers infected were infected with 5×10^5 pfu of the *in1312* recombinants expressing the EYFP-tagged UL82 homologues, and incubated at 38.5°C. Cell monolayers were fixed and permeabilised and images were captured on a confocal microscope. Images were selected specifically to illustrate the different patterns of fluorescence observed throughout this study .

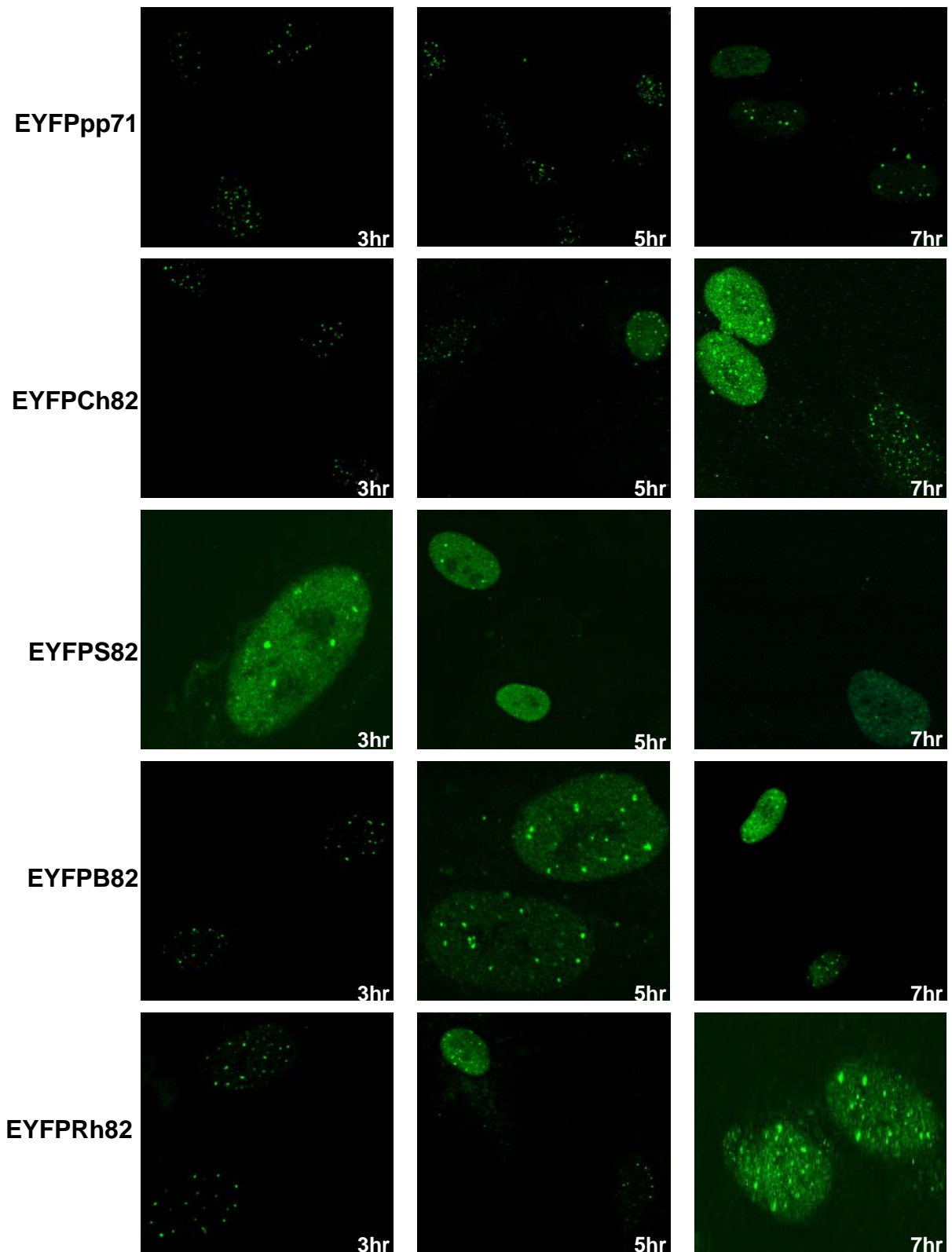


Figure. 5.2 Nuclear distribution of the EYFPUL82 homologues at 3 hr, 5 hr and 7 hr post-infection.

HFFF2 monolayers infected were mock-infected or infected with 5×10^5 pfu of the *in1312* recombinants expressing the EYFP-tagged UL82 homologues, and incubated at 38.5°C. At 3 hr, 5 hr, or 7 hr post-infection cell monolayers were fixed and permeabilised. Images were captured on a confocal microscope and the magnification of each image was optimised to fit the area of the cell(s) in the field.

counted and tabulated (table 5.1 and 5.2). At 5 hr post-infection cell monolayers infected with *in1310* showed no change from the distribution pattern observed at 3 hr post-infection (figure 5.2). Again pp71 localised to discrete punctate foci in the nucleus (95%) however, in some infected cells pp71 exhibited a punctate/diffuse pattern of fluorescence (5%) (table 5.2).

HFFF2 cells infected with *in0146* showed a change in distribution patterns at 5 hr. In HFFF2 cells infected with *in0146* a change in distribution patterns at 5 hr was observed compared to that at 3 hr post-infection (figure 5.2). At 5 hr post-infection, 54% of infected cells showed the Ch82 protein localising to discrete punctate foci, while an increasing proportion of infected cells (46%) showed Ch82 exhibiting a more punctate/diffuse pattern of fluorescence (tables 5.1 and 5.2). Therefore, at 5 hr post-infection, despite the nuclear localisation pattern of the Ch82 homologue continuing to show similarities to that of pp71, a change in the degree of similarity was observed. Cell monolayers infected with *in0145* and *in0144* showed little change in patterns of distribution at 5 hr compared to 3 hr. The majority of infected cells showed both B82 and Rh82 proteins localising as discrete punctate foci, however the number of cells exhibiting punctate/diffuse patterns of fluorescence increased (tables 5.1 and 5.2). When HFFF2 cells were infected with *in0150*, no significant change in nuclear distribution patterns was observed when compared to 3 hr post-infection. Tables 5.1 and 5.2 show that in cells infected with *in0150*, S82 exhibited a more diffuse pattern of fluorescence, and again no punctate foci were observed (figure 5.2). The nuclear distribution pattern of S82 continued to differ from that of pp71.

5.1.3. Distribution patterns of the EYFPUL82 homologues at 7 hr post-infection

HFFF2 cells (8×10^4 cells) infected with 5×10^5 pfu of the *in1312* recombinants expressing the EYFP-tagged UL82 homologues were fixed and mounted onto microscope slides. Nuclear distribution patterns were counted and tabulated (table 5.1 and 5.2). Cell monolayers infected with *in1310* showed a change in the nuclear distribution pattern. Tables 5.1 and 5.2 show that in the majority of cells infected with *in1310*, pp71 continued to localise to discrete punctate foci in the nucleus as observed at 3 hr and 5 hr post-infection. However a greater number of

infected cells showed pp71 exhibiting a more punctate/diffuse pattern of fluorescence (figure 5.2).

In HFFF2 cells infected with *in0146* a change in the distribution pattern at 7 hr post-infection compared to that at 3 hr and 5 hr post-infection was observed. The majority of infected cells showed Ch82 exhibiting a more punctate/diffuse pattern of fluorescence (80%), while fewer infected cells (20%) retained the discrete punctate foci exhibited at 3 hr and 5 hr post-infection (table 5.2). This was also found to be the case in those cell monolayers infected with *in0145* and *in0144*. A greater number of infected cells showed both B82 and Rh82 proteins exhibiting a more punctate/diffuse pattern of fluorescence at 7 hr post-infection compared to that observed at 3 hr and 5 hr post-infection, as presented in tables 5.1 and 5.2, and in figure 5.2. Cell monolayers infected with *in0150* showed little change in distribution patterns. The majority of infected cells (88%) showed S82 exhibiting a more diffuse pattern of fluorescence observed at earlier time points (tables 5.1 and 5.2). However, in a few infected cells S82 exhibited a punctate/diffuse pattern of fluorescence, as seen in figure 5.2. At later times of infection the Ch82, B82 and Rh82 homologues began to show a divergence from the discrete punctate foci exhibited by pp71.

This part of the study indicated that the majority of the non-human homologues (B82, Rh82 and Ch82) all displayed similar attributes to pp71 at 3 and 5 hr post-infection by localising to punctate foci. Unlike pp71, the S82 homologue exhibited a punctate/diffuse pattern of fluorescence at 3 hr post-infection which became increasingly diffuse throughout the time period examined. No discrete punctate foci were observed in any cells infected with *in0150* at any time post-infection. However, while pp71 predominantly localised to discrete punctate foci at 7 hr post-infection the B82, Rh82 and Ch82 homologues began to diverge away from the pattern exhibited by pp71 to localise to the punctate/diffuse pattern of fluorescence associated with the S82 homologue. These distinct changes in patterns of fluorescence exhibited by the non-human UL82 homologues were hypothesised to affect their ability to co-localise with the cellular proteins hDaxx and PML.

5. Part II

5.2. Introduction

Various studies have shown that pp71 co-localises with PML (Marshall et al., 2002) and also with the cellular protein hDaxx (Hofmann et al., 2002, Ishov et al., 2002). To investigate whether the non-human UL82 homologues also localised with these cellular proteins, initial experiments were carried out at 7 hr and 24 hr post-infection. It was observed that the Ch82, B82 and Rh82 homologues co-localised with hDaxx and PML at these times. However in those cells where S82 exhibited a diffuse pattern of fluorescence, hDaxx was seen to be dispersed from the larger more intense foci associated with this distribution pattern (data not shown). Experiments were carried out at the earlier times of 3 hr and 5 hr post-infection to establish whether the Ch82, B82 and Rh82 homologues co-localised with hDaxx and PML when their distribution patterns were more like those associated with pp71. Experiments at these time points also served to establish if the S82 homologue caused hDaxx to be dispersed at earlier times after infection or if this property was associated with later times of infection.

5.2.1. The EYFPUL82 homologues co-localise with the cellular proteins hDaxx and PML at 3 hr 5 hr and 7hr post-infection.

HFFF2 cells, seeded at 8×10^4 cells, were infected with the *in1312* recombinant viruses expressing the EYFP-tagged UL82 homologues. At 3 hr post-infection cell monolayers were fixed and stained with an anti-PML A-20 antibody or an anti-hDaxx antibody and their appropriate secondary antibodies.

Cell monolayers infected with *in1310* showed co-localisation of pp71 with hDaxx at the punctate foci observed at the three time points under investigation (figure 5.3a). Further staining showed that pp71 also co-localised with PML in these punctate foci (figure 5.3b). These results were in agreement with the reports by other groups that pp71 co-localises with hDaxx and PML at ND10 domains (Hofmann et al., 2002, Ishov et al., 2002). As time progressed, pp71 displayed a punctate/diffuse pattern of fluorescence in an increasing number of infected cells while maintaining discrete punctate foci in the majority of infected cells.

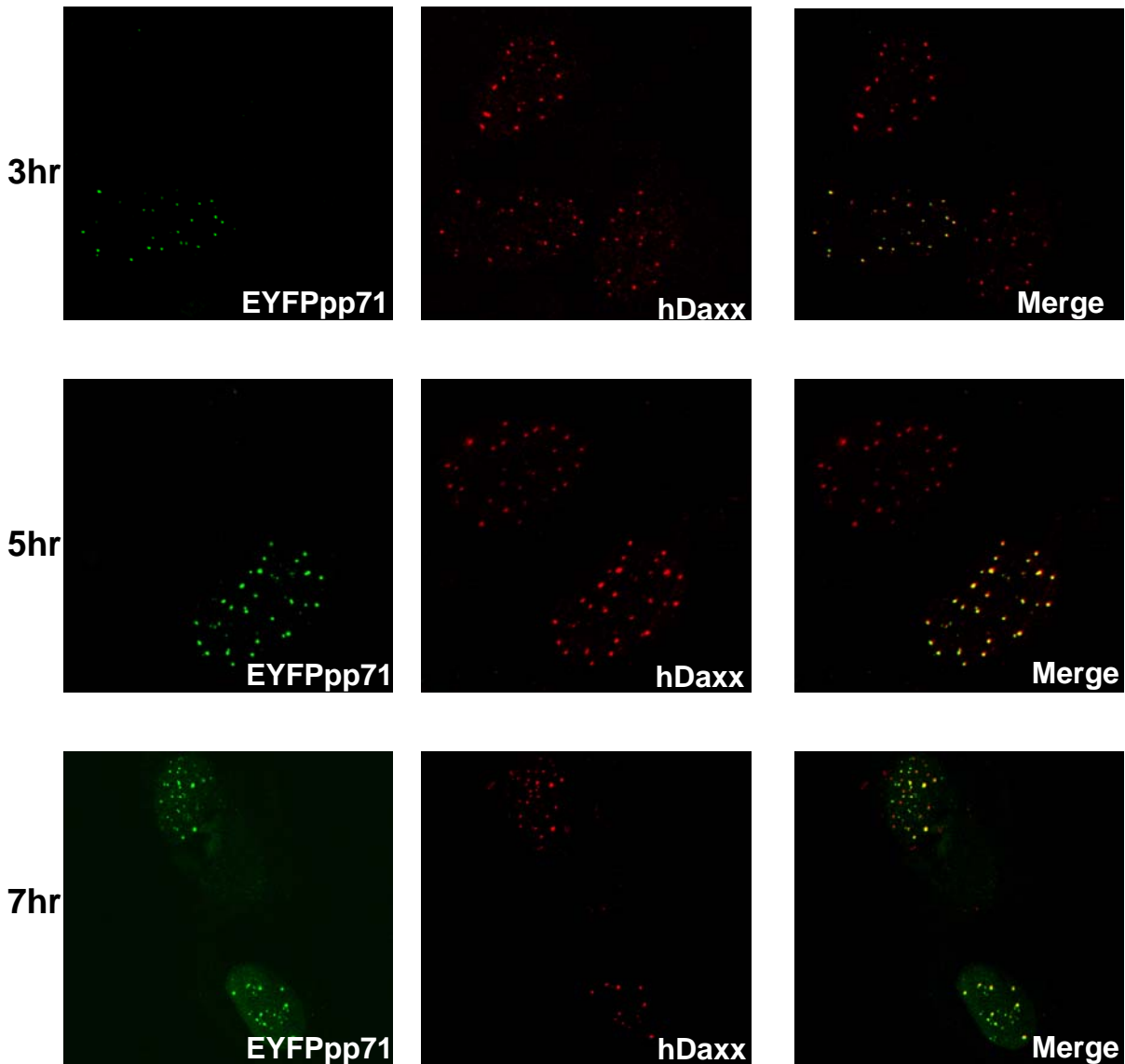


Figure 5.3a. EYFPpp71 co-localises with hDaxx at 3 hr, 5 hr and 7 hr post-infection.

HFFF2 monolayers were infected with 5×10^5 pfu of *in1310* (expressing EYFPpp71), and incubated at 38.5°C . At 3 hr, 5 hr and 7 hr post-infection cell monolayers were fixed and permeabilised. Cells were stained with anti-hDaxx primary antibody and subsequently with secondary antibody (anti-mouse Cy5-conjugated). Images were generated on a confocal microscope and the magnification of each image was optimised to fit the area of the cell(s) in the field of view.

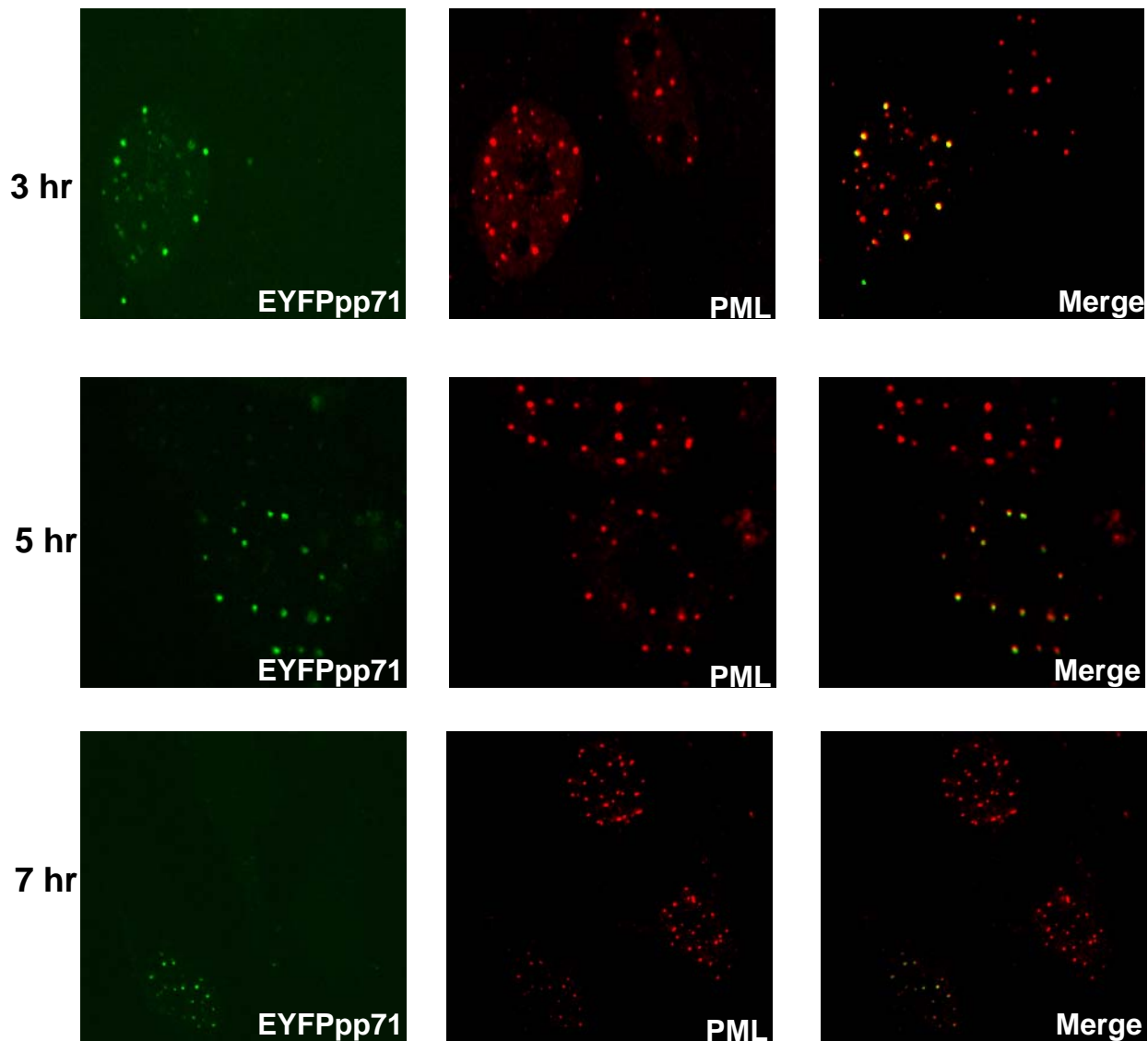


Figure 5.3b. EYFPpp71 co-localises with PML at 3 hr, 5 hr and 7 hr post-infection.

HFFF2 monolayers were infected with 5×10^5 pfu of *in1310* expressing EYFPpp71), and incubated at 38.5°C. At 3 hr, 5 hr and 7 hr post-infection cell monolayers were fixed and permeabilised. Cells were stained with primary antibody anti-PML A-20 for 1 hr followed by incubation with secondary antibody (Alexa 647-chicken anti-goat) for 1 hr. Images were captured on a confocal microscope and the magnification of each image was optimised to fit the area of the cell in the field of view.

Cell monolayers infected with *in0146* exhibited a distribution pattern analogous to that of pp71 at 3 hr post-infection. The Ch82 homologue localised to discrete punctate foci, which in turn co-localised with both hDaxx and PML. The pattern of fluorescence became more punctate/diffuse at 5 hr post-infection and by 7hr post-infection, the majority of infected cells displayed this pattern. Co-localisation with hDaxx and PML persisted at both these times of infection (figure 5.4a and 5.4b).

Unlike pp71, the S82 homologue expressed from virus *in0150* exhibited a punctate/diffuse or diffuse pattern of fluorescence at 3 hr post-infection (figure 5.2). However despite these distinct distribution patterns, foci co-localised with both hDaxx (figure 5.5a) and PML (figure 5.5b). Through 5 hr post-infection until 7hr post-infection an increasingly diffuse pattern of fluorescence was observed in most infected cell nuclei. While some co-localisation with PML was retained, hDaxx appeared to be dispersed throughout the nucleus (figure 5.5a and figure 5.5b).

In cells infected with *in0145* (figure 5.6a and 5.6b) and *in0144* (figure 5.7a and 5.7b) both homologues displayed the typical punctate foci associated with pp71, and again co-localised with hDaxx and PML at 3 hr post-infection. The pattern of fluorescence exhibited by both these homologues became more punctate/diffuse at 5 hr post-infection and by 7hr post-infection, the majority of infected cells displayed this pattern. Co-localisation with hDaxx and PML persisted at both these times of infection (figure 5.4a and 5.4b).

Data at all three times post-infection post-infection showed that the Ch82, B82 and Rh82 homologues appeared to be most like pp71 in terms of nuclear distribution patterns and in their ability to co-localise with hDaxx and PML at ND10 domains. The S82 homologue, though unlike pp71 in terms of nuclear distribution patterns, still behaved in a similar way to pp71 by co-localising with PML. However, as the patterns of fluorescence became increasingly diffuse, hDaxx was observed to be dispersed from the nucleus, suggesting that the changes in patterns of fluorescence may affect the ability of the homologues to co-localise with hDaxx. Further experiments with the B82, Rh82 and Ch82 homologues at later times would need to be carried out to establish if they also exhibit diffuse patterns of fluorescence and, like S82, disperse hDaxx.

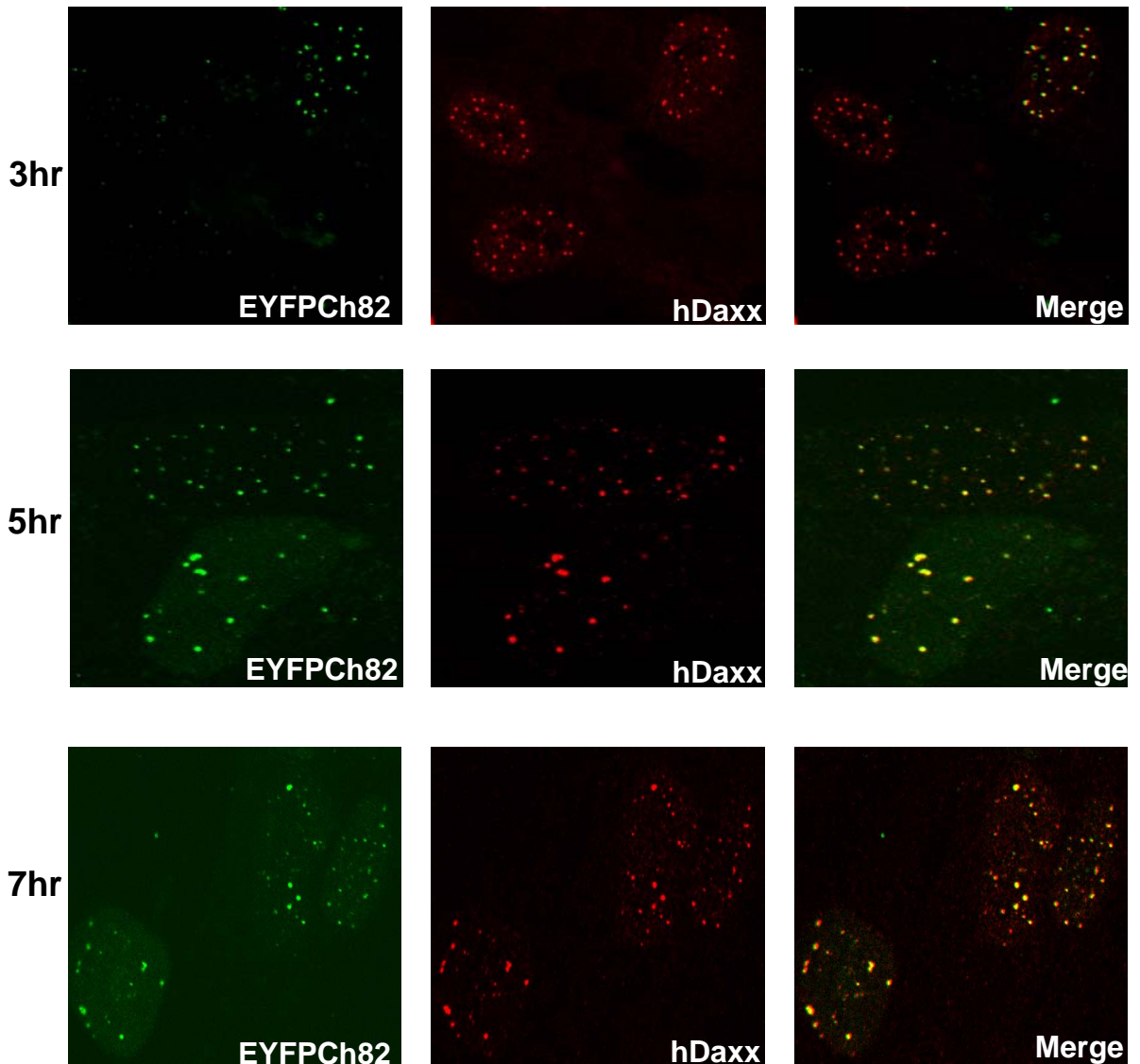


Figure 5.4a. EYFPCh82 co-localises with hDaxx at 3 hr, 5 hr and 7 hr post-infection.

HFFF2 monolayers were infected with 5×10^5 pfu of *in0146* (expressing EYFPCh82), and incubated at 38.5°C . At 3 hr, 5 hr and 7 hr post-infection cell monolayers were fixed and permeabilised. Cells were stained with anti-hDaxx primary antibody and subsequently with secondary antibody (anti-mouse Cy5-conjugated). Images were generated on a confocal microscope and the magnification of each image was optimised to fit the area of the cell(s) in the field of view.

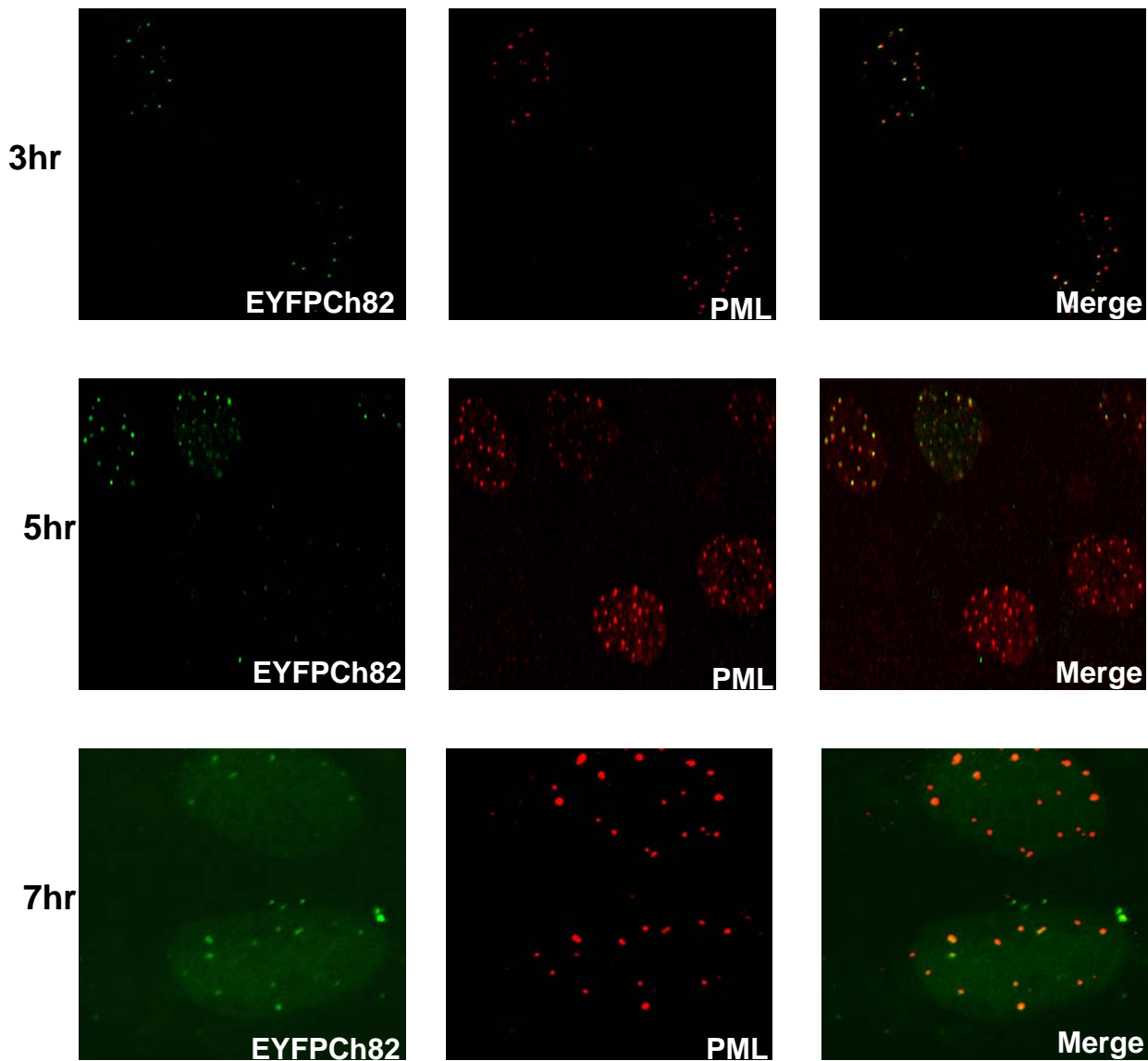


Figure 5.4b. EYFPCh82 co-localises with PML at 3 hr, 5 hr and 7 hr post-infection.

HFFF2 monolayers were infected with 5×10^5 pfu of *in0146* (expressing EYFPCh82), and incubated at 38.5°C . At 3 hr, 5 hr and 7 hr post-infection cell monolayers were fixed and permeabilised. Cells were stained with primary antibody anti-PML A-20 for 1 hr followed by incubation with secondary antibody (Alexa 647-chicken anti-goat) for 1 hr. Images were captured on a confocal microscope and the magnification of each image was optimised to fit the area of the cell in the field of view.

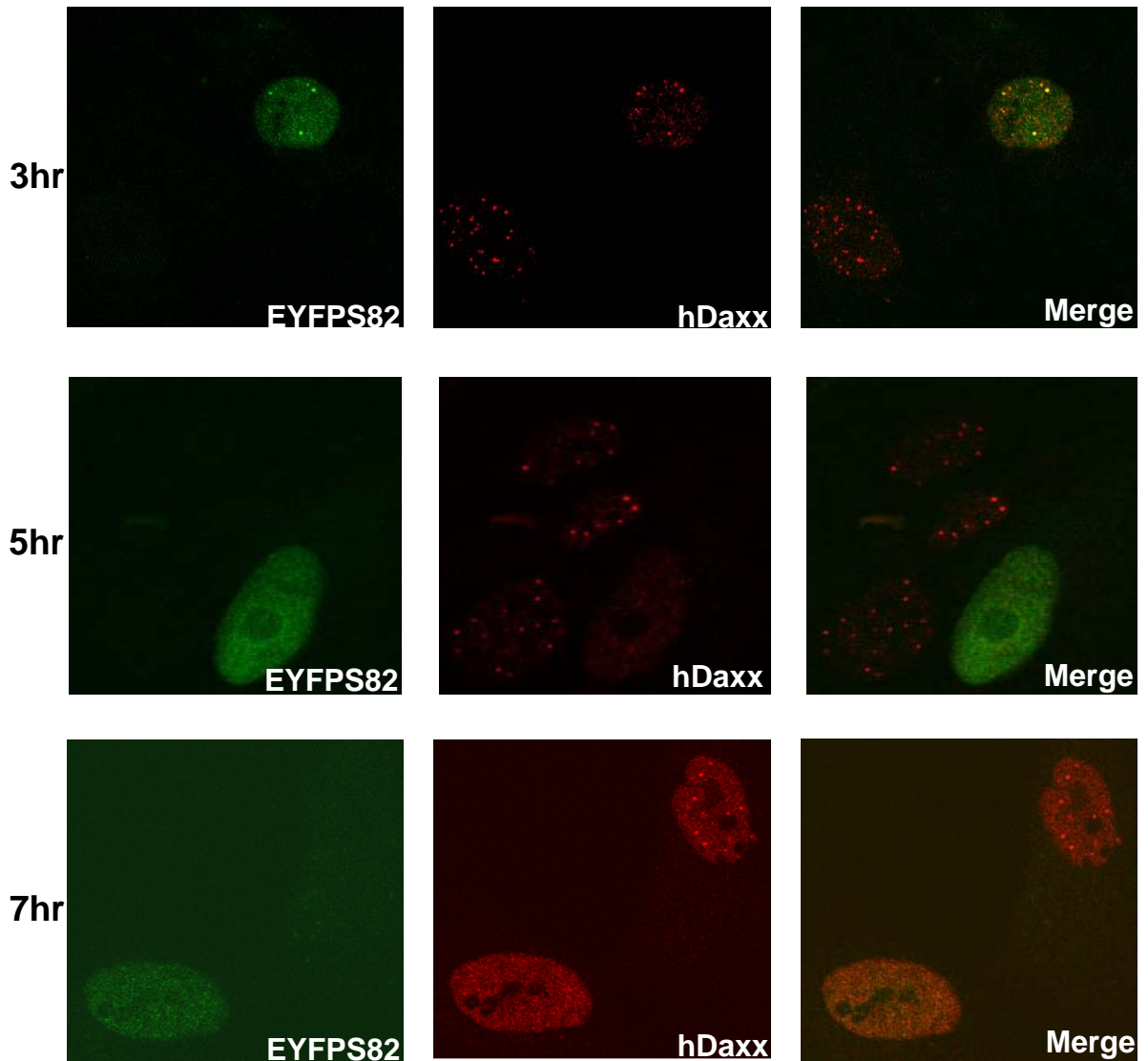


Figure 5.5a. EYFPS82 and hDaxx at 3 hr, 5 hr and 7 hr post-infection.

HFFF2 monolayers were infected with 5×10^5 pfu of *in0150* (expressing EYFPS82), and incubated at 38.5°C . At 3 hr, 5 hr and 7 hr post-infection cell monolayers were fixed and permeabilised. Cells were stained with anti-Daxx primary antibody and subsequently with secondary antibody (anti-mouse Cy5-conjugated). Images were generated on a confocal microscope and the magnification of each image was optimised to fit the area of the cell(s) in the field of view. (7 hr image courtesy of Dr. Chris Preston).

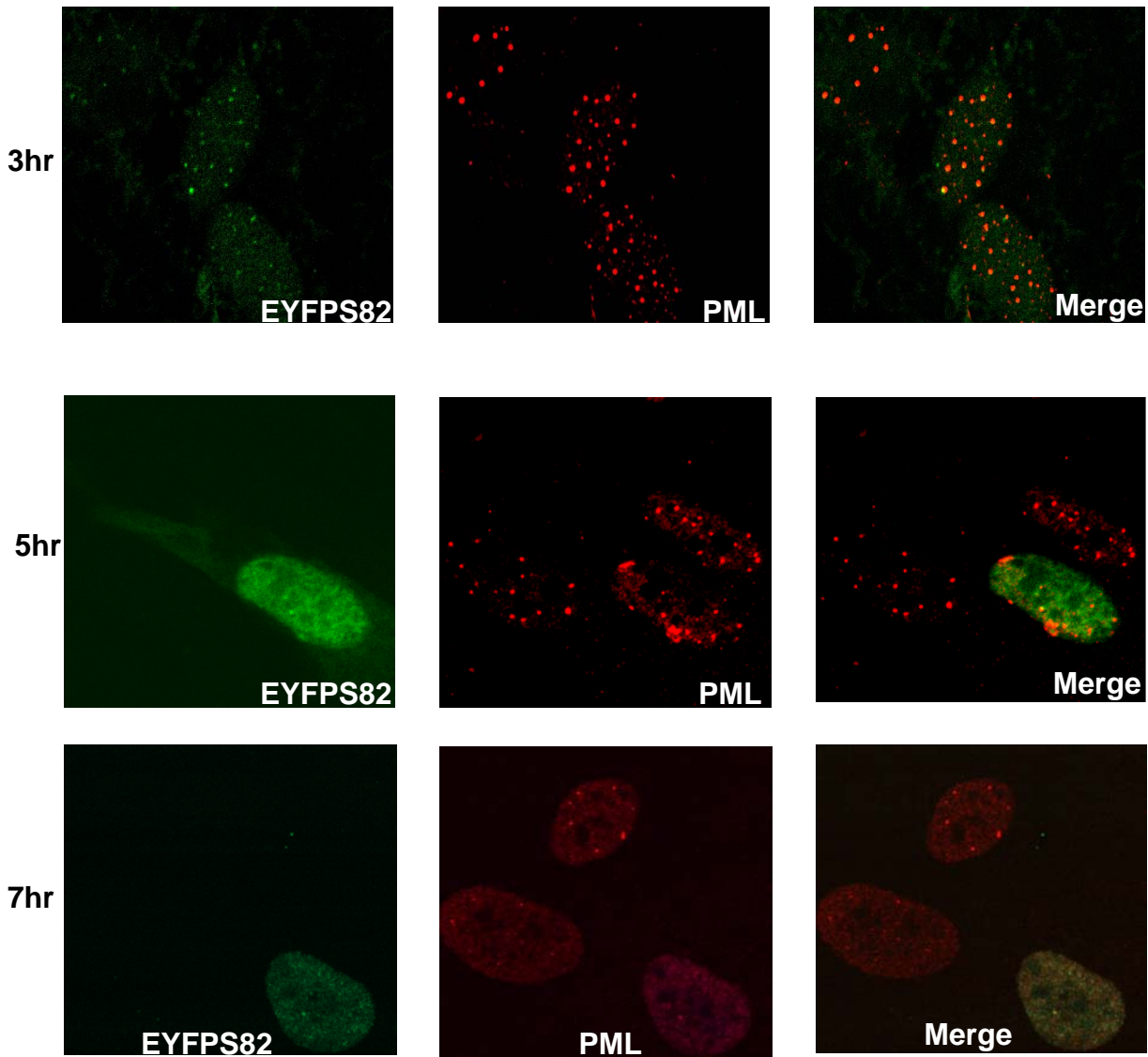


Figure 5.5b. EYFPS82 co-localises with PML at 3 hr, 5 hr and 7 hr post-infection.

HFFF2 monolayers were infected with 5×10^5 pfu of *in0150* (expressing EYFPS82), and incubated at 38.5°C . At 3 hr, 5 hr and 7 hr post-infection cell monolayers were fixed and permeabilised. Cells were stained with primary antibody anti-PML A-20 for 1 hr followed by incubation with secondary antibody (Alexa 647-chicken anti-goat) for 1 hr. Images were captured on a confocal microscope and the magnification of each image was optimised to fit the area of the cell in the field of view.

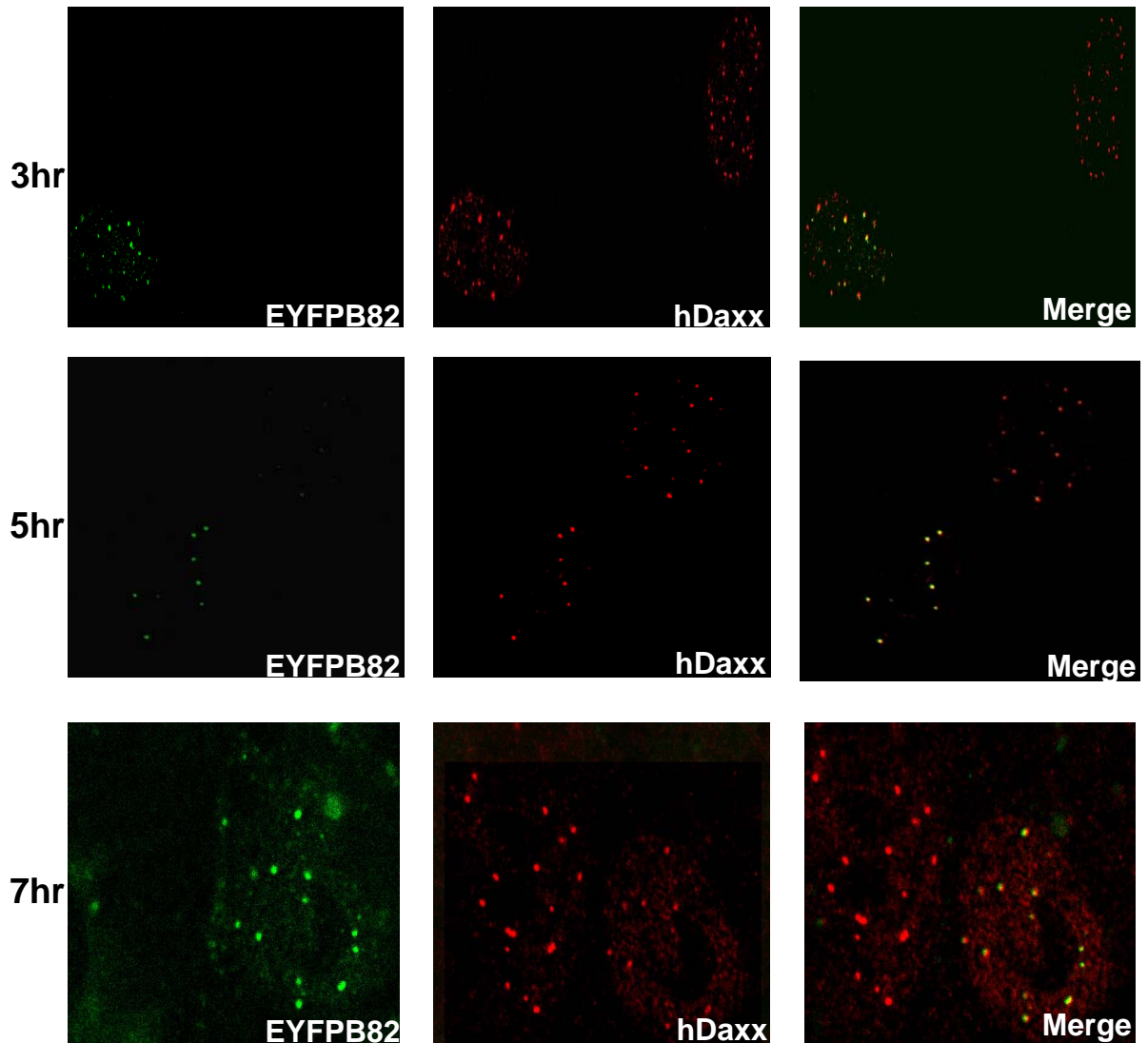


Figure 5.6a. EYFPB82 co-localises with hDaxx at 3 hr, 5 hr and 7 hr post-infection.

HFFF2 monolayers were infected with 5×10^5 pfu of *in0145* (expressing EYFPB82), and incubated at 38.5°C . At 3 hr, 5 hr and 7 hr post-infection cell monolayers were fixed and permeabilised. Cells were stained with anti-hDaxx primary antibody and subsequently with secondary antibody (anti-mouse Cy5-conjugated). Images were generated on a confocal microscope and the magnification of each image was optimised to fit the area of the cell(s) in the field of view.

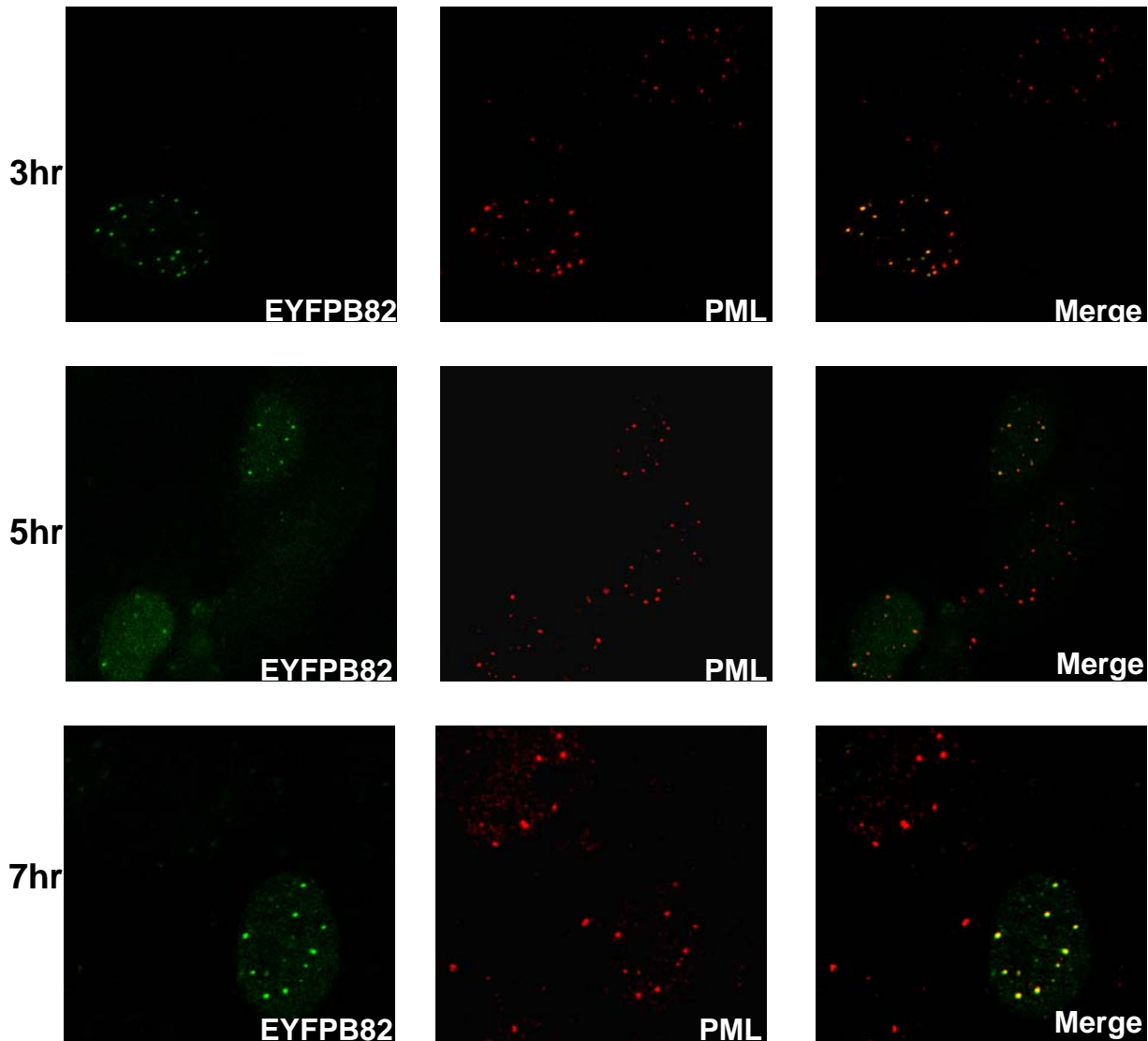


Figure 5.6b. EYFPB82 co-localises with PML at 3 hr, 5 hr and 7 hr post-infection.

HFFF2 monolayers were infected with 5×10^5 pfu of *in0145* (expressing EYFPB82), and incubated at 38.5°C . At 3 hr, 5 hr and 7 hr post-infection cell monolayers were fixed and permeabilised. Cells were stained with primary antibody anti-PML A-20 for 1 hr followed by incubation with secondary antibody (Alexa 647-chicken anti-goat) for 1 hr. Images were captured on a confocal microscope and the magnification of each image was optimised to fit the area of the cell in the field of view.

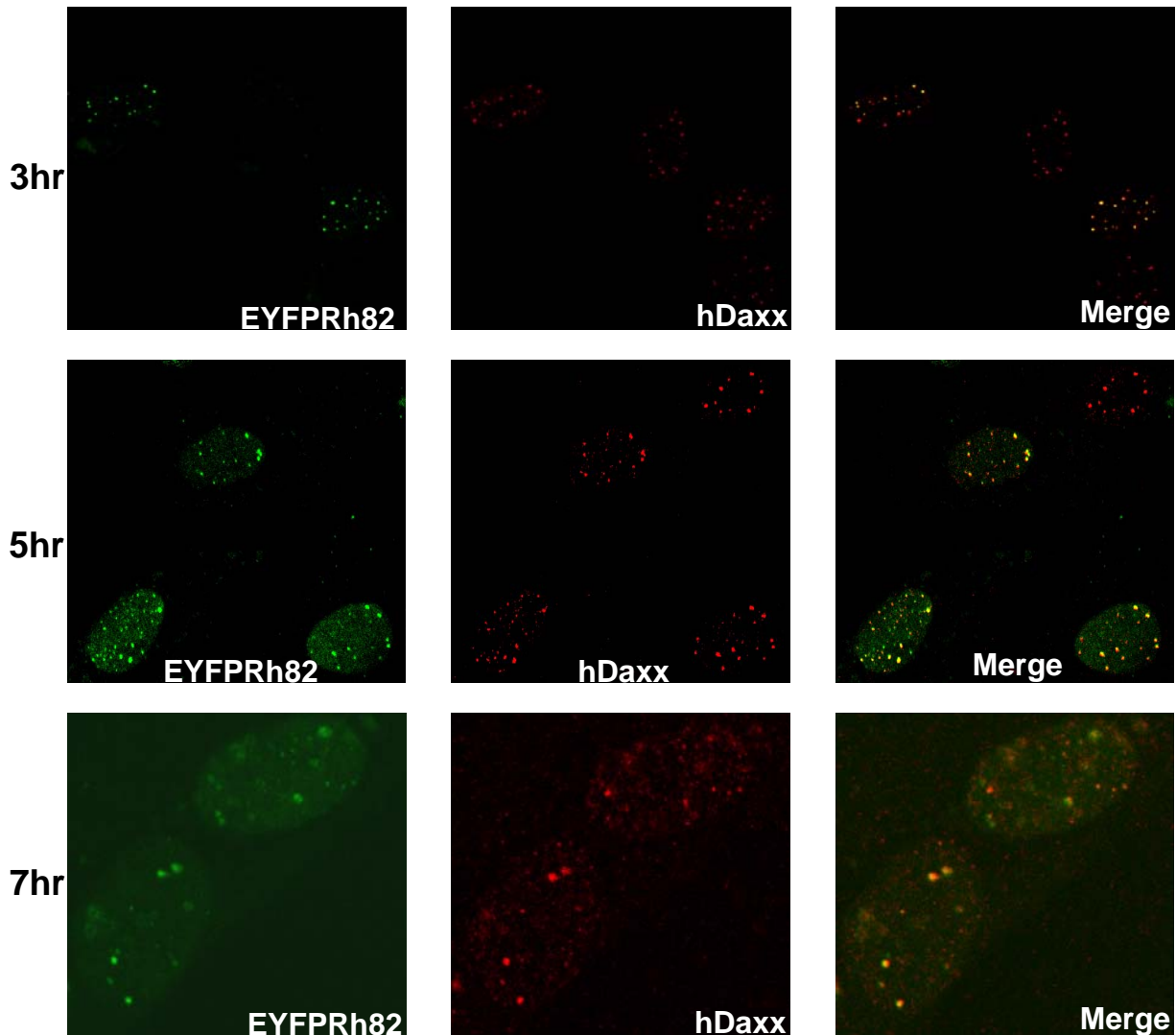


Figure 5.7a. EYFPRh82 co-localises with hDaxx at 3 hr, 5 hr and 7 hr post-infection.

HFFF2 monolayers were infected with 5×10^5 pfu of *in0144* (expressing EYFPRh82), and incubated at 38.5°C . At 3 hr, 5 hr and 7 hr post-infection cell monolayers were fixed and permeabilised. Cells were stained with anti-hDaxx primary antibody and subsequently with secondary antibody (anti-mouse Cy5-conjugated). Images were generated on a confocal microscope and the magnification of each image was optimised to fit the area of the cell(s) in the field of view.

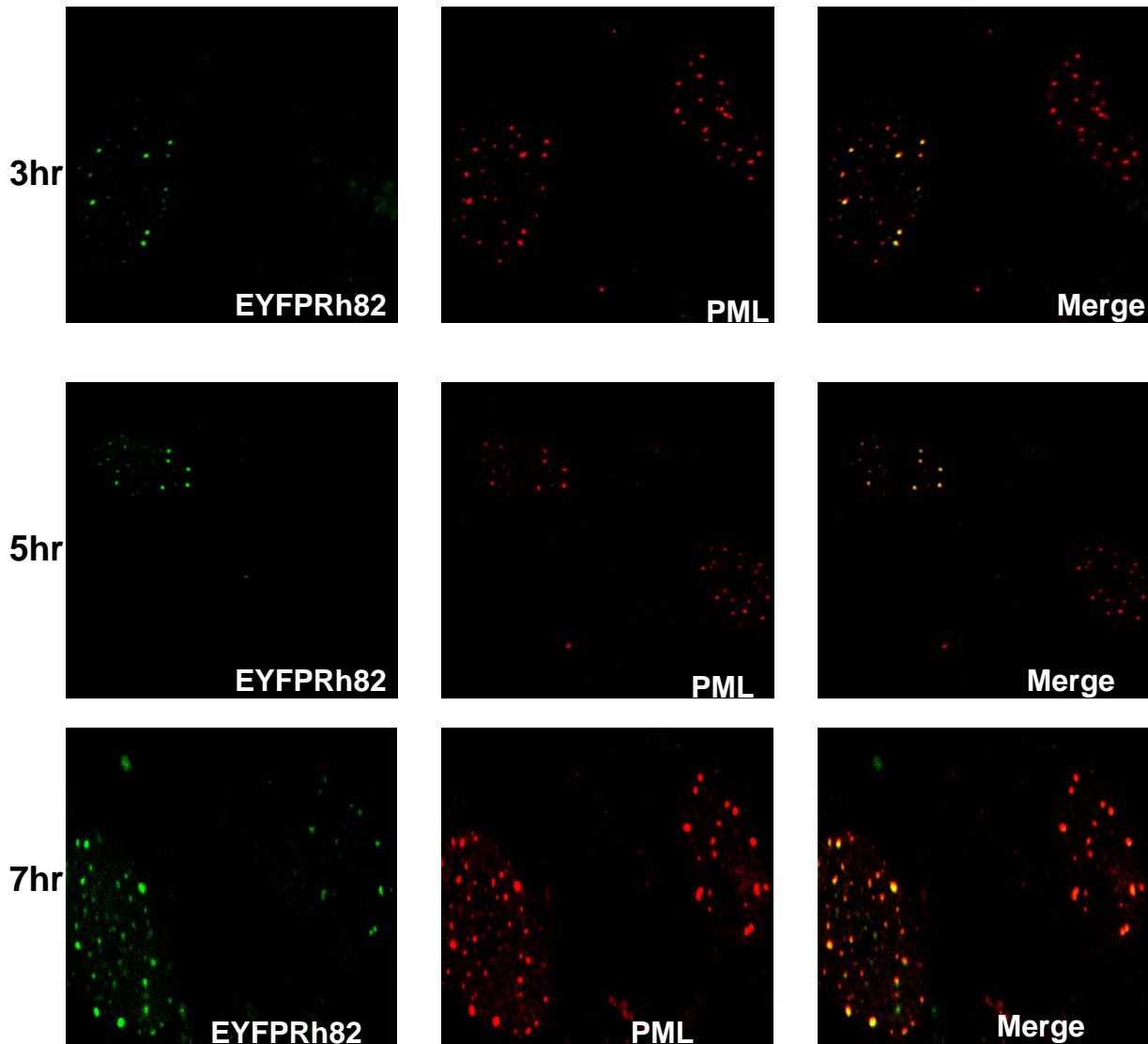


Figure 5.7b. EYFPRh82 co-localises with PML at 3 hr, 5 hr and 7 hr post-infection.

HFFF2 monolayers were infected with 5×10^5 pfu of *in0144* (expressing EYFPRh82), and incubated at 38.5°C . At 3 hr, 5 hr and 7 hr post-infection cell monolayers were fixed and permeabilised. Cells were stained with primary antibody anti-PML A-20 for 1 hr followed by incubation with secondary antibody (Alexa 647-chicken anti-goat) for 1 hr. Images were captured on a confocal microscope and the magnification of each image was optimised to fit the area of the cell in the field of view.

5. Part III

5.3. Introduction

In chapter 4 the hybrid protein EYFPTC6 (mid region of pp71 cloned into Ch82) was constructed and later recombined into a HSV-1 *in1312* recombinant virus named *in0156*. This hybrid was shown to retain some activity at 10 days post-infection however levels of activity appeared to be lower than that observed with pp71. The properties of this protein were further examined by observing its nuclear distribution patterns and co-localisation with the cellular proteins hDaxx and PML to establish if this hybrid behaved more like pp71 or Ch82.

5.3.1 Hybrid TC6 co-localises with the cellular proteins hDaxx and PML at 3 hr post-infection.

HFFF2 cells (8×10^4) were infected with 5×10^5 pfu of *in1310* (expressing EYFPpp71), *in0146* (EYFPCh82) or *in0156* (EYFPTC6). At 3 hr post-infection cell monolayers were fixed and stained with primary antibodies anti-PML A-20 or anti-hDaxx and their appropriate secondary antibodies.

Figure 5.1 shows that in cell monolayers infected with *in1310*, pp71 localised to discrete punctate foci. When cell monolayers were stained with an anti-hDaxx antibody (figure 5.3a), pp71 localised with hDaxx in these discrete punctate foci. When stained with an anti-PML antibody, co-localisation of pp71 with PML was also observed (figure 5.3b). Cell monolayers infected with *in0146* showed the Ch82 protein also localised to discrete punctate foci (figure 5.2). And, as expected, co-localisation with both hDaxx and PML was observed. These results were in agreement with those described previously (figure 5.4a and 5.4b). In cell monolayers infected with *in0156*, the same distribution pattern as both pp71 and Ch82 homologues was observed at 3 hr post-infection (figure 5.8a, panel a.) The hybrid protein TC6 also localised to discrete punctate foci in the nucleus. Figure 5.8a shows the discrete punctate foci of hybrid TC6 co-localising with hDaxx. Co-localisation was also observed in infected cells stained with anti-PML A20 antibody (figure 5.8b).

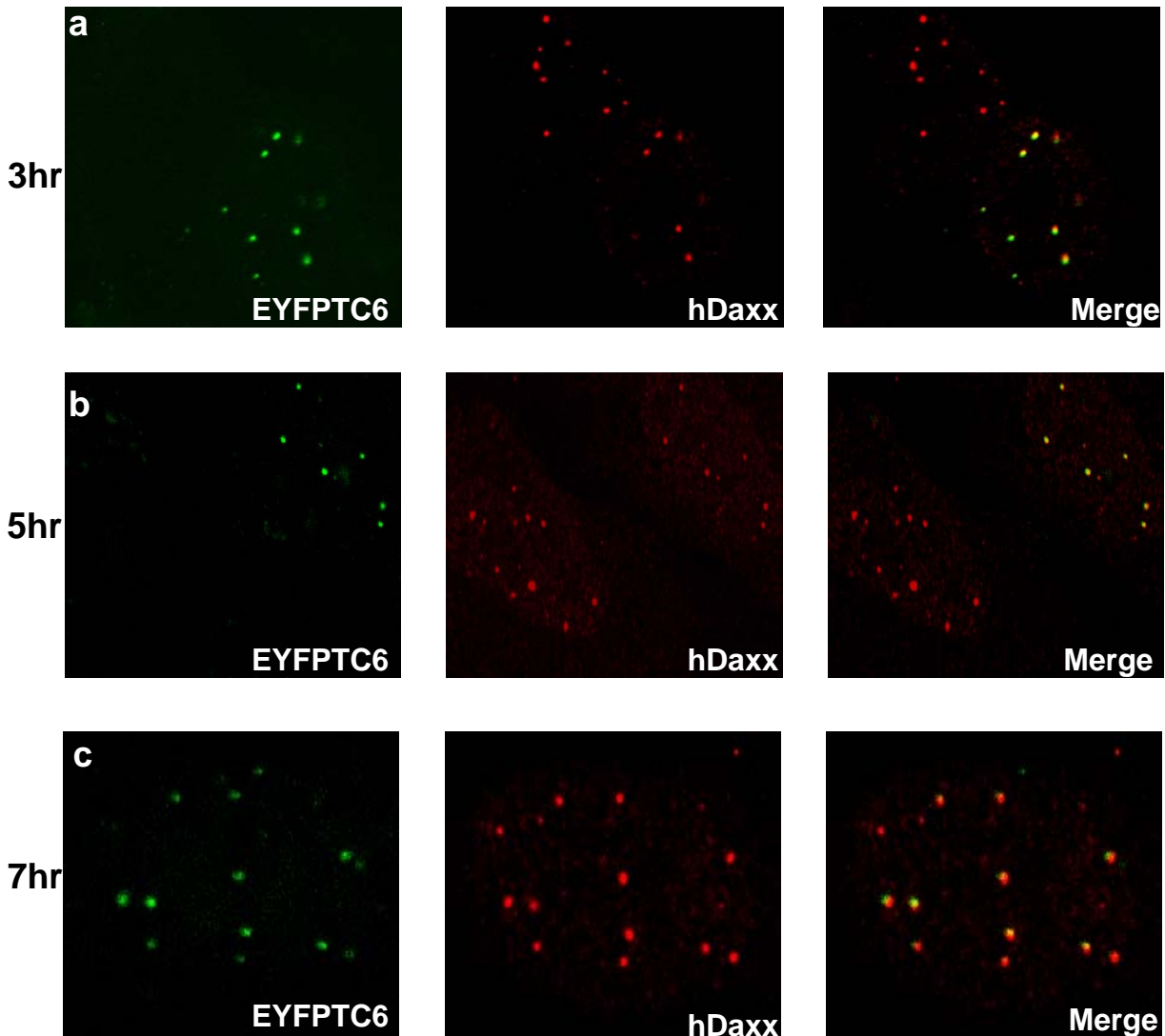


Figure 5.8a. EYFPTC6 co-localises with hDaxx at 3 hr, 5 hr and 7 hr post-infection.

HFFF2 monolayers were infected with 5×10^5 pfu of *in0156* (expressing EYFPTC6), and incubated at 38.5°C . At 3 hr, 5 hr and 7 hr post-infection cell monolayers were fixed and permeabilised. Cells were stained with anti-hDaxx primary antibody and subsequently with secondary antibody (anti-mouse Cy5-conjugated). Images were generated on a confocal microscope and the magnification of each image was optimised to fit the area of the cell(s) in the field of view.

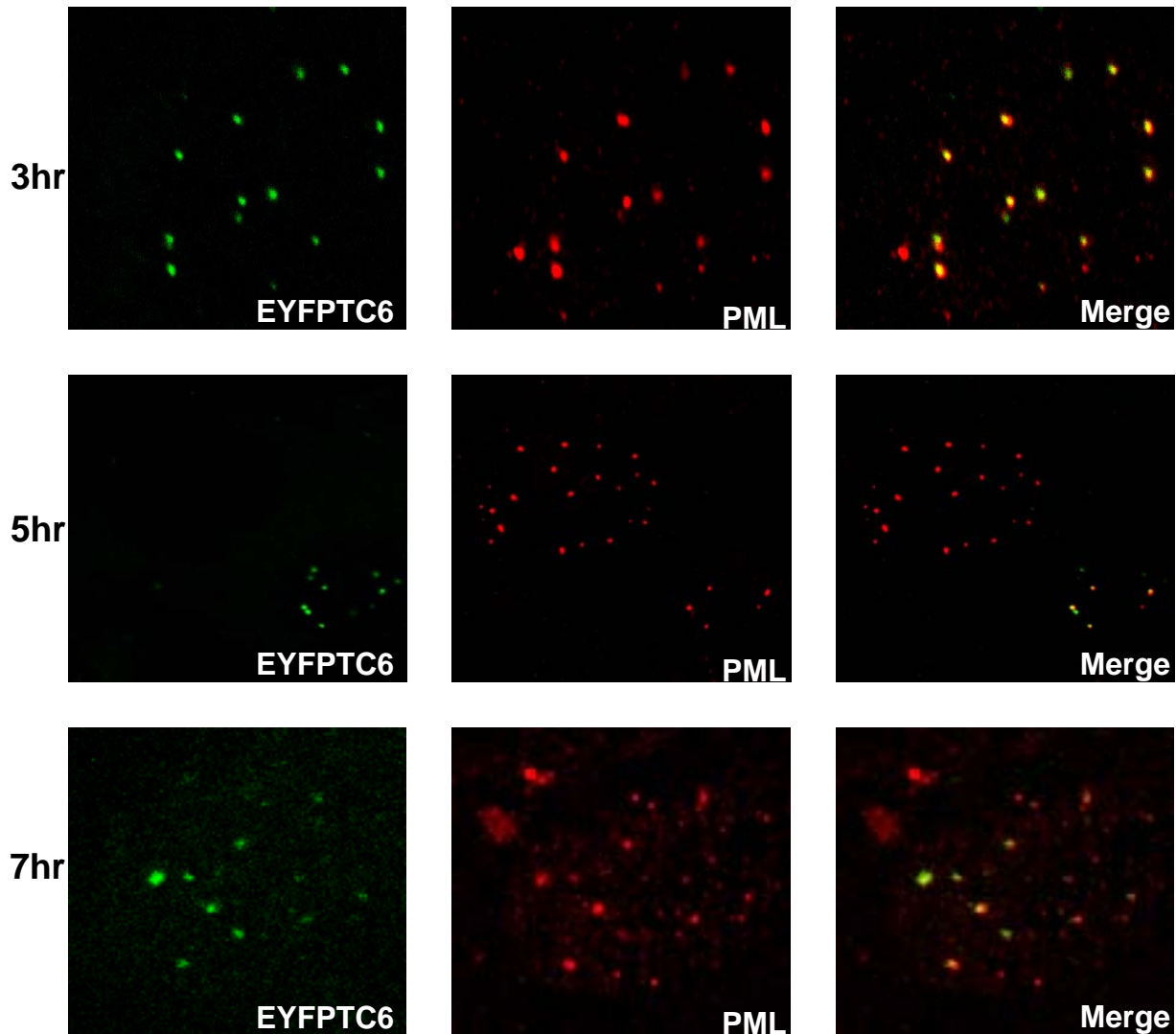


Figure 5.8b. EYFPTC6 co-localises with PML at 3 hr, 5 hr and 7 hr post-infection.

HFFF2 monolayers were infected with 5×10^5 pfu of *in0156* (expressing EYFPTC6), and incubated at 38.5°C . At 3 hr, 5 hr and 7 hr post-infection cell monolayers were fixed and permeabilised. Cells were stained with primary antibody anti-PML A-20 for 1 hr followed by incubation with secondary antibody (Alexa 647-chicken anti-goat) for 1 hr. Images were captured on a confocal microscope and the magnification of each image was optimised to fit the area of the cell in the field of view.

5.3.2. Hybrid TC6 co-localises with the cellular proteins hDaxx and PML at 5 hr post-infection.

HFFF2 cells (8×10^4) were infected with 5×10^5 pfu of *in1310* (expressing EYFPpp71), *in0146* (EYFPCh82), or *in0156* (EYFPTC6). At 5 hr post-infection cell monolayers were fixed and stained with either anti-hDaxx or anti-PML antibodies and their appropriate secondary antibodies.

Cell monolayers infected with *in1310* showed the same nuclear distribution patterns as observed at 3 hr post-infection whereby pp71 localised to discrete punctate foci in the nucleus (figure 5.2). When stained with antibodies raised against both hDaxx and PML, pp71 was found to co-localise with both cellular proteins (figure 5.3a and 5.3b). In cell monolayers infected with *in0146* a change in the nuclear distribution pattern of cells was observed. An increasing number of cells infected with *in0146* showed Ch82 exhibited a punctate/diffuse pattern of fluorescence (figure 5.2). However, as expected, both hDaxx and PML were seen to co-localise with these foci as presented in figures 5.4a and 5.4b. Surprisingly, cells infected with *in0156* showed no change in nuclear distribution patterns at 5 hr compared to that at 3 hr. In all cells observed, hybrid TC6 localised to discrete punctate foci associated with pp71 (figure 5.8a, panel b). When cell monolayers were stained with antibodies raised against hDaxx and PML the punctate foci of TC6 were found to co-localise with both cellular proteins (figure 5.8a and 5.8b).

5.3.3. Hybrid TC6 co-localises with the cellular proteins hDaxx and PML at 7 hr post-infection.

HFFF2 cells (8×10^4) were infected with 5×10^5 pfu of *in1310* (expressing EYFPpp71), *in0146* (EYFPCh82) or *in0156* (EYFPTC6). At 7 hr post-infection cell monolayers were fixed and stained with anti-hDaxx and anti-PML antibodies and their appropriate secondary antibodies. In the majority of cells infected with *in1310*, pp71 localised to discrete punctate foci, however some infected cells showed pp71 exhibiting a punctate/diffuse pattern of fluorescence (figure 5.2). When infected monolayers were stained with anti-hDaxx and anti-PML antibodies, all foci were seen to co-localise with both cellular proteins (figure 5.3a and 5.3b). As shown previously, as late as 7 hr post-infection pp71 co-localised with hDaxx and PML at ND10 domains. In cell monolayers infected with *in0146*, in the majority of cells Ch82 exhibited a punctate/diffuse pattern of fluorescence (figure

5.2), but continued to localise with both hDaxx and PML (figure 5.4a and 5.4b). Surprisingly, in cell monolayers infected with *in0156*, the nuclear distribution pattern continued to resemble that of pp71 (figure 5.8a, panel c), with hybrid TC6 localised to discrete punctate foci. When cell monolayers were stained with antibodies raised against hDaxx or PML, these punctate foci co-localised with both hDaxx and PML (figure 5.8a and 5.8b). Therefore, at 7 hr post-infection, hybrid TC6 behaved in a manner similar to that of pp71 in terms of both nuclear distribution and co-localisation with hDaxx and ND10 domains.

In previous experiments the difference in nuclear distribution patterns of pp71 and Ch82 were based on counting fluorescence patterns in cell nuclei. In the case of hybrid TC6, due to low levels of infection with *in0156* very few infected cells were observed at each time post-infection. At each time point hybrid TC6 localised to discrete punctate foci, mimicking the pattern of pp71. However it remains a possibility that the nuclear distribution pattern of hybrid F may become more like that of Ch82 at 5 hr and 7 hr post-infection. In order to investigate this further higher levels of infection with *in0156* would need to be obtained in order to observe a greater number of infected cells.

5. Part IV

5.4. Introduction

In various cell types the cellular protein hDaxx has been shown to bind to the transcription factors Ets-1 and Pax-3, thus exerting a repressive effect on the respective target genes (Hofmann et al., 2002, Li et al., 2000b). The repressive effect of hDaxx on IE gene expression is thought to occur via the action of a HDAC (Li et al., 2000a). Work by Saffert and Kalejta (2006) has shown that pp71 may act to mediate the proteasomal degradation of hDaxx in order to relieve its repressive effect and activate viral IE gene expression in infected cells. Preston and Nicholl (2006) also reported that the interaction of pp71 with hDaxx is important in relieving repression of IE gene expression and permitting the efficient initiation of productive replication.

As pp71 was recently reported to be sufficient to promote the degradation of hDaxx in the absence of every other HCMV protein (Saffert & Kalejta, 2006), (see section 1.10.3.2 for further details), work was carried out to establish if the non-human homologues also promote the degradation of hDaxx.

5.4.1. Infection with the *in1312* recombinants expressing EYFP-tagged homologues does not result in the degradation of hDaxx.

In order to determine whether the EYFP-tagged UL82 homologues were able to promote the degradation of hDaxx, 1.5×10^5 U373 cells were infected with 5×10^5 pfu of the *in1312* recombinant viruses expressing the EYFP-tagged UL82 homologues or HCMV AD169 (positive control). Following incubation at 38.5°C lysates were harvested at 7 hr and 24 hr post-infection for analysis by SDS PAGE, or cell monolayers were stained with X-gal in order to determine levels of infection.

Figure 5.9 shows a western blot of cell lysates harvested at 7 hr post-infection. The protein hDaxx was detected using an anti-hDaxx primary antibody and an HRP-conjugated anti-rabbit secondary antibody. Similar levels of hDaxx were observed in all lysates, including those from cells mock-infected or infected with the negative control (*in1374*). Figure 5.10 shows cell monolayers infected with the *in1312* recombinant viruses expressing EYFP-tagged UL82 homologues stained with X-gal at 7 hr post-infection. All five viruses expressing EYFP-tagged UL82

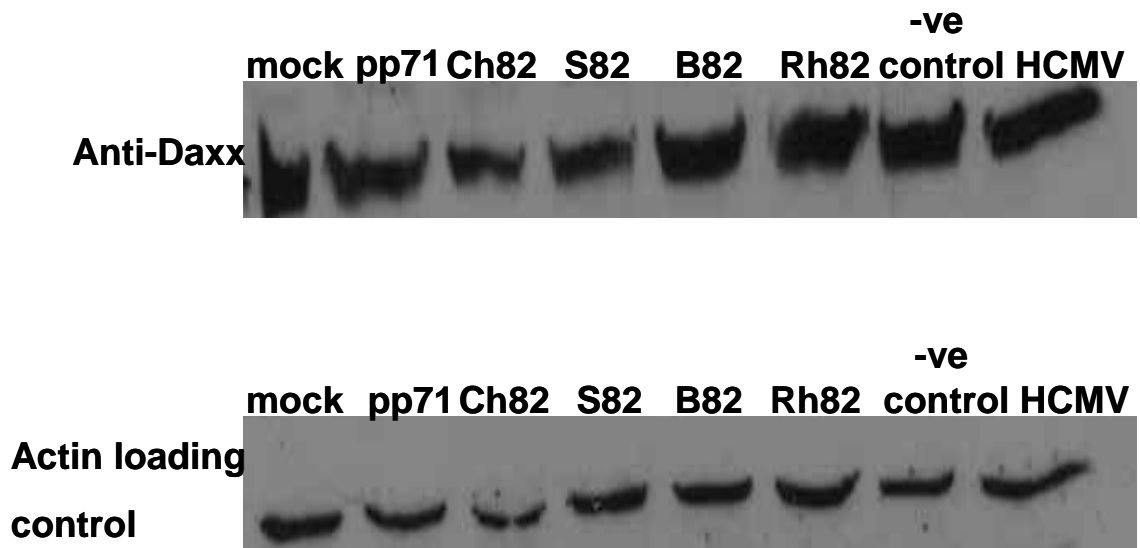


Figure 5.9. Western blot analysis of lysates of cells infected with *in1312* recombinants expressing UL82 homologues at 7 hr post infection.

U373 cell monolayers were infected with 5×10^5 pfu (MOI 3.3) of the *in1312* recombinants expressing the UL82 homologues or HCMV AD169 (control) and incubated 38.5°C . At 7 hr post-infection cell lysates were harvested and analysed by SDS PAGE. hDaxx was probed for using an anti-Daxx primary antibody and an anti-rabbit HRP conjugated secondary antibody. Blots were stripped and reprobed with an anti-actin primary antibody and an anti-mouse HRP conjugated secondary antibody, to control for loading.

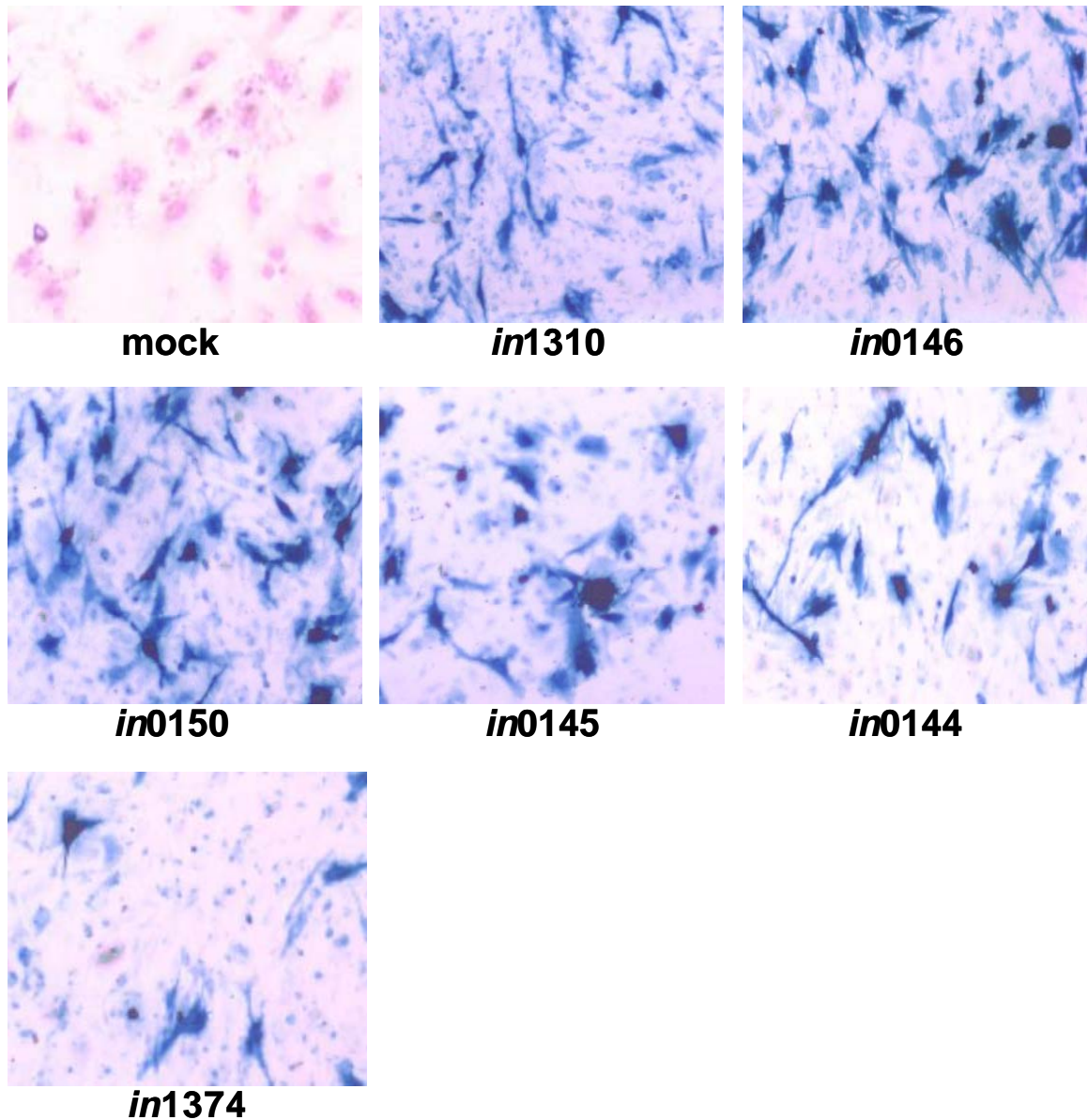


Figure 5.10. β -gal expression directed by the *in1312* recombinants expressing the EYFP-tagged UL82 homologues at 7 hr post-infection

U373 cell monolayers were mock-infected or infected with 5×10^5 pfu (MOI 3.3) of the *in1312* recombinants expressing the EYFP-tagged UL82 homologues and incubated at 38.5°C . At 7 hr post-infection cell monolayers were stained with X-gal and images were obtained.

The *in1310* virus expresses EYFPpp71, *in0146* expresses EYFPCh82, *in0150* expresses EYFPS82, *in0145* expresses EYFPB82, *in0144* expresses EYFPRh82, and *in1374* was used as a negative control.

homologues showed β -gal positive cells at levels above the negative control, implying that each homologue acts on the HCMV MIEP, to drive short-term gene expression to a similar extent.

Lysates of cell monolayers, infected with the *in1312* recombinant viruses expressing EYFP-tagged UL82 homologues and harvested at 24 hr post-infection, were analysed by SDS PAGE. Figure 5.11 shows a western blot containing all lysates probed with an anti-hDaxx primary antibody, and a HRP-conjugated anti-rabbit secondary antibody. At 24 hr post-infection no significant changes in the levels of hDaxx expression were observed in cell lysates compared to 7 hr post-infection. As expected, there was no change in the levels of hDaxx expression in lysates of cells infected with *in1374* (negative control) or mock-infected. X-gal staining showed that monolayers were infected to similar levels as presented in figure 5.12, ensuring lysates harvested at 24 hr post-infection were also infected at equivalent levels. Therefore no major change in levels of hDaxx was observed in lysates of cells infected with *in1312* recombinants expressing EYFP-tagged UL82 homologues or HCMV, and in these experiments none of the UL82 homologues detectably promoted the degradation of hDaxx.

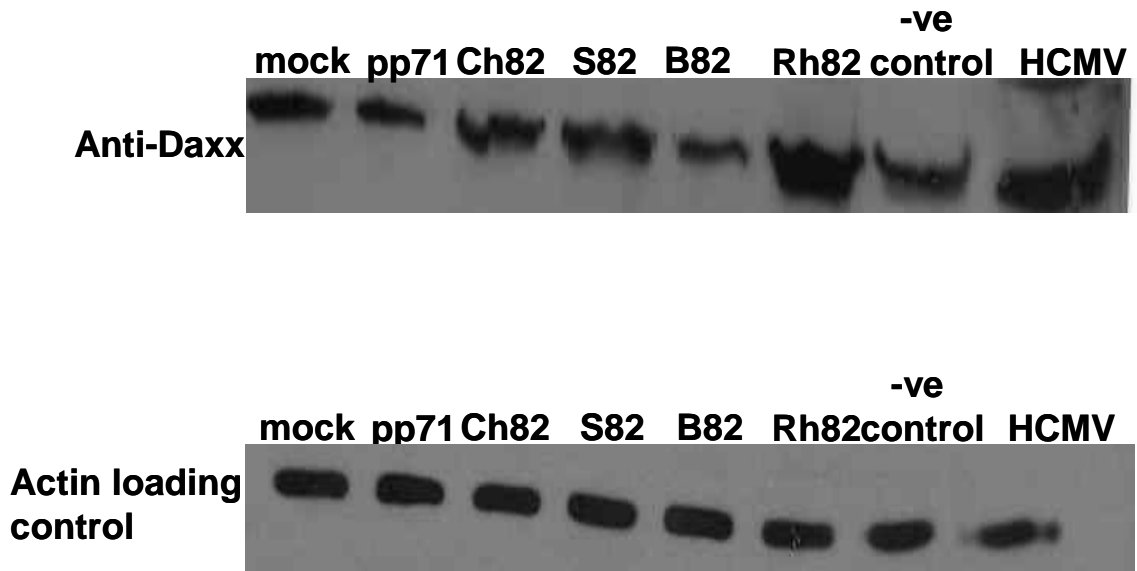


Figure 5.11. Western blot analysis of lysates of cells infected with *in1312* recombinants expressing UL82 homologues 24 hr post-infection.

U373 cell monolayers were infected with 5×10^5 pfu (MOI 3.3) of the *in1312* recombinants expressing the UL82 homologues or HCMV AD169 (control) and incubated 38.5°C . At 24 hr post-infection cell lysates were harvested and analysed by SDS PAGE. The protein hDaxx was probed for using an anti-Daxx primary antibody and an anti-rabbit HRP conjugated secondary antibody. Lysates were subjected to SDS PAGE again and probed with an anti-actin antibody and an anti-mouse HRP-conjugated secondary antibody, to act as a loading control.

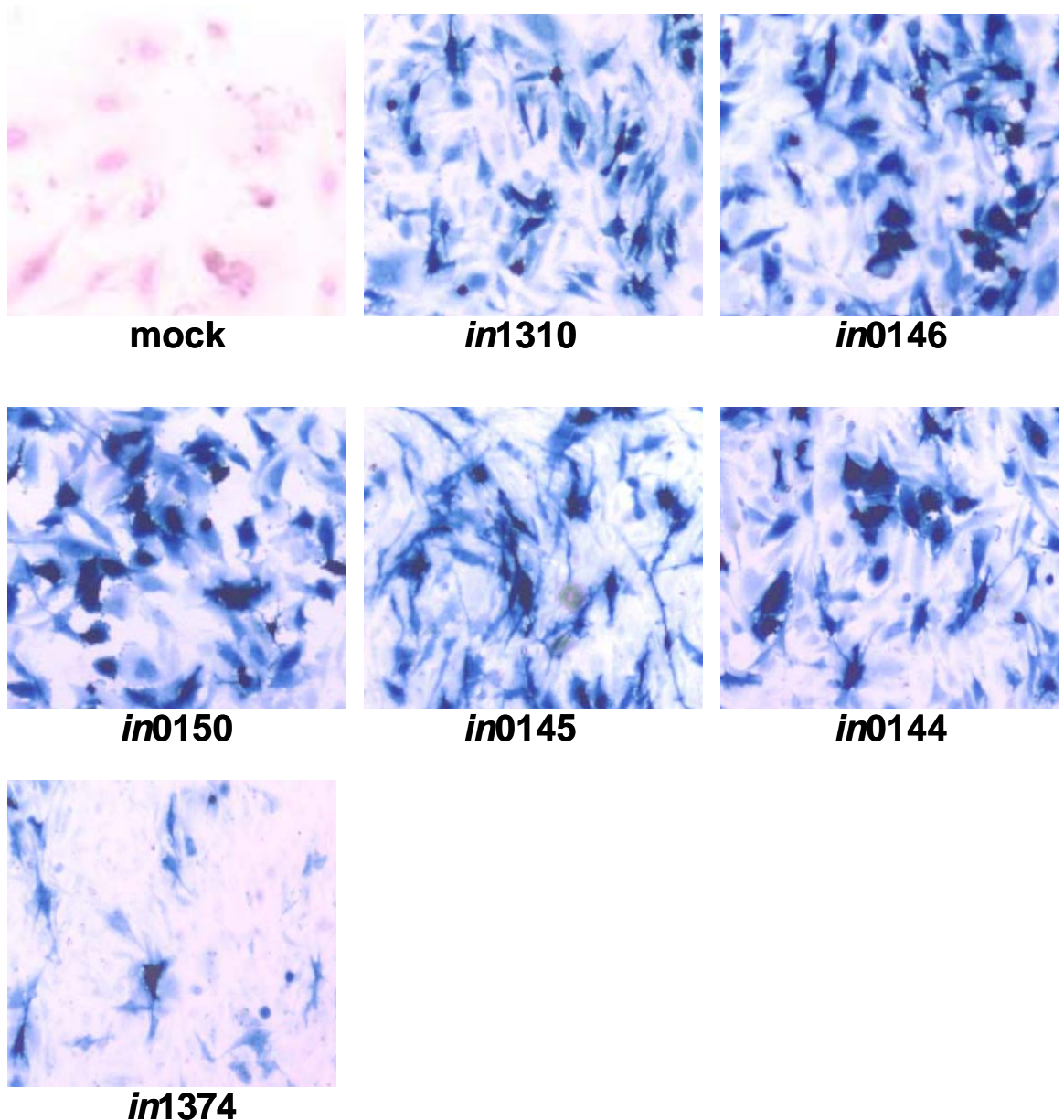


Figure 5.12. β -gal expression of the *in1312* recombinants expressing the EYFP-tagged UL82 homologues at 24 hr post-infection

U373 cell monolayers were mock-infected or infected with 5×10^5 pfu (MOI 3.3) of the *in1312* recombinants expressing the EYFP-tagged UL82 homologues and incubated at 38.5°C . At 24 hr post-infection cell monolayers were stained with X-gal and images were obtained.

The *in1310* virus expresses EYFPpp71, *in0146* expresses EYFPCh82, *in0150* expresses EYFPS82, *in0145* expresses EYFPB82, *in0144* expresses EYFPRh82, and *in1374* was used as a negative control.

5.5. Discussion

The study presented here has confirmed that pp71 is able to stimulate both short-term and long-term gene expression from the HCMV MIEP. Earlier work by Marshall et al. (2002) suggested that pp71 is a non-sequence-specific activator of gene expression, and could thus be compared to the HSV-1 IE protein ICP0. It is well known that ICP0 is a RING-finger ubiquitin E3 ligase protein that is able to induce the proteasome-dependent degradation of PML (Boutell & Everett, 2003, Everett et al., 1999a, Everett & Maul, 1994). The ICP0 induced degradation of PML at ND10 domains is a vital stage in the expression of HSV-1 early and late genes.

The HCMV protein pp71 is known to accumulate at ND10 domains, prior to the production of IE proteins, by co-localisation with hDaxx (Hofmann et al., 2002, Ishov et al., 2002). It is the interaction of pp71 with hDaxx, mediated by the interaction of the C-terminus of hDaxx with SUMO modified PML which trafficks pp71 to ND10 domains (Hofmann et al., 2002, Ishov et al., 2002). The data presented in the final part of this study aimed to characterise the UL82 homologues in terms of their nuclear distribution patterns and their interactions with the cellular proteins hDaxx and PML.

In tissue culture, cells infected with the viruses *in1310*, *in0146*, *in0150*, *in0145*, and *in0144* exhibited significant differences in terms of nuclear distribution patterns. The pp71 protein localised predominantly to discrete punctate foci up to 7 hr post-infection. The work presented in this study agrees with previous work that pp71 does indeed localise to discrete punctate foci.

At 3hr post-infection Ch82, B82, and Rh82 all appeared to localise to discrete punctate foci. However at 5 hr post-infection, a greater number of infected cells showed these proteins in a punctate/diffuse pattern of fluorescence and by 7 hr post-infection in the majority of cells infected with *in0146*, *in0145* and *in0144* the Ch82, B82 and Rh82 proteins exhibited a punctate/diffuse pattern of fluorescence. The S82 protein was markedly different from the outset, as it exhibited a punctate/diffuse diffuse pattern of fluorescence at 3 hr post-infection. At both 5 hr and 7 hr post-infection, the majority of infected cells exhibited a diffuse pattern of fluorescence. This indicated that at later times of infection, the attributes of the

non-human homologues diverge from those of pp71 to become increasingly like S82.

The distribution pattern exhibited by the EYFP-tagged hybrid protein TC6 was also investigated when cells were infected with *in0156*. At 3 hr, 5 hr and 7 hr post-infection, hybrid TC6 was observed to localise to discrete punctate foci similar to foci to which pp71 localises. However due to the low levels of initial infection, very few infected cells were observed and the possibility remains that the nuclear distribution pattern exhibited by hybrid TC6 could become more like the Ch82 homologue at later times of infection. Further experimental work is needed to confirm that data.

HFFF2 cell monolayers infected with the *in1312* recombinant viruses expressing the EYFP-tagged UL82 homologues or hybrid TC6 were stained for endogenous PML and hDaxx at 3 hr, 5 hr and 7 hr post-infection. The HCMV protein pp71 was observed to co-localise with hDaxx and PML at all times post-infection, in agreement with other studies (Hofmann et al., 2002, Ishov et al., 2002). Interestingly, the Ch82, B82 and Rh82 homologues were observed to co-localise with ND10 domains and interact with hDaxx at all time points investigated. It was observed that the various nuclear distribution patterns did little to alter the localisation of the homologues with these cellular proteins.

However in the case of S82 at 5 hr and 7 hr post-infection, few foci were observed to co-localise with hDaxx. In cells infected with *in0150* cells, where a diffuse pattern of fluorescence was observed, hDaxx appeared to be dispersed. Data presented here show that at 7 hr post-infection S82 appears to disperse hDaxx from within the nucleus. It is possible that the S82 protein may have a lower binding affinity for hDaxx at 7 hr post-infection compared to the other UL82 homologues. As this study shows no evidence of protein-protein interactions between S82 and hDaxx further experimental work would have to be carried out to establish if this is indeed the case. Also further studies would need to be carried out at later times post-infection to establish if the B82, Rh82 and Ch82 homologues also exhibit diffuse patterns of fluorescence and they also disperse hDaxx. Hybrid TC6 was also observed to interact with hDaxx and was able co-localise at ND10 domains at all times post-infection. Thus, indicating that this

hybrid protein possibly retains some of the attributes of pp71 and Ch82 which allow them to co-localise with hDaxx and PML.

This study has not only confirmed the co-localisation of pp71 and S82 with PML and hDaxx at ND10 domains (Hofmann et al., 2002, Ishov et al., 2002, Nicholson, 2004), it has also demonstrated that the remaining non-human homologues are also able to co-localise with these cellular proteins at ND10 domains.

It has been suggested that hDaxx acts as a transcriptional repressor by interacting with HDAC molecules, Dek and various transcription factors such as Pax1 or ETS1 (Hollenbach et al., 2002, Li et al., 2000a). Histone deacetylase activity occurs at sites of transcription where hDaxx facilitates the deacetylation of histone tails. The histone tails then bind to DNA, blocking access to the transcriptional machinery and causing repression of transcription. Dek has been reported to associate with chromatin, altering its condensed state and resulting in the repression of gene expression, as transcription factors are unable to access the DNA (Hollenbach et al., 2002, Kappes et al., 2001, Woodhall et al., 2006). Recent studies have proposed that pp71 acts to degrade hDaxx and relieve histone deacetylation. The histones associated with the MIEP during infection can then be acetylated (Cantrell & Bresnahan, 2006, Preston & Nicholl, 2006, Saffert & Kalejta, 2006). The mechanism whereby pp71 degrades hDaxx is believed to be by a proteasome-dependent ubiquitin independent pathway (Hwang & Kalejta, 2007).

Earlier in this study it was established that the non-human UL82 homologues act on the MIEP to drive short-term gene expression. As all the non-human homologues were observed to co-localise with hDaxx and PML, at ND10 domains, like pp71, it was hypothesised that the non-human homologues may also degrade hDaxx to relieve repression at the MIEP promoter during infection.

Cells infected with the *in1312* recombinant viruses expressing the EYFP-tagged UL82 homologues were probed for hDaxx at 7 hr and 24 hr post-infection by western analysis. Infected cell monolayers were also stained with X-gal to ensure similar levels of infection were obtained. Data from this study showed that at both 7 hr and 24 hr post-infection, no significant changes in levels of hDaxx were observed in lysates infected with *in0146*, *in0150*, *in0144*, *in0145*. Surprisingly, proteasomal degradation of hDaxx was not detected in lysates infected with

in1310 (expressing EYFPpp71) or in lysates infected with HCMV at either 7 hr or 24 hr post-infection. The data presented in this study showed that neither pp71 nor the non-human homologues appear to be directly involved in promoting the degradation of hDaxx.

Since there is considerable evidence to support the hypothesis that pp71 stimulates the proteasomal degradation of hDaxx (Cantrell & Bresnahan, 2006, Preston & Nicholl, 2006, Saffert & Kalejta, 2006, Saffert & Kalejta, 2007), it is possible that the lack of proteasomal degradation of hDaxx by pp71 in this study could be due to experimental differences. The proteasomal degradation of hDaxx by pp71 appears to be cell-type specific, and dependent on specific experimental conditions. Work by Saffert and Kalejta (2006) showed that pp71-induced hDaxx degradation in human foreskin fibroblast cells (HFFs) inoculated with virus at 4°C for a 1 hr incubation period, followed by a 5 min shift to 37°C where the virus inoculum was removed and the medium replaced. In studies described here, U373 cells were utilised and all infections were carried out at only 38.5°C. These differences may account for the lack of detectable proteasomal degradation, especially in the case of HCMV. Further work is required to establish if these differences in experimental conditions affect the pp71-induced degradation of hDaxx and if the homologues, like pp71, also induce proteasomal degradation of hDaxx. Work by Tavali et al. (2008) has recently shown that hDaxx is degraded by pp71 as early as 3 hr post-infection, but levels of hDaxx become stabilised by 12 hour post-infection to complement hDaxx levels observed in mock-infected cells.

All experiments carried out in this study employed HSV-1 recombinant viruses, thus it still remains unknown how the non-human UL82 homologues behave *in vivo*. Confocal microscopy studies have shown that S82 appears to disperse hDaxx at 7 hr post-infection; it is possible that at later times the other non-human homologues may not degrade hDaxx but instead disperse it to allow the onset of transcription. Therefore the non-human homologues may act by a different mechanism to eradicate hDaxx in order to relieve repression. It is also possible that *in vivo* the non-human UL82 homologues may employ a different repression mechanism or that they may need to degrade other cellular proteins in order to relieve repression at the MIEP to activate transcription.

Chapter 6

Final Discussion

6.Final Discussion

6.1. Introduction

HCMV pp71 has been established as a transactivator of gene expression, capable of acting on heterologous promoters (Homer et al., 1999, Liu & Stinski, 1992). It fulfils several functions as a tegument protein of HCMV and is conserved in chimpanzee (Ch82), simian (S82), baboon (B82), and rhesus (Rh82) CMV isolates. The aims of this study have been to characterise some of the attributes of B82, Ch82, Rh82 and S82 with regard to HCMV pp71. The focus of the work described here has been (a) to determine how the pp71 non-human UL82 homologues behave in terms of activation of short-term and long-term gene expression, (b) to map the region of pp71 involved in long-term gene expression and (c) to further characterise the non-human UL82 homologues by studying the intracellular localisation of these proteins.

6.1.1. UL82 homologues; short-term and long-term expression analyses

The first part of this study aimed to investigate the ability of the non-human UL82 homologues to direct short-term and long-term gene expression. Previous work by Nicholson (2004) and Preston and Nichol (2005) showed that pp71 was able to direct both short-term and long-term gene expression, while its non-human counter-part, S82, was only able to direct short-term gene expression.

To investigate if B82, Rh82 and Ch82 behaved like pp71 or S82, transfection assays were employed. Data from these experiments showed that pp71 appeared to be unique in its ability to stimulate long-term gene expression. Results from transfection experiments were confirmed by infection assays. The UL82 homologues were recombined into the HSV-1 genome, which was impaired for the transcriptional activity of VP16 and ICP0 and had a temperature sensitive mutation in ICP4. Each recombinant virus expressing the UL82 homologues had β -gal inserted into the non-essential UL43 locus under the control of the HCMV MIEP. The results from the infection assays confirmed those obtained previously from transfection assays whereby all the UL82 homologues were functional in the short-term. Only HCMV pp71 was observed to direct long-term gene expression.

6.1.2. The UL82 homologues and long-term gene expression

Preston and Nicholl (2005) suggested that when cells are infected with the HSV-1 recombinant viruses expressing EYFP-tagged pp71 (*in1310*), the quiescent state of the genome is incomplete. Low levels of gene expression, including pp71, continue thereby allowing pp71 to act on the MIEP which results in the eventual unblocking of the genome, leading to long-term gene expression. The non-human UL82 homologues (S82, B82, Rh82 and Ch82) were all found to be unable to stimulate long-term gene expression, and only short-term activation was observed. This may suggest that the quiescent state of the HSV-1 recombinant viruses expressing the non-human UL82 homologues is more complete than that of *in1310*. β -gal positive cells were observed at 24 hr post-infection, representing the population of infected cells that respond to short-term gene expression. At 10 days post-infection no β -gal positive plaques were observed in cells subjected to a temperature downshift i.e. at a temperature permissive for replication. The expression of the non-human UL82 homologues appears to be shut off, and there is no evidence of continued low level expression of these homologues to unblock the remainder of the genome. Evidence for this can be observed when infected cells are super-infected with *tsK*, unmasking the genomes that are still present in the cells but have become quiescent after short-term expression. Therefore the non-human UL82 homologues may lack the positive feedback mechanism thought to be associated with pp71. These data indicate that, like pp71, all the non-human UL82 homologues are able to stimulate short-term gene expression, possibly for the rapid initiation of the viral transcription program, but, unlike pp71, allow the genome to be completely shut off preventing long-term expression in these systems.

Alternatively, it is possible that short-term and long-term gene expression directed by the UL82 homologues is linked to differing chromatin structures in both situations. The initial short-term gene expression directed by all the non-human homologues investigated maybe indicative of an open chromatin formation around the HCMV MIEP, allowing the UL82 homologues to act on the HCMV MIEP to drive β -gal expression. It maybe the case that, at late times post-infection, the HCMV MIEP becomes repressed through the recruitment of HDACs resulting in a closed chromatin conformation. Therefore, in cells infected with the *in1312* recombinant viruses expressing the non-human UL82 homologues, a state similar

to latency is achieved at later times post-infection as the non-human UL82 homologues are unable to relieve repression at the HCMV MIEP, and thus are unable to direct long-term gene expression. In cells infected with *in1310* pp71 may act to relieve histone deacetylation allowing access for other transcription factors to give long-term gene expression.

Further work would be needed to establish the state of chromatin around at the MIEP at early and late times post-infection

6.1.3. Effects of the UL82 homologues on genome quiescence

Preston and Nichol (2005) showed that pp71 could act *in trans* to reactivate quiescent genomes. In this study, SEAP assays were carried out to investigate if the non-human homologue, Ch82, like pp71 could reactivate quiescent genomes. Results from the SEAP assays showed that upon super-infecting quiescent genomes with *in1310* and *in0146*, only pp71 was able to provoke resumption of gene expression. This confirmed work by Preston and Nichol (2005) and showed that pp71 appears to be unique in its ability to stimulate reactivation of quiescent genomes.

As pp71 has been demonstrated to be able to reactivate quiescent genomes, this protein can be considered to have some similar functions to HSV-1 ICP0. Various studies have shown that ICP0 is able to reactivate quiescent genomes (Harris & Preston, 1991, Preston & Nicholl, 1997, Russell et al., 1987, Samaniego et al., 1998, Stow & Stow, 1989), however the rate at which pp71 can induce reactivation of a quiescent genome is slower than that of ICP0 (Preston & Nicholl, 2005). Reactivation by pp71 is believed to be less effective than ICP0 as only small amounts of ICP0 are required to reverse the quiescent state (Hobbs et al., 2001, Preston & Nicholl, 2005). It has been suggested that ICP0 may counteract repression by stimulating the degradation of a number of cellular proteins via the ubiquitin proteasome pathway through the binding of its RING finger domain to USP7 (Boutell et al., 2002). The protein pp71 lacks a RING finger domain, however, despite this, it can mediate proteasomal degradation of the Rb family of proteins which may result in pp71 stimulating quiescent cells back into the cell cycle (Kalejta & Shenk, 2003c). Thus pp71, like ICP0, may utilise a proteasomal pathway to degrade cellular proteins and relieve repression, in this case of

quiescent cells. Previous studies have shown that quiescent HSV-1 can be reactivated upon super-infection with HCMV (Russell & Preston, 1986, Stow & Stow, 1989) suggesting that HCMV gene products act as a substitute for the absence of ICP0. It is possible that pp71 may have some effect upon this, as to date no additional HCMV gene products have been identified as playing a role in reactivation.

6.1.4. Promoter analysis of the UL82 homologues

The ability of pp71 to mediate long-term gene expression may be linked to the promoter stimulating activity of this protein. Consequently, long-term gene expression may be directed by the non-human UL82 homologues but only when they are controlled by their own MIEP promoters. The HCMV MIEP enhancer contains a number of interaction sites to which transcription factors can bind, to activate the MIEP. These sites include three copies of a 21 bp repeat element and four copies of an 18 bp repeat element. It also contains five copies of a 19 bp repeat element (CCCCATTGACGTCAATGGG) to which the cellular transcription factors ATF/CREB are known to bind. Various studies have shown that pp71-induced MIEP stimulation requires the presence of the ATF/CREB binding site within the enhancer region (Cherrington & Mocarski, 1989, Liu & Stinski, 1992). Deletion of the 19 bp repeat element containing the consensus ATF/CREB binding motif abolished responsiveness of the promoter to pp71 in co-transfection assays (Liu & Stinski, 1992).

Sequence analysis of the ChCMV MIEP enhancer region (data not shown) showed conserved 19 bp, 18 bp, 21 bp and 17 bp repeat elements. Four copies of the 19 bp repeat elements were found, one of which was a perfect match to the 19 bp sequence in HCMV, two sequences contained two nucleotide mismatches the first at residues 704-747 (GCCCCATTGACGTCAATGGI) and the second at residues 729-747 (TI~~CC~~ATTGACGTCAATGGG). The third sequence at residues 809-829 had three mismatches (CCCIATTGACGTCAATGAC). However, as the consensus sequence (TTGACGTCAA) to which the ATF/CREB proteins bind remains unaltered it seems unlikely that the mismatches would have any significant effect on activation. Indeed, variations also exist within the 19 bp repeat in the HCMV MIEP. Two copies of the 18 bp repeat sequence were found containing two and three mismatches. Two copies of the 21 bp repeat elements

were also found, one of which was a perfect match to that in HCMV while the other contained two mismatches. Only one copy of the 17 bp repeat element was found conserved within the ChCMV sequence and contained one mismatched nucleotide.

The 19 bp nucleotide repeat sequence is also believed to be highly conserved within the SCMV MIEP enhancer region, while the 18 and a 16 bp element are only marginally conserved (Thomsen et al., 1984). The 19 bp repeat element is also conserved in RhCMV (data not shown). Thus as these repeat elements appear to be conserved within both ChCMV, SCMV and RhCMV MIEPs, it is highly likely that they are also conserved within the BCMV MIEP. It is possible that the non-human UL82 homologues, like pp71, activate the ATF/CREB sequences at the 19bp repeat elements in the HCMV MIEP because they are conserved throughout their own promoters, resulting in short-term gene expression. This could provide an explanation as to why the non-human homologues were equally or more active than pp71 during short-term assays. The target promoter in all experiments was the HCMV MIEP, thus all the homologues were able to act on the conserved ATF/CREB sequences at the 19 bp repeat elements to drive short-term gene expression. It is possible that during long-term gene expression pp71 acts on a different part of the promoter, possibly by binding to cellular factors which attach to other repeat elements. Furthermore, this mode of action may also be the case for the non-human UL82 homologues acting on their own promoters.

6.1.5. The LXCXD motif

The LACSD motif within pp71 was found to induce the degradation of the Rb tumour suppressor protein family through a proteasome-dependent ubiquitin-independent mechanism (Kalejta & Shenk, 2003c). This motif was conserved in the S82 protein at residues 209-213 and in the B82 protein at residues 209-213. Within the Ch82 protein this motif is found as LSCSD at residues 212-216, while in Rh82 the motif appears as LACSN at residues 209-213 (figure 6.1a). However work by Preston and Nicholl (2005) eliminated the theory that the LACSD motif in pp71 played a role in directing long-term gene expression. Mutation of the central cysteine to glycine abolished the effect of pp71 on the degradation of the unphosphorylated Rb gene products but did not alter the ability of pp71 to mediate

A Conservation of Rb interaction domains in the UL82 homologues

Human (213) LEQ**LACSDPNT**
Chimp (210) VELL**SCSDRNT**
Simian(206)MDQ**LACSDADT**
Baboon(205)MDQ**LACSDGYT**
Rhesus(206)IDQ**LACSNNGDT**
Consensus MDQLACSDG T

B Conservation of DIDs in the UL82 homologues

DID I		DID II	
Human (206)	PL TLVDAL	Human (324)	PG VSIEAGP
Chimp (203)	PL RLVDAV	Chimp (321)	PG VSMEAGP
Simian(199)	PL TVVDAM	Simian(316)	PGL SIEAGP
Baboon(198)	PL TVVDAM	Baboon(315)	PGL SIECGP
Rhesus(199)	PL TLVDAI	Rhesus(316)	PGI SMDAGP
Consensus	PL TLVDAM	Consensus	PGL SIEAGP

Figure 6.1 Conservation of UL82 functional domains in homologous non-human CMV sequences

A: Conservation of the LASC domain. B: Conservation of the DIDs. For all domains, residues conserved across all sequences are shown in red.

long-term activity of the promoter (Preston & Nicholl, 2005). As changes to the LACSD motif in pp71 did not result in changes to long-term gene expression, it is unlikely that the conserved motifs within the non-human UL82 homologues are of any importance with regards to long-term gene expression. However, it is not known if the conserved motifs within non-human UL82 homologues promote the degradation of the Rb proteins, or if the amino acid substitutions to the motifs in the Ch82 and Rh82 proteins have any significance.

6.2. The significance of the DIDs in the UL82 homologues

Sequencing of pp71 and the non-human UL82 homologues has revealed certain similarities and differences. Hensel et al. (1996) showed that pp71 has a bi-partite nuclear localisation signal (NLS), however this region is not conserved in the non-human homologues (Nicholson, 2004). As the Ch82, S82, B82 and Rh82 proteins are all targeted to the nucleus it seems unlikely that the proposed NLS in pp71 has any significant role in targeting this protein to the nuclei of cells. Hofmann et al. (2002) identified two putative DIDs (DID I at residues 206-213; DID II at residues 324-331). Deletion of either of these domains resulted in the pp71-hDaxx interaction being abolished. Point mutations of these motifs failed to identify the amino acid residues essential for hDaxx binding. As these DIDs are found within the most ordered region of pp71, deletion of these domains or mutations to individual residues may result in the disruption of the structure of pp71, resulting in the inability of the protein to bind to hDaxx.

Sequence analysis of the non-human homologues has revealed that these DIDs are well conserved within the protein sequences of all the non-human homologues, with the greatest degree of conservation occurring in DID II (figure 6.1b) (Nicholson, 2004). It is possible that these conserved DIDs within the non-human UL82 homologue sequences are involved in the hDaxx interactions observed in this study.

The role of the proposed pp71 DIDs in interactions with hDaxx (Hofmann et al., 2002) is borne out by the observed pattern of co-localisation of hybrid F with both hDaxx and PML. This indicated that this protein not only co-localises with hDaxx but also is trafficked to PML at ND10 domains. This hybrid protein is likely to co-localise with hDaxx and PML as the DIDs in pp71 have remained intact, despite the change to the structure of pp71. This suggests that as long as this highly

ordered region of pp71 remains undisrupted it is still able to retain a certain degree of functionality in terms of localising to hDaxx and PML at ND10 domains. In order to establish that the DIDs conserved in the Ch82 homologue are indeed functional, comparative experiments would have to be carried out using hybrid E which contains the middle region of Ch82 flanked by the N- and C- terminal regions of pp71.

6.3. Conclusions

This study has sought to characterise the non-human UL82 homologues of pp71 in terms of their effects on gene expression, intracellular localisation and interactions with the cellular proteins hDaxx and PML. Each UL82 homologue was shown to act in a similar way to pp71 with the exception that pp71 remains unique in its ability to direct long-term gene expression and reactivate quiescent genomes. Moreover, the non-human UL82 homologues exhibited slightly different intracellular distribution patterns to pp71 over the time period examined. Also hDaxx and PML interactions of the S82 homologue were different compared to that of pp71. This work, in combination with further analysis of structure, sequence motifs and cellular interactions, will help to progress the continued elucidation of pp71 function.

6.4. Future work

- Sequence analysis of the UL82 homologues has shown regions of highly conserved motifs including the DIDs and the LASCD motifs. Further study is needed to establish if the conserved DIDs in the non-human UL82 homologues are important in hDaxx interactions. Further work is also required to establish if the conserved LASCD motifs in the non-human UL82 homologues cause proteasome-dependent ubiquitin-independent degradation of the Rb tumour protein families.
- Further analysis of pp71 and the proteasomal degradation of hDaxx is required to establish if pp71 alone degrades hDaxx or if any other cellular interactions occur.
- Further analysis of the non-human UL82 homologues is needed to establish if they degrade or disperse hDaxx to relieve transcriptional repression.

- Elucidation of the 3D structure of pp71 would be helpful investigate protein folding, and to establish how deletions or changes to the structure of pp71 affect its other properties.

References

References

- Ablashi, D. V., Eastman, H. B., Owen, C. B., Roman, M. M., Friedman, J., Zabriskie, J. B., Peterson, D. L., Pearson, G. R. & Whitman, J. E. (2000). Frequent HHV-6 reactivation in multiple sclerosis (MS) and chronic fatigue syndrome (CFS) patients. *J Clin Virol* **16**, 179-91.
- Ace, C. I., Dalrymple, M. A., Ramsay, F. H., Preston, V. G. & Preston, C. M. (1988). Mutational analysis of the herpes simplex virus type 1 trans-inducing factor Vmw65. *J Gen Virol* **69**, 2595-605.
- Ace, C. I., McKee, T. A., Ryan, J. M., Cameron, J. M. & Preston, C. M. (1989). Construction and characterization of a herpes simplex virus type 1 mutant unable to transinduce immediate-early gene expression. *J Virol* **63**, 2260-9.
- Adair, R., Liebisch, G. W. & Colberg-Poley, A. M. (2003). Complex alternative processing of human cytomegalovirus UL37 pre-mRNA. *J Gen Virol* **84**, 3353-8.
- Adamson, W. E., McNab, D., Preston, V. G. & Rixon, F. J. (2006). Mutational analysis of the herpes simplex virus triplex protein VP19C. *J Virol* **80**, 1537-48.
- Ahmed, M., Lock, M., Miller, C. G. & Fraser, N. W. (2002). Regions of the herpes simplex virus type 1 latency-associated transcript that protect cells from apoptosis in vitro and protect neuronal cells in vivo. *J Virol* **76**, 717-29.
- Ahn, J. H., Brignole, E. J., 3rd & Hayward, G. S. (1998). Disruption of PML subnuclear domains by the acidic IE1 protein of human cytomegalovirus is mediated through interaction with PML and may modulate a RING finger-dependent cryptic transactivator function of PML. *Mol Cell Biol* **18**, 4899-913.
- Ahn, J. H. & Hayward, G. S. (1997). The major immediate-early proteins IE1 and IE2 of human cytomegalovirus colocalize with and disrupt PML-associated nuclear bodies at very early times in infected permissive cells. *J Virol* **71**, 4599-613.
- Ahn, J. H. & Hayward, G. S. (2000). Disruption of PML-associated nuclear bodies by IE1 correlates with efficient early stages of viral gene expression and DNA replication in human cytomegalovirus infection. *Virology* **274**, 39-55.
- Ahn, J. H., Xu, Y., Jang, W. J., Matunis, M. J. & Hayward, G. S. (2001). Evaluation of interactions of human cytomegalovirus immediate-early IE2 regulatory protein with small ubiquitin-like modifiers and their conjugation enzyme Ubc9. *J Virol* **75**, 3859-72.
- Amelio, A. L., Giordani, N. V., Kubat, N. J., O'Neil, J. E. & Bloom, D. C. (2006a). Deacetylation of the herpes simplex virus type 1 latency-associated transcript (LAT) enhancer and a decrease in LAT abundance precede an increase in ICP0 transcriptional permissiveness at early times postexplant. *J Virol* **80**, 2063-8.
- Amelio, A. L., McAnany, P. K. & Bloom, D. C. (2006b). A chromatin insulator-like element in the herpes simplex virus type 1 latency-associated transcript region binds CCCTC-binding factor and displays enhancer-blocking and silencing activities. *J Virol* **80**, 2358-68.
- Anders, D. G., Kacica, M. A., Pari, G. & Punturieri, S. M. (1992). Boundaries and structure of human cytomegalovirus oriLyt, a complex origin for lytic-phase DNA replication. *J Virol* **66**, 3373-84.
- Anders, D. G. & Punturieri, S. M. (1991). Multicomponent origin of cytomegalovirus lytic-phase DNA replication. *J Virol* **65**, 931-7.
- Arthur, J. L., Scarpini, C. G., Connor, V., Lachmann, R. H., Tolkovsky, A. M. & Efstathiou, S. (2001). Herpes simplex virus type 1 promoter activity during

- latency establishment, maintenance, and reactivation in primary dorsal root neurons in vitro. *J Virol* **75**, 3885-95.
- Ascoli, C. A. & Maul, G. G. (1991). Identification of a novel nuclear domain. *J Cell Biol* **112**, 785-95.
- AuCoin, D. P., Smith, G. B., Meiring, C. D. & Mocarski, E. S. (2006). Betaherpesvirus-conserved cytomegalovirus tegument protein ppUL32 (pp150) controls cytoplasmic events during virion maturation. *J Virol* **80**, 8199-210.
- Awasthi, S., Isler, J. A. & Alwine, J. C. (2004). Analysis of splice variants of the immediate-early 1 region of human cytomegalovirus. *J Virol* **78**, 8191-200.
- Baldick, C. J., Jr., Marchini, A., Patterson, C. E. & Shenk, T. (1997). Human cytomegalovirus tegument protein pp71 (ppUL82) enhances the infectivity of viral DNA and accelerates the infectious cycle. *J Virol* **71**, 4400-8.
- Barry, P. A., Alcendor, D. J., Power, M. D., Kerr, H. & Luciw, P. A. (1996). Nucleotide sequence and molecular analysis of the rhesus cytomegalovirus immediate-early gene and the UL121-117 open reading frames. *Virology* **215**, 61-72.
- Baskin, G. B. (1987). Disseminated cytomegalovirus infection in immunodeficient rhesus monkeys. *Am J Pathol* **129**, 345-52.
- Batchelor, A. H., Wilcox, K. W. & O'Hare, P. (1994). Binding and repression of the latency-associated promoter of herpes simplex virus by the immediate early 175K protein. *J Gen Virol* **75**, 753-67.
- Baxter, M. K. & Gibson, W. (2001). Cytomegalovirus basic phosphoprotein (pUL32) binds to capsids in vitro through its amino one-third. *J Virol* **75**, 6865-73.
- Becker, Y., Dym, H. & Sarov, I. (1968). Herpes simplex virus DNA. *Virology* **36**, 184-92.
- Bego, M., Maciejewski, J., Khaiboullina, S., Pari, G. & St Jeor, S. (2005). Characterization of an antisense transcript spanning the UL81-82 locus of human cytomegalovirus. *J Virol* **79**, 11022-34.
- Berger, S. L. (2002). Histone modifications in transcriptional regulation. *Curr Opin Genet Dev* **12**, 142-8.
- Bernardi, R. & Pandolfi, P. P. (2003). Role of PML and the PML-nuclear body in the control of programmed cell death. *Oncogene* **22**, 9048-57.
- Bhella, D., Rixon, F. J. & Dargan, D. J. (2000). Cryomicroscopy of human cytomegalovirus virions reveals more densely packed genomic DNA than in herpes simplex virus type 1. *J Mol Biol* **295**, 155-61.
- Blewett, E. L., Black, D. H., Lerche, N. W., White, G. & Eberle, R. (2000). Simian foamy virus infections in a baboon breeding colony. *Virology* **278**, 183-93.
- Blewett, E. L., White, G., Saliki, J. T. & Eberle, R. (2001). Isolation and characterization of an endogenous cytomegalovirus (BaCMV) from baboons. *Arch Virol* **146**, 1723-38.
- Boehmer, P. E. & Lehman, I. R. (1997). Herpes simplex virus DNA replication. *Annu Rev Biochem* **66**, 347-84.
- Bogner, E., Reschke, M., Reis, B., Reis, E., Britt, W. & Radsak, K. (1992). Recognition of compartmentalized intracellular analogs of glycoprotein H of human cytomegalovirus. *Arch Virol* **126**, 67-80.
- Bold, S., Ohlin, M., Garten, W. & Radsak, K. (1996). Structural domains involved in human cytomegalovirus glycoprotein B-mediated cell-cell fusion. *J Gen Virol* **77**, 2297-302.
- Booy, F. P., Newcomb, W. W., Trus, B. L., Brown, J. C., Baker, T. S. & Steven, A. C. (1991). Liquid-crystalline, phage-like packing of encapsidated DNA in herpes simplex virus. *Cell* **64**, 1007-15.

- Boppana, S. B., Pass, R. F., Britt, W. J., Stagno, S. & Alford, C. A. (1992). Symptomatic congenital cytomegalovirus infection: neonatal morbidity and mortality. *Pediatr Infect Dis J* **11**, 93-9.
- Borst, E. M., Mathys, S., Wagner, M., Muranyi, W. & Messerle, M. (2001). Genetic evidence of an essential role for cytomegalovirus small capsid protein in viral growth. *J Virol* **75**, 1450-8.
- Boshart, M., Weber, F., Jahn, G., Dorsch-Hasler, K., Fleckenstein, B. & Schaffner, W. (1985). A very strong enhancer is located upstream of an immediate early gene of human cytomegalovirus. *Cell* **41**, 521-30.
- Boutell, C., Canning, M., Orr, A. & Everett, R. D. (2005). Reciprocal activities between herpes simplex virus type 1 regulatory protein ICP0, a ubiquitin E3 ligase, and ubiquitin-specific protease USP7. *J Virol* **79**, 12342-54.
- Boutell, C. & Everett, R. D. (2003). The herpes simplex virus type 1 (HSV-1) regulatory protein ICP0 interacts with and Ubiquitinates p53. *J Biol Chem* **278**, 36596-602.
- Boutell, C., Orr, A. & Everett, R. D. (2003). PML residue lysine 160 is required for the degradation of PML induced by herpes simplex virus type 1 regulatory protein ICP0. *J Virol* **77**, 8686-94.
- Boutell, C., Sadis, S. & Everett, R. D. (2002). Herpes simplex virus type 1 immediate-early protein ICP0 and its isolated RING finger domain act as ubiquitin E3 ligases in vitro. *J Virol* **76**, 841-50.
- Bresnahan, W. A. & Shenk, T. E. (2000). UL82 virion protein activates expression of immediate early viral genes in human cytomegalovirus-infected cells. *Proc Natl Acad Sci U S A* **97**, 14506-11.
- Burgos, J. S., Serrano-Saiz, E., Sastre, I. & Valdivieso, F. (2006). ICP47 mediates viral neuroinvasiveness by induction of TAP protein following intravenous inoculation of herpes simplex virus type 1 in mice. *J Neurovirol* **12**, 420-7.
- Buser, C., Walther, P., Mertens, T. & Michel, D. (2007). Cytomegalovirus primary envelopment occurs at large infoldings of the inner nuclear membrane. *J Virol* **81**, 3042-8.
- Butcher, S. J., Aitken, J., Mitchell, J., Gowen, B. & Dargan, D. J. (1998). Structure of the human cytomegalovirus B capsid by electron cryomicroscopy and image reconstruction. *J Struct Biol* **124**, 70-6.
- Cai, W. & Schaffer, P. A. (1992). Herpes simplex virus type 1 ICP0 regulates expression of immediate-early, early, and late genes in productively infected cells. *J Virol* **66**, 2904-15.
- Canning, M., Boutell, C., Parkinson, J. & Everett, R. D. (2004). A RING finger ubiquitin ligase is protected from autocatalyzed ubiquitination and degradation by binding to ubiquitin-specific protease USP7. *J Biol Chem* **279**, 38160-8.
- Cantrell, S. R. & Bresnahan, W. A. (2005). Interaction between the human cytomegalovirus UL82 gene product (pp71) and hDaxx regulates immediate-early gene expression and viral replication. *J Virol* **79**, 7792-802.
- Cantrell, S. R. & Bresnahan, W. A. (2006). Human cytomegalovirus (HCMV) UL82 gene product (pp71) relieves hDaxx-mediated repression of HCMV replication. *J Virol* **80**, 6188-91.
- Casaday, R. J., Bailey, J. R., Kalb, S. R., Brignole, E. J., Loveland, A. N., Cotter, R. J. & Gibson, W. (2004). Assembly protein precursor (pUL80.5 homolog) of simian cytomegalovirus is phosphorylated at a glycogen synthase kinase 3 site and its downstream "priming" site: phosphorylation affects interactions of protein with itself and with major capsid protein. *J Virol* **78**, 13501-11.
- Castillo, J. P. & Kowalik, T. F. (2002). Human cytomegalovirus immediate early proteins and cell growth control. *Gene* **290**, 19-34.

- Cha, T. A., Tom, E., Kemble, G. W., Duke, G. M., Mocarski, E. S. & Spaete, R. R. (1996). Human cytomegalovirus clinical isolates carry at least 19 genes not found in laboratory strains. *J Virol* **70**, 78-83.
- Challberg, M. D. (1986). A method for identifying the viral genes required for herpesvirus DNA replication. *Proc Natl Acad Sci U S A* **83**, 9094-8.
- Chambers, J., Angulo, A., Amaratunga, D., Guo, H., Jiang, Y., Wan, J. S., Bittner, A., Frueh, K., Jackson, M. R., Peterson, P. A., Erlander, M. G. & Ghazal, P. (1999). DNA microarrays of the complex human cytomegalovirus genome: profiling kinetic class with drug sensitivity of viral gene expression. *J Virol* **73**, 5757-66.
- Champier, G., Hantz, S., Couvreur, A., Stuppfler, S., Mazon, M. C., Bouaziz, S., Denis, F. & Alain, S. (2007). New functional domains of human cytomegalovirus pUL89 predicted by sequence analysis and three-dimensional modelling of the catalytic site DEXDc. *Antivir Ther* **12**, 217-32.
- Chang, H. Y., Yang, X. & Baltimore, D. (1999). Dissecting Fas signaling with an altered-specificity death-domain mutant: requirement of FADD binding for apoptosis but not Jun N-terminal kinase activation. *Proc Natl Acad Sci U S A* **96**, 1252-6.
- Chau, N. H., Vanson, C. D. & Kerry, J. A. (1999). Transcriptional regulation of the human cytomegalovirus US11 early gene. *J Virol* **73**, 863-70.
- Chee, M. S., Bankier, A. T., Beck, S., Bohni, R., Brown, C. M., Cerny, R., Horsnell, T., Hutchison, C. A., 3rd, Kouzarides, T., Martignetti, J. A. & et al. (1990). Analysis of the protein-coding content of the sequence of human cytomegalovirus strain AD169. *Curr Top Microbiol Immunol* **154**, 125-69.
- Chen, D. H., Jiang, H., Lee, M., Liu, F. & Zhou, Z. H. (1999). Three-dimensional visualization of tegument/capsid interactions in the intact human cytomegalovirus. *Virology* **260**, 10-6.
- Chen, J. & Silverstein, S. (1992). Herpes simplex viruses with mutations in the gene encoding ICP0 are defective in gene expression. *J Virol* **66**, 2916-27.
- Cherrington, J. M. & Mocarski, E. S. (1989). Human cytomegalovirus ie1 transactivates the alpha promoter-enhancer via an 18-base-pair repeat element. *J Virol* **63**, 1435-40.
- Choi, K. S., Kim, S. J. & Kim, S. (1995). The retinoblastoma gene product negatively regulates transcriptional activation mediated by the human cytomegalovirus IE2 protein. *Virology* **208**, 450-6.
- Cirone, M., Campadelli-Fiume, G., Foa-Tomasi, L., Torrisi, M. R. & Faggioni, A. (1994). Human herpesvirus 6 envelope glycoproteins B and H-L complex are undetectable on the plasma membrane of infected lymphocytes. *AIDS Res Hum Retroviruses* **10**, 175-9.
- Compton, T., Nepomuceno, R. R. & Nowlin, D. M. (1992). Human cytomegalovirus penetrates host cells by pH-independent fusion at the cell surface. *Virology* **191**, 387-95.
- Dai-Ju, J. Q., Li, L., Johnson, L. A. & Sandri-Goldin, R. M. (2006). ICP27 interacts with the C-terminal domain of RNA polymerase II and facilitates its recruitment to herpes simplex virus 1 transcription sites, where it undergoes proteasomal degradation during infection. *J Virol* **80**, 3567-81.
- Dargan, D. J., Jamieson, F. E., MacLean, J., Dolan, A., Addison, C. & McGeoch, D. J. (1997). The published DNA sequence of human cytomegalovirus strain AD169 lacks 929 base pairs affecting genes UL42 and UL43. *J Virol* **71**, 9833-6.
- Davison, A. J., Akter, P., Cunningham, C., Dolan, A., Addison, C., Dargan, D. J., Hassan-Walker, A. F., Emery, V. C., Griffiths, P. D. & Wilkinson, G. W. (2003b). Homology between the human cytomegalovirus RL11 gene family and human adenovirus E3 genes. *J Gen Virol* **84**, 657-63.

- Davison, A. J., Dolan, A., Akter, P., Addison, C., Dargan, D. J., Alcendor, D. J., McGeoch, D. J. & Hayward, G. S. (2003a). The human cytomegalovirus genome revisited: comparison with the chimpanzee cytomegalovirus genome. *J Gen Virol* **84**, 17-28.
- Davison, A. J. & Wilkie, N. M. (1981). Nucleotide sequences of the joint between the L and S segments of herpes simplex virus types 1 and 2. *J Gen Virol* **55**, 315-31.
- Dellaire, G., Ching, R. W., Dehghani, H., Ren, Y. & Bazett-Jones, D. P. (2006). The number of PML nuclear bodies increases in early S phase by a fission mechanism. *J Cell Sci* **119**, 1026-33.
- Depto, A. S. & Stenberg, R. M. (1992). Functional analysis of the true late human cytomegalovirus pp28 upstream promoter: cis-acting elements and viral trans-acting proteins necessary for promoter activation. *J Virol* **66**, 3241-6.
- Deshmane, S. L. & Fraser, N. W. (1989). During latency, herpes simplex virus type 1 DNA is associated with nucleosomes in a chromatin structure. *J Virol* **63**, 943-7.
- Dittmer, A. & Bogner, E. (2005). Analysis of the quaternary structure of the putative HCMV portal protein PUL104. *Biochemistry* **44**, 759-65.
- Dittmer, D. & Mocarski, E. S. (1997). Human cytomegalovirus infection inhibits G1/S transition. *J Virol* **71**, 1629-34.
- Dohner, K., Wolfstein, A., Prank, U., Echeverri, C., Dujardin, D., Vallee, R. & Sodeik, B. (2002). Function of dynein and dynactin in herpes simplex virus capsid transport. *Mol Biol Cell* **13**, 2795-809.
- Dolan, A., Cunningham, C., Hector, R. D., Hassan-Walker, A. F., Lee, L., Addison, C., Dargan, D. J., McGeoch, D. J., Gatherer, D., Emery, V. C., Griffiths, P. D., Sinzger, C., McSharry, B. P., Wilkinson, G. W. & Davison, A. J. (2004). Genetic content of wild-type human cytomegalovirus. *J Gen Virol* **85**, 1301-12.
- Dolan, A., Jamieson, F. E., Cunningham, C., Barnett, B. C. & McGeoch, D. J. (1998). The genome sequence of herpes simplex virus type 2. *J Virol* **72**, 2010-21.
- Dyck, J. A., Maul, G. G., Miller, W. H., Jr., Chen, J. D., Kakizuka, A. & Evans, R. M. (1994). A novel macromolecular structure is a target of the promyelocyte-retinoic acid receptor oncoprotein. *Cell* **76**, 333-43.
- Efstathiou, S. & Preston, C. M. (2005). Towards an understanding of the molecular basis of herpes simplex virus latency. *Virus Res* **111**, 108-19.
- Everett, R. D. (1988). Analysis of the functional domains of herpes simplex virus type 1 immediate-early polypeptide Vmw110. *J Mol Biol* **202**, 87-96.
- Everett, R. D. (2000). ICP0, a regulator of herpes simplex virus during lytic and latent infection. *Bioessays* **22**, 761-70.
- Everett, R. D., Boutell, C. & Orr, A. (2004a). Phenotype of a herpes simplex virus type 1 mutant that fails to express immediate-early regulatory protein ICP0. *J Virol* **78**, 1763-74.
- Everett, R. D., Earnshaw, W. C., Findlay, J. & Lomonte, P. (1999a). Specific destruction of kinetochore protein CENP-C and disruption of cell division by herpes simplex virus immediate-early protein Vmw110. *Embo J* **18**, 1526-38.
- Everett, R. D., Freemont, P., Saitoh, H., Dasso, M., Orr, A., Kathoria, M. & Parkinson, J. (1998a). The disruption of ND10 during herpes simplex virus infection correlates with the Vmw110- and proteasome-dependent loss of several PML isoforms. *J Virol* **72**, 6581-91.
- Everett, R. D., Lomonte, P., Sternsdorf, T., van Driel, R. & Orr, A. (1999b). Cell cycle regulation of PML modification and ND10 composition. *J Cell Sci* **112**, 4581-8.

- Everett, R. D. & Maul, G. G. (1994). HSV-1 IE protein Vmw110 causes redistribution of PML. *Embo J* **13**, 5062-9.
- Everett, R. D., Meredith, M. & Orr, A. (1998b). The ability of herpes simplex virus type 1 immediate-early protein Vmw110 to bind to a ubiquitin-specific protease contributes to its roles in the activation of gene expression and stimulation of virus replication. *J Virol* **73**, 417-26.
- Everett, R. D., Meredith, M., Orr, A., Cross, A., Kathoria, M. & Parkinson, J. (1997). A novel ubiquitin-specific protease is dynamically associated with the PML nuclear domain and binds to a herpesvirus regulatory protein. *Embo J* **16**, 1519-30.
- Everett, R. D. & Murray, J. (2005). ND10 components relocate to sites associated with herpes simplex virus type 1 nucleoprotein complexes during virus infection. *J Virol* **79**, 5078-89.
- Everett, R. D., Orr, A. & Elliott, M. (1991). High level expression and purification of herpes simplex virus type 1 immediate early polypeptide Vmw110. *Nucleic Acids Res* **19**, 6155-61.
- Everett, R. D., Rechter, S., Papior, P., Tavalai, N., Stamminger, T. & Orr, A. (2006). PML contributes to a cellular mechanism of repression of herpes simplex virus type 1 infection that is inactivated by ICP0. *J Virol* **80**, 7995-8005.
- Everett, R. D., Sourvinos, G., Leiper, C., Clements, J. B. & Orr, A. (2004b). Formation of nuclear foci of the herpes simplex virus type 1 regulatory protein ICP4 at early times of infection: localization, dynamics, recruitment of ICP27, and evidence for the de novo induction of ND10-like complexes. *J Virol* **78**, 1903-17.
- Fagioli, M., Alcalay, M., Pandolfi, P. P., Venturini, L., Mencarelli, A., Simeone, A., Acampora, D., Grignani, F. & Pelicci, P. G. (1992). Alternative splicing of PML transcripts predicts coexpression of several carboxy-terminally different protein isoforms. *Oncogene* **7**, 1083-91.
- Farrell, M. J., Dobson, A. T. & Feldman, L. T. (1991). Herpes simplex virus latency-associated transcript is a stable intron. *Proc Natl Acad Sci U S A* **88**, 790-4.
- Fisher, S., Genbacev, O., Maidji, E. & Pereira, L. (2000). Human cytomegalovirus infection of placental cytotrophoblasts in vitro and in utero: implications for transmission and pathogenesis. *J Virol* **74**, 6808-20.
- Flint, J. & Shenk, T. (1997). Viral transactivating proteins. *Annu Rev Genet* **31**, 177-212.
- Fogal, V., Gostissa, M., Sandy, P., Zacchi, P., Sternsdorf, T., Jensen, K., Pandolfi, P. P., Will, H., Schneider, C. & Del Sal, G. (2000). Regulation of p53 activity in nuclear bodies by a specific PML isoform. *Embo J* **19**, 6185-95.
- French, J. D., Dunn, J., Smart, C. E., Manning, N. & Brown, M. A. (2006). Disruption of BRCA1 function results in telomere lengthening and increased anaphase bridge formation in immortalized cell lines. *Genes Chromosomes Cancer* **45**, 277-89.
- Gandhi, M. K. & Khanna, R. (2004). Human cytomegalovirus: clinical aspects, immune regulation, and emerging treatments. *Lancet Infect Dis* **4**, 725-38.
- Garner, J. A. (2003). Herpes simplex virion entry into and intracellular transport within mammalian cells. *Adv Drug Deliv Rev* **55**, 1497-513.
- Gawn, J. M. & Greaves, R. F. (2002). Absence of IE1 p72 protein function during low-multiplicity infection by human cytomegalovirus results in a broad block to viral delayed-early gene expression. *J Virol* **76**, 4441-55.
- Ghazal, P., DeMattei, C., Giulietti, E., Kliwer, S. A., Umesono, K. & Evans, R. M. (1992). Retinoic acid receptors initiate induction of the cytomegalovirus enhancer in embryonal cells. *Proc Natl Acad Sci U S A* **89**, 7630-4.

- Ghazal, P., Lubon, H., Fleckenstein, B. & Hennighausen, L. (1987). Binding of transcription factors and creation of a large nucleoprotein complex on the human cytomegalovirus enhancer. *Proc Natl Acad Sci U S A* **84**, 3658-62.
- Ghazal, P., Lubon, H. & Hennighausen, L. (1988). Specific interactions between transcription factors and the promoter-regulatory region of the human cytomegalovirus major immediate-early gene. *J Virol* **62**, 1076-9.
- Gibson, W. (1981). Structural and nonstructural proteins of strain Colburn cytomegalovirus. *Virology* **111**, 516-37.
- Gibson, W., Clopper, K. S., Britt, W. J. & Baxter, M. K. (1996). Human cytomegalovirus (HCMV) smallest capsid protein identified as product of short open reading frame located between HCMV UL48 and UL49. *J Virol* **70**, 5680-3.
- Glickman, M. H. & Ciechanover, A. (2002). The ubiquitin-proteasome proteolytic pathway: destruction for the sake of construction. *Physiol Rev* **82**, 373-428.
- Gonelli, A., Boccia, S., Boni, M., Pozzoli, A., Rizzo, C., Querzoli, P., Cassai, E. & Di Luca, D. (2001). Human herpesvirus 7 is latent in gastric mucosa. *J Med Virol* **63**, 277-83.
- Goodrum, F. D., Jordan, C. T., High, K. & Shenk, T. (2002). Human cytomegalovirus gene expression during infection of primary hematopoietic progenitor cells: a model for latency. *Proc Natl Acad Sci U S A* **99**, 16255-60.
- Granzow, H., Klupp, B. G. & Mettenleiter, T. C. (2005). Entry of pseudorabies virus: an immunogold-labeling study. *J Virol* **79**, 3200-5.
- Greaves, R. F. & Mocarski, E. S. (1998). Defective growth correlates with reduced accumulation of a viral DNA replication protein after low-multiplicity infection by a human cytomegalovirus ie1 mutant. *J Virol* **72**, 366-79.
- Gretch, D. R., Kari, B., Rasmussen, L., Gehrz, R. C. & Stinski, M. F. (1988). Identification and characterization of three distinct families of glycoprotein complexes in the envelopes of human cytomegalovirus. *J Virol* **62**, 875-81.
- Griffiths, P. D. & Baboonian, C. (1984). A prospective study of primary cytomegalovirus infection during pregnancy: final report. *Br J Obstet Gynaecol* **91**, 307-15.
- Grondin, B. & DeLuca, N. (2000). Herpes simplex virus type 1 ICP4 promotes transcription preinitiation complex formation by enhancing the binding of TFIID to DNA. *J Virol* **74**, 11504-10.
- Groves, I. J. & Sinclair, J. H. (2007). Knockdown of hDaxx in normally non-permissive undifferentiated cells does not permit human cytomegalovirus immediate-early gene expression. *J Gen Virol* **88**, 2935-40.
- Gu, B., Kuddus, R. & DeLuca, N. A. (1995). Repression of activator-mediated transcription by herpes simplex virus ICP4 via a mechanism involving interactions with the basal transcription factors TATA-binding protein and TFIIB. *Mol Cell Biol* **15**, 3618-26.
- Gussow, A. M., Giordani, N. V., Tran, R. K., Imai, Y., Kwiatkowski, D. L., Rall, G. F., Margolis, T. P. & Bloom, D. C. (2006). Tissue-specific splicing of the herpes simplex virus type 1 latency-associated transcript (LAT) intron in LAT transgenic mice. *J Virol* **80**, 9414-23.
- Hagemeier, C., Caswell, R., Hayhurst, G., Sinclair, J. & Kouzarides, T. (1994). Functional interaction between the HCMV IE2 transactivator and the retinoblastoma protein. *Embo J* **13**, 2897-903.
- Halford, W. P., Kemp, C. D., Isler, J. A., Davido, D. J. & Schaffer, P. A. (2001). ICP0, ICP4, or VP16 expressed from adenovirus vectors induces reactivation of latent herpes simplex virus type 1 in primary cultures of latently infected trigeminal ganglion cells. *J Virol* **75**, 6143-53.

- Hamzeh, F. M., Lietman, P. S., Gibson, W. & Hayward, G. S. (1990). Identification of the lytic origin of DNA replication in human cytomegalovirus by a novel approach utilizing ganciclovir-induced chain termination. *J Virol* **64**, 6184-95.
- Hancock, M. H., Corcoran, J. A. & Smiley, J. R. (2006). Herpes simplex virus regulatory proteins VP16 and ICP0 counteract an innate intranuclear barrier to viral gene expression. *Virology* **352**, 237-52.
- Hansen, S. G., Strelow, L. I., Franchi, D. C., Anders, D. G. & Wong, S. W. (2003). Complete sequence and genomic analysis of rhesus cytomegalovirus. *J Virol* **77**, 6620-36.
- Harris, R. A., Everett, R. D., Zhu, X. X., Silverstein, S. & Preston, C. M. (1989). Herpes simplex virus type 1 immediate-early protein Vmw110 reactivates latent herpes simplex virus type 2 in an in vitro latency system. *J Virol* **63**, 3513-5.
- Harris, R. A. & Preston, C. M. (1991). Establishment of latency in vitro by the herpes simplex virus type 1 mutant in1814. *J Gen Virol* **72**, 907-13.
- He, H., Rinaldo, C. R., Jr. & Morel, P. A. (1995). T cell proliferative responses to five human cytomegalovirus proteins in healthy seropositive individuals: implications for vaccine development. *J Gen Virol* **76**, 1603-10.
- Hensel, G. M., Meyer, H. H., Buchmann, I., Pommerehne, D., Schmolke, S., Plachter, B., Radsak, K. & Kern, H. F. (1996). Intracellular localization and expression of the human cytomegalovirus matrix phosphoprotein pp71 (ppUL82): evidence for its translocation into the nucleus. *J Gen Virol* **77**, 3087-97.
- Herold, B. C., Visalli, R. J., Susmarski, N., Brandt, C. R. & Spear, P. G. (1994). Glycoprotein C-independent binding of herpes simplex virus to cells requires cell surface heparan sulphate and glycoprotein B. *J Gen Virol* **75**, 1211-22.
- Hobbs, W. E., Brough, D. E., Kovesdi, I. & DeLuca, N. A. (2001). Efficient activation of viral genomes by levels of herpes simplex virus ICP0 insufficient to affect cellular gene expression or cell survival. *J Virol* **75**, 3391-403.
- Hobom, U., Brune, W., Messerle, M., Hahn, G. & Koszinowski, U. H. (2000). Fast screening procedures for random transposon libraries of cloned herpesvirus genomes: mutational analysis of human cytomegalovirus envelope glycoprotein genes. *J Virol* **74**, 7720-9.
- Hofmann, H., Sindre, H. & Stamminger, T. (2002). Functional interaction between the pp71 protein of human cytomegalovirus and the PML-interacting protein human Daxx. *J Virol* **76**, 5769-83.
- Hollenbach, A. D., McPherson, C. J., Mientjes, E. J., Iyengar, R. & Grosveld, G. (2002). Daxx and histone deacetylase II associate with chromatin through an interaction with core histones and the chromatin-associated protein Dek. *J Cell Sci* **115**, 3319-30.
- Homer, E. G., Rinaldi, A., Nicholl, M. J. & Preston, C. M. (1999). Activation of herpesvirus gene expression by the human cytomegalovirus protein pp71. *J Virol* **73**, 8512-8.
- Homman-Loudiyi, M., Hultenby, K., Britt, W. & Soderberg-Naucler, C. (2003). Envelopment of human cytomegalovirus occurs by budding into Golgi-derived vacuole compartments positive for gB, Rab 3, trans-golgi network 46, and mannosidase II. *J Virol* **77**, 3191-203.
- Huang, L., Zhu, Y. & Anders, D. G. (1996). The variable 3' ends of a human cytomegalovirus oriLyt transcript (SRT) overlap an essential, conserved replicator element. *J Virol* **70**, 5272-81.

- Huber, M. T. & Compton, T. (1997). Characterization of a novel third member of the human cytomegalovirus glycoprotein H-glycoprotein L complex. *J Virol* **71**, 5391-8.
- Huber, M. T. & Compton, T. (1998). The human cytomegalovirus UL74 gene encodes the third component of the glycoprotein H-glycoprotein L-containing envelope complex. *J Virol* **72**, 8191-7.
- Huber, M. T. & Compton, T. (1999). Intracellular formation and processing of the heterotrimeric gH-gL-gO (gCIII) glycoprotein envelope complex of human cytomegalovirus. *J Virol* **73**, 3886-92.
- Huszar, D. & Bacchetti, S. (1981). Partial purification and characterization of the ribonucleotide reductase induced by herpes simplex virus infection of mammalian cells. *J Virol* **37**, 580-8.
- Hwang, J. & Kalejta, R. F. (2007). Proteasome-dependent, ubiquitin-independent degradation of Daxx by the viral pp71 protein in human cytomegalovirus-infected cells. *Virology* **367**, 334-8.
- Hwang, J. S. & Bogner, E. (2002). ATPase activity of the terminase subunit pUL56 of human cytomegalovirus. *J Biol Chem* **277**, 6943-8.
- Inman, M., Perng, G. C., Henderson, G., Ghiasi, H., Nesburn, A. B., Wechsler, S. L. & Jones, C. (2001). Region of herpes simplex virus type 1 latency-associated transcript sufficient for wild-type spontaneous reactivation promotes cell survival in tissue culture. *J Virol* **75**, 3636-46.
- Ishov, A. M., Sotnikov, A. G., Negorev, D., Vladimirova, O. V., Neff, N., Kamitani, T., Yeh, E. T., Strauss, J. F., 3rd & Maul, G. G. (1999). PML is critical for ND10 formation and recruits the PML-interacting protein daxx to this nuclear structure when modified by SUMO-1. *J Cell Biol* **147**, 221-34.
- Ishov, A. M., Vladimirova, O. V. & Maul, G. G. (2002). Daxx-mediated accumulation of human cytomegalovirus tegument protein pp71 at ND10 facilitates initiation of viral infection at these nuclear domains. *J Virol* **76**, 7705-12.
- Ishov, A. M., Vladimirova, O. V. & Maul, G. G. (2004). Heterochromatin and ND10 are cell-cycle regulated and phosphorylation-dependent alternate nuclear sites of the transcription repressor Daxx and SWI/SNF protein ATRX. *J Cell Sci* **117**, 3807-20.
- Isomura, H. & Stinski, M. F. (2003). The human cytomegalovirus major immediate-early enhancer determines the efficiency of immediate-early gene transcription and viral replication in permissive cells at low multiplicity of infection. *J Virol* **77**, 3602-14.
- Jamieson, D. R., Robinson, L. H., Daksis, J. I., Nicholl, M. J. & Preston, C. M. (1995). Quiescent viral genomes in human fibroblasts after infection with herpes simplex virus type 1 Vmw65 mutants. *J Gen Virol* **76**, 1417-31.
- Jarvis, M. A. & Nelson, J. A. (2002). Mechanisms of human cytomegalovirus persistence and latency. *Front Biosci* **7**, d1575-82.
- Javier, R. T., Stevens, J. G., Dissette, V. B. & Wagner, E. K. (1988). A herpes simplex virus transcript abundant in latently infected neurons is dispensable for establishment of the latent state. *Virology* **166**, 254-7.
- Jeang, K. T., Chin, G. & Hayward, G. S. (1982). Characterization of cytomegalovirus immediate-early genes. I. Nonpermissive rodent cells overproduce the IE94K protein form CMV (Colburn). *Virology* **121**, 393-403.
- Jeang, K. T., Rawlins, D. R., Rosenfeld, P. J., Shero, J. H., Kelly, T. J. & Hayward, G. S. (1987). Multiple tandemly repeated binding sites for cellular nuclear factor 1 that surround the major immediate-early promoters of simian and human cytomegalovirus. *J Virol* **61**, 1559-70.
- Jenson, H. B., Ench, Y., Gao, S. J., Rice, K., Carey, D., Kennedy, R. C., Arrand, J. R. & Mackett, M. (2000). Epidemiology of herpesvirus papio infection in a

- large captive baboon colony: similarities to Epstein-Barr virus infection in humans. *J Infect Dis* **181**, 1462-6.
- Kalejta, R. F., Bechtel, J. T. & Shenk, T. (2003a). Human cytomegalovirus pp71 stimulates cell cycle progression by inducing the proteasome-dependent degradation of the retinoblastoma family of tumor suppressors. *Mol Cell Biol* **23**, 1885-95.
- Kalejta, R. F. & Shenk, T. (2003b). The human cytomegalovirus UL82 gene product (pp71) accelerates progression through the G1 phase of the cell cycle. *J Virol* **77**, 3451-9.
- Kalejta, R. F. & Shenk, T. (2003c). Proteasome-dependent, ubiquitin-independent degradation of the Rb family of tumor suppressors by the human cytomegalovirus pp71 protein. *Proc Natl Acad Sci U S A* **100**, 3263-8.
- Kalter, S. S. & Heberling, R. L. (1990). Primate viral diseases in perspective. *J Med Primatol* **19**, 519-35.
- Kappes, F., Burger, K., Baack, M., Fackelmayer, F. O. & Gruss, C. (2001). Subcellular localization of the human proto-oncogene protein DEK. *J Biol Chem* **276**, 26317-23.
- Keil, G. M., Ebeling-Keil, A. & Koszinowski, U. H. (1984). Temporal regulation of murine cytomegalovirus transcription and mapping of viral RNA synthesized at immediate early times after infection. *J Virol* **50**, 784-95.
- Kim, S., Yu, S. S., Lee, I. S., Ohno, S., Yim, J. & Kang, H. S. (1999). Human cytomegalovirus IE1 protein activates AP-1 through a cellular protein kinase(s). *J Gen Virol* **80**, 961-9.
- Koffa, M. D., Clements, J. B., Izaurralde, E., Wadd, S., Wilson, S. A., Mattaj, I. W. & Kuersten, S. (2001). Herpes simplex virus ICP27 protein provides viral mRNAs with access to the cellular mRNA export pathway. *Embo J* **20**, 5769-78.
- Kondo, K., Xu, J. & Mocarski, E. S. (1996). Human cytomegalovirus latent gene expression in granulocyte-macrophage progenitors in culture and in seropositive individuals. *Proc Natl Acad Sci U S A* **93**, 11137-42.
- Korioth, F., Maul, G. G., Plachter, B., Stamminger, T. & Frey, J. (1996). The nuclear domain 10 (ND10) is disrupted by the human cytomegalovirus gene product IE1. *Exp Cell Res* **229**, 155-8.
- Kouzarides, T. (2002). Histone methylation in transcriptional control. *Curr Opin Genet Dev* **12**, 198-209.
- Kravitz, R. H., Sciabica, K. S., Cho, K., Luciw, P. A. & Barry, P. A. (1997). Cloning and characterization of rhesus cytomegalovirus glycoprotein B. *J Gen Virol* **78 (Pt 8)**, 2009-13.
- Kristie, T. M., Vogel, J. L. & Sears, A. E. (1999). Nuclear localization of the C1 factor (host cell factor) in sensory neurons correlates with reactivation of herpes simplex virus from latency. *Proc Natl Acad Sci U S A* **96**, 1229-33.
- Kropff, B. & Mach, M. (1997). Identification of the gene coding for rhesus cytomegalovirus glycoprotein B and immunological analysis of the protein. *J Gen Virol* **78**, 1999-2007.
- Kubat, N. J., Tran, R. K., McAnany, P. & Bloom, D. C. (2004). Specific histone tail modification and not DNA methylation is a determinant of herpes simplex virus type 1 latent gene expression. *J Virol* **78**, 1139-49.
- Kuddus, R., Gu, B. & DeLuca, N. A. (1995). Relationship between TATA-binding protein and herpes simplex virus type 1 ICP4 DNA-binding sites in complex formation and repression of transcription. *J Virol* **69**, 5568-75.
- Kuddus, R. H. & DeLuca, N. A. (2007). DNA-dependent oligomerization of herpes simplex virus type 1 regulatory protein ICP4. *J Virol* **81**, 9230-7.
- LaBoissiere, S. & O'Hare, P. (2000). Analysis of HCF, the cellular cofactor of VP16, in herpes simplex virus-infected cells. *J Virol* **74**, 99-109.

- Larralde, O., Smith, R. W., Wilkie, G. S., Malik, P., Gray, N. K. & Clements, J. B. (2006). Direct stimulation of translation by the multifunctional herpesvirus ICP27 protein. *J Virol* **80**, 1588-91.
- Larsson, S., Soderberg-Naucler, C., Wang, F. Z. & Moller, E. (1998). Cytomegalovirus DNA can be detected in peripheral blood mononuclear cells from all seropositive and most seronegative healthy blood donors over time. *Transfusion* **38**, 271-8.
- Lee, H. R., Kim, D. J., Lee, J. M., Choi, C. Y., Ahn, B. Y., Hayward, G. S. & Ahn, J. H. (2004). Ability of the human cytomegalovirus IE1 protein to modulate sumoylation of PML correlates with its functional activities in transcriptional regulation and infectivity in cultured fibroblast cells. *J Virol* **78**, 6527-42.
- Lee, J. M., Kang, H. J., Lee, H. R., Choi, C. Y., Jang, W. J. & Ahn, J. H. (2003). PIAS1 enhances SUMO-1 modification and the transactivation activity of the major immediate-early IE2 protein of human cytomegalovirus. *FEBS Lett* **555**, 322-8.
- Leuzinger, H., Ziegler, U., Schraner, E. M., Fraefel, C., Glauser, D. L., Heid, I., Ackermann, M., Mueller, M. & Wild, P. (2005). Herpes simplex virus 1 envelopment follows two diverse pathways. *J Virol* **79**, 13047-59.
- Li, H., Leo, C., Zhu, J., Wu, X., O'Neil, J., Park, E. J. & Chen, J. D. (2000a). Sequestration and inhibition of Daxx-mediated transcriptional repression by PML. *Mol Cell Biol* **20**, 1784-96.
- Li, L., Nelson, J. A. & Britt, W. J. (1997). Glycoprotein H-related complexes of human cytomegalovirus: identification of a third protein in the gCIII complex. *J Virol* **71**, 3090-7.
- Li, R., Pei, H., Watson, D. K. & Papas, T. S. (2000b). EAP1/Daxx interacts with ETS1 and represses transcriptional activation of ETS1 target genes. *Oncogene* **19**, 745-53.
- Lin, D. Y., Huang, Y. S., Jeng, J. C., Kuo, H. Y., Chang, C. C., Chao, T. T., Ho, C. C., Chen, Y. C., Lin, T. P., Fang, H. I., Hung, C. C., Suen, C. S., Hwang, M. J., Chang, K. S., Maul, G. G. & Shih, H. M. (2006). Role of SUMO-interacting motif in Daxx SUMO modification, subnuclear localization, and repression of sumoylated transcription factors. *Mol Cell* **24**, 341-54.
- Liu, B., Hermiston, T. W. & Stinski, M. F. (1991). A cis-acting element in the major immediate-early (IE) promoter of human cytomegalovirus is required for negative regulation by IE2. *J Virol* **65**, 897-903.
- Liu, B. & Stinski, M. F. (1992). Human cytomegalovirus contains a tegument protein that enhances transcription from promoters with upstream ATF and AP-1 cis-acting elements. *J Virol* **66**, 4434-44.
- Liu, R., Baillie, J., Sissons, J. G. & Sinclair, J. H. (1994). The transcription factor YY1 binds to negative regulatory elements in the human cytomegalovirus major immediate early enhancer/promoter and mediates repression in non-permissive cells. *Nucleic Acids Res* **22**, 2453-9.
- Liu, Y. & Biegelke, B. J. (2002). The human cytomegalovirus UL35 gene encodes two proteins with different functions. *J Virol* **76**, 2460-8.
- Lomonte, P., Sullivan, K. F. & Everett, R. D. (2001). Degradation of nucleosome-associated centromeric histone H3-like protein CENP-A induced by herpes simplex virus type 1 protein ICP0. *J Biol Chem* **276**, 5829-35.
- Lundquist, C. A., Meier, J. L. & Stinski, M. F. (1999). A strong negative transcriptional regulatory region between the human cytomegalovirus UL127 gene and the major immediate-early enhancer. *J Virol* **73**, 9039-52.
- Lurain, N. S., Fox, A. M., Lichy, H. M., Bhorade, S. M., Ware, C. F., Huang, D. D., Kwan, S. P., Garrity, E. R. & Chou, S. (2006). Analysis of the human cytomegalovirus genomic region from UL146 through UL147A reveals

- sequence hypervariability, genotypic stability, and overlapping transcripts. *Virology* **3**, 4.
- Mach, M., Kropff, B., Dal Monte, P. & Britt, W. (2000). Complex formation by human cytomegalovirus glycoproteins M (gpUL100) and N (gpUL73). *J Virol* **74**, 11881-92.
- Mach, M., Osinski, K., Kropff, B., Schloetzer-Schrehardt, U., Krzyzaniak, M. & Britt, W. (2007). The carboxy-terminal domain of glycoprotein N of human cytomegalovirus is required for virion morphogenesis. *J Virol* **81**, 5212-24.
- Malm, G. & Engman, M. L. (2007). Congenital cytomegalovirus infections. *Semin Fetal Neonatal Med* **12**, 154-9.
- Marchini, A., Liu, H. & Zhu, H. (2001). Human cytomegalovirus with IE-2 (UL122) deleted fails to express early lytic genes. *J Virol* **75**, 1870-8.
- Margolis, T. P., Sedarati, F., Dobson, A. T., Feldman, L. T. & Stevens, J. G. (1992). Pathways of viral gene expression during acute neuronal infection with HSV-1. *Virology* **189**, 150-60.
- Marshall, K. R., Lachmann, R. H., Efstathiou, S., Rinaldi, A. & Preston, C. M. (2000). Long-term transgene expression in mice infected with a herpes simplex virus type 1 mutant severely impaired for immediate-early gene expression. *J Virol* **74**, 956-64.
- Marshall, K. R., Rowley, K. V., Rinaldi, A., Nicholson, I. P., Ishov, A. M., Maul, G. G. & Preston, C. M. (2002). Activity and intracellular localization of the human cytomegalovirus protein pp71. *J Gen Virol* **83**, 1601-12.
- Masse, M. J., Karlin, S., Schachtel, G. A. & Mocarski, E. S. (1992). Human cytomegalovirus origin of DNA replication (oriLyt) resides within a highly complex repetitive region. *Proc Natl Acad Sci U S A* **89**, 5246-50.
- Maul, G. G. & Everett, R. D. (1994). The nuclear location of PML, a cellular member of the C3HC4 zinc-binding domain protein family, is rearranged during herpes simplex virus infection by the C3HC4 viral protein ICP0. *J Gen Virol* **75**, 1223-33.
- Maul, G. G., Negorev, D., Bell, P. & Ishov, A. M. (2000). Review: properties and assembly mechanisms of ND10, PML bodies, or PODs. *J Struct Biol* **129**, 278-87.
- McGeoch, D. J., Dalrymple, M. A., Davison, A. J., Dolan, A., Frame, M. C., McNab, D., Perry, L. J., Scott, J. E. & Taylor, P. (1988). The complete DNA sequence of the long unique region in the genome of herpes simplex virus type 1. *J Gen Virol* **69**, 1531-74.
- McGeoch, D. J., Dolan, A., Donald, S. & Rixon, F. J. (1985). Sequence determination and genetic content of the short unique region in the genome of herpes simplex virus type 1. *J Mol Biol* **181**, 1-13.
- McLauchlan, J. & Rixon, F. J. (1992). Characterization of enveloped tegument structures (L particles) produced by alphaherpesviruses: integrity of the tegument does not depend on the presence of capsid or envelope. *J Gen Virol* **73**, 269-76.
- Meier, J. L. & Pruessner, J. A. (2000). The human cytomegalovirus major immediate-early distal enhancer region is required for efficient viral replication and immediate-early gene expression. *J Virol* **74**, 1602-13.
- Meier, J. L. & Stinski, M. F. (1996). Regulation of human cytomegalovirus immediate-early gene expression. *Intervirology* **39**, 331-42.
- Meier, J. L. & Stinski, M. F. (1997). Effect of a modulator deletion on transcription of the human cytomegalovirus major immediate-early genes in infected undifferentiated and differentiated cells. *J Virol* **71**, 1246-55.
- Mendelson, M., Monard, S., Sissons, P. & Sinclair, J. (1996). Detection of endogenous human cytomegalovirus in CD34+ bone marrow progenitors. *J Gen Virol* **77**, 3099-102.

- Meredith, M., Orr, A., Elliott, M. & Everett, R. (1995). Separation of sequence requirements for HSV-1 Vmw110 multimerisation and interaction with a 135-kDa cellular protein. *Virology* **209**, 174-87.
- Meredith, M., Orr, A. & Everett, R. (1994). Herpes simplex virus type 1 immediate-early protein Vmw110 binds strongly and specifically to a 135-kDa cellular protein. *Virology* **200**, 457-69.
- Mettenleiter, T. C. (2002). Herpesvirus assembly and egress. *J Virol* **76**, 1537-47.
- Mettenleiter, T. C. (2004). Budding events in herpesvirus morphogenesis. *Virus Res* **106**, 167-80.
- Michaels, M. G., Jenkins, F. J., St George, K., Nalesnik, M. A., Starzl, T. E. & Rinaldo, C. R., Jr. (2001). Detection of infectious baboon cytomegalovirus after baboon-to-human liver xenotransplantation. *J Virol* **75**, 2825-8.
- Miller-Kittrell, M., Sai, J., Penfold, M., Richmond, A. & Sparer, T. E. (2007). Functional characterization of chimpanzee cytomegalovirus chemokine, vCXCL-1(CCMV). *Virology* **364**, 454-65.
- Mocarski, E. S., and Courcelle C.T (2001). Cytomegaloviruses and their replication". In *Fields Virology*, 4th edn, pp. 2447-91. *Fields Virology*, 4th edn. Edited by Knipe.D.M Lippincott-Williams & Wilkins Publishers. Philadelphia.
- Mostoufi-zadeh, M., Driscoll, S. G., Bianco, S. A. & Kundsins, R. B. (1984). Placental evidence of cytomegalovirus infection of the fetus and neonate. *Arch Pathol Lab Med* **108**, 403-6.
- Mueller, N. J. & Fishman, J. A. (2004). Herpesvirus infections in xenotransplantation: pathogenesis and approaches. *Xenotransplantation* **11**, 486-90.
- Murchie, M. J. & McGeoch, D. J. (1982). DNA sequence analysis of an immediate-early gene region of the herpes simplex virus type 1 genome (map coordinates 0.950 to 0.978). *J Gen Virol* **62**, 1-15.
- Murphy, E., Rigoutsos, I., Shibuya, T. & Shenk, T. E. (2003a). Reevaluation of human cytomegalovirus coding potential. *Proc Natl Acad Sci U S A* **100**, 13585-90.
- Murphy, E., Yu, D., Grimwood, J., Schmutz, J., Dickson, M., Jarvis, M. A., Hahn, G., Nelson, J. A., Myers, R. M. & Shenk, T. E. (2003b). Coding potential of laboratory and clinical strains of human cytomegalovirus. *Proc Natl Acad Sci U S A* **100**, 14976-81.
- Murphy, J. C., Fischle, W., Verdin, E. & Sinclair, J. H. (2002). Control of cytomegalovirus lytic gene expression by histone acetylation. *Embo J* **21**, 1112-20.
- Navarro, D., Paz, P., Tugizov, S., Topp, K., La Vail, J. & Pereira, L. (1993). Glycoprotein B of human cytomegalovirus promotes virion penetration into cells, transmission of infection from cell to cell, and fusion of infected cells. *Virology* **197**, 143-58.
- Negorev, D. & Maul, G. G. (2001). Cellular proteins localized at and interacting within ND10/PML nuclear bodies/PODs suggest functions of a nuclear depot. *Oncogene* **20**, 7234-42.
- Nevels, M., Brune, W. & Shenk, T. (2004a). SUMOylation of the human cytomegalovirus 72-kilodalton IE1 protein facilitates expression of the 86-kilodalton IE2 protein and promotes viral replication. *J Virol* **78**, 7803-12.
- Nevels, M., Paulus, C. & Shenk, T. (2004b). Human cytomegalovirus immediate-early 1 protein facilitates viral replication by antagonizing histone deacetylation. *Proc Natl Acad Sci U S A* **101**, 17234-9.
- Newcomb, W. W., Homa, F. L. & Brown, J. C. (2005). Involvement of the portal at an early step in herpes simplex virus capsid assembly. *J Virol* **79**, 10540-6.

- Newcomb, W. W., Homa, F. L. & Brown, J. C. (2006). Herpes simplex virus capsid structure: DNA packaging protein UL25 is located on the external surface of the capsid near the vertices. *J Virol* **80**, 6286-94.
- Newcomb, W. W., Thomsen, D. R., Homa, F. L. & Brown, J. C. (2003). Assembly of the herpes simplex virus capsid: identification of soluble scaffold-portal complexes and their role in formation of portal-containing capsids. *J Virol* **77**, 9862-71.
- Nicholl, M. J. & Preston, C. M. (1996). Inhibition of herpes simplex virus type 1 immediate-early gene expression by alpha interferon is not VP16 specific. *J Virol* **70**, 6336-9.
- Nicholson, I. P. (2004). Characterisation of two homologues of the human cytomegalovirus transactivating protein pp71. In *MRC Virology Unit*. Glasgow: University of Glasgow.
- Nixon, D. E. & McVoy, M. A. (2002). Terminally repeated sequences on a herpesvirus genome are deleted following circularization but are reconstituted by duplication during cleavage and packaging of concatemeric DNA. *J Virol* **76**, 2009-13.
- Nowak, B., Sullivan, C., Sarnow, P., Thomas, R., Bricout, F., Nicolas, J. C., Fleckenstein, B. & Levine, A. J. (1984). Characterization of monoclonal antibodies and polyclonal immune sera directed against human cytomegalovirus virion proteins. *Virology* **132**, 325-38.
- Ogawa-Goto, K., Tanaka, K., Gibson, W., Moriishi, E., Miura, Y., Kurata, T., Irie, S. & Sata, T. (2003). Microtubule network facilitates nuclear targeting of human cytomegalovirus capsid. *J Virol* **77**, 8541-7.
- Ojala, P. M., Sodeik, B., Ebersold, M. W., Kutay, U. & Helenius, A. (2000). Herpes simplex virus type 1 entry into host cells: reconstitution of capsid binding and uncoating at the nuclear pore complex in vitro. *Mol Cell Biol* **20**, 4922-31.
- Orlando, J. S., Balliet, J. W., Kushnir, A. S., Astor, T. L., Kosz-Vnenchak, M., Rice, S. A., Knipe, D. M. & Schaffer, P. A. (2006). ICP22 is required for wild-type composition and infectivity of herpes simplex virus type 1 virions. *J Virol* **80**, 9381-90.
- Parkinson, J. & Everett, R. D. (2000). Alphaherpesvirus proteins related to herpes simplex virus type 1 ICP0 affect cellular structures and proteins. *J Virol* **74**, 10006-17.
- Pass, R. F. (2001). "Cytomegaloviruses". In *Fields Virology*, 4th edn edn, pp. 2675-2706. Edited by a. P. M. H. D. M. Knipe: Philadelphia: Lippincott-Williams & Wilkins Publishers.
- Perng, G. C., Jones, C., Ciacci-Zanella, J., Stone, M., Henderson, G., Yukht, A., Slanina, S. M., Hofman, F. M., Ghiasi, H., Nesburn, A. B. & Wechsler, S. L. (2000). Virus-induced neuronal apoptosis blocked by the herpes simplex virus latency-associated transcript. *Science* **287**, 1500-3.
- Perry, L. J. & McGeoch, D. J. (1988). The DNA sequences of the long repeat region and adjoining parts of the long unique region in the genome of herpes simplex virus type 1. *J Gen Virol* **69**, 2831-46.
- Pizzorno, M. C. & Hayward, G. S. (1990). The IE2 gene products of human cytomegalovirus specifically down-regulate expression from the major immediate-early promoter through a target sequence located near the cap site. *J Virol* **64**, 6154-65.
- Plafker, S. M., Woods, A. S. & Gibson, W. (1999). Phosphorylation of simian cytomegalovirus assembly protein precursor (pAPNG.5) and proteinase precursor (pAPNG1): multiple attachment sites identified, including two adjacent serines in a casein kinase II consensus sequence. *J Virol* **73**, 9053-62.

- Preston, C. M. (2000). Repression of viral transcription during herpes simplex virus latency. *J Gen Virol* **81**, 1-19.
- Preston, C. M. (2007). Reactivation of expression from quiescent herpes simplex virus type 1 genomes in the absence of immediate-early protein ICP0. *J Virol* **81**, 11781-9.
- Preston, C. M., Frame, M. C. & Campbell, M. E. (1988). A complex formed between cell components and an HSV structural polypeptide binds to a viral immediate early gene regulatory DNA sequence. *Cell* **52**, 425-34.
- Preston, C. M., Mabbs, R. & Nicholl, M. J. (1997). Construction and characterization of herpes simplex virus type 1 mutants with conditional defects in immediate early gene expression. *Virology* **229**, 228-39.
- Preston, C. M. & Nicholl, M. J. (1997). Repression of gene expression upon infection of cells with herpes simplex virus type 1 mutants impaired for immediate-early protein synthesis. *J Virol* **71**, 7807-13.
- Preston, C. M. & Nicholl, M. J. (2005). Human cytomegalovirus tegument protein pp71 directs long-term gene expression from quiescent herpes simplex virus genomes. *J Virol* **79**, 525-35.
- Preston, C. M. & Nicholl, M. J. (2006). Role of the cellular protein hDaxx in human cytomegalovirus immediate-early gene expression. *J Gen Virol* **87**, 1113-21.
- Preston, C. M., Rinaldi, A. & Nicholl, M. J. (1998). Herpes simplex virus type 1 immediate early gene expression is stimulated by inhibition of protein synthesis. *J Gen Virol* **79**, 117-24.
- Prichard, M. N., Penfold, M. E., Duke, G. M., Spaete, R. R. & Kemble, G. W. (2001). A review of genetic differences between limited and extensively passaged human cytomegalovirus strains. *Rev Med Virol* **11**, 191-200.
- Quirici, N., Soligo, D., Caneva, L., Servida, F., Bossolasco, P. & Deliliers, G. L. (2001). Differentiation and expansion of endothelial cells from human bone marrow CD133(+) cells. *Br J Haematol* **115**, 186-94.
- Reeves, M., Murphy, J., Greaves, R., Fairley, J., Brehm, A. & Sinclair, J. (2006). Autorepression of the human cytomegalovirus major immediate-early promoter/enhancer at late times of infection is mediated by the recruitment of chromatin remodeling enzymes by IE86. *J Virol* **80**, 9998-10009.
- Reeves, M. B., Lehner, P. J., Sissons, J. G. & Sinclair, J. H. (2005a). An in vitro model for the regulation of human cytomegalovirus latency and reactivation in dendritic cells by chromatin remodelling. *J Gen Virol* **86**, 2949-54.
- Reeves, M. B., MacAry, P. A., Lehner, P. J., Sissons, J. G. & Sinclair, J. H. (2005b). Latency, chromatin remodeling, and reactivation of human cytomegalovirus in the dendritic cells of healthy carriers. *Proc Natl Acad Sci U S A* **102**, 4140-5.
- Reid, G. G., Ellsmore, V. & Stow, N. D. (2003). An analysis of the requirements for human cytomegalovirus oriLyt-dependent DNA synthesis in the presence of the herpes simplex virus type 1 replication fork proteins. *Virology* **308**, 303-16.
- Rixon, F. J. (1993). Structure and assembly of herpesviruses. *Seminars in VIROLOGY* **4**, 135-144.
- Rixon, F. J., Addison, C. & McLauchlan, J. (1992). Assembly of enveloped tegument structures (L particles) can occur independently of virion maturation in herpes simplex virus type 1-infected cells. *J Gen Virol* **73**, 277-84.
- Robson, L. & Gibson, W. (1989). Primate cytomegalovirus assembly protein: genome location and nucleotide sequence. *J Virol* **63**, 669-76.
- Roizman, B. & Baines, J. (1991). The diversity and unity of Herpesviridae. *Comp Immunol Microbiol Infect Dis* **14**, 63-79.

- Roizman, B. Knipe, D. M. (2001). Herpes simplex viruses and their replication. In *Fields Virology*, 4th edn, pp. 2399-2459. Edited by Knipe, D.M Lippincott-Williams & Wilkins Publishers. Philadelphia:
- Ross, T. G., Rogers, R. P., Elfrink, N., Bray, N. & Blewett, E. L. (2005). Detection of baboon cytomegalovirus (BaCMV) by PCR using primers directed against the glycoprotein B gene. *J Virol Methods* **125**, 119-24.
- Ruger, B., Klages, S., Walla, B., Albrecht, J., Fleckenstein, B., Tomlinson, P. & Barrell, B. (1987). Primary structure and transcription of the genes coding for the two virion phosphoproteins pp65 and pp71 of human cytomegalovirus. *J Virol* **61**, 446-53.
- Ruggero, D., Wang, Z. G. & Pandolfi, P. P. (2000). The puzzling multiple lives of PML and its role in the genesis of cancer. *Bioessays* **22**, 827-35.
- Russell, J. & Preston, C. M. (1986). An in vitro latency system for herpes simplex virus type 2. *J Gen Virol* **67**, 397-403.
- Russell, J., Stow, N. D., Stow, E. C. & Preston, C. M. (1987). Herpes simplex virus genes involved in latency in vitro. *J Gen Virol* **68**, 3009-18.
- Saad, A., Zhou, Z. H., Jakana, J., Chiu, W. & Rixon, F. J. (1999). Roles of triplex and scaffolding proteins in herpes simplex virus type 1 capsid formation suggested by structures of recombinant particles. *J Virol* **73**, 6821-30.
- Sacks, W. R., Greene, C. C., Aschman, D. P. & Schaffer, P. A. (1985). Herpes simplex virus type 1 ICP27 is an essential regulatory protein. *J Virol* **55**, 796-805.
- Sacks, W. R. & Schaffer, P. A. (1987). Deletion mutants in the gene encoding the herpes simplex virus type 1 immediate-early protein ICP0 exhibit impaired growth in cell culture. *J Virol* **61**, 829-39.
- Saffert, R. T. & Kalejta, R. F. (2006). Inactivating a cellular intrinsic immune defense mediated by Daxx is the mechanism through which the human cytomegalovirus pp71 protein stimulates viral immediate-early gene expression. *J Virol* **80**, 3863-71.
- Saffert, R. T. & Kalejta, R. F. (2007). Human cytomegalovirus gene expression is silenced by Daxx-mediated intrinsic immune defense in model latent infections established in vitro. *J Virol* **81**, 9109-20.
- Sagedal, S., Hartmann, A. & Rollag, H. (2005). The impact of early cytomegalovirus infection and disease in renal transplant recipients. *Clin Microbiol Infect* **11**, 518-30.
- Salomoni, P. & Khelifi, A. F. (2006). Daxx: death or survival protein? *Trends Cell Biol* **16**, 97-104.
- Samaniego, L. A., Neiderhiser, L. & DeLuca, N. A. (1998). Persistence and expression of the herpes simplex virus genome in the absence of immediate-early proteins. *J Virol* **72**, 3307-20.
- Sanchez, V., Greis, K. D., Sztul, E. & Britt, W. J. (2000a). Accumulation of virion tegument and envelope proteins in a stable cytoplasmic compartment during human cytomegalovirus replication: characterization of a potential site of virus assembly. *J Virol* **74**, 975-86.
- Sanchez, V., Sztul, E. & Britt, W. J. (2000b). Human cytomegalovirus pp28 (UL99) localizes to a cytoplasmic compartment which overlaps the endoplasmic reticulum-golgi-intermediate compartment. *J Virol* **74**, 3842-51.
- Sandri-Goldin, R. M. (1998). ICP27 mediates HSV RNA export by shuttling through a leucine-rich nuclear export signal and binding viral intronless RNAs through an RGG motif. *Genes Dev* **12**, 868-79.
- Sarisky, R. T. & Hayward, G. S. (1996). Evidence that the UL84 gene product of human cytomegalovirus is essential for promoting oriLyt-dependent DNA replication and formation of replication compartments in cotransfection assays. *J Virol* **70**, 7398-413.

- Sawtell, N. M. & Thompson, R. L. (2004). Comparison of herpes simplex virus reactivation in ganglia in vivo and in explants demonstrates quantitative and qualitative differences. *J Virol* **78**, 7784-94.
- Schierling, K., Stamminger, T., Mertens, T. & Winkler, M. (2004). Human cytomegalovirus tegument proteins ppUL82 (pp71) and ppUL35 interact and cooperatively activate the major immediate-early enhancer. *J Virol* **78**, 9512-23.
- Schlessinger, J. (2000). Cell signaling by receptor tyrosine kinases. *Cell* **103**, 211-25.
- Shahin, V., Hafezi, W., Oberleithner, H., Ludwig, Y., Windoffer, B., Schillers, H. & Kuhn, J. E. (2006). The genome of HSV-1 translocates through the nuclear pore as a condensed rod-like structure. *J Cell Sci* **119**, 23-30.
- Shen, T. H., Lin, H. K., Scaglioni, P. P., Yung, T. M. & Pandolfi, P. P. (2006). The mechanisms of PML-nuclear body formation. *Mol Cell* **24**, 331-9.
- Sinclair, J. & Sissons, P. (2006). Latency and reactivation of human cytomegalovirus. *J Gen Virol* **87**, 1763-79.
- Smith, J. S. & Robinson, N. J. (2002). Age-specific prevalence of infection with herpes simplex virus types 2 and 1: a global review. *J Infect Dis* **186**, S3-28.
- Smith, M. S., Bentz, G. L., Alexander, J. S. & Yurochko, A. D. (2004). Human cytomegalovirus induces monocyte differentiation and migration as a strategy for dissemination and persistence. *J Virol* **78**, 4444-53.
- Smuda, C., Bogner, E. & Radsak, K. (1997). The human cytomegalovirus glycoprotein B gene (ORF UL55) is expressed early in the infectious cycle. *J Gen Virol* **78**, 1981-92.
- Sodeik, B. (2000). Mechanisms of viral transport in the cytoplasm. *Trends Microbiol* **8**, 465-72.
- Sommer, M. H., Scully, A. L. & Spector, D. H. (1994). Transactivation by the human cytomegalovirus IE2 86-kilodalton protein requires a domain that binds to both the TATA box-binding protein and the retinoblastoma protein. *J Virol* **68**, 6223-31.
- Spaete, R. R. & Frenkel, N. (1982). The herpes simplex virus amplicon: a new eucaryotic defective-virus cloning-amplifying vector. *Cell* **30**, 295-304.
- Spaete, R. R. & Mocarski, E. S. (1985). Regulation of cytomegalovirus gene expression: alpha and beta promoters are trans activated by viral functions in permissive human fibroblasts. *J Virol* **56**, 135-43.
- Spaete, R. R., Perot, K., Scott, P. I., Nelson, J. A., Stinski, M. F. & Pachl, C. (1993). Coexpression of truncated human cytomegalovirus gH with the UL115 gene product or the truncated human fibroblast growth factor receptor results in transport of gH to the cell surface. *Virology* **193**, 853-61.
- Spear, P. G. (2002). Viral interactions with receptors in cell junctions and effects on junctional stability. *Dev Cell* **3**, 462-4.
- Spear, P. G. (2004). Herpes simplex virus: receptors and ligands for cell entry. *Cell Microbiol* **6**, 401-10.
- Spengler, M. L., Kurapatwinski, K., Black, A. R. & Azizkhan-Clifford, J. (2002). SUMO-1 modification of human cytomegalovirus IE1/IE72. *J Virol* **76**, 2990-6.
- Stanier, P., Kitchen, A. D., Taylor, D. L. & Tynms, A. S. (1992). Detection of human cytomegalovirus in peripheral mononuclear cells and urine samples using PCR. *Mol Cell Probes* **6**, 51-8.
- Steiner, I., Spivack, J. G., Lirette, R. P., Brown, S. M., MacLean, A. R., Subak-Sharpe, J. H. & Fraser, N. W. (1989). Herpes simplex virus type 1 latency-associated transcripts are evidently not essential for latent infection. *Embo J* **8**, 505-11.

- Stinski, M. F. & Roehr, T. J. (1985). Activation of the major immediate early gene of human cytomegalovirus by cis-acting elements in the promoter-regulatory sequence and by virus-specific trans-acting components. *J Virol* **55**, 431-41.
- Stow, E. C. & Stow, N. D. (1989). Complementation of a herpes simplex virus type 1 Vmw110 deletion mutant by human cytomegalovirus. *J Gen Virol* **70**, 695-704.
- Stow, N. D. (1982). Localization of an origin of DNA replication within the TRS/IRS repeated region of the herpes simplex virus type 1 genome. *Embo J* **1**, 863-7.
- Stow, N. D. (2001). Packaging of genomic and amplicon DNA by the herpes simplex virus type 1 UL25-null mutant KUL25NS. *J Virol* **75**, 10755-65.
- Stow, N. D. & McMonagle, E. C. (1983). Characterization of the TRS/IRS origin of DNA replication of herpes simplex virus type 1. *Virology* **130**, 427-38.
- Stow, N. D. & Stow, E. C. (1986). Isolation and characterization of a herpes simplex virus type 1 mutant containing a deletion within the gene encoding the immediate early polypeptide Vmw110. *J Gen Virol* **67**, 2571-85.
- Su, Y. H., Zhang, X., Wang, X., Fraser, N. W. & Block, T. M. (2006). Evidence that the immediate-early gene product ICP4 is necessary for the genome of the herpes simplex virus type 1 ICP4 deletion mutant strain d120 to circularize in infected cells. *J Virol* **80**, 11589-97.
- Taylor-Wiedeman, J., Sissons, J. G., Borysiewicz, L. K. & Sinclair, J. H. (1991). Monocytes are a major site of persistence of human cytomegalovirus in peripheral blood mononuclear cells. *J Gen Virol* **72**, 2059-64.
- Taylor-Wiedeman, J., Sissons, P. & Sinclair, J. (1994). Induction of endogenous human cytomegalovirus gene expression after differentiation of monocytes from healthy carriers. *J Virol* **68**, 1597-604.
- Thompson, R. L. & Sawtell, N. M. (2006). Evidence that the herpes simplex virus type 1 ICP0 protein does not initiate reactivation from latency in vivo. *J Virol* **80**, 10919-30.
- Thomsen, D. R., Stenberg, R. M., Goins, W. F. & Stinski, M. F. (1984). Promoter-regulatory region of the major immediate early gene of human cytomegalovirus. *Proc Natl Acad Sci U S A* **81**, 659-63.
- Trgovcich, J., Cebulla, C., Zimmerman, P. & Sedmak, D. D. (2006). Human cytomegalovirus protein pp71 disrupts major histocompatibility complex class I cell surface expression. *J Virol* **80**, 951-63.
- Trus, B. L., Gibson, W., Cheng, N. & Steven, A. C. (1999). Capsid structure of simian cytomegalovirus from cryoelectron microscopy: evidence for tegument attachment sites. *J Virol* **73**, 2181-92.
- Ullrich, A. & Schlessinger, J. (1990). Signal transduction by receptors with tyrosine kinase activity. *Cell* **61**, 203-12.
- Wang, K., Lau, T. Y., Morales, M., Mont, E. K. & Straus, S. E. (2005). Laser-capture microdissection: refining estimates of the quantity and distribution of latent herpes simplex virus 1 and varicella-zoster virus DNA in human trigeminal Ganglia at the single-cell level. *J Virol* **79**, 14079-87.
- Wang, X., Huong, S. M., Chiu, M. L., Raab-Traub, N. & Huang, E. S. (2003). Epidermal growth factor receptor is a cellular receptor for human cytomegalovirus. *Nature* **424**, 456-61.
- Watson, R. J. & Clements, J. B. (1980). A herpes simplex virus type 1 function continuously required for early and late virus RNA synthesis. *Nature* **285**, 329-30.
- Weir, J. P. (2001). Regulation of herpes simplex virus gene expression. *Gene* **271**, 117-30.

- Weller, S. K., Lee, K. J., Sabourin, D. J. & Schaffer, P. A. (1983). Genetic analysis of temperature-sensitive mutants which define the gene for the major herpes simplex virus type 1 DNA-binding protein. *J Virol* **45**, 354-66.
- Whitley, R. J. (2001). Herpes simplex viruses. In *Fields Virology*. Edited by K. D. M. H. P. M. Fields B. N. Philadelphia: Lippincott-Raven.
- Wiertz, E. J., Jones, T. R., Sun, L., Bogoy, M., Geuze, H. J. & Ploegh, H. L. (1996). The human cytomegalovirus US11 gene product dislocates MHC class I heavy chains from the endoplasmic reticulum to the cytosol. *Cell* **84**, 769-79.
- Wilkinson, G. W., Kelly, C., Sinclair, J. H. & Rickards, C. (1998). Disruption of PML-associated nuclear bodies mediated by the human cytomegalovirus major immediate early gene product. *J Gen Virol* **79 (Pt 5)**, 1233-45.
- Woodhall, D. L., Groves, I. J., Reeves, M. B., Wilkinson, G. & Sinclair, J. H. (2006). Human Daxx-mediated Repression of Human Cytomegalovirus Gene Expression Correlates with a Repressive Chromatin Structure around the Major Immediate Early Promoter. *J Biol Chem* **281**, 37652-60.
- Wright, E., Bain, M., Teague, L., Murphy, J. & Sinclair, J. (2005). Ets-2 repressor factor recruits histone deacetylase to silence human cytomegalovirus immediate-early gene expression in non-permissive cells. *J Gen Virol* **86**, 535-44.
- Wu, C. A., Nelson, N. J., McGeoch, D. J. & Challberg, M. D. (1988). Identification of herpes simplex virus type 1 genes required for origin-dependent DNA synthesis. *J Virol* **62**, 435-43.
- Wysocka, J. & Herr, W. (2003). The herpes simplex virus VP16-induced complex: the makings of a regulatory switch. *Trends Biochem Sci* **28**, 294-304.
- Xu, Y., Cei, S. A., Rodriguez Huete, A., Colletti, K. S. & Pari, G. S. (2004). Human cytomegalovirus DNA replication requires transcriptional activation via an IE2- and UL84-responsive bidirectional promoter element within oriLyt. *J Virol* **78**, 11664-77.
- Yang, X., Khosravi-Far, R., Chang, H. Y. & Baltimore, D. (1997). Daxx, a novel Fas-binding protein that activates JNK and apoptosis. *Cell* **89**, 1067-76.
- Yao, F. & Courtney, R. J. (1989). A major transcriptional regulatory protein (ICP4) of herpes simplex virus type 1 is associated with purified virions. *J Virol* **63**, 3338-44.
- Yao, F. & Schaffer, P. A. (1994). Physical interaction between the herpes simplex virus type 1 immediate-early regulatory proteins ICP0 and ICP4. *J Virol* **68**, 8158-68.
- Yao, F. & Schaffer, P. A. (1995). An activity specified by the osteosarcoma line U2OS can substitute functionally for ICP0, a major regulatory protein of herpes simplex virus type 1. *J Virol* **69**, 6249-58.
- York, I. A. & Rock, K. L. (1996). Antigen processing and presentation by the class I major histocompatibility complex. *Annu Rev Immunol* **14**, 369-96.
- York, I. A., Roop, C., Andrews, D. W., Riddell, S. R., Graham, F. L. & Johnson, D. C. (1994). A cytosolic herpes simplex virus protein inhibits antigen presentation to CD8+ T lymphocytes. *Cell* **77**, 525-35.
- Yue, Y., Kaur, A., Zhou, S. S. & Barry, P. A. (2006). Characterization and immunological analysis of the rhesus cytomegalovirus homologue (Rh112) of the human cytomegalovirus UL83 lower matrix phosphoprotein (pp65). *J Gen Virol* **87**, 777-87.
- Yurochko, A. D., Hwang, E. S., Rasmussen, L., Keay, S., Pereira, L. & Huang, E. S. (1997). The human cytomegalovirus UL55 (gB) and UL75 (gH) glycoprotein ligands initiate the rapid activation of Sp1 and NF-kappaB during infection. *J Virol* **71**, 5051-9.

- Zabierowski, S. & DeLuca, N. A. (2004). Differential cellular requirements for activation of herpes simplex virus type 1 early (tk) and late (gC) promoters by ICP4. *J Virol* **78**, 6162-70.
- Zhu, X. X., Chen, J. X., Young, C. S. & Silverstein, S. (1990). Reactivation of latent herpes simplex virus by adenovirus recombinants encoding mutant IE-0 gene products. *J Virol* **64**, 4489-98.

Appendices

Appendices

Appendix A: Recombinant Viruses

EYP-tagged HSV-1 recombinant viruses

Virus	Transgene locus	Mutations to HSV-1 recombinants
in1374 Negative control	<i>E.coli lacZ</i> inserted in to the UL43 locus	VP16, ICP0. ICP4
in1310 HCMV EYFPpp71 inserted into the TK locus	<i>E.coli lacZ</i> inserted in to the UL43 locus	VP16, ICP0. ICP4
in0150 SCMV EYFPS82 inserted into the TK locus	<i>E.coli lacZ</i> inserted in to the UL43 locus	VP16, ICP0. ICP4
in0146 ChCMV EYFPCh82 inserted into the TK locus	<i>E.coli lacZ</i> inserted in to the UL43 locus	VP16, ICP0. ICP4
in0144 RhCMV EYFPRh82 inserted into the TK locus	<i>E.coli lacZ</i> inserted in to the UL43 locus	VP16, ICP0. ICP4
in0145 BCMV EYFPB82 inserted into the TK locus	<i>E.coli lacZ</i> inserted in to the UL43 locus	VP16, ICP0. ICP4

myc-tagged HSV-1 recombinant viruses

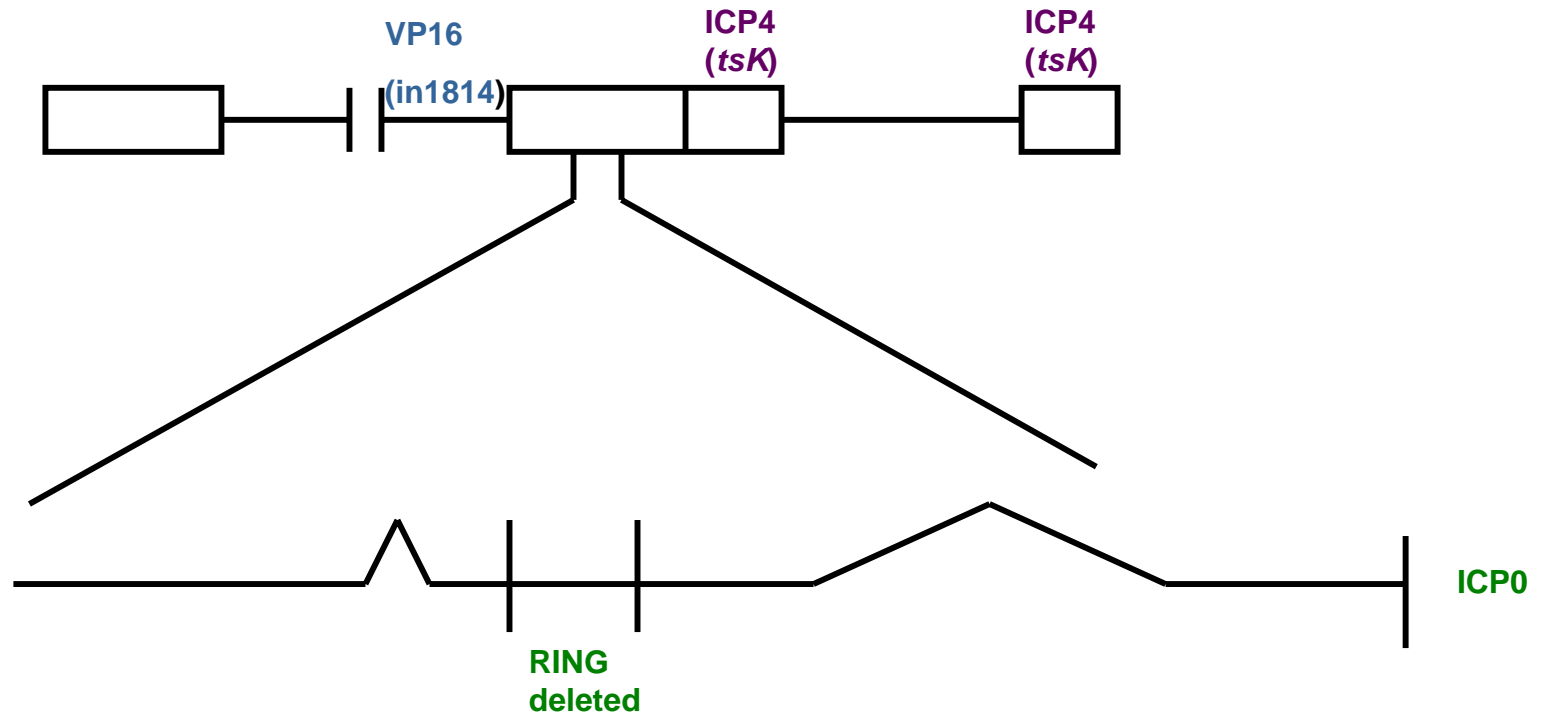
Virus	Transgene locus	Mutations to HSV-1 recombinants
in0149 ChCMV82 mycCh82 inserted into the TK locus	<i>E.coli lacZ</i> inserted in to the UL43 locus	VP16, ICP0. ICP4
in0151 HCMV mycpp71 inserted into the TK locus	<i>E.coli lacZ</i> inserted in to the UL43 locus	VP16, ICP0. ICP4

Other HSV-1 recombinant viruses used in this study

Virus	Transgene locus	Mutations to HSV-1 recombinants
in1382	<i>E.coli lacZ</i> inserted in to the TK locus	VP16, ICP0. ICP4
in0156 EYFPTC6 inserted into the TK locus	<i>E.coli lacZ</i> inserted in to the UL43 locus	VP16, ICP0. ICP4
in1318 Secreted alkaline phosphatase (SEAP) inserted into the TK locus		VP16, ICP0. ICP4

All HSV-1 recombinant viruses used in this study were impaired for the transcriptional stimulating activity of VP16 the IE proteins ICP0 and ICP4 were rendered non-functional by deletion and temperature sensitive mutations respectively.

HSV-1 multiple mutant *in1312*



A multiple mutant inactive for the functions of the three major HSV-1 transcription activators VP16, ICP0 and ICP4 at 38.5° but contains lacZ under the control of the HCMV MIEP.

***In1312* based recombinant expressing the EYFP/myc-tagged UL82 homologues or EYFP-tagged hybrid protein TC6**

pp71

Ch82

S82

B82

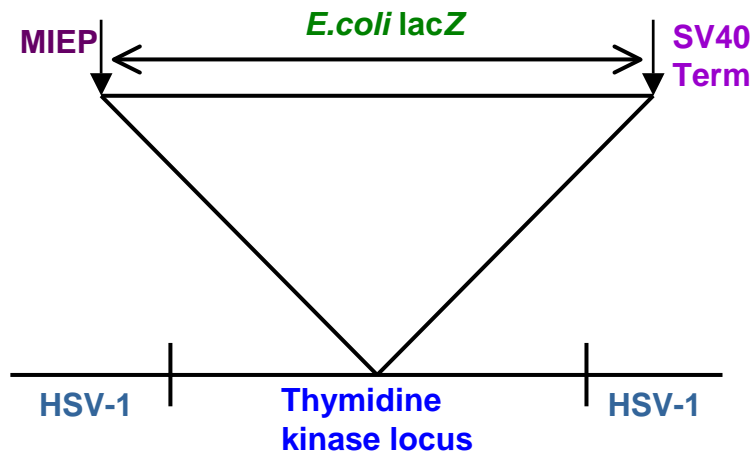
Rh82

Hybrid TC6

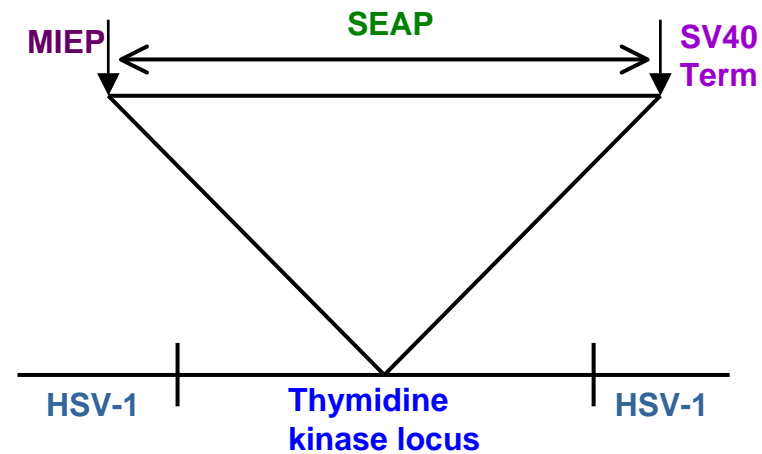


The *in1312* HSV-1 multiple mutant was used to construct the negative control *in1374*, which has *lacZ* inserted into the UL43 locus. *in1374* was used as a vector to express the UL82 homologues or hybrid protein TC6 by insertion of the appropriate DNA cassette into the TK locus. All the HSV-1 recombinant viruses lack VP16, ICP0 and ICP4 function at 38.5⁰

Other HSV-1 in1312 based recombinant viruses used in this study



In1382



In1318

In1382 was constructed by inserting the *E.coli lacZ* reporter gene into the TK locus, *in1318* was constructed by inserting the gene expressing SEAP into the TK locus. Each HSV-1 mutant virus was impaired for the transcriptional activity of VP16, ICP0 and contained a temperature sensitive mutation at ICP4 rendering the viruses inactive at 38.5⁰

Appendix B

Genome organisation of the HCMV Strain Merlin

Coloured arrows indicate protein-coding regions and the name of each gene is indicated below.

The Merlin image was kindly provided by Dr. Andrew Davison

